UNIVERSITY OF SOUTHAMPTON

FACULTY OF SOCIAL SCIENCES
Mathematical Sciences

Black hole microstate geometries and their holographic duals

by

Sami Rawash

Thesis for the degree of Doctor of Philosophy

DATE: February 2023

UNIVERSITY OF SOUTHAMPTON

ABSTRACT

FACULTY OF SOCIAL SCIENCES
Mathematical Sciences

Doctor of Philosophy

BLACK HOLE MICROSTATE GEOMETRIES AND THEIR HOLOGRAPHIC DUALS

by Sami Rawash

In this thesis we exploit various tools to investigate aspects of black hole microstate geometries within the context of the "fuzzball proposal", which follows from the string theory construction of black holes in terms of strings and branes. This thesis comprises three parts.

In Part I, we make use of the gauge-gravity duality to discuss the precision holographic dictionary, that relates the asymptotic expansion of black hole microstates near the AdS boundary with the expectation values of certain operators in the dual CFT. In particular, we derive the dictionary for scalar chiral primary operators of dimension two and a class of superdescendants of these operators, in the single-particle basis.

In Part II, we construct the first family of three-charge supersymmetric solutions containing a shockwave and we give a proposal for their holographic duals, which passes non-trivial checks. These gravitational solutions do not represent a single pure state in gravity: they provide a collective description of a family of microstates whose details are not resolved in supergravity.

In Part III, we use computer science tools to derive approximate examples of microstate geometries. In particular, we present an optimization algorithm, based on evolutionary algorithm and Bayesian optimization, to construct numerical multi-center solutions with a high number of centers in generic configurations.

The research conducted in this thesis supports the ideas of the fuzzball paradigm, and develops techniques which can prove useful to examine and test the conjecture in future scenarios.

Contents

List of Figures

List of Tables

Declaration of Authorship

I, Sami Rawash, declare that this thesis entitled "Black hole microstate geometries and their holographic duals" and the work presented in it are my own and have been generated by me as the result of my own original research.

I confirm that:

- This work was done wholly or mainly while in candidature for a research degree at this University;
- Where any part of this thesis has previously been submitted for a degree or any other qualification at this University or any other institution, this has been clearly stated;
- Where I have consulted the published work of others, this is always clearly attributed;
- Where I have quoted from the work of others, the source is always given. With the exception of such quotations, this thesis is entirely my own work;
- I have acknowledged all main sources of help;
- Where the thesis is based on work done by myself jointly with others, I have made clear exactly what was done by others and what I have contributed myself;
- Parts of this work have been published as: [1–4]

Signed: .....

Date: .....

Acknowledgements

First of all, I would like to thank my supervisor David Turton for his support and guidance in these years, and for the several things he has thought me with patience and enthusiasm. Perhaps more importantly, I would like to thank him for his human support, without which the transition outside academia would have been much harder.

I feel in debt with Stefano Giusto, for having introduced me to the mysteries of black holes and fuzzballs: the clarity of his explanations have been rarely beaten. I want to thank Bidisha Chakrabarty, for our collaboration on shockwaves and for a delicious indian dinner. It is a pleasure to thank Iosif Bena, Davide Bufalini, Oscar Dias, Pierre Heidmann, Hynek Paul, Rodolfo Russo, Michele Santagata, Kostas Skenderis, Marika Taylor, Joan Garcia i Tormo and Nicholas P. Warner for stimulating discussions during the PhD.

A special thanks goes to Michele, for having shared part of this experience with me and for his help in bringing back light when the sleep of reason produced monsters. See you on the other side of the globe! And to Davide, my academic younger brother, severe but fair.

Many days spent at Uni would have not been so pleasant without my office mates: Enrico, Davide, Adam, Alex, Daniel, Elliot, George, Ivan and Federico, the chattiest. I want to thank Adam, Matt, Lorenzo, Mike, Michele and Alessandra for our great trip in Cornwall. When I arrived in the UK I promised myself I would have not hung out with italians: Federico, Michele, Davide, Thomas, Giuseppe and Lorenzo made me realize that this promise was worth breaking. Many other people have enriched my permanence in Southampton and I want to list at least a few of them: Billy, Stacy, Tracy, Marcos, Francesco, Zhora, Ross, Giovanna, Elena, Kostas, Dalius, Aaron, Ivan, Martina, Nico, Pantelis, Fabian, Hao, Leire, Kostantine, Andy and Richard.

I fill lucky thinking that I have friends like Massimo, Michelangelo, Matteo and Giovanni, as close as brothers, despite the five of us leaving in four different countries. Cities change, friends remain. Thanks to Massimo, Sergio, Michele and Federico for their hospitality in the south of Italy and for having shown me the vibes of the southern culture.

These acknowledgments would not be complete without mentioning the Paduans: Amarilli, Dani, Marco, Ale, Bea, Lorenzo, Giacomo, Sara, Linda and Michelino. A special thanks goes to Silvia and Michele.

Last, I feel grateful to my parents for their unconditional love. And to my sisters: so different to me, and yet so similar.

"...anyone who thinks that all fruits ripen at the same time as strawberries, knows nothing of grapes."

Paracelsus

Chapter 1

Introduction

1.1 Puzzles and paradoxes

In the last few years, we have witnessed a very exciting period for black hole physics. The gravitational waves detected by LIGO [5] and the release of the first picture of a black hole by the Event Horizon Telescope [6] not only support the idea that black hole like objects do exist in Nature, but also show that their description in general relativity (GR) is accurate within our experimental error. These discoveries are another experimental example indicating the validity of GR, which add to several experimental tests that general relativity has already passed [7]. Even though there are no empirical motivations (and thus guidelines) to modify this theory, we have strong theoretical arguments to believe that the description of black hole physics provided by GR is not the most fundamental one. This can be motivated at different levels.

First of all, a black hole in general relativity is a singular solution of Einstein's equations in which the curvature singularity is hidden behind an event horizon, a one-way membrane that separates those spacetime points that are connected to infinity by a time-like path from those that are not. Singularities indicate a breakdown of the theory in describing phenomena at certain scales, so when dealing with black holes GR predicts its own failure and we shall look for a more fundamental theory in which the singularity is resolved.

Deeper motivations come from a closer analysis of black holes in general relativity. The classical phase space of a black hole is protected by uniqueness theorems, known as "no-hair theorems" [8]. For example, they state that given a stationary, asymptotically flat black hole solution coupled to electromagnetism that is non singular outside the horizon, the solution is fully characterized by its conserved charges (the mass M, the charge Q and the angular momentum J). Suppose a black hole is formed by gravitational collapse: no matter the details of the initial configuration, once the system has settled down to a stationary state its back reaction on spacetime is described only by three parameters.

This does not imply that the information on the initial state is lost: classically, we can think of it as hidden behind the horizon. We will see that quantum mechanically the situation is much more puzzling.

Another important property of black holes is their thermodynamic behaviour. By using Einstein's equations one can derive a set of mechanical laws that look analogous to the laws of thermodynamics [9]. These are (for a review see e.g. [10, 11]):

- Zeroth law: the surface gravity κ is constant over the horizon. This is the law of thermal equilibrium, with κ playing the role of a temperature.
- First law: the variation of the mass M of a black hole is related to the change of its horizon area A, angular momentum J and charge Q via

$$\delta M = \frac{\kappa}{8\pi G_N}\delta A + \Omega_H \delta J + \Phi \delta Q\,, \tag{1.1}$$

  where Ω_H and Φ are the angular velocity and electrostatic potential, respectively. This is the law of conservation of energy.
- Second law: in any mechanical process the area of the event horizon can never decrease $\delta A \geq 0$. This is the analog of the law stating that entropy is a non-decreasing function of time, with the area of the event horizon playing the role of the entropy of the black hole S_{BH}. The relation between these two quantities, in units where $c = \hbar = k_B = 1$, is:

$$S_{BH} \,=\, \frac{A}{4G_N}\,. \tag{1.2}$$

  The second law has then been generalized by Bekenstein [12]:

$$d\big(S_{BH} + S_{\text{Matter}}\big) \,\geq\, 0\,. \tag{1.3}$$

  This relation states that the total entropy, given by the sum of the entropy of the black hole and that of the matter in the exterior of the black hole, never decreases.

Even though this analogy between thermodynamics and black hole mechanics seems quite remarkable, it is not obvious that it should be taken seriously. Black holes, as the name states, are objects from which nothing can escape: what does it mean to associate a temperature to a body that does not emit radiation? Moreover, Boltzman has taught us that the entropy of a thermodynamic system can be understood as the degeneracy of microstates associated to the macroscopic system:

$$S \propto \ln(\#\text{ microstates})\,. \tag{1.4}$$

It is useful at this stage to give an order of magnitude of the entropy of a black hole: by restoring the physical units in Eq. (1.2), one has that a Schwarzschild black hole of

mass M has a thermodynamic entropy given by:

$$S_{\text{Schw}} \sim 10^{76}\Big(\frac{M}{M_{\text{Sun}}}\Big)\,, \tag{1.5}$$

which is a remarkably large number. Is this point of view compatible with the no-hair theorems, i.e. with the triviality of the black hole's classical phase space? Because of these conflicts one would be tempted not to take this correspondence seriously and interpret it as nothing more but a vague analogy.

Taking into account quantum field theory on the curved (fixed) background produced by a black hole, Hawking showed that the physics is much more mysterious. Even though classically black holes are black, semi-classically they emit a black body radiation at a temperature [13, 14]

$$T_{BH} \,=\, \frac{\kappa}{2\pi}\,. \tag{1.6}$$

In a nutshell, Hawking's computation arises as follows (see e.g. [15] for a review). We consider a black hole solution coupled with a quantum field and we remind that the Equivalence Principle implies that a free falling observer crossing the horizon experiences nothing out of ordinary. The vacuum state of the quantum field is observer dependent in curved spacetime: when the free falling observer crossing the horizon experiences the vacuum, an observer at infinity will see a flux of particles. By energy conservation, we conclude that the particles are emitted by the black hole, which decreases in mass. This emission process turns out to be exactly thermal, with no correlations between early and late radiation. An heuristic but useful picture to visualise the Hawking radiation process is as follows. We can think of the black hole radiation as due to pair production near the horizon: one member of the entangled pair falls into the black hole, decreasing its mass, and the other member escapes to infinity, giving rise to the radiation.

This phenomenon enforces the case for taking seriously the thermodynamic behaviour of black holes and gives rise to puzzling questions. As we outlined above, a thermodynamic system should be governed by an underlying statistical mechanics: in this view, the macroscopic system with entropy S is a coarse grained description of e^S microstates which are lumped into the same macroscopic state, meaning that they cannot be distinguished by macroscopic observables. In the case of a black hole, what/where are the $e^{S_{BH}}$ microstates? This is the so called entropy puzzle.

Hawking process has another important consequence that has puzzled high energy theoretical physicist for over fifty years, which is the so called information paradox [16]. Hawking radiation, in the simplest setup, implies the evaporation of the black hole: once the emitted radiation has carried away all the energy, the black hole is expected to disappear. Let us consider the process of creation and evaporation of a black hole as a scattering experiment. We start from an initial configuration in a pure state which, under the gravitational interaction, collapses to form a black hole. Under time evolution, the black hole evaporates and eventually disappears so that the final state is the

thermal radiation. This process describes the temporal evolution of an initial pure state to a mixed state: this violates the quantum mechanical principle of unitary.

Of course, one could support the idea that the fundamental laws of nature are not unitary: with this perspective Hawking evaporation process not only would not be a problem, but would also provide an indication of this non-unitary behaviour. In this thesis we will acquire the perspective (and we will give motivations for this in due course) that quantum gravity is unitary: in this sense, Hawking's computation is a paradox. We refer the reader to [17–23] for further discussions on the information paradox.

It has been suggested [24] that black holes do not evaporate completely: the Hawking process, being a semi-classical computation, should be trusted until the black hole becomes Planck-size[1]. Next, quantum gravity effects take over and they could stabilize the evaporation process leaving an eternal, or simply a very long-lived, remnant, i.e. an object which is bounded in mass and size but that can have an unbounded amount of entanglement with a system far away. In this case, the final state, being the union of the remnant and the Hawking radiation, is in a pure state. This proposal is problematic for several reasons. First, this time evolution is in conflict with the Page curve [18, 25], which states that unitary evolution requires the entanglement entropy between the black hole and the radiation to start decreasing when about half of the degrees of freedom have evaporated. Second, having an unbounded amount of entanglement entropy in a finite size system is in conflict with Bekenstein's entropy bound and the generalized second law of thermodynamics [26, 27]. See also [28, 29] for other critics of remnants.

Another general guideline that was suggested to solve the information paradox was that small quantum gravity effects could restore unitarity. Hawking's computation neglects these effects and represents the leading order contribution. We thus expect small, even though in principle arbitrarily complicated, corrections to the Hawking process due to unknown quantum gravity physics. Despite being small, these effects are integrated over a very large number of evaporating bits (see Eq. (1.5)). It was argued that these small corrections could introduce subtle correlations between the early and late radiation, resulting in an order one correction to the final state of the evaporation process that restores unitarity.

However, the "small correction theorem" proven in [30] (see also [20, 31] for further discussions) shows that this common lore is a misconception: small corrections to Hawking evaporation process that are localized in the neighborhood of the horizon cannot restore unitarity. One has either to incorporate (and justify) order one corrections to Hawking evaporation process that are localized near the horizon or non-local effects that can be arbitrarily small but have to extend across the full space-like slice that connects the horizon with the observer at infinity.

These examples show that, even if we expect that a UV complete theory of gravity

[1] Assuming there is no new physics before the Planck scale.

should shed light upon the information paradox, it is not obvious a priori how this may happen. Hawking's computation treats the gravitational field as a classical background. At a fundamental level we believe that all physical fields should undergo the general framework of quantum physics: gravity is no exception [32]. However, we generally expect quantum gravity effects to become important at some fundamental scale which we typically take to be the Planck scale l_p. On the other hand, Hawking process is sensitive to a scale (i.e. the radius of the event horizon R) which, at least while the black hole is large, is macroscopic and we have $l_p \ll R$: it is thus not obvious how quantum gravity effects can resolve the information paradox. Why should the semi-classical approximation fail for Hawking's computation? And when does it cease to be a good approximation?

It would be unfair to proceed further without mentioning some recent advances to solve the information paradox, that go under the general framework of the "island paradigm" [33–36] (see [37] for a review). In these papers, the entanglement entropy of the radiation was computed via the gravitational path integral, with a method that is similar in spirit to the computation of the entropy of an Euclidean black hole [38]. The resulting formula prescribes that in order to compute the entanglement entropy of the radiation, one has to take into account an "island" contribution, i.e. one has to consider the entropy of a system that is the union of the radiation and a part of the interior of the black hole. Since the information paradox arises from the entangled nature of black hole and radiation, by prescribing that in order to compute the fine-grained entropy of the radiation one has to consider also Hawking modes in the interior, the Page curve is recovered. Note that this is a semi-classical computation that does not require knowledge on the UV completion of gravity.

This computation does not give the details of the actual outgoing modes, i.e. of the final state of the evaporation process: the subsystem containing only the radiation is still in a mixed state, and the prescription is interpreted as the "unreasonable effectiveness" of the semi-classical limit. At a fundamental level, the meaning of this prescription and of the statement "that the interior belongs to [...] the radiation" [37] remains quite mysterious. In particular, it has been argued in [39] that, as a consequence of the "small correction theorem", the island paradigm requires the presence of non-local effects across the full space-like slice in the quantum theory.

In this thesis we will follow a different paradigm, according to which the information paradox is solved because of order one corrections to the evolution of Hawking modes at the horizon. In the next section we will discuss how this can be realised in a theory of quantum gravity, string theory.

1.2 The fuzzball proposal

As it is well known, the canonical quantization approach to GR fails because it is a non-renormalizable theory. The attempts to define a consistent theory of quantum gravity have led in the past decades to different approaches, guided by different underlying ideas: string theory, loop quantum gravity, asymptotic safety (just to name a few). String theory is one of the most promising attempts, and we will work within this framework. The fundamental objects of the theory are not point-like particles, but one dimensional objects - the strings - whose different modes of oscillation give rise to a spectrum that contains, among others, a spin-two massless particle (the graviton). A black hole in string theory is a bound state of the fundamental objects of the theory: namely strings and D-branes. To be more precise, changing the string coupling constant g_s, which controls the strength of the gravitational coupling ($g_s^2 \sim G_N$), one can interpolate between the bound state description of the system, when there is no gravitational interaction, and the black hole regime, when gravity is turned on. Using this paradigm, remarkable progress has been made in the last decades.

To start with, for a class of supersymmetric black holes, it is possible [40] to reproduce the Bekenstein-Hawking entropy via a microscopic computation[2] (see e.g. [43] for a review). In fact, one can compute the degeneracy of the microstates at vanishing coupling, exploit the fact that it is protected by supersymmetry as one moves in the moduli space and compare it with the black hole entropy[3].

The agreement between these two quantities not only implies that the Bekenstein-Hawking entropy has a statistical origin, but also that, at least for certain classes of black holes, string theory captures correctly the microscopic degrees of freedom of the gravitational system. This result can be interpreted as a first indication that the black hole evaporation process is unitary: string theory is a unitary theory and it seems to be able to describe black holes at the microscopic level. However, since this computation is based on an extrapolation from weak to strong coupling, it does not give us insight on the gravitational properties of the microstates: understanding how the microstates manifest themselves in the black hole regime would be important to shed light upon the unitary process that replaces Hawking evaporation process at the microscopic level.

One of the ideas in this direction has been motivated by the explicit construction of microstate solutions of the supersymmetric D1-D5 black hole [44–47]. The D1-D5 system is connected via a set of string dualities to the F1-P system: a fundamental string carrying momentum. Indeed, these solutions were first constructed in the F1-P frame and then dualized to D1-D5. The different microstates of the black hole correspond to the different

[2] See e.g. [41, 42] for examples of microscopic entropy counting of non-extremal black holes.

[3] To be precise, the protected quantity is an index that counts the difference between bosonic and fermionic degrees of freedom. One then exploits the fact that the index and the absolute degeneracy agree at leading order.

ways in which the string carrying momentum can vibrate. The common lore before the explicit solutions were constructed was that, by increasing the gravitational coupling, the string configuration would shrink until its characteristic size becomes smaller then the associated Schwarzshild radius: at that point a horizon would form and the resulting geometry would be that of a conventional black hole [48]. The resulting geometries, instead, turned out to be different: they are smooth (in the D1-D5 duality frame [49]) and horizonless. In particular, a microstate is indistinguishable from the classical black hole solution asymptotically, but start to differ from it already at the characteristic scale set by the string vibrations, which is the scale of the would-be horizon. These microstates include both low curvature solutions which are well described in supergravity and limits in which the curvature is string scale. All of them together reproduce the black hole entropy. A typical microstate is a superposition of these solutions and, thus, is highly quantum in nature.

This result motivated the fuzzball proposal [30, 50–52]: according to this conjecture, there are strong quantum gravity effects already at the horizon scale due to the size of the underlying bound state. At the fundamental level, a black hole solution should be replaced with $e^{S_{BH}}$ microstates, which are indistinguishable from the black hole asymptotically, but start to differ from it at the horizon scale: in particular, they are horizonless and non-singular. Importantly, typical microstates are expected to be highly quantum in nature and to be solutions of the full string theory: only a subset of these are low curvature supergravity solutions. According to this paradigm, the (naive) black hole solution represents the coarse grained description of the system, which is not accurate enough to describe the evaporation process.

Some comments are in order. First, the fact that the black hole microstates do not have an horizon enables to interpret them as pure states of the ensemble. If they had an horizon, we could have associated an entropy to each them. But does it make sense to associate an entropy to a microstate? A microstate is any of the possible microscopic description of the system which gives rise to the same thermodynamics: in this sense, entropy is hidden information. However, since a microstate provides a complete description of the system, we shall not associate an entropy to it. Secondly, it is commonly accepted that quantum modifications to GR should become important at some fundamental microscopic scale and, in particular, that the quantum gravity effects that resolve the singularity would be localized in its neighborhood. The fuzzball proposal conjectures that the classical black hole solution should be modified long before: corrections occur already at the horizon scale. This paradigm has the potential to solve the information paradox: the generic microstate is a very non-trivial quantum bound state in the region where the horizon would have been, instead of the smooth vacuum as Hawking assumed.

Let us now briefly review the status of the fuzzball proposal. We have a good understanding of all the microstates responsible for the entropy of the D1-D5 extremal black

hole [46, 47, 53–55] and they all satisfy the properties conjectured by the fuzzball proposal. The D1-D5 black hole, however, is microscopically small, i.e. its horizon area is zero in supergravity. The next challenge is to study how much of this physics is carried over by the microstates of a macroscopic black hole: the main playground in this direction has been the study of microstates of the supersymmetric D1-D5-P black hole. Two main classes have been constructed (and we will review both of them in this thesis): one goes under the name of "superstrata" solutions (see e.g. [56–66]) and the second one is given by a subset of the multi-center solutions (see e.g. [51, 67–75]). Again, the structure of these microstates are compatible with the fuzzball proposal, but it has been shown that these alone are not enough to account for the entropy of the black hole [66, 76, 77].

Last, it is important to develop further our understanding of microstates of non-extremal black holes, as this could give further insight on the unitary process that replaces Hawking evaporation at the microscopic level. An important progress in this direction has been the example provided in [78]: these microstates, that go under the name of JMaRT solutions, do not have a horizon but do have an ergoregion. In this context, Hawking evaporation has been reinterpreted as a process of ergoregion emission [79–85]: this process produces entangled pairs, but in this case the inner particle stays in the ergoregion, affects the evolution of the later quanta and can itself evaporate at a later time. The resulting evaporation process is unitary, in the very same way in which a piece of coal burns in a unitary way. See also [86–89] for further examples and discussions on non-supersymmetric microstates.

The fuzzball proposal has been also discussed in the context of the AdS formulation of the information paradox [90]. Large AdS black holes do not evaporate completely: the AdS boundary is reflective, so that the radiation bounces at the boundary and falls back into the black hole. For this reason, the formulation of the information paradox that we have introduced in the previous section does not hold in general. However, one can characterize the loss of information for AdS black holes by looking at the late-time behaviour of two-point functions of light boundary operators [90]. In the naive black hole geometry (see e.g. [91] for the result in a BTZ) the two-point function decays at late Lorentzian time: this is an indication of information loss. An intuitive interpretation of this behaviour is that the more the boundary operators are separated, the deeper the dual gravitational excitation probes the bulk of spacetime: when the probe crosses the horizon, its correlation with the exterior decays and the information gets lost in the black hole.

It was suggested in [92] that, in order to restore unitarity, higher order corrections in G_N had to be included. By following the fuzzball paradigm, the authors in [93] (see also [94, 95]) proposed a different conclusion: they analyzed the late time behaviour of a two-point function on a fuzzball geometry background and found no signal of information loss. This provides an example that black hole microstates are not accurately described by the naive black hole geometry. In this perspective, the full higher dimensional geometry

contributes to the correlator and the traditional black hole does not have enough degrees of freedom to restore unitarity.

It is fair to say that, despite these examples, the fuzzball proposal is a conjecture at the present state of things. In order to further explore the validity of the proposal the tools provided by the AdS/CFT duality come at hand, as we shall now discuss.

1.3 The role of holography

In order to introduce the role that holography can play within the context of the fuzzball proposal, let us briefly introduce the setup that will be used throughout this thesis (we will provide a more detailed description in Chapters 2 and 3). We consider Type IIB string theory in $\mathbb{R}^{1,4} \times S^1 \times \mathcal{M}$, where $\mathcal{M}$ is either T^4 or $K3$. We take the S^1 to be large and the characteristic size of the internal manifold $\mathcal{M}$ to be microscopic. Even though working in four non-compact direction is more interesting for phenomenological reasons, the spacetime topology we chose simplifies the problem: in five non-compact dimensions three charges are enough to construct a macroscopic black hole. Had we chosen to work in four non-compact dimensions, we would have needed to add a fourth charge [96] (and, of course, the fewer the number of charges the simpler the system).

The black hole under consideration is a bound state of N_1 D1 branes that extend along S^1, N_5 D5 branes that wrap the compact directions and possibly n_p units of momentum P along S^1. The resulting geometry has a near horizon region which is asymptotically $\mathrm{AdS}_3 \times \mathrm{S}^3 \times \mathcal{M}$, so holography is applicable: the gauge side of the duality involves a two dimensional CFT, known as D1-D5 CFT. The basic rules of holography in its mature formulation were described in [97–99]. The duality relates the spectrum (and the dynamics) of string theory in a spacetime that is asymptotically AdS with that of gauge invariant operators in the dual CFT. In particular, holography provides a map between states in the bulk and states in the CFT. Note that, since holography conjectures an exact equivalence between the bulk and the boundary theory, and the latter is unitary, holography is another indication that the microscopic dynamics of black hole should not lead to information loss. Our main interest is in black hole microstates: supersymmetric D1-D5(-P) microstates are understood to be dual to CFT states $|H\rangle$ in the RR sector, which break 1/4 (1/8) of the supercharges and have a conformal dimension of order of the central charge $c = 6N_1N_5 \equiv 6N$ [52, 100, 101]. We work in the best controlled limit of the AdS/CFT duality: when the supergravity approximation is a good description of the bulk physics and $1/N$ and α' corrections are ignored.

On the gauge side, this regime is dual to a strongly coupled point in the moduli space, which makes it difficult to gain a complete understanding of the gravitational physics from the CFT side of the duality. However, one can focus on quantities which, being protected by supersymmetry, are moduli independent: they can be computed at the

free orbifold point of the CFT (where the theory reduces to a collection of free bosons and fermions) and reliably compared with the bulk duals. Quantities of this type are the expectation values of chiral primary operators (and descendants) on 1/4 or 1/8-BPS states [102, 103]: on the gravity side these quantities are encoded in the asymptotic expansion of the bulk solution around $AdS_3 \times S^3$. Roughly speaking, expectation values of such operators on the state $|H\rangle$ characterize the deviation of the dual microstate from the vacuum.

In general, a complete description of the CFT state $|H\rangle$ is determined by the expectation values $\langle H| O_i |H\rangle$, where O_i denotes all operators in the theory (not only the chiral primary ones). On the bulk side, the equivalent statement is that the deviation of one microstate from another is encoded in the different deviation of the fields from pure AdS: these fields are generically those of the full string theory. Restricting our attention to chiral primary operators (and descendants) means probing a microstate at the level of its supergravity modes [100].

A general result of statistical mechanics implies that most of the pure states of an ensemble, when probed with simple operators of the theory (i.e. with operator whose dimension does not scale with the central charge), are indistinguishable from each other and from the thermal state up to exponentially suppressed terms in the large N limit [104, 105]. This means that, according to the fuzzball paradigm, a black hole microstate is a solution of the full string theory which is typically not reliably distinguishable from the corresponding black hole solution in the low energy approximation. Restricting ourselves to the supergravity regime means dealing with atypical states which fill a very small volume of the phase space, but, nonetheless, might be valuable to gain insight on the typical structure of the microstates.

An analysis of the map between expectation values of operators in a CFT state and asymptotic expansion of the dual geometry was pioneered in [54, 55, 106, 107], where it was applied to D1-D5 configurations. A complete study of the dictionary for operators of (total) conformal dimension one, and its extension to 1/8-BPS black hole microstates was given in [103].

1.4 Outline of the thesis

This thesis collects the results presented in [1–4]. The fil rouge of this work is to extend our current understanding of black hole microstates in the black hole regime by exploiting holographic, supergravity and computer science tools. The thesis is organized in three parts, as follows.

In Part 1 we review the precision holographic dictionary for chiral primary operators of dimension one, and extend it to two other sectors: scalar chiral primary operators of

dimension two and superdescendants of such operators. In doing this, we will present the dictionary in the single-particle basis, applying to the AdS_3 case some recent developments occurred in the context of AdS_5 holography.

In Part 2 we will derive the first family of three-charge supersymmetric solutions containing a shockwave in their core region, and propose a holographic description for these gravitational solutions. We will discuss that this new geometries do not describe a single pure state in gravity, but rather provide a collective description of a family of microstates as the microscopic details of the shockwave are not resolved in supergravity.

In Part 3 we will discuss why obtaining analytic multi-center solutions with a high number of centers (> 4) in generic configurations is a hard task. This is mainly because physical consistency - smoothness, charge quantization and absence of closed time-like curves (CTCs) - impose several constraints on the equations that have to be solved. We present an optimization algorithm, based on evolutionary algorithm and Bayesian optimization, to construct numerical multi-center solutions with a high number of centers in generic configurations that satisfy all the flux quantization conditions and are free of CTCs.

Part I

Precision holographic dictionary

Chapter 2

AdS_3 holography at dimension 2

This chapter reports the work presented in [1]. The aims of this project are to construct a fully explicit holographic dictionary for chiral primary operators (CPOs) of dimension $(1,1)$ and use it to perform new precision holography tests on the class of three-charge microstate solutions constructed in [56, 58, 62].

Holographic studies involving expectation values of operators of total dimension higher than one present some interesting complications. As pointed out in [107], the map between CFT operators and supergravity fields cannot be uniquely fixed by the quantum numbers, because of degeneracies present in the CFT: first of all, single-trace operators O_i with the same quantum number can mix, which means that the dictionary proposed in [54] needs to be rotated by a mixing matrix $\mathcal{M}$, whose explicit form has been identified in [107]. Moreover, for some time it has been understood that the identification of supergravity fields and single-trace operators (or a linear combination of single-trace operators) fails to give a consistent result for all observables [107–109], even at leading order in large N. An example of this are extremal correlators, i.e. correlators in which the conformal dimension of the heaviest operator equals the sum of the conformal dimensions of the other two. To fix these inconsistencies, one needs to take into account the mixing between single-trace and multi-trace operators with the same quantum numbers. Aside from extremal correlators, the correct dictionary must be used also in certain (non-extremal) heavy-light-heavy correlators, which are the observables we will focus on in this work. Even though multi-trace operators naturally involve powers of $1/N$, their Wick contraction with heavy operators can produce other factors of N: as a result, multi-trace operators can contribute to the value of the correlator at leading order in large N.

The holographic dictionary involves an identification between expectation value of operators in the CFT state and expansion of the dual gravitational solution around $AdS_3 \times S^3$: the geometric quantities relevant for CPOs at dimension $(1,1)$ have been computed in [54, 55]. We will compute the the precise linear combination of single and multi-trace

operators relevant for the holographic dictionary in this sector of the theory, by applying the following strategy. After imposing a consistent normalization of both the CFT operators and the asymptotic expansion of the gravity solution, we consider the most general linear combination of single and multi-trace operators allowed by the quantum numbers. Next, we fix the numerical coefficients that define the operators mixing by matching the CFT predictions with some reference D1-D5 geometries, whose dual CFT states are already well-established. This procedure determines the single-trace operators mixing matrix $\mathcal{M}$, in agreement with the result in [107], and the admixture of multi-trace operators.

Consistency of the holographic dictionary imposes some stringent requirements on its explicit form. First, the numerical coefficients defining the operators admixture have to be independent of the state. Second, they have to respect invariance under the R-symmetry group, which implies that the coefficients defining the holographic map should be the same for all the operators in the same R-charge multiplet. Beside analysing these general features, consistency of the dictionary has been checked by performing several tests both on two-charge and three-charge microstates.

This Chapter is organized as follows. We review the correspondence between 1/4-BPS coherent states of the orbifold CFT and the family of D1-D5 supergravity solutions in Section 2.1. The holographic map for chiral primary operators (CPOs) of dimension 1 is summarized in Section 2.2; this is mostly a recollection of previous results [54, 55, 103, 106], however we clarify some minus signs that are needed to make the dictionary for the $SU(2)_L \times SU(2)_R$ R-currents consistent. In Section 2.3 we describe all the CPOs of dimension $(1,1)$, including single and double-trace operators, and we first work out the holographic dictionary for the simpler subsector of operators, which does not involve mixing between different single-traces. The more complicated subsector is analyzed in Section 2.4, in which we fix in turn each of the coefficients defining the holographic dictionary, and then make some non-trivial tests on 1/4 BPS states. In Section 2.5 we apply our results to perform new precision holographic tests of D1-D5-P superstrata.

2.1 Holography for D1-D5 black hole microstates

In this section we give a brief review of holography for D1-D5 black hole microstates, with the main purpose of setting up notation that is needed in the rest of the chapter.

The dual gravitational description of the Ramond-Ramond (RR) ground states of the D1-D5 CFT is well known [46, 47, 55, 101, 106, 110]. There is a family of supergravity solutions that can be associated with coherent RR ground states of the D1-D5 CFT, in the sense that protected correlators involving such states agree, as discussed in the Introduction.

The states of the D1-D5 CFT have a simple description at the free orbifold locus in moduli space, where the CFT is the $(4,4)$ sigma-model with target space $\mathcal{M}^N/S_N$, with $\mathcal{M}$ either T^4 or K3 (recall $N = n_1 n_5$). A review of the orbifold CFT can be found for example in [111]. We will use the notation and the conventions of [60, 103]. A generic state of the orbifold CFT is described by a collection of "strands" involving spin-twist operators; the ground state of each strand is characterized by a spin s and a winding number k and is denoted by $|s\rangle_k$. We will consider bosonic ground states, and excitations thereof, that are insensitive to the structure of the internal manifold $\mathcal{M}$, so that our results apply when $\mathcal{M}$ is either T^4 or K3 (the generalization to more general states is straightforward). For this class of ground states, there are five possible spin configurations: $s = (0,0), (\pm,\pm), (\pm,\mp)$, where $(j,\bar{j})$ denotes a state with $SU(2)_L$ charge j and $SU(2)_R$ charge $\bar{j}$; $SU(2)_L \times SU(2)_R$ is the R-symmetry of the $(4,4)$ theory, which corresponds on the gravity side to rotations in the four spatial directions. A RR ground state with $N_k^{(s)}$ strands of type $|s\rangle_k$ is denoted by

$$\psi_{\{N_k^{(s)}\}} \equiv \prod_{k,s} (|s\rangle_k)^{N_k^{(s)}} , \tag{2.1}$$

and is an allowed state if the total winding number sums up to N:

$$\sum_{k,s} k N_k^{(s)} = N . \tag{2.2}$$

It will be convenient to work with non-normalized states; for later use we record the norm of the states (2.1), which was derived in [103]:

$$\left|\psi_{\{N_k^{(s)}\}}\right|^2 = \frac{N!}{\prod_{k,s} N_k^{(s)}!\, k^{N_k^{(s)}}} . \tag{2.3}$$

States of the form (2.1) are eigenstates of the $SU(2)_L \times SU(2)_R$ currents $(J^3, \tilde{J}^3)$; we are interested in coherent states that are linear combinations of R-symmetry eigenstates labeled by complex coefficients $A_k^{(s)}$,

$$\psi(\{A_k^{(s)}\}) \equiv \sum_{\{N_k^{(s)}\}}{}' \prod_{k,s} (A_k^{(s)}\, |s\rangle_k)^{N_k^{(s)}} , \tag{2.4}$$

where the sum $\sum_{\{N_k^{(s)}\}}{}'$ is restricted by the constraint (2.2). The states that admit a good supergravity description are those for which this sum is peaked over large values of $N_k^{(s)}$: as shown in [103], in this semiclassical limit the parameters $A_k^{(s)}$ determine the average numbers $\overline{N}_k^{(s)}$ of strands of type $|s\rangle_k$, via

$$k\, \overline{N}_k^{(s)} = |A_k^{(s)}|^2 . \tag{2.5}$$

The constraint (2.2) then implies

$$\sum_{k,s} |A_k^{(s)}|^2 = N\,. \tag{2.6}$$

The supergravity solutions describing coherent bound states of large numbers of D1 and D5 branes are well-known and are given in terms of a profile function $g_i(v')$ (parametrized by a null coordinate v') in $\mathbb{R}^8$ [47, 55, 110]. For configurations invariant on the internal manifold $\mathcal{M}$, the profile function takes values in $\mathbb{R}^5$:

$$\begin{aligned} g_1(v') + ig_2(v') &= \sum_{k>0} \left(\frac{\bar{a}_k^{(++)}}{k} e^{\frac{2\pi i k}{L} v'} + \frac{a_k^{(--)}}{k} e^{-\frac{2\pi i k}{L} v'} \right), \\ g_3(v') + ig_4(v') &= \sum_{k>0} \left(\frac{\bar{a}_k^{(+-)}}{k} e^{\frac{2\pi i k}{L} v'} - \frac{a_k^{(-+)}}{k} e^{-\frac{2\pi i k}{L} v'} \right), \\ g_5(v') &= -\mathrm{Im} \left(\sum_{k>0} \frac{\bar{a}_k^{(00)}}{k} e^{\frac{2\pi i k}{L} v'} \right). \end{aligned} \tag{2.7}$$

The map between the CFT states in (2.4) and the supergravity solutions parameterized by the profile $g_i(v')$ which will be described in more detail below, is given by relating the Fourier modes $a_k^{(s)}$ to the coherent state parameters $A_k^{(s)}$, via[1]

$$A_k^{(\pm\pm)} = R\sqrt{\frac{N}{Q_1 Q_5}} a_k^{(\pm\pm)}\,, \qquad A_k^{(00)} = R\sqrt{\frac{N}{2\,Q_1 Q_5}} a_k^{(00)}\,. \tag{2.8}$$

The curve $g_i(v')$ arises because the D1-D5 system is U-dual to a fundamental string (F1) carrying momentum (P): in the F1-P duality frame, the curve (2.7) represents the oscillation profile of the string in the five transverse directions that are U-dual to D1-D5 states invariant on $\mathcal{M}$. The D1-D5 supergravity solution associated with a curve $g_i(v')$ is as follows. The 6D Einstein metric of this solution is given by

$$ds_6^2 \;=\; -\frac{2}{\sqrt{\mathcal{P}}}(dv + \boldsymbol{\beta}) \left(du + \omega + \frac{\mathcal{F}}{2}(dv + \boldsymbol{\beta}) \right) + \sqrt{\mathcal{P}} ds_4^2\,, \tag{2.9}$$

with

$$\mathcal{P} \;=\; Z_1 Z_2 - Z_4^2\,. \tag{2.10}$$

The 4D metric ds_4^2 describes the four spatial non-compact directions x_i, and, for all the solutions considered in this article, is the flat $\mathbb{R}^4$ metric

$$ds_4^2 \;=\; dx_i dx_i\,. \tag{2.11}$$

[1] We note that in Eq. (2.7), the minus sign in front of $a_k^{(-+)}$ and the complex conjugations differ from those given in [103]. We will see in due course that these details in Eq. (2.7) are needed for consistency of the holographic map (2.8) and the rest of our conventions.

The u and v coordinates parametrize time t and the S^1 direction y, which we take to have radius R_y:

$$u \equiv \frac{t-y}{\sqrt{2}} \quad , \quad v \equiv \frac{t+y}{\sqrt{2}} \, . \tag{2.12}$$

The D1 and D5 charges of the solution are given by

$$Q_1 \, = \, \frac{(2\pi)^4 \, n_1 \, g_s \, \alpha'^4}{V_4} \, , \qquad Q_5 \, = \, n_5 \, g_s \, \alpha' \, , \tag{2.13}$$

where g_s is the string coupling, and V_4 is the coordinate volume of $\mathcal{M}$. The periodicity L of the curve $g_i(v')$ is $L = 2\pi Q_5/R_y$. The solution is specified by the scalar functions Z_1, Z_2, Z_4 and $\mathcal{F}$ and by the 1-forms with legs along $\mathbb{R}^4$, $\boldsymbol{\beta}$ and ω. The solutions dual to RR ground states have $\mathcal{F} = 0$ and all the other scalars and 1-forms are only functions of x_i, specified by the curve $g_i(v')$ as follows:

$$\begin{aligned}
Z_1 \, &= \, \frac{Q_5}{L} \int_0^L dv' \, \frac{|\dot{g}_i(v')|^2 + |\dot{g}_5(v')|^2}{|x_i - g_i(v')|^2} \, , \qquad & Z_2 \, &= \, \frac{Q_5}{L} \int_0^L dv' \, \frac{1}{|x_i - g_i(v')|^2} \, , \\
Z_4 \, &= \, -\frac{Q_5}{L} \int_0^L dv' \, \frac{\dot{g}_5(v')}{|x_i - g_i(v')|^2} \, , & \mathbf{A} \, &= \, -\frac{Q_5}{L} \int_0^L dv' \, \frac{\dot{g}_j(v') dx_j}{|x_i - g_i(v')|^2} \, , \\
d\mathbf{B} \, &= \, - *_4 \, d\mathbf{A} \, , \qquad \boldsymbol{\beta} = \frac{-\mathbf{A} + \mathbf{B}}{\sqrt{2}} \, , & \omega \, &= \, -\frac{\mathbf{A} + \mathbf{B}}{\sqrt{2}} \, ,
\end{aligned} \tag{2.14}$$

where the dot indicates the derivative with respect to v' and $*_4$ is the Hodge dual with respect to the flat metric ds_4^2. Besides the 6D metric ds_6^2 in (2.9), the solution contains all other NSNS and RR fields of type IIB supergravity: their form is entirely specified by the curve $g_i(v')$ through the above functions, and is recorded for completeness in Eq. (C.1).

In summary, the geometry dual to the RR ground state (2.4) is completely specified by the curve $g_i(v')$ (2.7), through Eqs. (2.9)–(2.14). Given the identification between gravity and CFT parameters in Eq. (2.8), the CFT constraint (2.6) becomes

$$\sum_{k>0} \left(|a_k^{(++)}|^2 + |a_k^{(--)}|^2 + |a_k^{(+-)}|^2 + |a_k^{(-+)}|^2 + \frac{1}{2} |a_k^{(00)}|^2 \right) \, = \, \frac{Q_1 Q_5}{R_y^2} \, , \tag{2.15}$$

which, on the gravity side, is the regularity condition for the solution (2.9)–(2.14).

Let us note that the holographic map does not relate D1-D5 supergravity solutions that have generic classical profile functions with individual basis states of the usual basis of RR ground states of the D1-D5 CFT, as originally suggested in [47], but with coherent superpositions thereof [54] (see also [106]). The reason being that, because of charge conservation, expectation values of charged operators on RR ground states are trivially zero, while, as we will see in various examples in this chapter, holographic one-point function of charged operators on D1-D5 microstates are generically non zero.

The holographic map can also be extended to a subset of the BPS states carrying D1, D5

and momentum (P) charge, which in CFT terms are states with $L_0 > \tilde{L}_0 = \frac{c}{24}$. There is not yet a general understanding of the full class of D1-D5-P states, however there has been much recent progress in constructing large families of explicit solutions known as "superstrata" [56–63, 112–114]. There is an explicit proposal for the dual CFT states of these solutions [56–58, 60, 62]. This family of solutions, and the proposed map to states of the orbifold CFT, will be reviewed in Section 2.5. Their 6D metric can still be written in the form (2.9) with a flat ds_4^2, but now $\mathcal{F} \neq 0$ and the scalars and 1-forms specifying the solution are functions of v as well as x_i. Given the similarities of the supergravity description of this class of D1-D5-P states with the D1-D5 states, one can formulate a unified recipe to extract expectation values of operators of dimension one and two from the geometry. We proceed to do this in the next three sections.

2.2 Expectation values of operators of dimension one

In this section we review the holographic map for expectation values of operators of dimension one, making precise some details that will be important in the following sections.

We start by setting up some notation for the field content of the D1-D5 orbifold CFT. We label the N copies of the CFT on $\mathcal{M}$ by the index $r = 1, \ldots, N$. The orbifold CFT has R-symmetry group $SU(2)_L \times SU(2)_R$, whose spinorial indices we denote by $\alpha, \dot{\alpha} = \pm$, and there is also an $SU(2)_1 \times SU(2)_2$ group of rotations on the tangent space of $\mathcal{M}$ that is useful for labelling operators, whose spinorial indices we denote by $A, \dot{A} = 1, 2$. On each copy of the CFT, the fundamental fields are four bosons $X_{(r)}^{A\dot{A}}$, and four left-moving plus four right-moving fermions $\psi_{(r)}^{\alpha\dot{A}}$, $\tilde{\psi}_{(r)}^{\dot{\alpha}\dot{A}}$.

The theory also contains spin-twist operators, that change the boundary conditions of the fields, and that are labelled by permutations of S_N. For example, the 'bare' twist operator $\sigma_{(rs)}$ joins or splits the copies r and s. When acting on untwisted strands in their respective NS vacuum state, $\sigma_{(rs)}$ creates the state that is the lowest state on a twist-two strand, which is the NS vacuum of the two-fold covering space. A brief review of covering space methods and a more general definition of spin-twist operators is given in Appendix B. We also have left and right-moving spin-fields S^{α}, $\bar{S}^{\dot{\alpha}}$ in each twisted sector, that map NS ground states to R ground states.

Though this description in terms of free fields ceases in general to be useful away from the orbifold point, there are physical quantities that are guaranteed to be independent of the moduli, and hence can be quantitatively described by the free orbifold CFT. We will focus on the expectation values of chiral primary operators (CPOs) and their (global) $SU(2)_L \times SU(2)_R$ descendents in states preserving eight or four supercharges [102]: the first class of states are the RR ground states described in the previous section and the states in the second class include the D1-D5-P states that will be considered in

Section 2.5. Note that in both classes, the states are "heavy", in the sense that their left and right dimensions h and $\bar{h}$ are of order of the CFT central charge $c = 6N$: one has $h = \bar{h} = c/24$ for the D1-D5 states and $h > \bar{h} = c/24$ for the D1-D5-P states. The CPOs we will consider are instead "light", having $h, \bar{h}$ of order c^0. In particular we will restrict to CPOs with $h + \bar{h} \leq 2$. The purpose of the next two sections is to formulate and test a recipe to compute the expectation values of light CPOs in heavy states from the asymptotic expansion of the geometries dual to the heavy states.

Expectation values of CPOs with total dimension $\Delta = h + \bar{h} = 1$ have already been considered in [54, 55, 103]. The only operators with $h = \pm j = 1$, $\bar{h} = \bar{j} = 0$ are the $SU(2)_L$ generators $J^{\pm}$:

$$J^{\pm} = \sum_r J^{\pm}_{(r)} = \pm \sum_r \psi^{\pm 1}_{(r)} \psi^{\pm 2}_{(r)} ; \tag{2.16}$$

analogously one has the $SU(2)_R$ generators $\tilde{J}^{\pm}$, with $h = j = 0$, $\bar{h} = \pm\bar{j} = 1$:

$$\tilde{J}^{\pm} = \sum_r \tilde{J}^{\pm}_{(r)} = \pm \sum_r \tilde{\psi}^{\pm 1}_{(r)} \tilde{\psi}^{\pm 2}_{(r)} . \tag{2.17}$$

We define J^3 to be normalized according to the standard commutation relation $[J^+, J^-] = 2J^3$ and such that the eigenvalue of J^3 on the RR ground state $|{\pm}{+}\rangle$ is $\pm 1/2$; similarly for $\tilde{J}^3$; see Appendix B for more details. We normalize the corresponding vector spherical harmonics in the same way, see Appendix A for details. Note that this convention means that the normalized affine descendant of J^+ is $\frac{1}{\sqrt{2}}[J^-, J^+] = -\sqrt{2}J^3$, which means that some factors of $\sqrt{2}$ will show up in equations such as (2.25).

Next we have the operators with $h = j = \bar{h} = \bar{j} = 1/2$. The first of these is the twist-two operator

$$\Sigma_2^{++} \;=\; \sum_{r<s} \sigma^{++}_{(rs)} , \qquad\qquad \sigma^{++}_{(rs)} \;=\; S^+_{(rs)} \bar{S}^+_{(rs)} \sigma_{(rs)} \tag{2.18}$$

where the operator $\sigma_{(rs)}$ is the 'bare' twist operator that joins or splits the copies r and s, and $S^+_{(rs)}$, $\bar{S}^+_{(rs)}$ are spin fields. When acting on untwisted strands in the NS vacuum state, $\sigma^{++}_{(rs)}$ creates the twisted RR vacuum state $|{+}{+}\rangle_2$.

The second chiral primary with $h = j = \bar{h} = \bar{j} = 1/2$ is the untwisted operator

$$O^{++} \;=\; \sum_r O^{++}_{(r)} \;=\; \sum_r \frac{-i}{\sqrt{2}} \epsilon_{\dot{A}\dot{B}} \, \psi^{+\dot{A}}_{(r)} \tilde{\psi}^{+\dot{B}}_{(r)} . \tag{2.19}$$

More generally, one has operators like in (2.19) for each of the $h^{1,1}(\mathcal{M})$ elements of the $(1,1)$ cohomology of $\mathcal{M}$: we focus on the unique $SU(2)_1 \times SU(2)_2$ operator O^{++} because it is the only one that has non-trivial expectation values on the $\mathcal{M}$-invariant class of states introduced in Section 2.1.

For any CPO one also has the whole multiplet of (global) $SU(2)_L \times SU(2)_R$ descendants, obtained in the usual way by acting on the CPO with J_0^- and/or $\tilde{J}_0^-$. We denote the

generic elements of the multiplet by J^a, $\tilde{J}^a$, with $a = +, 3, -$, and $O^{\alpha,\dot{\alpha}}$, $\Sigma^{\alpha,\dot{\alpha}}$, with $\alpha, \dot{\alpha} = \pm$. For later use we record our convention that $O^{--} = (O^{++})^\dagger$, whereupon consistency with the $SU(2)_L \times SU(2)_R$ algebra implies that $O^{-+} = -(O^{+-})^\dagger$, since $(O^{+-})^\dagger = ([\tilde{J}_0^-, O^{++}])^\dagger = -[\tilde{J}_0^+, O^{--}] = -O^{-+}$. Analogous expressions hold for $\Sigma^{\alpha,\dot{\alpha}}$.

The expectation values of the CPOs and their descendants in a heavy state are encoded in the asymptotic expansion of the dual geometry near their $\mathrm{AdS}_3 \times S^3$ boundary. Roughly speaking, given a radial coordinate r, operators of increasing dimension correspond to terms of higher order in $1/r$. The precise map involves identifying gauge-invariant quantities [54, 115]; having done so, in practice it is convenient to choose a particular gauge in which to work. Though there is, in general, no canonical choice for r, for the class of geometries of the form (2.9) with a *flat* ds_4^2 one can canonically identify r with the radial coordinate of $\mathbb{R}^4$ in standard polar coordinates:

$$ds_4^2 = dr^2 + r^2(d\theta^2 + \sin^2\theta\, d\phi^2 + \cos^2\theta\, d\psi^2)\,. \tag{2.20}$$

Similarly we can use the θ, ϕ, ψ coordinates to define spherical harmonics on S^3. This leaves us with the only ambiguity of choosing the origin of polar coordinates, which will be fixed shortly. One can then define the following asymptotic expansion[2] [54, 55]:

$$\begin{aligned}
Z_1 &= \frac{Q_1}{r^2}\left(1 + \sum_{k=1}^{2}\sum_{m_k,\bar{m}_k=-k/2}^{k/2} f^1_{k\,(m_k,\bar{m}_k)}\,\frac{Y_k^{m_k,\bar{m}_k}}{r^k} + O(r^{-3})\right),\\
Z_2 &= \frac{Q_5}{r^2}\left(1 + \sum_{k=1}^{2}\sum_{m_k,\bar{m}_k=-k/2}^{k/2} f^5_{k\,(m_k,\bar{m}_k)}\,\frac{Y_k^{m_k,\bar{m}_k}}{r^k} + O(r^{-3})\right),\\
Z_4 &= \frac{\sqrt{Q_1Q_5}}{r^2}\left(\sum_{k=1}^{2}\sum_{m_k,\bar{m}_k=-k/2}^{k/2} \mathcal{A}_{k\,(m_k,\bar{m}_k)}\,\frac{Y_k^{m_k,\bar{m}_k}}{r^k} + O(r^{-3})\right),\\
\mathbf{A} &= \frac{\sqrt{Q_1Q_5}}{r^2}\sum_{a=1}^{3}(a_{a+}Y_1^{a+} + a_{a-}Y_1^{a-}) + O(r^{-3})\,, \qquad \mathcal{F} = -\frac{2Q_p}{r^2} + O(r^{-3})\,,
\end{aligned} \tag{2.21}$$

where $Y_k^{m_k,\bar{m}_k}$ are S^3 scalar harmonics of degree k and $Y_1^{a\pm}$ are vector harmonics of degree one; we list our definitions and conventions regarding the spherical harmonics in Appendix A.

The D1, D5 charges Q_1, Q_5 have been defined in (2.13); Q_p represents the momentum charge and is quantized in terms of the integer n_p as

$$Q_p = \frac{(2\pi)^4\, n_p\, g_s^2\, \alpha'^4}{R_y^2\, V_4}\,. \tag{2.22}$$

[2]This equations has been changed compared to the one in [1]. The expression reported in [1] is valid when the Z_is are harmonic functions, which is true only for a 1/4-BPS microstates. When the P charge is not vanishing, the second equation in (C.8) shows that the Z_is satisfy a Laplace equation with a source term.

By an appropriate choice of the $\mathbb{R}^4$ origin, one can choose

$$f^1_{1(\alpha,\dot\alpha)} + f^5_{1(\alpha,\dot\alpha)} = 0 \quad \text{for} \quad \alpha,\dot\alpha = \pm\,, \tag{2.23}$$

which completely fixes the coordinate system (for notational convenience we use the indices $(\alpha,\dot\alpha) = (\pm,\pm)$ instead of $(m_1,\bar m_1) = (\pm 1/2, \pm 1/2)$ for $k = 1$). At the first non-trivial order, one thus has the independent coefficients $f^1_{1(\alpha,\dot\alpha)}$, $\mathcal{A}_{1(\alpha,\dot\alpha)}$ and $a_{a\pm}$, and these encode the expectation values of the dimension one operators $\Sigma_2^{\alpha\dot\alpha}$, $O^{\alpha\dot\alpha}$, J^a, and $\tilde J^a$.

In the CFT we will mostly use null coordinates on the cylinder, which we also denote by (u,v), and which are related to the CFT time and spatial coordinates analogously to the corresponding spacetime coordinate relations (2.12). All the CFT one-point functions in this work will consist of a light operator O_i inserted at a generic point (u,v) in the background of a heavy state:

$$\langle O_i\rangle \;\equiv\; \langle H|O_i(u,v)|H\rangle\,. \tag{2.24}$$

The dependence on the insertion point (u,v) is determined by conformal invariance, and in fact the expectation values of the operators we consider in RR ground states are independent of (u,v) and are controlled solely by the zero mode of the light operator O_i. For the superstratum states that we shall study in Section 2.5, some of the one-point functions will however have non-trivial v dependence.

When the expectation value is taken in the heavy state dual to the geometry corresponding to (2.21), the precise map[3] is [54, 55, 103]

$$\begin{gathered}
\frac{\sqrt{2}}{N}\langle\Sigma_2^{\alpha\dot\alpha}\rangle = (-1)^{\alpha\dot\alpha}\,2\sqrt{\frac{N}{Q_1Q_5}}R_y\,f^1_{1(-\alpha,-\dot\alpha)}\\
\frac{1}{\sqrt{N}}\langle O^{\alpha\dot\alpha}\rangle = (-1)^{\alpha\dot\alpha}\,2\sqrt{\frac{N}{Q_1Q_5}}R_y\,\mathcal{A}_{1(-\alpha,-\dot\alpha)}\,,\\
\frac{1}{\sqrt{N}}\langle J^\pm\rangle = \sqrt{2}\sqrt{\frac{N}{Q_1Q_5}}R_y\,a_{\mp,+}, \qquad \frac{1}{\sqrt{N}}\langle \tilde J^\pm\rangle = \sqrt{2}\sqrt{\frac{N}{Q_1Q_5}}R_y\,a_{\mp,-}\,,\\
\frac{1}{\sqrt{N}}\langle J^3\rangle = \sqrt{\frac{N}{Q_1Q_5}}R_y\,a_{0,+}, \qquad \frac{1}{\sqrt{N}}\langle \tilde J^3\rangle = \sqrt{\frac{N}{Q_1Q_5}}R_y\,a_{0,-}\,,
\end{gathered} \tag{2.25}$$

where the numerical factors have been chosen in such a way that the operators on the left-hand side have unit norm in the large N limit. As anticipated below Eq. (2.17), our (standard) choice of normalization of J^a, $\tilde J^a$ introduces different coefficients for $J^\pm$ and J^3 in this dictionary. Taking into account that the correctly normalized descendant of

[3]The term $(-1)^{\alpha\dot\alpha}$ gives a minus sign when $(\alpha,\dot\alpha) = (\pm,\mp)$. This is required by $SU(2)_L \times SU(2)_R$ invariance: the scalar product between two operators $\mathcal{O}_1$ and $\mathcal{O}_2$ with indices in the fundamental of $SU(2)_L \times SU(2)_R$ is given by $\mathcal{O}_1\cdot\mathcal{O}_2 = \epsilon_{\alpha\beta}\epsilon_{\dot\alpha\dot\beta}\mathcal{O}_1^{\alpha\dot\alpha}\mathcal{O}_2^{\beta\dot\beta}$.

J^+ is $-\sqrt{2}J^3$, and likewise for $\tilde{J}^a$, the above expressions indeed respect the $SU(2)_L$ and $SU(2)_R$ R-symmetries.

2.2.1 An example

Several non-trivial tests of the map (2.25) have already been performed in [103]. We present here one further example, which concentrates on the expectation values of J^a and $\tilde{J}^a$, because it will justify the choice of sign for $a_k^{(-+)}$ in (2.7); this sign will be relevant in testing the map for dimension two operators.

Consider the state

$$\sum_{p,q}(A\,|{+}{+}\rangle_1)^{N-p-q}\,(B\,|{+}{-}\rangle_1)^p\,(C\,|{-}{+}\rangle_1)^q\,. \tag{2.26}$$

From Eq. (2.7), the profile function associated to this state has the following components:

$$g_1(v')+ig_2(v')=\bar{a}\,e^{\frac{2\pi i}{L}v'}\,,\qquad g_3(v')+ig_4(v')=\bar{b}\,e^{\frac{2\pi i}{L}v'}-c\,e^{-\frac{2\pi i}{L}v'}\,,\qquad g_5(v')=0\,. \tag{2.27}$$

This profile encodes the data needed to generate the dual geometry through Eq. (2.14): since we are interested in the expectation values of the left and right currents, it follows from Eq. (2.25) that the coefficients we need are

$$\begin{aligned}
a_{++}&=\frac{R_y}{\sqrt{Q_1Q_5}}\frac{a\bar{c}}{\sqrt{2}}\,, & a_{-+}&=\frac{R_y}{\sqrt{Q_1Q_5}}\frac{\bar{a}c}{\sqrt{2}}\,,\\
a_{--}&=\frac{R_y}{\sqrt{Q_1Q_5}}\frac{\bar{a}b}{\sqrt{2}}\,, & a_{+-}&=\frac{R_y}{\sqrt{Q_1Q_5}}\frac{a\bar{b}}{\sqrt{2}}\,,\\
a_{0+}&=\frac{R_y}{\sqrt{Q_1Q_5}}\frac{|a|^2+|b|^2-|c|^2}{2}\,, & a_{0-}&=\frac{R_y}{\sqrt{Q_1Q_5}}\frac{|a|^2-|b|^2+|c|^2}{2}\,.
\end{aligned} \tag{2.28}$$

The zero-mode of the CFT operator J^3, i.e. J_0^3, has eigenvalue $1/2$ on the strands $|{+}{+}\rangle_1$ and $|{+}{-}\rangle_1$ while it has eigenvalue $-1/2$ on the strands of type $|{-}{+}\rangle_1$. Since each component of the superposition in (2.26) is an eigenstate of J_0^3, its expectation value is controlled by the average number of strands of each type:

$$\langle J^3\rangle=\frac{1}{2}\big(\bar{N}^{++}+\bar{N}^{+-}-\bar{N}^{-+}\big)=\frac{1}{2}\frac{R_y^2\,N}{Q_1Q_5}\Big(|a|^2+|b|^2-|c|^2\Big)\,, \tag{2.29}$$

where we have used Eqs. (2.5) and (2.8). Analogously one can compute the expectation value of the operator $\tilde{J}^3$, which gives

$$\langle \tilde{J}^3\rangle=\frac{1}{2}\big(\bar{N}^{++}-\bar{N}^{+-}+\bar{N}^{-+}\big)=\frac{1}{2}\frac{R_y^2\,N}{Q_1Q_5}\Big(|a|^2-|b|^2+|c|^2\Big)\,. \tag{2.30}$$

Let us now consider the operator J^+. Its zero-mode, J_0^+, maps a strand of type $|{-}{+}\rangle_1$

into $|{+}{+}\rangle_1$; the strand $|{+}{-}\rangle_1$ is annihilated, so is just a spectator. Thus the expectation value is determined by the following process (here and in similar expressions, to lighten the notation we suppress the subscript 0 and it should be understood that we are considering the zero mode of the operator, since this is the only mode that contributes to the correlator for RR ground states):

$$J^+\left(|{+}{+}\rangle_1^{N-p-q}\,|{+}{-}\rangle_1^{p}\,|{-}{+}\rangle^{q}\right)=(N{-}p{-}q{+}1)\left(|{+}{+}\rangle_1^{N-p-q+1}\,|{+}{-}\rangle_1^{p}\,|{-}{+}\rangle^{q-1}\right). \quad (2.31)$$

Here the factor $N-p-q+1$ arises from observing that J^+ can transform any of the q strands of type $|{-}{+}\rangle_1$ and imposing that the total number of terms on the left and right-hand sides of the equation match. (We will explain similar steps in more detail in Section 2.3.1). Thus we obtain

$$\langle J^+\rangle=\frac{C}{A}(N-\bar p-\bar q)=\frac{R_y^2\,N}{Q_1Q_5}\bar a c\,. \quad (2.32)$$

As in Eq. (2.5), the bar over p and q denote the average number of strands of each type. Using $J^-=(J^+)^\dagger$, we have

$$\langle J^-\rangle=\langle J^+\rangle^*=\frac{R_y^2\,N}{Q_1Q_5}a\bar c\,. \quad (2.33)$$

Analogously we obtain

$$\langle \tilde J^+\rangle=\frac{B}{A}(N-\bar p-\bar q)=\frac{R_y^2\,N}{Q_1Q_5}\bar a b\,,\quad \langle \tilde J^-\rangle=\langle \tilde J^+\rangle^*=\frac{R_y^2\,N}{Q_1Q_5}a\bar b\,. \quad (2.34)$$

Comparing the gravity coefficients in Eq. (2.28) and the CFT results in Eqs. (2.29)–(2.34), one can verify the consistency of (2.7), (2.8) and (2.25).

2.3 D1-D5 holography at dimension two

Deriving the holographic map for operators of total dimension two involves two new levels of complication. First, as pointed out in [54], not all operators are distinguished by their quantum numbers, and the map between the operator expectation values and the coefficients obtained from the asymptotic expansion of the geometry (2.21) may involve a non-trivial mixing matrix. The mixing matrix was subsequently derived in [107], and our explicit tests confirm this result. Second, single-trace dimension-two operators can also mix with "double-trace" operators given by sums of products of dimension-one operators evaluated on different CFT copies. This possibility was also discussed in [107], however the precise structure of the mixing was not worked out in full detail.

In this section we derive the full explicit holographic dictionary for all single and double-trace operators of dimension $(h,\bar h)=(1,1)$. We choose to study operators of dimension

(1,1) as it is for these operators that the mixing is most non-trivial, and because these operators enable us to perform new precision holographic tests of superstrata.

Single-trace operators in a symmetric product orbifold CFT are operators that involve a single sum over copies of the CFT (the 'trace' is over the discrete gauge group S_N). We begin by describing the single-trace CPOs of dimension (1,1), which are as follows:

- An operator of twist three,

$$\Sigma_3^{++} = \sum_{r<s<t} (\sigma^{++}_{(rst)} + \sigma^{++}_{(rts)}) , \qquad \sigma^{++}_{(rst)} \equiv \tilde{J}^+_{-\frac{1}{3}} J^+_{-\frac{1}{3}} \sigma_{(rst)} \tag{2.35}$$

  where it should be understood that the fractional moded operators in the definition of the chiral primary $\sigma^{++}_{(rst)}$ are those associated with the permutation (rst); more details can be found in Appendix B.

- An operator of twist two,

$$O_2^{++} \equiv \sum_{r<s} O^{++}_{(rs)} , \qquad O^{++}_{(rs)} \equiv \left(O^{++}_{(r)} + O^{++}_{(s)}\right) \sigma^{++}_{(rs)} . \tag{2.36}$$

  Here $O^{++}_{(rs)}$ is the operator (of unit norm) that joins or splits the copies r and s and raises the spin by $(1/2, 1/2)$; for example, when acting on copies 1 and 2:

$$O^{++}_{(12)} \, |--\rangle^2_1 = |00\rangle_2 \ , \qquad O^{++}_{(12)} \, |00\rangle_2 = |++\rangle^2_1 \ . \tag{2.37}$$

  As we discussed for the operator O^{++} below (2.19), there are $h^{1,1}(\mathcal{M})$ similar operators, and we focus on the one that has non-zero expectation values in the states we consider.

- An operator in the untwisted sector,

$$\Omega^{++} = \sum_r \psi^{+1}_{(r)} \psi^{+2}_{(r)} \tilde{\psi}^{+1}_{(r)} \tilde{\psi}^{+2}_{(r)} = \sum_r J^+_{(r)} \tilde{J}^+_{(r)} . \tag{2.38}$$

As usual one can also consider the global $SU(2)_L \times SU(2)_R$ descendants of these CPOs: the multiplet of Σ_3^{++} will be denoted by $\Sigma_3^{a\dot{a}}$ with $a, \dot{a} = +, 0, -$, and analogously for the other operators. We define the descendants to have the same norm as the highest weight state, thus for example $\Omega^{0+} = \frac{1}{\sqrt{2}} [J_0^-, \Omega^{++}] = -\sqrt{2} \sum_r J^3_{(r)} \tilde{J}^+_{(r)}$ and $\Omega^{00} = 2 \sum_r J^3_{(r)} \tilde{J}^3_{(r)}$.

As mentioned above, double-trace operators also play an important role: they are defined by taking products of single-trace operators acting on disconnected subsets of the N

copies. The double-trace operators with dimension $(1,1)$ are

$$\begin{aligned}
(\Sigma_2\cdot\Sigma_2)^{++} &\equiv \frac{2}{N^2}\sum_{(r<s)\neq(p<q)}\sigma^{++}_{(rs)}\sigma^{++}_{(pq)}\,, & (J\cdot\tilde J)^{++} &\equiv \frac{1}{N}\sum_{r\neq s}J^{+}_{(r)}\tilde J^{+}_{(s)}\,,\\
(\Sigma_2\cdot O)^{++} &\equiv \frac{\sqrt{2}}{N^{3/2}}\sum_{\substack{r<s\\ t\neq r,s}}\sigma^{++}_{(rs)}O^{++}_{(t)}\,, & (O\cdot O)^{++} &\equiv \frac{1}{N}\sum_{r\neq s}O^{++}_{(r)}O^{++}_{(s)}
\end{aligned} \tag{2.39}$$

and descendants thereof; we have chosen the N-dependent factors to normalize the operators. The constraints in the sum defining the double-trace $(\Sigma_2\cdot\Sigma_2)$ mean that we are summing over all couples of pairs that have no indices in common and where, in each pair, the first entry is smaller than the second one.

On the gravity side, the asymptotic expansion of the bulk quantities in (2.21) gives, at the next order in $1/r$, the set of coefficients $f^1_{2\,I}$, $f^5_{2\,I}$ and $\mathcal{A}_{2\,I}$, where for brevity $I\equiv(a,\dot a)$ with $a,\dot a=+,0,-$. These coefficients are related to the expectation values of the three single-trace CPOs in (2.35), (2.36), (2.38) [54, 55], eventually mixed with the double-traces in (2.39). Since the operator O_2 is in fact part of a set of $h^{1,1}(\mathcal{M})$ operators, it is natural to assume that it does not mix with the other two, and that the associated gravity coefficient is $\mathcal{A}_{2\,I}$; the quantum numbers related with $\mathcal{M}$-rotations suggest that O_2 may mix with the double-trace $(\Sigma_2\cdot O)$. We will examine this simple subset in the next subsection. A more intricate and interesting structure involves Σ_3, Ω and the remaining double-traces $(\Sigma_2\cdot\Sigma_2)$, $(J\cdot\tilde J)$, $(O\cdot O)$ in (2.39). This will be the focus of Section 2.4.

2.3.1 The operator O_2

On the gravity side, the only relevant coefficient in this sector is $\mathcal{A}_{2\,(a,\dot a)}$ [55]; on the CFT side, this should be mapped to the expectation value of $O_2^{a\dot a}$, with a possible mixing with the double-trace $(\Sigma_2\cdot O)$:

$$\frac{\sqrt{2}}{N}\langle O_2^{a\dot a}\rangle + c_1\langle(\Sigma_2\cdot O)^{a\dot a}\rangle = (-1)^{a+\dot a}\,\gamma\,\mathcal{A}_{2\,(-a,-\dot a)}\,, \tag{2.40}$$

where the sign $(-1)^{a+\dot a}$ is needed for $SU(2)_L\times SU(2)_R$ invariance, as one can understand following the same logic explained in Footnote 3. We will determine the coefficients γ and c_1 by calibrating the map (2.40) using some appropriately chosen RR ground states. Tests of this map will be performed in Section 2.5, by comparing with some three-charge superstratum states.

A set of states in which O_2^{--} and O_2^{++} have a non-vanishing expectation value is

$$\sum_{p=1}^{N/2}(A_1\,|{+}{+}\rangle_1)^{N-2p}(B_1\,|00\rangle_2)^p\,. \tag{2.41}$$

This expectation value can be computed following the general logic explained in [103], which we now briefly review. Acting on two chosen strands of type $|{+}{+}\rangle_1$, (the zero mode of) O_2^{--} joins them into the strand $|00\rangle_2$:

$$O_2^{--}\ |{+}{+}\rangle_1^2\ =\ |00\rangle_2\ . \tag{2.42}$$

When acting on the full state $(|{+}{+}\rangle_1)^{N-2p}(|00\rangle_2)^p$, there are $\binom{N-2p}{2}$ ways to choose two out of $N-2p$ strands $|{+}{+}\rangle_1$; one should also take into account that the states $\psi_{\{N_k^{(s)}\}}$ defined in (2.1) are composed of $\left|\psi_{\{N_k^{(s)}\}}\right|^2$ terms, with $\left|\psi_{\{N_k^{(s)}\}}\right|^2$ given in (2.3). This leads to

$$O_2^{--}\left(|{+}{+}\rangle_1^{N-2p}\,|00\rangle_2^p\right)\ =\ (p+1)\ |{+}{+}\rangle_1^{N-2p-2}\,|00\rangle_2^{p+1}\ , \tag{2.43}$$

where the factor $p+1$ is the one needed to match the number of terms on the two sides of the equation, since

$$\binom{N-2p}{2}\ \left|(|{+}{+}\rangle_1)^{N-2p}(|00\rangle_2)^p\right|^2\ =\ (p+1)\ \left|(|{+}{+}\rangle_1)^{N-2p-2}(|00\rangle_2)^{p+1}\right|^2\ . \tag{2.44}$$

The expectation value of O_2^{--} in the state (2.41) then follows from (2.43) and the definition of the state (2.41):

$$\langle O_2^{--}\rangle\ =\ \frac{A_1^2}{B_1}\,(\overline{p}+1)\ \approx\ \frac{A_1^2}{B_1}\,\overline{p}\ =\ \frac{A_1^2\,\bar{B}_1}{2}\,, \tag{2.45}$$

where we have taken the large N (and large p) limit and used (2.5). On the gravity side the state (2.41) is dual to the D1-D5 geometry associated with the profile

$$g_1(v')+ig_2(v')\ =\ \bar{a}_1\,e^{\frac{2\pi i}{L}v'}\,,\qquad g_3(v')\ =\ g_4(v')\ =\ 0\ ,\qquad g_5(v')\ =\ -\mathrm{Im}\left(\frac{\bar{b}_1}{2}\,e^{\frac{4\pi i}{L}v'}\right), \tag{2.46}$$

with the a_1, b_1 parameters linked to A_1, B_1 by (2.8). Using the definition of Z_4 in (2.14) it is immediate to extract from the expansion (2.21) the coefficients $\mathcal{A}_{2\,(a,\dot{a})}$:

$$\mathcal{A}_{2\,(+,+)}\ =\ \left(\mathcal{A}_{2\,(-,-)}\right)^*\ =\ \frac{R_y}{2\sqrt{3}\,(Q_1Q_5)^{1/2}}\,a_1^2\,\bar{b}_1\ =\ \frac{Q_1Q_5}{N^{3/2}R_y^2}\,\frac{A_1^2\,\bar{B}_1}{\sqrt{6}}\,. \tag{2.47}$$

Note that $\mathcal{A}_{1\,(\alpha,\dot{\alpha})}=0$, consistently with the fact that the expectation value of $O^{\alpha,\dot{\alpha}}$ in the state (2.41) vanishes. Comparing the CFT (2.45) and gravity (2.47) results with the general map (2.40), one determines the parameter γ:

$$\gamma\ =\ \sqrt{3}\,\frac{N^{1/2}\,R_y^2}{Q_1Q_5}\,. \tag{2.48}$$

To fix the coefficient c_1 we must consider a state with a non-vanishing expectation value

for the double-trace $(\Sigma_2 \cdot O)^{++}$. An example is

$$\sum_{q=1}^{N/2} \sum_{p=1}^{N-2q} (A_2 \, |{+}{+}\rangle_1)^{N-p-2q} (B_2 \, |00\rangle_1)^p (C_2 \, |{+}{+}\rangle_2)^q \, . \tag{2.49}$$

The geometry associated with this state is sourced by the following profile:

$$g_1(v') + i g_2(v') = \bar{a}_2 \, e^{\frac{2\pi i}{L} v'} + \frac{\bar{c}_2}{2} \, e^{\frac{4\pi i}{L} v'} \, , \quad g_3(v') = g_4(v') = 0 \, , \quad g_5(v') = -\mathrm{Im} \left(\bar{b}_2 \, e^{\frac{2\pi i}{L} v'} \right) . \tag{2.50}$$

Choosing coordinates in which (2.23) is satisfied and using (2.14), we obtain that the coefficient encoding the expectation value of $(\Sigma_2 \cdot O)$ takes the following value for this microstate:

$$\mathcal{A}_{2\,(1,1)} \;=\; \frac{R_y^3}{(Q_1 Q_5)^{3/2}} \, \frac{\bar{a}_2 (b_2^3 \, \bar{c}_2 + 8 \bar{a}_2^2 \, b_2 \, c_2)}{16 \sqrt{3}} \, . \tag{2.51}$$

We now consider the action of $(\Sigma_2 \cdot O)^{++} = \sqrt{2} N^{-3/2} \Sigma_2^{++} O^{++}$ on the state (2.49). The operator O^{++} contributes via the basic process $O^{++} \, |00\rangle_1 = |{+}{+}\rangle_1$, so that we have:

$$\begin{aligned} &(\Sigma_2 \cdot O)^{++} \big(\, |{+}{+}\rangle_1^{N-p-2q} \, |00\rangle_1^p \, |{+}{+}\rangle_2^q \, \big) \\ &\qquad = \frac{\sqrt{2}}{N^{3/2}} \Sigma_2^{++} (N - p - 2q + 1) \big(\, |{+}{+}\rangle_1^{N-p-2q+1} \, |00\rangle_1^{p-1} \, |{+}{+}\rangle_2^q \, \big) \, , \end{aligned} \tag{2.52}$$

where the factor $(N - p - 2q + 1)$ arises from imposing that the number of terms on the two sides of the equation match, after taking into account that the operator O^{++} can act on any of the p strands of type $|00\rangle_1$. The action of the operator Σ_2^{++} is slightly more complicated: its expectation value receives a contribution both by the splitting a strand of type $|{+}{+}\rangle_2$ into two $|{+}{+}\rangle_1$ and from the joining of two $|{+}{+}\rangle_1$ to form a $|{+}{+}\rangle_2$. We thus have to consider the following basic processes (as before, the zero mode should be understood):

$$\Sigma_2^{++} \, |{+}{+}\rangle_2 = |{+}{+}\rangle_1 \, |{+}{+}\rangle_1 \, , \qquad \Sigma_2^{++} \, |00\rangle_1 \, |00\rangle_1 = \frac{1}{4} \, |{+}{+}\rangle_2 \, , \tag{2.53}$$

where the coefficient of the latter process is computed in Appendix B, see Eq. (B.32). Continuing from Eq. (2.52), we obtain

$$\begin{aligned} (\Sigma_2 \cdot O)^{++} (\, |{+}{+}\rangle_1^{N-p-2q} \, |00\rangle_1^p \, |{+}{+}\rangle_2^q) \;=\; & \frac{\sqrt{2}}{N^{3/2}} (N - p - 2q + 1) \\ & \Big[\frac{1}{2} (N - p - 2q + 2)(N - p - 2q + 3) (|{+}{+}\rangle_1^{N-p-2q+3} \, |00\rangle_1^{p-1} \, |{+}{+}\rangle_2^{q-1}) \\ & \quad + \frac{q+1}{4} (|{+}{+}\rangle_1^{N-p-2q+1} \, |00\rangle_1^{p-3} \, |{+}{+}\rangle_2^{q+1}) \Big] \, , \end{aligned} \tag{2.54}$$

where the combinatorial factors again arise from matching the norms of the states on

both sides of the equation. In the large N limit, this gives rise to the one-point function:

$$\langle (\Sigma_2 \cdot O)^{++} \rangle \;=\; \frac{\sqrt{2}}{N^{3/2}} \Big(\frac{\bar{A}_2^3\, B_2\, C_2}{2} + \frac{\bar{A}_2\, B_2^3\, \bar{C}_2}{8} \Big) \;=\; \frac{R_y^5 N}{(Q_1 Q_5)^{5/2}} \Big(\frac{\bar{a}_2^3\, b_2\, c_2}{2} + \frac{\bar{a}_2\, b_2^3\, \bar{c}_2}{16} \Big) , \tag{2.55}$$

where we have used Eqs. (2.6) and (2.8). By comparing the results in Eqs. (2.51) and (2.55) and the map (2.40), we determine the unknown coefficient to be

$$c_1 \;=\; -\frac{1}{N^{1/2}} \, . \tag{2.56}$$

The holographic map in this subsector can then be summarized as

$$\frac{\sqrt{2}}{N} \langle \widetilde{O}_2^{a\dot{a}} \rangle \;=\; (-1)^{a+\dot{a}} \sqrt{3}\, \frac{N^{1/2}\, R_y^2}{Q_1 Q_5}\, \mathcal{A}_{2\,(-a,-\dot{a})} \, , \tag{2.57}$$

where

$$\widetilde{O}_2^{++} \;\equiv\; \sum_{r<s} O_{(rs)}^{++} - \frac{1}{N} \sum_{\substack{r<s \\ t \neq r,s}} \sigma_{(rs)}^{++} O_{(t)}^{++} \, . \tag{2.58}$$

Note that the extremal three-point functions containing the operator $\widetilde{O}_2^{++}$ vanish [54, 107–109, 116]. The only extremal correlator that is not trivially zero because of the quantum numbers is

$$\langle \widetilde{O}_2^{++}\, O^{--}\, \Sigma_2^{--} \rangle = \frac{N^2}{2} \langle O_{(12)}^{++}\, (O_{(1)}^{--} + O_{(2)}^{--})\, \sigma_{(12)}^{--} \rangle - \frac{N^2}{2} \, , \tag{2.59}$$

where the first term on the right-hand side comes from the single-trace part of $\widetilde{O}_2^{++}$ and the second term is produced by the double-trace part. The definition of $O_{(12)}^{++}$, Eq. (2.37), implies that

$$\langle O_{(12)}^{++}\, (O_{(1)}^{--} + O_{(2)}^{--})\, \sigma_{(12)}^{--} \rangle = 1 \, , \tag{2.60}$$

and thus the extremal correlator (2.59) vanishes.

2.4 The operators Σ_3 and Ω

In this section we turn to the sector of dimension (1,1) operators that contains Σ_3 and Ω, in which the mixing is more involved. We begin this section by importing the results of [54, 55] that for a metric of the form (2.9), with the choice of coordinates defined by (2.20) and (2.23), the geometric quantities dual to the operator expectation values in this sector are linear combinations of the following gauge-invariant quantities (evaluated in this gauge) [54, Eq. (6.4)],[55, Eq. (5.27)]:

$$g_I \;\equiv\; \sqrt{6}\, (f_{2\,I}^1 - f_{2\,I}^5) \, , \qquad \tilde{g}_I \;\equiv\; \sqrt{2}\, (-(f_{2\,I}^1 + f_{2\,I}^5) + 8\, a_{a+} a_{b-}\, f_{Iab}) \, , \tag{2.61}$$

where the coefficients f_{Iab} are defined by the overlap between a scalar S^3 spherical harmonic of degree two and the scalar product of two vector spherical harmonics of degree one, and are given in Appendix A.

A first guess for the holographic dictionary might have been that g_I should be dual to the expectation value of Σ_3^{-I} and $\tilde{g}_I$ should be dual to the expectation value Ω^{-I}, however in [54] it was pointed out that this guess was inconsistent with the structure of known CFT correlators, and a modified map was proposed in [107]. In what follows we shall not assume any previous results on the holographic dictionary beyond (2.61), and we shall simply start with the most general map, allowing for generic mixings with the double-traces that can mix with Σ_3 and Ω:

$$\begin{aligned}
&\frac{\sqrt{3}}{N^{3/2}}\langle\Sigma_3^{a\dot{a}}\rangle + a_1\langle(J\cdot\tilde{J})^{a\dot{a}}\rangle + a_2\langle(\Sigma_2\cdot\Sigma_2)^{a\dot{a}}\rangle + a_3\langle(O\cdot O)^{a\dot{a}}\rangle \\
&\qquad\qquad = (-1)^{a+\dot{a}}\Big[\alpha\, g_{(-a,-\dot{a})} + \tilde{\alpha}\,\tilde{g}_{(-a,-\dot{a})}\Big], \\
&\frac{1}{N^{1/2}}\langle\Omega^{a\dot{a}}\rangle + b_1\langle(J\cdot\tilde{J})^{a\dot{a}}\rangle + b_2\langle(\Sigma_2\cdot\Sigma_2)^{a\dot{a}}\rangle + b_3\langle(O\cdot O)^{a\dot{a}}\rangle \\
&\qquad\qquad = (-1)^{a+\dot{a}}\Big[\beta\, g_{(-a,-\dot{a})} + \tilde{\beta}\,\tilde{g}_{(-a,-\dot{a})}\Big].
\end{aligned} \tag{2.62}$$

As usual the numerical factors in front of Σ_3 and Ω have the purpose of normalizing the operators, and the sign $(-1)^{a+\dot{a}}$ is required by $SU(2)_L \times SU(2)_R$ invariance.

In the following, we shall determine in turn the unknown coefficients α, $\tilde{\alpha}$, β, $\tilde{\beta}$, a_i and b_i by applying the holographic map to an appropriate set of D1-D5 RR ground states. Note that we have implemented $SU(2)_L \times SU(2)_R$ invariance by requiring that coefficients be independent of the R-symmetry indices $(a, \dot{a})$. (The real coefficients α, β should not be confused with the one-form $\boldsymbol{\beta}$ or the spinorial indices of the R-symmetry group $SU(2)_L \times SU(2)_R$ used elsewhere.) We will then perform a set of non-trivial checks of the resulting dictionary by testing it on a wider class of states. Further tests involving D1-D5-P superstrata will be performed in Section 2.5.

2.4.1 Determining the first set of coefficients

To determine the values of the coefficients α, $\tilde{\alpha}$, β, $\tilde{\beta}$, we consider states in which Σ_3 and Ω have non-zero expectation values, and in which the expectation values of the double-traces in (2.62) vanish. Two simple choices are

$$\psi^{(1)}(A_1, B_1) \;=\; \sum_{p=1}^{N/3} \big(A_1\,|{+}{+}\rangle_1\big)^{N-3p}\big(B_1\,|{+}{+}\rangle_3\big)^p\,, \tag{2.63}$$

and

$$\psi^{(2)}(A_2, B_2) \;=\; \sum_{p=1}^{N} \big(A_2\,|{+}{+}\rangle_1\big)^{N-p}\big(B_2\,|{-}{-}\rangle_1\big)^p\,, \tag{2.64}$$

which, according to the map in Section 2.1, correspond respectively to the profiles

$$g_1^{(1)}(v') + ig_2^{(1)}(v') = \bar{a}_1\, e^{\frac{2\pi i}{L}v'} + \frac{\bar{b}_1}{3}\, e^{\frac{6\pi i}{L}v'}\,, \qquad g_3^{(1)}(v') = g_4^{(1)}(v') = g_5^{(1)}(v') = 0\,, \tag{2.65}$$

and

$$g_1^{(2)}(v') + ig_2^{(2)}(v') = \bar{a}_2\, e^{\frac{2\pi i}{L}v'} + b_2\, e^{-\frac{2\pi i}{L}v'}\,, \qquad g_3^{(2)}(v') = g_4^{(2)}(v') = g_5^{(2)}(v') = 0\,. \tag{2.66}$$

The computation of the gravity parameters g_I and $\tilde{g}_I$ follows straightforwardly from Eqs. (2.14), (2.21) and (2.61); for the state $\psi^{(1)}$ one obtains

$$\begin{aligned} g^{(1)}_{(0,0)} &= -6\sqrt{2}\frac{R_y^2}{Q_1Q_5}\,|a_1|^2\,|b_1|^2\,, & \tilde{g}^{(1)}_{(0,0)} &= \frac{14\sqrt{6}}{27}\frac{R_y^2}{Q_1Q_5}\,|a_1|^2\,|b_1|^2\,, \\ g^{(1)}_{(1,1)} &= (g^{(1)}_{(-1,-1)})^* = \sqrt{2}\frac{R_y^2}{Q_1Q_5}\,a_1^3\,\bar{b}_1\,, & \tilde{g}^{(1)}_{(1,1)} &= (\tilde{g}^{(1)}_{(-1,-1)})^* = -\frac{\sqrt{2}}{\sqrt{3}}\frac{R_y^2}{Q_1Q_5}\,a_1^3\,\bar{b}_1\,, \end{aligned} \tag{2.67}$$

and for the state $\psi^{(2)}$ one obtains

$$\begin{aligned} g^{(2)}_{(0,0)} &= 2\sqrt{2}\frac{R_y^2}{Q_1Q_5}\,|a_2|^2\,|b_2|^2\,, & \tilde{g}^{(2)}_{(0,0)} &= 2\sqrt{6}\frac{R_y^2}{Q_1Q_5}\,|a_2|^2\,|b_2|^2\,, \\ g^{(2)}_{(1,1)} &= g^{(2)}_{(-1,-1)})^* = -\sqrt{2}\,a_2\,\bar{b}_2\,, & \tilde{g}^{(2)}_{(1,1)} &= (\tilde{g}^{(2)}_{(-1,-1)})^* = -\sqrt{6}\,a_2\,\bar{b}_2\,. \end{aligned} \tag{2.68}$$

On the CFT side, Σ_3^{--} and Ω^{--} have non-vanishing expectation values respectively in $\psi^{(1)}$ and $\psi^{(2)}$, while the expectation values of all the double-trace operators in (2.62) with spin $(-1,-1)$ are zero, as can be easily seen from the fact that the action of the dimension-one operators Σ_2^{--}, J^-, $\tilde{J}^-$ or O^{--} on either $\psi^{(1)}$ or $\psi^{(2)}$ would produce strands of a type that is not present in the state itself.

The expectation value of Σ_3^{--} in $\psi^{(1)}$ arises from the process in which three strands of winding one are joined into a strand of winding three. In general one has (as before the zero mode should be understood here and in similar equations that follow)

$$\sigma^{--}_{(3)}\,|{+}{+}\rangle_{k_1}\,|{+}{+}\rangle_{k_2}\,|{+}{+}\rangle_{k_3} = c_{k_1,k_2,k_3}\,|{+}{+}\rangle_{k_1+k_2+k_3}\,, \tag{2.69}$$

where (3) denotes a permutation that joins together the three strands $|{+}{+}\rangle_{k_i}$ and where $c_{k_1,k_2,k_3} = \frac{k_1+k_2+k_3}{3k_1k_2k_3}$ [117]. We first focus on three particular strands of winding one and one particular permutation, say (123), of the three strands, for which we thus have

$$\sigma^{--}_{(123)}\big(\,|{+}{+}\rangle_1\,\big)^3 = |{+}{+}\rangle_3\,. \tag{2.70}$$

When considering the action of the full operator Σ_3^{--} on the state $|{+}{+}\rangle_1^{N-3p}\,|{+}{+}\rangle_3^p$, one must also include the appropriate combinatorial factors, as follows. The twist operator can act on any three of the $N-3p$ strands of winding one, and for each choice of the three strands there are two inequivalent three-cycles (c.f. Eq. (2.35)). Thus Σ_3^{--} can act in

$2\binom{N-3p}{3}$ ways on $(|{+}{+}\rangle_1)^{N-3p}(|{+}{+}\rangle_3)^p$ to produce the state $(|{+}{+}\rangle_1)^{N-3p-3}(|{+}{+}\rangle_3)^{p+1}$. Moreover one has to take into account that the initial and final states have a non-trivial norm given by (2.3). Matching the norm of the states on both sides of the following equation, one finds

$$\Sigma_3^{--}\left((|{+}{+}\rangle_1)^{N-3p}(|{+}{+}\rangle_3)^p\right) = (p+1)\,(|{+}{+}\rangle_1)^{N-3p-3}(|{+}{+}\rangle_3)^{p+1}\,. \tag{2.71}$$

The above result and the definition of the state $\psi^{(1)}$ in (2.63) imply that, in the large N limit, the expectation value of Σ_3^{--} in the state $\psi^{(1)}$ is:

$$\langle\Sigma_3^{--}\rangle_1 \;=\; \frac{A_1^3}{B_1}\,\bar{p} \;=\; \frac{A_1^3\,\bar{B}_1}{3} \;=\; \frac{N^2\,R_y^2}{3\,(Q_1Q_5)^2}\,a_1^3\,\bar{b}_1\,, \tag{2.72}$$

where we have used $\bar{p} = |B|^2/3$ (from (2.5)) and the relation (2.8).

Next, the expectation value of Ω^{--} in the state $\psi^{(2)}$ arises from the basic process where Ω^{--} maps $|{+}{+}\rangle_1$ to $|{-}{-}\rangle_1$. There are $N-p$ choices of strand for Ω^{--} to act on the state $(|{+}{+}\rangle_1)^{N-p}(|{-}{-}\rangle_1)^p$ to give $(|{+}{+}\rangle_1)^{N-p-1}(|{-}{-}\rangle_1)^{p+1}$. Matching the norms of left and right-hand sides gives

$$\Omega^{--}\left((|{+}{+}\rangle_1)^{N-p}(|{-}{-}\rangle_1)^p\right) = (p+1)\,(|{+}{+}\rangle_1)^{N-p-1}(|{-}{-}\rangle_1)^{p+1}\,, \tag{2.73}$$

and thus the expectation value of Ω^{--} on $\psi^{(2)}$ is

$$\langle\Omega^{--}\rangle_2 \;=\; \frac{A_2}{B_2}\,\bar{p} \;=\; A_2\,\bar{B}_2 \;=\; \frac{N\,R_y^2}{Q_1Q_5}\,a_2\,\bar{b}_2\,, \tag{2.74}$$

where we have again used (2.5) and (2.8).

Comparing $\langle\Sigma_3^{--}\rangle_1$ and $\langle\Omega^{--}\rangle_2$ with the gravity data $g^{(i)}_{-1,-1}$, $\tilde{g}^{(i)}_{-1,-1}$ $(i=1,2)$ uniquely fixes α, $\tilde{\alpha}$, β, $\tilde{\beta}$ to be

$$\alpha \;=\; -\tilde{\beta} \;=\; \frac{\sqrt{3}}{4\sqrt{2}}\,\frac{N^{1/2}\,R_y^2}{Q_1Q_5}\,, \qquad \tilde{\alpha} \;=\; \beta \;=\; -\frac{1}{4\sqrt{2}}\,\frac{N^{1/2}\,R_y^2}{Q_1Q_5}\,. \tag{2.75}$$

These values agree precisely with the results of [107]. The expectation values of Σ_3^{++} and Ω^{++} are simply the complex conjugates of the ones considered above, and do not add new information. The expectation values of Σ_3^{00} and Ω^{00} are also non-vanishing, and should be compared with $g^{(i)}_{0,0}$. For this value of the spin, however, double-trace operators play a role and so we will return to this comparison in Section 2.4.6, where we will perform some non-trivial consistency checks of the full dictionary.

2.4.2 Determining the coefficients a_1, b_1

The coefficients a_1, b_1 in the general map (2.62) correspond to the double-trace operator $(J\cdot\tilde{J})$. An RR ground state in which $(J\cdot\tilde{J})^{++}$ is the only operator with $j=\bar{j}=1$ to have non-vanishing expectation value is the state given in Eq. (2.26). It is straightforward to compute this one-point function in the orbifold CFT, where $\tilde{J}^+$ can map any of the p strands of type $|+-\rangle_1$ into $|++\rangle_1$, and likewise J^+ can act on any of the q $|-+\rangle_1$ strands. Taking into account the normalization (2.3) of the states, one finds

$$\begin{aligned}&(J\cdot\tilde{J})^{++}\left(|++\rangle_1^{N-p-q}\,|+-\rangle_1^{p}\,|-+\rangle_1^{q}\right)\\&\quad=\frac{(N-p-q+1)(N-p-q+2)}{N}\,|++\rangle_1^{N-p-q+2}\,|+-\rangle_1^{p-1}\,|-+\rangle_1^{q-1}\ ,\end{aligned}\tag{2.76}$$

and, in the large N limit,

$$\langle(J\cdot\tilde{J})^{++}\rangle=\frac{B\,C}{A^2}\,\frac{(N-\bar{p}-\bar{q})^2}{N}=\frac{\bar{A}^2\,B\,C}{N}=\frac{N\,R_y^4}{(Q_1Q_5)^2}\,\bar{a}^2\,b\,c\,.\tag{2.77}$$

Notice that, up to the normalization factor N^{-1}, the expectation value of $(J\cdot\tilde{J})^{++}$ is just the product of the expectation values of J^+ and $\tilde{J}^+$, at large N.

On the gravity side, the relevant coefficients extracted from the metric associated with the profile (2.27) are

$$g_{1,1}=(g_{-1,-1})^*=\sqrt{2}\,\frac{R_y^2}{Q_1Q_5}\,a^2\,\bar{b}\,\bar{c}\,,\qquad \tilde{g}_{1,1}=(\tilde{g}_{-1,-1})^*=\sqrt{6}\,\frac{R_y^2}{Q_1Q_5}\,a^2\,\bar{b}\,\bar{c}\,,\tag{2.78}$$

which, taking into account the values of α, $\tilde{\alpha}$, β, $\tilde{\beta}$ derived in (2.75), implies that

$$\alpha\,g_{-1,-1}+\tilde{\alpha}\,\tilde{g}_{-1,-1}\;=\;0\ ,\qquad \beta\,g_{-1,-1}+\tilde{\beta}\,\tilde{g}_{-1,-1}\;=\;-\frac{N^{1/2}\,R_y^4}{(Q_1Q_5)^2}\,.\tag{2.79}$$

Then comparison with (2.62) yields

$$a_1=0\quad,\quad b_1=-\frac{1}{N^{1/2}}\,.\tag{2.80}$$

Using the above value of b_1, one sees that the combination appearing in the holographic map is

$$\frac{1}{N^{1/2}}\left(\Omega^{++}-\frac{1}{N}\sum_{r\neq s}J^+\tilde{J}^+\right)\equiv\frac{1}{N^{1/2}}\,\widetilde{\Omega}^{++}\,.\tag{2.81}$$

We note that the operator $\widetilde{\Omega}^{++}$ has the property that its extremal three-point function with J^- and $\tilde{J}^-$ vanishes,

$$\langle\widetilde{\Omega}^{++}\,J^-\,\tilde{J}^-\rangle=0\,.\tag{2.82}$$

2.4.3 Determining the coefficients a_2, b_2

The coefficients a_2, b_2 in the map (2.62) correspond to the operator $(\Sigma_2 \cdot \Sigma_2)$. An RR ground state in which $(\Sigma_2 \cdot \Sigma_2)^{--}$ is the only operator with $j = \bar{j} = -1$ to have non-vanishing expectation value is

$$\sum_{p=1}^{N/2} (A\ |{+}{+}\rangle_1)^{N-2p} (B\ |{+}{+}\rangle_2)^p \,. \tag{2.83}$$

The CFT expectation value follows from the relation

$$(\Sigma_2 \cdot \Sigma_2)^{--}\ \Big(|{+}{+}\rangle_1^{N-2p}\ |{+}{+}\rangle_2^p\Big) = \frac{2(p+1)(p+2)}{N^2}\ |{+}{+}\rangle_1^{N-2p-4}\ |{+}{+}\rangle_2^{p+2}\ ; \tag{2.84}$$

the combinatorial factor is derived by noting that the first σ_2^{--} in the double-trace can act in $\binom{N-2p}{2}$ ways on the $N-2p$ strands $|{+}{+}\rangle_1$ and similarly the second σ_2^{--} can act in $\binom{N-2p-2}{2}$ ways on the remaining $N-2p-2$ strands $|{+}{+}\rangle_1$; one then, as usual, equates the numbers of terms composing the states on the two sides of (2.84) and multiplies by the normalization factor $2/N^2$. The expectation value in the coherent state (2.83), for which $2\bar{p} = |B|^2$, is then

$$\langle (\Sigma_2 \cdot \Sigma_2)^{--} \rangle = \frac{A^4}{B^2}, \frac{2\,\bar{p}^2}{N^2} = \frac{A^4\,\bar{B}^2}{2\,N^2} = \frac{N\,R_y^6}{(Q_1Q_5)^3}\,\frac{a^4\,\bar{b}^2}{2}\,. \tag{2.85}$$

We note that, in the large N limit, the expectation value of the double-trace $(\Sigma_2 \cdot \Sigma_2)^{--}$ is given again by the square of the normalized single trace $(\sqrt{2}/\sqrt{N})\,\Sigma_2^{--}$, which was computed in Eq. (4.14) of [103].

The geometry dual to the state (2.83) is generated from the profile

$$g_1(v') + i g_2(v') = \bar{a}\, e^{\frac{2\pi i}{L} v'} + \frac{\bar{b}}{2}\, e^{\frac{4\pi i}{L} v'} - \frac{R_y^2}{2Q_1Q_5}\,\bar{a}^2\, b\,, \qquad g_3(v') = g_4(v') = g_5(v') = 0\,, \tag{2.86}$$

where we have shifted the profile centre in order to implement the gauge condition $f_1^1 + f_1^5 = 0$. From this geometry one derives

$$g_{1,1} = (g_{-1,-1})^* = -\sqrt{2}\frac{R_y^4}{(Q_1Q_5)^2}\,a^4\,\bar{b}^2 \quad , \quad \tilde{g}_{1,1} = (\tilde{g}_{-1,-1})^* = \frac{1}{\sqrt{6}}\frac{R_y^4}{(Q_1Q_5)^2}\,a^4\,\bar{b}^2\,. \tag{2.87}$$

Comparing with (2.62) and using the values (2.75), one deduces

$$a_2 \;=\; -\frac{7}{4\sqrt{3}}\frac{1}{N^{1/2}}\,, \qquad b_2 \;=\; \frac{1}{4}\frac{1}{N^{1/2}}\,. \tag{2.88}$$

2.4.4 Determining the coefficients a_3, b_3

The coefficients a_3, b_3 in the map (2.62) correspond to the double-trace operator $(O\cdot O)$. A set of RR ground states in which $(O\cdot O)^{--}$ is the only operator with $j=\bar{j}=-1$ to have non-vanishing one-point function is

$$\sum_{p=1}^{N}(A\,|{+}{+}\rangle_1)^{N-p}(B\,|00\rangle_1)^p\,, \tag{2.89}$$

which is just a particular case of the state (2.49) with $C_2=0$ and $A_2=A$, $B_2=B$. The expectation value $\langle(O\cdot O)^{--}\rangle$ is, as usual, proportional to the square of the single-trace expectation value $\langle O^{--}\rangle = A\,\bar{B}$, as computed in [118]. We obtain

$$\langle(O\cdot O)^{--}\rangle \;=\; \frac{A^2\bar{B}^2}{N} \;=\; \frac{N\,R_y^4}{(Q_1Q_5)^2}\frac{a^2\,\bar{b}^2}{2}\,. \tag{2.90}$$

The relevant gravity coefficients are

$$g_{1,1}\;=\;(g_{-1,-1})^*\;=\;\frac{\sqrt{2}}{4}\frac{R_y^2}{Q_1Q_5}\,a^2\,\bar{b}^2\,,\qquad \tilde{g}_{1,1}\;=\;(\tilde{g}_{-1,-1})^*\;=\;-\frac{\sqrt{2}}{4\sqrt{3}}\frac{R_y^2}{Q_1Q_5}\,a^2\,\bar{b}^2\,, \tag{2.91}$$

which determines a_3 and b_3 to be

$$a_3\;=\;\frac{1}{2\sqrt{3}}\frac{1}{N^{1/2}}\,,\qquad b_3\;=\;0\,. \tag{2.92}$$

2.4.5 The holographic dictionary at dimension (1,1)

We can now summarize our results and write the explicit holographic map in the Σ_3, Ω sector as:

$$\begin{aligned}\frac{\sqrt{3}}{N^{3/2}}\langle\Sigma_3^{a\dot{a}}\rangle+\frac{1}{4\sqrt{3}}\frac{1}{N^{1/2}}\Big[-7\big\langle(\Sigma_2\cdot\Sigma_2)^{a\dot{a}}\big\rangle+2\,\big\langle(O\cdot O)^{a\dot{a}}\big\rangle\Big]\;&=\;(-1)^{a+\dot{a}}\,h_{(-a,-\dot{a})}\,,\\ \frac{1}{N^{1/2}}\langle\Omega^{a\dot{a}}\rangle-\frac{1}{N^{1/2}}\left[\big\langle(J\cdot\tilde{J})^{a\dot{a}}\big\rangle-\frac{1}{4}\,\big\langle(\Sigma_2\cdot\Sigma_2)^{a\dot{a}}\big\rangle\right]\;&=\;(-1)^{a+\dot{a}}\,\tilde{h}_{(-a,-\dot{a})}\,,\end{aligned} \tag{2.93}$$

where (recall that g, $\tilde{g}$ were defined in (2.61))

$$\begin{aligned}h_{(a,\dot{a})}\;&\equiv\;\frac{N^{1/2}\,R_y^2}{4\sqrt{2}\,Q_1Q_5}\Big[\sqrt{3}\,g_{(a,\dot{a})}-\tilde{g}_{(a,\dot{a})}\Big]\,,\\ \tilde{h}_{(a,\dot{a})}\;&\equiv\;-\frac{N^{1/2}\,R_y^2}{4\sqrt{2}\,Q_1Q_5}\Big[g_{(a,\dot{a})}+\sqrt{3}\,\tilde{g}_{(a,\dot{a})}\Big]\,.\end{aligned} \tag{2.94}$$

We also repeat for the reader's convenience the results from the O_2 sector, (2.57) and (2.58):

$$\frac{\sqrt{2}}{N}\langle\widetilde{O}_2^{a\dot{a}}\rangle\;=\;(-1)^{a+\dot{a}}\,\sqrt{3}\,\frac{N^{1/2}\,R_y^2}{Q_1Q_5}\,\mathcal{A}_{2\,(-a,-\dot{a})}\,, \tag{2.95}$$

where

$$\widetilde{O}_2^{++} \equiv \sum_{r<s} O_{(rs)}^{++} - \frac{1}{N} \sum_{\substack{r<s \\ t\neq r,s}} \sigma_{(rs)}^{++} O_{(t)}^{++} \,. \tag{2.96}$$

For the class of $\mathcal{M}$-invariant supergravity solutions with a flat four-dimensional base space, Eqs. (2.93)–(2.96) comprise the holographic dictionary at dimension $(1,1)$.

One can check that not all extremal three-point functions of the operator combinations dual to g, $\tilde{g}$ vanish. Based on general expectations, there should be an appropriate field redefinition such that all extremal three-point functions vanish [54, 107–109, 116]. We will discuss this further in Chapter 3.

2.4.6 Tests of the holographic dictionary on two-charge states

Having determined all the coefficients in the holographic map (2.93), we can now use the map as a non-trivial consistency check on the correspondence (2.8) between the 1/4-BPS RR ground states (2.4) and the supergravity solutions (2.14). We re-emphasize that the $SU(2)_L \times SU(2)_R$ symmetry requires the coefficients in (2.93) to be independent of the spin $(a, \dot{a})$; thus, even if the most efficient way to fix the coefficients is to focus on the highest (or the lowest) spin component, as we have done in the previous subsections, the same coefficients must necessarily reproduce the expectation values of all other components. A relatively involved example is given by the operators

$$\Omega^{00} = 2 \sum_r J_{(r)}^3 \tilde{J}_{(r)}^3 \qquad \text{and} \qquad \Sigma_3^{00} = \frac{1}{2} \left[J_0^-, [\tilde{J}_0^-, \Sigma_3^{++}] \right] . \tag{2.97}$$

We will next work out a couple of examples that demonstrate how the one-point functions of these operators are correctly reproduced by the map (2.93). More examples involving 1/8-BPS D1-D5-P states will be examined in the next section.

- First, consider the state $(A\,|{+}{+}\rangle_k)^{\frac{N}{k}}$ with $k \in \mathbb{N}$.

The dual geometry is generated from the profile

$$g_1(v') + i g_2(v') = \frac{\bar{a}}{k}\, e^{\frac{2\pi i\, k}{L} v'} \,, \qquad g_3(v') = g_4(v') = g_5(v') = 0 \,, \tag{2.98}$$

and from the asymptotic expansion of the geometry one deduces that

$$h_{(a,\dot{a})} = \tilde{h}_{(a,\dot{a})} = 0 \qquad \text{for all} \quad (a, \dot{a}) \,. \tag{2.99}$$

This is a reflection of the fact that the geometry is a $\mathbb{Z}_k$ quotient of $\mathrm{AdS}_3 \times S^3$, with non-trivial constant gauge fields mixing S^3 and AdS_3.

Given the simple structure of the geometry, one would naively expect that on the CFT side only the R-symmetry currents, which couple to the S^3 gauge fields, have non-trivial expectation values; the situation is however a bit more interesting. While it is true that to leading order at large N all expectation values appearing in the first line of (2.93) vanish[4], the expectation values of the single-trace Ω^{00} and of the double-trace $(J\cdot\tilde{J})^{00}$ are non-trivial; consistency with the map (2.93) requires that the two expectation values precisely cancel. To compute the expectation value of Ω^{00} one notes that

$$\Omega^{00}\,|{+}{+}\rangle_k = \frac{1}{2k}\,|{+}{+}\rangle_k\ . \tag{2.100}$$

The $1/k$ factor in this equation is not a-priori obvious and can be understood as follows. Consider the action of the zero-mode of the $SU(2)_L$ current J^3_0 on a strand of winding k, such as $|{+}{+}\rangle_k$. Since there are identical copies of the $SU(2)_L$ algebra in any twist sector of the orbifold theory, the value of J^3_0 cannot depend on k: $J^3_0\,|{+}{+}\rangle_k = 1/2\,|{+}{+}\rangle_k$; on the other hand $J^3_0 = \sum_{r=1}^k J^3_{(r),0} = k\,J^3_{(r),0}$, with $J^3_{(r),0}$ the zero-mode of the operator acting on a single copy of the CFT. One deduces that, in the k-twisted sector, $J^3_{(r),0} = 1/k\,J^3_0$ and analogously $\tilde{J}^3_{(r),0} = 1/k\,\tilde{J}^3_0$. This implies that $\Omega^{00}_0 = 2\sum_{r=1}^k J^3_{(r),0}\tilde{J}^3_{(r),0} = 2/k\,J^3_0\tilde{J}^3_0$, from which (2.100) immediately follows.

The action of Ω^{00} on the full state $(|{+}{+}\rangle_k)^{\frac{N}{k}}$ is then given by multiplying by the number of strands N/k:

$$\Omega^{00}\left(|{+}{+}\rangle_k\right)^{\frac{N}{k}} \;=\; \frac{N}{2k^2}\left(|{+}{+}\rangle_k\right)^{\frac{N}{k}}. \tag{2.101}$$

This immediately implies

$$\left\langle\Omega^{00}\right\rangle \;=\; \frac{N}{2k^2}\,. \tag{2.102}$$

As for the expectation value of the double-trace $(J\cdot\tilde{J})^{00}$, one should first note that the correctly normalized affine descendant of $(J\cdot\tilde{J})^{++}$, which is what appears in the map (2.93), is given by

$$(J\cdot\tilde{J})^{00} \;=\; \frac{2}{N}\sum_{r\neq s} J^3_{(r)}\tilde{J}^3_{(s)}\,. \tag{2.103}$$

When acting on the state $(|{+}{+}\rangle_k)^{\frac{N}{k}}$, J^3 can be applied on any of the N/k strands, and it has eigenvalue $1/2$. The same happens for $\tilde{J}^3$ on the remaining $N/k-1$ strands. In the large N limit one finds

$$(J\cdot\tilde{J})^{00}\left(|{+}{+}\rangle_k\right)^{\frac{N}{k}} \;=\; \frac{2}{N}\frac{N^2}{k^2}\frac{1}{4}\left(|{+}{+}\rangle_k\right)^{\frac{N}{k}} \;=\; \frac{N}{2\,k^2}\left(|{+}{+}\rangle_k\right)^{\frac{N}{k}}, \tag{2.104}$$

[4]Naively one could think that the expectation value of the double-trace $(\Sigma_2\cdot\Sigma_2)^{00}\sim\sum\sigma^{++}_{(rs)}\sigma^{--}_{(pq)} + \sigma^{+-}_{(rs)}\sigma^{-+}_{(pq)}$ could receive a contribution, for example, from the process in which a σ^{--} joins two strands $|{+}{+}\rangle_k$ into $|{+}{+}\rangle_{2k}$ and a σ^{++} splits the newly created $|{+}{+}\rangle_{2k}$ strand again into two $|{+}{+}\rangle_k$ strands. One can however see that this expectation value, unlike the one computed in (2.85), does not grow with N, and hence it does not contribute to the holographic map at the leading order in the large N expansion. The origin of the difference with (2.85) is that in the present situation the second twist operator can only act on a particular strand, while in (2.85) it could act on $O(N)$ strands. This observation confirms the general rule that the expectation value of a double-trace operator is given by the product of the expectation values of the single-trace components at leading order in N.

and thus

$$\langle (J\cdot\tilde{J})^{00}\rangle \;=\; \frac{N}{2\,k^2}\,. \tag{2.105}$$

The two expectation values (2.102) and (2.105) are equal, as required by the holographic map.

- Second, let us consider the state

$$\sum_{p=1}^{N/k} (A\,|{+}{+}\rangle_1)^{N-k\,p} (B\,|{+}{+}\rangle_k)^p\,, \qquad\qquad k\in\mathbb{N}\,,\quad k\geq 3\,. \tag{2.106}$$

The supergravity analysis is done along the usual lines: starting from the dual profile

$$g_1(v')+ig_2(v') = \bar{a}\,e^{\frac{2\pi i}{L}v'} + \frac{\bar{b}}{k}\,e^{\frac{2\pi i\,k}{L}v'}\,, \qquad g_3(v')=g_4(v')=g_5(v')=0\,, \tag{2.107}$$

(where for simplicity we take $a,b\in\mathbb{R}$) one extracts the supergravity data defined in (2.94):

$$h_{(0,0)} = \frac{\sqrt{3}}{6}\,\frac{(k+1)^2}{k^2}\,\frac{N^{1/2}\,R_y^4}{(Q_1Q_5)^2}\,a^2\,b^2\,, \qquad \tilde{h}_{(0,0)} = \frac{1}{2}\,\frac{(k-1)^2}{k^2}\,\frac{N^{1/2}\,R_y^4}{(Q_1Q_5)^2}\,a^2\,b^2\,. \tag{2.108}$$

Note that in the following manipulations the regularity constraint $a^2+b^2=\frac{Q_1Q_5}{R_y^2}$ (2.15) will be used.

The second line of (2.93) works in a way that is qualitatively similar to the previous example. We take $k\geq 3$ for simplicity, where the non-vanishing expectation values are $\langle\Omega^{00}\rangle$ and $\langle(J\cdot\tilde{J})^{00}\rangle$ (for $k=2$, one would also need to include $\langle(\Sigma_2\cdot\Sigma_2)^{00}\rangle$). The one-point functions can be computed by applying the rules already explained:

$$\begin{aligned}\langle\Omega^{00}\rangle \;&=\; \frac{1}{2}\,\frac{N\,R_y^4}{(Q_1Q_5)^2}\,\frac{k^2a^4+(k^2+1)a^2b^2+b^4}{k^2}\,,\\ \langle(J\cdot\tilde{J})^{00}\rangle \;&=\; \frac{1}{2}\,\frac{N\,R_y^4}{(Q_1Q_5)^2}\,\frac{k^2a^4+2ka^2b^2+b^4}{k^2}\,.\end{aligned} \tag{2.109}$$

One can verify that substituting these expectation values in the second line of (2.93) reproduces the value of $\tilde{h}_{(0,0)}$ given in (2.108).

The first line of (2.93) introduces a novel ingredient: the expectation value of Σ_3^{00} (the other double-trace operators clearly do not play a role in this example, at large N). The mechanism by which Σ_3^{00} acquires a non-zero expectation value in the state (2.106) for any $k>1$ is as follows. Take for example $k=3$ and consider the action of Σ_3^{00} on the strands $|{+}{+}\rangle_1$ and $|{+}{+}\rangle_3$ corresponding to the permutation $(1)\,(234)$; when the twist 3 operator acts with the permutation (132) it produces a state described by the permutation $(2)\,(341)$, which represents again two strands of type $|{+}{+}\rangle_1$ and $|{+}{+}\rangle_3$. In

other words, the operator Σ_3^{00} maps the state (2.106) into itself, permuting the copy $|{+}{+}\rangle_1$ with one of the copies forming the strand $|{+}{+}\rangle_3$. To compute the expectation value associated with this process we need to know the coefficient $C_{k,3,k}^{-,-(1),-}$ defined by

$$\sigma_{(3)}^{00}\ |{+}{+}\rangle_1\,|{+}{+}\rangle_k = C_{k,3,k}^{-,-(1),-}\ |{+}{+}\rangle_1\,|{+}{+}\rangle_k\ , \tag{2.110}$$

where (3) denotes any three cycle that maps the state on the left to the state on the right. This coefficient is equal to $C_{3,k,k}^{-(1),-,-}$, corresponding to a three-point function that differs from the one giving $C_{k,3,k}^{-,-(1),-}$ by the ordering of the operators. One can see that the coefficients are equal using e.g. [119, Eq. (2.2.48)]. The coefficient $C_{3,k,k}^{-(1),-,-}$ was computed in [120, Eq. (6.28)] using the techniques reviewed in Appendix B, giving

$$C_{k,3,k}^{-,-(1),-} = \frac{(k+1)^2}{6\,k^2}\,. \tag{2.111}$$

The full expectation value of Σ_3^{00} is given by dressing $C_{k,3,k}^{-,-(1),-}$ by the appropriate combinatorial factors: the twist operator can act on any of the $(N-k\,p)\,p$ pairs of strands $|{+}{+}\rangle_1\,|{+}{+}\rangle_k$ and can cut the $|{+}{+}\rangle_k$ strand in k different positions (note that only one of the two permutations (rst) and (rts) that appear in the definition of Σ_3 (2.35) contributes to the present process, and thus one does not have an additional factor of 2). We thus find

$$\Sigma_3^{00}\ |{+}{+}\rangle_1^{N-k\,p}\ |{+}{+}\rangle_k^{p}\ =\ C_{k,3,k}^{-,-(1),-}\,(N-k\,p)\,p\,k\ |{+}{+}\rangle_1^{N-k\,p}\ |{+}{+}\rangle_k^{p}\ , \tag{2.112}$$

which gives

$$\langle\Sigma_3^{00}\rangle\ =\ \frac{(k+1)^2}{6\,k^2}\,A^2\,B^2\ =\ \frac{(k+1)^2}{6\,k^2}\,\frac{N^2\,R_y^4}{(Q_1Q_5)^2}\,a^2\,b^2\,. \tag{2.113}$$

The CFT prediction agrees, via the map (2.93), with the gravity coefficient $h_{(0,0)}$ in (2.108).

2.5 Precision holographic tests of superstrata

We now perform new precision tests of the proposed holographic dictionary for a recently constructed set of superstratum solutions and proposed dual CFT microstates. The term 'superstratum' refers to a large class of supergravity solutions describing black hole microstates [56–63, 112–114]. The key property of superstrata is that the isometries preserved by the black hole are explicitly broken (apart from the single null isometry guaranteed by supersymmetry). These solutions include sub-classes whose proposed dual CFT states display momentum fractionation [57], and include solutions that have parametrically long AdS_2 throats (in full, the throats are approximately $AdS_2{\times}S^1{\times}S^3{\times}T^4$) [58, 60], which have potentially important implications for AdS_2 holography [112]. Some special sub-families have the remarkable property of having completely integrable null

geodesics [61]; for some recent studies of superstrata, see [114, 121–123].

We will perform tests on a couple of specific sub-families of superstrata, including some of the most recently constructed solutions [62]. In all cases the proposed CFT description passes these new precision tests, which lends strong support to the proposed families of holographically dual CFT states.

2.5.1 Key properties of superstrata

We now briefly summarize the elements of the superstratum construction that will be relevant for our studies. The main purpose will be to introduce the necessary notation for the holographic tests that follow. For a more comprehensive introduction to superstrata, we refer the reader to [60].

The superstrata that have been constructed to date are six-dimensional solutions where the four-dimensional base is flat $\mathbb{R}^4$. The six-dimensional metric, four-dimensional base and relation between t, y and u, v coordinates are as given in Eqs. (2.9)–(2.12). The one-form $\boldsymbol{\beta}$ takes the value

$$\boldsymbol{\beta} \;=\; \frac{R_y a^2}{\sqrt{2}\,\Sigma}\left(\sin^2\theta\, d\phi - \cos^2\theta\, d\psi\right). \tag{2.114}$$

The remaining quantities in the supergravity ansatz (C.1) are organized by the almost-linear structure of the six-dimensional BPS equations. For completeness we give the full Type IIB ansatz and BPS equations in Appendix C, and we summarize the content here. The four-dimensional base and the one-form $\boldsymbol{\beta}$ are referred to as the data of the "zeroth" layer of equations. Then the first layer of BPS equations involves the scalars Z_1, Z_2, Z_4 and two-forms Θ^1, Θ^2, Θ^4. By convention Z_3 is related to $\mathcal{F}$, and $\Theta^3 = d\boldsymbol{\beta}$. Finally, the second layer of equations determines the scalar $\mathcal{F}$ and the one-form ω.

In the class of superstratum solutions that we will consider, Z_2 has the simple form

$$Z_2 \;=\; \frac{Q_5}{\Sigma}\,. \tag{2.115}$$

The first important feature of the solutions is encoded in the function Z_4 which enters directly into the Type IIB NS-NS two-form B_2, and the RR forms $C^{(0)}$ and $C^{(4)}$, and also into the metric via the combination $\mathcal{P} = Z_1 Z_2 - Z_4^2$. The function Z_4 takes the general form (more generally a phase could also be introduced in the definition of Z_4)

$$Z_4 \;=\; R_y \sum_{k,m,n,q} \delta_{q,0}\, b_4^{k,m,n,q}\, \frac{\Delta_{k,m,n}}{\Sigma} \cos\hat{v}_{k,m,n}\,, \tag{2.116}$$

where $b_4^{k,m,n,q}$ are real coefficients (the inclusion of q in the indices is somewhat super-

fluous because of the $\delta_{q,0}$, however we choose to keep the notation general), and where

$$\begin{aligned} \Delta_{k,m,n} &\equiv \left(\frac{a}{\sqrt{r^2+a^2}}\right)^k \left(\frac{r}{\sqrt{r^2+a^2}}\right)^n \cos^m\theta\, \sin^{k-m}\theta\,, \\ \hat{v}_{k,m,n} &\equiv (m+n)\frac{\sqrt{2}\,v}{R_y} + (k-m)\phi - m\psi\,, \qquad \Sigma \equiv r^2 + a^2\cos^2\theta\,. \end{aligned} \tag{2.117}$$

The ansatz for Z_1 involves a linear combination of terms similar to those appearing in Z_4, with coefficients chosen to facilitate the construction of smooth solutions without horizons. This procedure is known as "coiffuring" [56, 124, 125]. In practical terms, this means making the combination $\mathcal{P} = Z_1 Z_2 - Z_4^2$ have desired properties, which in the simplest cases means arranging that $\mathcal{P}$ is independent of $\hat{v}_{k,m,n}$. Several families of asymptotically AdS$_3$ solutions have this property, and in fact have the property that the full metric is also independent of the phase $\hat{v}_{k,m,n}$ and all explicit dependence on this phase is in the matter fields. We will discuss the explicit form of Z_1 that exhibits "coiffuring" once we specialize the discussion to the solutions that we consider in this section.

The proposed CFT interpretation of the superstratum solutions involves coherent superpositions of several strands of the following type. The states are labelled by integers (m,n,k,q) with[5] $q = 0,1$; $n \geq 1$; and $k > 0, k-q \geq m \geq 1$. For ease of notation it is convenient to define the states in the NS-NS sector, where they are given by [56–58, 60, 62]

$$|k,m,n,q\rangle^{\rm NS} = \frac{1}{(m-q)!(n-q)!}(J_0^+)^{m-q} L_{-1}^{n-q} \left(G^{+1}_{-\frac{1}{2}} G^{+2}_{-\frac{1}{2}} + \frac{1}{k} J_0^+ L_{-1}\right)^q |O^{--}\rangle_k^{\rm NS}\,, \tag{2.118}$$

with $|O^{--}\rangle_k^{\rm NS}$ the NS-sector anti-chiral primary corresponding to the RR ground state $|00\rangle_k$. Then the states we are interested in are the RR states obtained by performing left and right spectral flow transformations with parameters $(1/2, 1/2)$, and for ease of notation we shall denote the resulting RR states by $|k_i, m_i, n_i, q_i\rangle$, where i runs over the different types of superstratum strands that are present in a given state. Our spectral flow conventions are recorded in Eqs. (B.14)–(B.16) and are such that spectral flow with parameters $(1/2, 1/2)$ on an individual copy of the CFT maps the NS-NS vacuum to the RR ground state $|{+}{+}\rangle$.

We are interested in coherent superpositions of the states involving N_i copies of the above superstratum-type strands $|k_i, m_i, n_i, q_i\rangle$ and $N_k^{(s)}$ copies of the bosonic RR ground state strands $|s\rangle_k$ introduced around Eq. (2.1):

$$\psi_{\{N_k^{(s)}, n_i\}} \equiv \prod_{s=1}^{4} \prod_k |s\rangle_k^{N_k^{(s)}} \prod_i |k_i, m_i, n_i, q_i\rangle^{N_i}\,. \tag{2.119}$$

[5] We use the notation of [63] which differs from that of CRS [62] by $(m-q)_{\rm here} = m_{\rm CRS}$ and $(n-q)_{\rm here} = n_{\rm CRS}$.

The resulting family of (non-normalized) CFT states $\psi(\{A_k^{(s)}, B_i\})$ is defined, in a way similar to (2.4), as

$$\psi(\{A_k^{(s)}, B_i\}) \equiv \sum_{\{N_i, N_k^{(s)}\}}{}' \left[\prod_{s=1}^{4} \prod_k \left(A_k^{(s)} |s\rangle_k \right)^{N_k^{(s)}} \prod_i \left(B_i |k_i, m_i, n_i, q_i\rangle \right)^{N_i} \right] . \quad (2.120)$$

where the prime on the overall sum indicates that it is a restricted sum (as in Eq. (2.4)) over all states whose total number of copies adds up to N:

$$\sum_{k,s} k N_k^{(s)} + \sum_i k_i N_i = N . \quad (2.121)$$

Having defined the general class of superstratum states, we now specialize to those that we will consider in this chapter. We consider states with one type of ground state strands, with winding $k = 1$ and polarization $s = ++$, and one type of superstratum strand:

$$\psi(A_1, B_{k,m,n,q}) = \sum_{p=1}^{N/p} \left(A_1 |{++}\rangle_1 \right)^{N-pk} \left(B_{k,m,n,q} |k, m, n, q\rangle \right)^p . \quad (2.122)$$

This class is both sufficiently tractable and sufficiently interesting to enable the new precision holographic tests that follow.

The computations in the following subsections make use of a number of technical results, such as the norm of the states $\psi_{\{N_1, N_{k,m,n,q}\}}$, the average numbers $\overline{N}_i$ of strands in the coherent state (2.120), and the map between the CFT parameters A_1, $B_{k,m,n,q}$ and the coefficients a, $b_4^{k,m,n,q}$ that define the supergravity solution. For the examples considered below, it will be sufficient to present these results for $q = 0$, whose derivation can be found in [60]:

$$\left| \psi_{\{N_1, N_{k,m,n,0}\}} \right|^2 = \frac{N!}{N_1!} \prod_{k,m,n} \frac{1}{N_{k,m,n,0}!} \left[\frac{1}{k} \binom{k}{m} \binom{n+k-1}{n} \right]^{N_{k,m,n,0}} , \quad (2.123)$$

$$\overline{N}_1 = |A_1|^2 , \qquad k\overline{N}_{k,m,n,0} = \binom{k}{m} \binom{n+k-1}{n} |B_{k,m,n,0}|^2 , \quad (2.124)$$

$$|A_1| = R_y \sqrt{\frac{N}{Q_1 Q_5}}\, a , \qquad |B_{k,m,n,0}| = R_y \sqrt{\frac{N}{2Q_1 Q_5}} \binom{k}{m}^{-1} \binom{n+k-1}{n}^{-1} b_4^{k,m,n,0} . \quad (2.125)$$

2.5.2 Holographic tests of superstrata with the operator O_2

We now make the first precision holographic test of superstrata at dimension two, focusing on the expectation value of the operator O_2. Since the one-point function of O_2 is

extracted from the metric function Z_4, which is the basic ingredient in the construction of the superstrata solutions, these are the most direct tests of the identification between superstrata and CFT states.

Superstrata with $k = 2$, $m = 1$

We now consider the following set of states:

$$\sum_{p=1}^{\frac{N}{2}} \left(A\,|{+}{+}\rangle_1\right)^{N-2p} \left(B\frac{(L_{-1}-J^3_{-1})^n}{n!}J^+_{-1}\,|00\rangle_2\right)^p . \tag{2.126}$$

To begin with we will set $n = 0$, before extending to general n. We thus first consider the states

$$\sum_{p=1}^{\frac{N}{2}} \left(A\,|{+}{+}\rangle_1\right)^{N-2p} \left(BJ^+_{-1}\,|00\rangle_2\right)^p . \tag{2.127}$$

In the CFT, of the operators O_2 and $(\Sigma_2 \cdot O)$ entering in the holographic dictionary (2.40), only the single-trace O_2 has a non trivial expectation value: the expectation value of the operators O and Σ_2 are zero on this state, thus also that of the double-trace $(\Sigma_2 \cdot O)$ is zero.

Moreover, since the strands $|{+}{+}\rangle_1$ and $J^+_{-1}\,|00\rangle_2$ carry spin $(\frac{1}{2},\frac{1}{2})$ and $(1,0)$ respectively, by angular momentum conservation we conclude that only O_2^{0-} and its hermitian conjugate have non-vanishing one-point functions. The basic process is that in which O_2^{0-} links two strands $|{+}{+}\rangle_1$ into a strand $J^+_{-1}\,|00\rangle_2$ and the corresponding amplitude is

$$_{(12)}\langle 00|\, J^-_{+1}O_2^{0-}(v,u)\,|{+}{+}\rangle_{(1)}\,|{+}{+}\rangle_{(2)} \;=\; \sqrt{2}e^{\,i\frac{\sqrt{2}\,v}{R_y}} . \tag{2.128}$$

In deriving this result we have used the fact that the ground state is annihilated by the positive modes of the current operator to replace $J^-_{+1}O_2^{0-}(v,u)$ by their commutator[6]

$$[J^-_{+1}, O_2^{0-}(v,u)] \;=\; \sqrt{2}\,e^{\,i\frac{\sqrt{2}\,v}{R_y}}\; O_2^{--}(v,u)\,, \tag{2.129}$$

and the hermitian conjugate of the second relation in (2.37). Note that it is important to insert the operator O_2^{0-} at a generic worldsheet point (v,u) to obtain a non-trivial result: had we inserted it at past infinity, it would have killed the initial state $|{+}{+}\rangle_{(1)}\,|{+}{+}\rangle_{(2)}$.

We must now dress the result (2.128) with the proper combinatorial factor: the operator O_2^{0-} can act on any of the $\binom{N-2p}{2}$ pairs of $|{+}{+}\rangle_1$ to produce the state $J^+_{-1}\,|00\rangle_2$. Using (2.123) and requiring that both sides of the equation contain the same number of terms,

[6] The factor $\sqrt{2}$ in the commutator (2.129) ensures, as usual, that all components of $O_2^{a\dot{a}}$ have unit norm.

we obtain

$$O_2^{0-}\big(\,|{+}{+}\rangle_1\,\big)^{N-2p}\big(J_{-1}^{+}\,|00\rangle_2\,\big)^{p} \;=\; \frac{p+1}{\sqrt{2}}e^{i\frac{\sqrt{2}v}{R_y}}\big(\,|{+}{+}\rangle_1\,\big)^{N-2(p+1)}\big(J_{-1}^{+}\,|00\rangle_2\,\big)^{p+1}\,. \tag{2.130}$$

This implies that

$$\big\langle O_2^{0-}(v,u)\big\rangle \;=\; \frac{A^2}{\sqrt{2}B}\,\bar{p}\,e^{i\frac{\sqrt{2}v}{R_y}} \;=\; \frac{A^2\bar{B}}{\sqrt{2}}e^{i\frac{\sqrt{2}v}{R_y}} \;=\; \frac{N^{\frac{3}{2}}\,R_y^3}{4(Q_1Q_5)^{\frac{3}{2}}}a^2\,\bar{b}\,e^{i\frac{\sqrt{2}v}{R_y}}\,, \tag{2.131}$$

where we have used (2.124) to compute $\bar{p}$ and (2.125) to express the final result in terms of the gravity parameters.

On the supergravity side, we require the first non-trivial terms in the large r expansion of the function Z_4 given in (2.116) where $k=2$, $m=1$, $n=0$, $q=0$ and $b_4^{2,1,0,0}=b$:

$$Z_4 \;\sim\; \frac{\sqrt{Q_1Q_5}}{r^4}\frac{R_y\,a^2\,b}{2\sqrt{6}\sqrt{Q_1Q_5}}\left(-e^{i\frac{\sqrt{2}v}{R_y}}Y_2^{0,1}+e^{-i\frac{\sqrt{2}v}{R_y}}Y_2^{0,-1}\right)\,. \tag{2.132}$$

Comparing the result (2.131) with (2.132) using the dictionary in (2.57) and (2.58), one obtains exact agreement.

It is now straightforward to generalize the $n=0$ computation to the general set of states (2.126). On the CFT side the computation proceeds along the same lines as before, with the only difference that the correlator (2.128) should be replaced by

$${}_{(12)}\langle 00|\,\frac{(L_1-J_1^3)^n}{n!}J_{+1}^{-}O_2^{0-}(v,u)\,|{+}{+}\rangle_{(1)}\,|{+}{+}\rangle_{(2)} \;=\; \sqrt{2}e^{i(n+1)\frac{\sqrt{2}v}{R_y}}\,. \tag{2.133}$$

The extra factor $e^{in\frac{\sqrt{2}v}{R_y}}$ is produced by commuting the operator $(L_1-J_1^3)^n$ with $O_2^{--}(v,u)$, using

$$\big[(L_1-J_1^3)^n,O_2^{--}(v,u)\big] \;=\; n!\,e^{in\frac{\sqrt{2}v}{R_y}}\,O_{2,0}^{--}\,, \tag{2.134}$$

where $O_{2,0}^{--}$ denotes the zero-mode of O_2^{--}, which is the only one contributing to the correlator after having eliminated the momentum-carrying operators. On the gravity side, it follows immediately from (2.116) that the only modification to Z_4 at order r^{-4} is an extra factor $e^{in\frac{\sqrt{2}v}{R_y}}$. We thus see that the exact agreement persists for any value of n.

Superstrata with $k=2$, $m=2$

As a further consistency check, we consider the set of superstratum states with $k=2$, $m=2$:

$$\sum_{p=1}^{\frac{N}{2}}(A\,|{+}{+}\rangle_1)^{N-2p}\left(B\,\frac{(L_{-1}-J_{-1}^3)^n}{n!}\,\frac{(J_{-1}^{+})^2}{2}\,|00\rangle_2\right)^{p}\,. \tag{2.135}$$

We follow the same presentation and first set $n = 0$, before extending to general n. Thus, we first consider the coherent state

$$\sum_{p=1}^{\frac{N}{2}} (A\,|{+}{+}\rangle_1)^{N-2p} \left(B\,\frac{(J_{-1}^+)^2}{2}\,|00\rangle_2 \right)^p . \tag{2.136}$$

The strand $(J_{-1}^+)^2\,|00\rangle_2$ carries spin $(2,0)$, thus, by conservation of angular momentum, we conclude that only the operator $O_2^{+-} = \frac{1}{2}\left[(\tilde{J}_0^-)^2, O_2^{++}\right]$ and its hermitian conjugate will have non-trivial expectation values; the expectation value of the multi-trace $(\Sigma_2 \cdot O)$ is trivially zero. This operator carries out the fundamental process

$$O_2^{+-}(v,u)\;|{+}{+}\rangle_1\,|{+}{+}\rangle_1 = e^{i\frac{2\sqrt{2}v}{R_y}}\,\frac{(J_{-1}^+)^2}{2}\,|00\rangle_2\;, \tag{2.137}$$

where we have used the commutation relation $[(J_1^-)^2, O_2^{+-}(v,u)] = 2\,e^{i\frac{2\sqrt{2}v}{R_y}}\,O_2^{--}(v,u)$, the relation defining O^{--}, given by the hermitian conjugate of (2.37), and the fact that $\frac{(J_{-1}^+)^2}{2}\,|00\rangle_2$ has unit norm. The complete action of the operator O_2^{+-} on the state is obtained implementing the appropriate combinatorial factor (which follows, as usual, noticing that O_2^{+-} can choose among $\binom{N-2p}{2}$ pairs of $|{+}{+}\rangle_1$ and imposing that the norms on the two sides of the equation are equal). We obtain

$$\begin{aligned} &O_2^{+-}(v,u)\left[(|{+}{+}\rangle_1)^{N-2p}\left(\frac{(J_{-1}^+)^2}{2}\,|00\rangle_2\right)^p\right] \\ &\qquad = \; e^{i\frac{2\sqrt{2}v}{R_y}}(p+1)(|{+}{+}\rangle_1)^{N-2p-2}\left(\frac{(J_{-1}^+)^2}{2}\,|00\rangle_2\right)^{p+1} . \end{aligned} \tag{2.138}$$

This gives rise to the expectation value

$$\left\langle O_2^{+,-}(v,u)\right\rangle \;=\; e^{i\frac{2\sqrt{2}v}{R_y}}\,\bar{p}\frac{A^2}{B} \;=\; e^{i\frac{2\sqrt{2}v}{R_y}}\,\frac{A^2\bar{B}}{2} \;=\; e^{i\frac{2\sqrt{2}v}{R_y}}\,\frac{N^{\frac{3}{2}}\,R_y^3}{2\sqrt{2}(Q_1Q_5)^{\frac{3}{2}}}a^2\,\bar{b}\,. \tag{2.139}$$

Expanding the Z_4 function of the dual geometry (2.116) (with $k=2$, $m=2$, $n=q=0$, $b_4^{2,2,0,0} = b$) for large r up to the first non-trivial order, we obtain

$$Z_4 \;\sim\; \frac{\sqrt{Q_1Q_5}}{r^4}\,\frac{R_y\,a^2 b}{2\sqrt{3}\sqrt{Q_1Q_5}}\left(e^{i\frac{2\sqrt{2}v}{R_y}}Y_2^{-1,1} + e^{-i\frac{2\sqrt{2}v}{R_y}}Y_2^{+1,-1}\right). \tag{2.140}$$

Eqs. (2.139) and (2.140) are in exact agreement with the dictionary given in Eqs. (2.57) and (2.58).

As explained around Eq. (2.134), it is straightforward to extend this result to the states with general n given in Eq. (2.135): both the CFT and the gravity results are simply multiplied by the factor $e^{in\frac{\sqrt{2}v}{R_y}}$.

2.5.3 Holographic tests of superstrata with the operators Ω^{00} and Σ_3^{00}

We now consider the class of states with $m = 1$, $n = 0$, $q = 0$ and general (positive integer) k:

$$\sum_{p=1}^{N/k} \left(A\,|{+}{+}\rangle_1\right)^{N-kp} \left(B\,J_{-1}^{+}\,|00\rangle_k\right)^p . \tag{2.141}$$

The one-point function of O_2 in the state with $k = 2$ has already been considered in the previous subsection; here we concentrate on the other dimension-two operators, with the purpose of testing the dictionary (2.93). This enables us to check some features of the dual geometry other than Z_4, and in particular the metric function Z_1. Setting for ease of notation $b_4^{k,1,0,0} = b$, for this class of metrics Z_1 is given by (see e.g. [60, Eq. (4.3)]):

$$Z_1 \;=\; \frac{Q_1}{\Sigma} + \frac{R_y^2\, b^2}{2Q_5}\,\frac{\Delta_{k,1,0}}{\Sigma}\,\cos\hat{v}_{2k,2,0}\,, \tag{2.142}$$

where

$$Q_1 \;=\; \frac{R_y^2}{Q_5}\left(a^2 + \frac{b^2}{2k}\right). \tag{2.143}$$

The term proportional to Q_1 is the standard term encoding the dependence on the D1 charge; the term proportional to b^2 is more subtle, since it cannot be inferred simply on the basis of the global charges or of the supergravity equations, which would be satisfied also in the absence of that term. Its presence is however crucial for the smoothness of the solution. The general mechanism by which regularity is ensured in the superstratum construction has been dubbed "coiffuring" [124, 125], and in this example it amounts to choosing the ansatz for the function Z_1 such that the combination $\mathcal{P} = Z_1 Z_2 - Z_4^2$ is independent of v.

The holographic dictionary can provide a more direct CFT understanding of the coiffuring construction: we will show that the b^2 contribution to Z_1 originates from the mixing of both Ω and Σ_3 with the double-trace operator $(O \cdot O)$.

We first consider the second line of the holographic dictionary (2.93), which involves the expectation values of Ω^{00} and $(J{\cdot}\tilde{J})^{00}$ (in these states the one-point function of $(\Sigma_2{\cdot}\Sigma_2)^{00}$ is trivially zero for any k). Since these operators act in a way that has essentially already been explained in Section 2.4.6, we will be brief in the following. The operator Ω^{00} acts non-trivially only on the $|{+}{+}\rangle_1$ strands, for which $\Omega^{00}\,|{+}{+}\rangle_1 = 1/2\;|{+}{+}\rangle_1$, so we obtain

$$\left\langle \Omega^{00} \right\rangle \;=\; \frac{|A|^2}{2} \;=\; \frac{1}{2}\,\frac{N\,R_y^2}{Q_1 Q_5}\,a^2 \;=\; \frac{1}{2}\,\frac{N\,R_y^4}{(Q_1 Q_5)^2}\,a^2\left(a^2 + \frac{b^2}{2k}\right), \tag{2.144}$$

where we used (2.125) and, for later convenience, the regularity constraint (2.143). The expectation value of the double-trace $(J \cdot \tilde{J})^{00}$ can be expressed, as usual, as the product

of the expectation values of J^3 and $\tilde{J}^3$:

$$\left\langle (J\cdot\tilde{J})^{00}\right\rangle \;=\; \frac{2}{N}\left\langle J^3\right\rangle\left\langle \tilde{J}^3\right\rangle \;=\; \frac{|A|^2}{N}\left(\frac{|A|^2}{2}+|B|^2\right) \;=\; \frac{1}{2}\,\frac{N\,R_y^4}{(Q_1Q_5)^2}\,a^2\left(a^2+\frac{b^2}{k^2}\right). \tag{2.145}$$

Substituting in the second line of (2.93), we find a value of $\tilde{h}_{(0,0)}$ in exact agreement with the one extracted from the geometry:

$$\tilde{h}_{(0,0)} \;=\; \frac{N^{1/2}\,R_y^4}{(Q_1Q_5)^2}\,\frac{k-2}{4\,k^2}\,a^2b^2\,. \tag{2.146}$$

The first line of the holographic dictionary (2.93) works in a more interesting way, and it requires us to distinguish the states with $k=1$ from the ones with $k>1$. For $k=1$ we have $\langle\Sigma_3\rangle=0$, however the following components of the double-trace $(O\cdot O)$ play a role:

$$(O\cdot O)^{00}=\frac{1}{N}\sum_{r\neq s}\left(O^{++}_{(r)}O^{--}_{(s)}+O^{+-}_{(r)}O^{-+}_{(s)}\right), \qquad (O\cdot O)^{+-}=\frac{1}{N}\sum_{r\neq s}O^{+-}_{(r)}O^{+-}_{(s)}\,, \tag{2.147}$$

as well as the hermitian conjugate $(O\cdot O)^{-+}$. On the CFT side the expectation values are straightforward to compute as the product of the expectation values of the single-particle operators O^{+-} and O^{-+}, which were derived in Eqs. (4.38), (4.39) of [103]:

$$\left\langle (O\cdot O)^{00}\right\rangle \;=\; -\frac{|A|^2\,|B|^2}{N}\,, \qquad \left\langle (O\cdot O)^{+-}\right\rangle \;=\; e^{i\frac{2\sqrt{2}v}{R_y}}\,\frac{A^2\,\bar{B}^2}{N}\,. \tag{2.148}$$

On the gravity side the term responsible for $\langle(O\cdot O)^{+-}\rangle$ is the term quadratic in b in the metric function Z_1 (2.142), from which one extracts

$$h_{(-,+)} \;=\; (h_{(+,-)})^* \;=\; \frac{N^{1/2}R_y^4}{Q_1^2Q_5^2}e^{i\frac{2\sqrt{2}v}{R_y}}\,\frac{a^2b^2}{4\sqrt{3}} \qquad \text{and} \qquad h_{(0,0)} \;=\; -\frac{N^{1/2}R_y^4}{Q_1^2Q_5^2}\,\frac{a^2b^2}{4\sqrt{3}}\,, \tag{2.149}$$

which agree precisely with the CFT results. As we discussed below Eq. (2.142), the term contributing to $h_{(-,+)}$ is the one deduced, quite indirectly, from the "coiffuring" method. It is satisfying to see that holography provides a sharp CFT explanation of this supergravity construction.

When $k>1$ the relevant operator is Σ_3^{00}, which, as we have already seen, has to be analyzed with some care. The non-trivial part of the computation is in the derivation of the coefficient $C_{k3k}^{00(m=1)}$, which captures the action of the twist-three operator on a particular pair of states $|{+}{+}\rangle_1$ and $J^+_{-1}\,|00\rangle_k$:

$$\sigma^{00}_{(3)}\left(\,|{+}{+}\rangle_1\;J^+_{-1}\,|00\rangle_k\,\right) \;=\; C_{k3k}^{00(m=1)}\left(\,|{+}{+}\rangle_1\;J^+_{-1}\,|00\rangle_k\,\right). \tag{2.150}$$

Similarly to our explanation of the process (2.110), the twist operator $\sigma^{00}_{(3)}$ can cut the strand $|00\rangle_k$ and join it with the strand $|{+}{+}\rangle_1$, while at the same permuting the spins of

the two copies involved in the process. To our knowledge the coefficient $C_{k3k}^{00(m=1)}$ does not appear in the literature, and we thus derive it in Appendix B.2, by evaluating the three-point function (B.17). The result is

$$C_{k3k}^{00(m=1)} \;=\; \frac{k-2}{6k}\,. \tag{2.151}$$

When acting on the full state, the twist operator Σ_3^{00} can act on any of the $N-pk$ strands $|{+}{+}\rangle_1$ and on any of the p strands $J_{-1}^+\,|00\rangle_k$, and can cut the latter in k positions (after this choice is made, the permutation by which the twist operator can act is completely fixed); this translates, according to the usual logic, into the identity

$$\Sigma_3^{00}\,\left(|{+}{+}\rangle_1^{N-kp}\,\left(J_{-1}^+\,|00\rangle_k\,\right)^p\right) \;=\; C_{k3k}^{00(m=1)}\,(N-kp)\,p\,k\;|{+}{+}\rangle_1^{N-kp}\,\left(J_{-1}^+\,|00\rangle_k\,\right)^p\,, \tag{2.152}$$

and thus, using the result (2.124) to compute $\bar{p}$ and the CFT–gravity parameter map (2.125), one arrives at

$$\left\langle \Sigma_3^{00} \right\rangle \;=\; C_{k3k}^{00(m=1)}\,k\,A^2\,B^2 \;=\; \frac{k-2}{12\,k^2}\,\frac{N^2\,R_y^4}{(Q_1Q_5)^2}\,a^2\,b^2\,. \tag{2.153}$$

From the dual gravity solution one extracts:

$$h_{0,0} \;=\; \frac{k-2}{4\sqrt{3}\,k^2}\,\frac{N^{1/2}\,R_y^4}{(Q_1Q_5)^2}\,a^2\,b^2\,, \tag{2.154}$$

which agrees precisely with the prediction of the map (2.93).

Let us note that Eq. (2.154) reduces to the second term in Eq. (2.149) when $k = 1$. This is quite a non-trivial result: as we have just discussed, the geometric term $h_{0,0}$ is sourced by different CFT operators depending on the value of k.

2.5.4 A holographic test of supercharged superstrata

A more recently constructed, and therefore less-studied, class of superstrata is that of [62], where some of the momentum is carried by the CFT supercurrents G. We will focus here on the simplest state in that class, the one with $k = 2$, $m = 1$, $n = 0$, $q = 1$ in the notation of (2.118), which we rewrite in the Ramond sector as:

$$\sum_{p=1}^{N/2}(A\,|{+}{+}\rangle_1)^{N-2p}\left[B\left(G_{-1}^{+1}G_{-1}^{+2}+\frac{1}{2}J_{-1}^+(L_{-1}-J_{-1}^3)\right)|00\rangle_2\right]^p. \tag{2.155}$$

We now verify the important feature of the supergravity solution dual to this state, namely that $Z_4 = 0$ (as indicated by the $\delta_{q,0}$ in Eq. (2.116)). For consistency with the holographic dictionary (2.57)–(2.58), one expects that the expectation values of O_2 and $(\Sigma_2 \cdot O)$ vanish. While this is obvious for the double-trace $(\Sigma_2 \cdot O)$, at first sight one

could have a non-vanishing expectation value for O_2^{0+}, generated by the correlator

$$ {}_1\langle ++|\ {}_1\langle ++|\ O_2^{0+}(z,\bar z)\left(G^{+1}_{-1}G^{+2}_{-1}+\frac{1}{2}J^+_{-1}(L_{-1}-J^3_{-1})\right)|00\rangle_2\ . \tag{2.156} $$

It is simpler to perform the computation in the NS sector, where this correlator becomes

$$ \bar z\ {}_{\rm NS}\langle 0|\ O_2^{0+}(z,\bar z)\left(G^{+1}_{-1/2}G^{+2}_{-1/2}+\frac{1}{2}J^+_0L_{-1}\right)\left|O^{--}\right\rangle_2^{\rm NS}\ , \tag{2.157} $$

with ${}_{\rm NS}\langle 0|$ the NS vacuum and $|O^{--}\rangle_2^{\rm NS}\equiv O_2^{--}(0,0)\,|0\rangle^{\rm NS}$ the anti-chiral-primary state with $h=\bar h=1$ and $j=\bar j=-1$ introduced after Eq. (2.118). One can write

$$ O_2^{0+}(z,\bar z)\ =\ [J_0^-,O_2^{++}(z,\bar z)]\ =\ [J_0^-,O_2^{++}(\infty)]+z^{-1}\,[J_0^-,[L_1,[O_2^{++}(\infty)]]+\dots\ , \tag{2.158} $$

where the dots represent terms with higher powers of L_1 or $\tilde L_1$, which cannot contribute to the correlator. Inserting (2.158) in (2.157), one finds that the correlator is proportional to

$$ \begin{aligned} {}^{\rm NS}_2\langle O^{--}|\ J_0^-\ L_1\Big(G^{+1}_{-1/2}G^{+2}_{-1/2}+\frac{1}{2}J^+_0L_{-1}\Big)\left|O^{--}\right\rangle_2^{\rm NS} \\ =\ {}^{\rm NS}_2\langle O^{--}|\ J_0^-\left(-J_0^++J_0^+L_0\right)\left|O^{--}\right\rangle_2^{\rm NS}=0\,, \end{aligned} \tag{2.159} $$

where we have used the chiral algebra commutation relations and the fact that $L_0\,|O^{--}\rangle_2^{\rm NS}=|O^{--}\rangle_2^{\rm NS}$, as in [62, Eq. (2.7)]. The vanishing of Z_4 for the state (2.155) is thus in exact agreement with the CFT prediction.

2.6 Discussion

The main result of this chapter is the derivation of the holographic map relating the expectation values of chiral primary operators of dimension $(1,1)$ in a 1/4 or 1/8-BPS state of the D1-D5 CFT with the geometric coefficients extracted from the asymptotic expansion of the supergravity solution dual to the state. The precision holographic dictionary in this sector is consistent with the requirements coming from the R-symmetry and has passed non-trivial tests performed on two-charge geometries, whose CFT duals are well understood.

The usefulness of this dictionary for the development of the fuzzball program can be justified at different levels. First of all, it is a powerful tool to perform high precision test on three-charge microstate solutions and dual CFT states. Given a gravitational solution, the identification of the dual CFT state is generically a difficult task, the reason being that the point in the moduli space where CFT states can be easily described (i.e. the free orbifold point) is far from the supergravity regime. By focusing on protected quantities, the holographic dictionary provides a bridge between the two description and

might simplify this task.

Despite the tests we have performed, the precision holographic dictionary we have constructed cannot prove that the proposed holographic description of superstrata conducted in [56–63, 112–114] is correct in all its details; the limitation being the one discussed in Section 1.3: there can be many states with the same one-point function of low dimensional chiral primary operators. Nonetheless, the fact that the candidate CFT duals have passed the tests performed in Section 2.5 is non-trivial and provides strong and stringent evidences on its validity.

This holographic description, moreover, shows that the coefficients in the geometry are sourced by the operators in the CFT; this point of view might turn valuable in constructing new gravitational microstates: evaluating correlators in free CFT may in certain contexts be easier than solving the supergravity equation of motion. In particular, it has been shown in this work that certain terms entering in the gravitational solution that were determined using the so-called "coiffuring" technique (i.e. by requiring the smoothness of the geometry) could in principle have been predicted simply by computing correlators in the orbifold CFT: their CFT interpretation is simply a consequence of the mixing between single and multi-trace operators.

Chapter 3

Supercharged AdS_3 holography

This chapter contains the work presented in [2]. The main goal is to construct the precision holographic dictionary in a novel sector of the theory and use it to perform tests of supercharged superstrata [62] and of a family of multi-mode superstrata derived in [63, 64]. The novel sector is given by superdescendants of chiral primary operators of conformal dimension $(1, 1)$.

As discussed in the previous chapter, the identification of the precise CFT operator dual to a supergravity excitation is a non-trivial task, as it usually involves mixing between single-trace and multi-trace operators that are degenerate in their quantum numbers. In this chapter we resolve this mixing in the sector of interest by exploiting a different strategy with respect to the one presented in Chapter 2. In particular, it has been proposed in the context of $AdS_5 \times S^5$ holography that single-particle supergravity excitations are dual to $\mathcal{N} = 4$ SYM operators (in short multiplets) that are orthogonal to all multi-trace operators [126, 127]. This property, in AdS_5, uniquely fixes (up to a normalization constant) the admixture between single and multi-trace operators in the single-particle basis, and it has passed recent checks [127].

In this chapter we will consider this perspective in the context of $AdS_3 \times S^3$ and we will discuss that in this case the situation is more complicated than in $AdS_5 \times S^5$. In the AdS_3 case, in fact, while orthogonality between single-particle operators and multi-trace operators provides constraints, one must resolve additional operator mixing. Such mixing has been studied previously in [107]. We will resolve this point fully in the sector in which we work, by combining and improving upon the results of [1] and [107]. As we will discuss in more detail later, this residual ambiguity in the AdS_3 case is due to the fact that there are degeneracies between single-trace operators, which are not present in the AdS_5 case.

We will construct the holographic dictionary in the single-particle basis as follows. First, we recast the dictionary in Section 2.4.5 in the single-particle basis. On the CFT side,

this requires taking slightly different admixtures of single and multi-trace operators, such that all extremal three-point functions involving these operators vanish; on the bulk side, we have to consider the expansion of different geometric quantities. Having derived the mixing for chiral single-particle operators of dimension $(1,1)$, we generate their superdescendants by using the supercharges of the small $\mathcal{N}=4$ superconformal algebra: by construction, the resulting operators will be orthogonal to all multi-trace operators.

Next, we use the method introduced in [115] to construct the gauge-invariant combinations of supergravity fields that describe the single-particle excitations of interest. We then determine the proportionality coefficient between the asymptotic expansion of these gravitational quantities and the expectation values of the dual single-particle operators by calibrating the holographic dictionary on some reference states. We finally check that this proportionality coefficients is universal, i.e. depends only on the charges and moduli of the theory, but not on the precise details of the microstate chosen for calibration.

Having derived the dictionary, we make two non-trivial holographic tests of superstrata: first we test the coiffuring proposal of general non-supercharged superstrata of [63, 64]. Second, we test a 'hybrid' superstratum involving both supercharged and non-supercharged modes. These tests also represent further cross-checks on the holographic dictionary itself.

The structure of this chapter is as follows. In Sections 3.1 we report some technical results relevant for the holographic description of supercharged superstrata. Section 3.2 is a review of relevant aspects of the supergravity theory, superstrata, and precision holography. In Sections 3.4 and 3.5 we begin the construction of the dictionary in both gravity and CFT. In Section 3.6 we fix the normalization coefficients in the dictionary and perform tests of two distinct families of superstrata. In Section 3.8 we discuss our results; technical details are recorded in four appendices.
To avoid confusions with other quantities, in this Section we will denote by $\mathsf{k},\mathsf{m},\mathsf{n},\mathsf{q}$ the CFT paramenters that in the previous section were denoted by k,m,n,q.

3.1 Supercharged superstrata: some technical results

One of the aims of this project is to extend the tests on the recently constructed supercharged superstrata. Thus, let us resume the discussion in Section 2.5.1 in order to derive and develop the technical results summarized in Eqs.(2.123) , (2.124) and (2.125) for supercharged superstrata.

Chiral primary operators (CPOs) are the top components of the short multiplets of the $SU(1,1|2)_L \times SU(1,1|2)_R$ symmetry. These operators, together with their descendants under the generators of the anomaly-free part of the small $\mathcal{N}=(4,4)$ superconformal

State	J^3	L_0	$\bar{J}^3$	$\bar{L}_0$	$SU(2)_1$
$\|CP\rangle$	h	h	$\bar{h}$	$\bar{h}$	$\mathbf{1}$
$G^2\|CP\rangle$	$h-1$	$h+1$	$\bar{h}$	$\bar{h}$	$\mathbf{1}$
$\bar{G}^2\|CP\rangle$	h	h	$\bar{h}-1$	$\bar{h}+1$	$\mathbf{1}$
$G\bar{G}\|CP\rangle$	$h-1/2$	$h+1/2$	$\bar{h}-1/2$	$\bar{h}+1/2$	$\mathbf{1}\oplus\mathbf{3}$
$G^2\bar{G}^2\|CP\rangle$	$h-1$	$h+1$	$\bar{h}-1$	$\bar{h}+1$	$\mathbf{1}$

Table 3.1: Bosonic structure of the short multiplets. The group $SU(2)_1$ is introduced at the beginning of Section 2.2.

algebra, i.e. $\{J_0^-, L_{-1}, G^{-,A}_{-1/2}\}$ and $\{\bar{J}_0^-, \bar{L}_{-1}, \bar{G}^{-,A}_{-1/2}\}$, play a central role in the construction of the holographic dictionary, because of their relation to single-particle excitations in supergravity [128–130].

The bosonic structure of the $SU(1,1|2)_L \times SU(1,1|2)_R$ short multiplets is sketched in Table 3.1. In Table 3.1, G^2 is a short hand for the combination

$$G^{+1}_{-\frac{1}{2}} G^{+2}_{-\frac{1}{2}} + \frac{1}{2h} J_0^+ L_{-1}\,, \tag{3.1}$$

where h is the eigenvalue of L_0 for the CPO we act upon; similarly for $\bar{G}^2$. By working with this linear combination, one obtains a state that is orthogonal to the other descendants of the CPO, which is then dual to an independent supergravity fluctuation [62, 76, 111]. Moreover, this combination gives a state that is an eigenstate of the Casimirs of $SU(2)_L \times SU(2)_R$ and $SL(2,\mathbb{R}) \times SL(2,\mathbb{R})$, as one can check making use of the anomaly-free part of the chiral algebra in the NS-NS sector, composed of L_0, $L_{\pm 1}$, J_0^a, $G^{\alpha A}_{\pm 1/2}$. Setting temporarily $m, n = 1, 0, -1$ and $r, s = \pm\frac{1}{2}$, the anomaly-free part of the chiral superconformal algebra is

$$\begin{aligned}
\big[L_m, L_n\big] &= (m-n)L_{m+n}\,, \qquad \big[J_0^a, J_0^b\big] = i\epsilon^{abc} J_0^c\,, \qquad \big[L_n, J_0^a\big] = 0\,,\\
\big[J_0^a, G_s^{\alpha A}\big] &= \frac{1}{2} G_s^{\beta A} \big(\sigma^a\big)^\alpha_\beta\,, \qquad \big[L_m, G_s^{\alpha A}\big] = \Big(\frac{m}{2} - s\Big) G^{\alpha A}_{m+s}\,,\\
\big\{G_r^{\alpha A}, G_s^{\beta B}\big\} &= \epsilon^{\alpha\beta}\epsilon^{AB} L_{r+s} + (r-s)\epsilon^{AB}\big(\sigma^{aT}\big)^\alpha_\gamma \epsilon^{\gamma\beta} J^a_{r+s}\,,
\end{aligned} \tag{3.2}$$

where $a, b, c = \{\pm, 3\}$ are indices in the adjoint of $SU(2)_L$. When discussing superstrata, it will be convenient for our conventions to work with anti-chiral primary operators (ACPOs): these are descendants of CPOs obtained acting the maximal number of times with the generators $J_0^-, \bar{J}_0^-$ and are characterized by $h = -j$, $\bar{h} = -\bar{j}$.

The momentum-carrying building blocks of the 1/8-BPS states dual to superstrata are the descendant states obtained by acting upon the anti-chiral primary $\big|O^{--}_{\mathsf{k}}\big\rangle_{\rm NS}$, which corresponds to the RR ground state $|00\rangle_{\mathsf{k}}$, with the holomorphic generators of the small $\mathcal{N} = 4$ superconformal algebra J_0^+, L_{-1} and $G^{+A}_{-\frac{1}{2}}$. We will denote these by $|\mathsf{k}, \mathsf{m}, \mathsf{n}, \mathsf{q}\rangle$,

and one has [56–58, 60, 62, 63]

$$|\mathsf{k},\mathsf{m},\mathsf{n},\mathsf{q}\rangle \;=\; \frac{1}{(\mathsf{m}-\mathsf{q})!(\mathsf{n}-\mathsf{q})!}(J_0^+)^{\mathsf{m}-\mathsf{q}}L_{-1}^{\mathsf{n}-\mathsf{q}}\left(G^{+1}_{-\frac{1}{2}}G^{+2}_{-\frac{1}{2}}+\frac{1}{\mathsf{k}}J_0^+L_{-1}\right)^{\mathsf{q}}|O_{\mathsf{k}}^{--}\rangle_{\rm NS}\,, \quad (3.3)$$

where the parameters can take values $\mathsf{q}=0$ or 1, $\mathsf{n}\geq\mathsf{q}$, $\mathsf{k}>0$, and $\mathsf{q}\leq\mathsf{m}\leq\mathsf{k}-\mathsf{q}$ [62] (our notation follows [63]). We describe states with $\mathsf{q}=1$ as supercharged states. We are interested in superstrata whose CFT dual state is made up of strands of type $|\mathsf{k},\mathsf{m},\mathsf{n},\mathsf{q}\rangle$ and the NS-NS vacuum $|0\rangle_1$: a basis for these states is given by the following eigenstates of the $SU(2)_L\times SU(2)_R$ currents

$$\psi_{\{N_0,N_i\}}\equiv|0\rangle_1^{N_0}\prod_i|\mathsf{k}_i,\mathsf{m}_i,\mathsf{n}_i,\mathsf{q}_i\rangle^{N_i} \quad (3.4)$$

subject to the constraint that the total number of copies must saturate the strand-budget:

$$N_0+\sum_i\mathsf{k}_iN_i=N \quad (3.5)$$

The black hole microstates that are well described in supergravity limit are coherent states [52] that are linear combinations of the $\psi_{\{N_0,N_i\}}$, weighted by complex coefficients A,B_i

$$\psi(\{A,B_i\})\;\equiv\;{\sum_{\{N_0,N_i\}}}'\left[\prod_i\Big(A\,|0\rangle_1\Big)^{N_0}\Big(B_i\,|\mathsf{k}_i,\mathsf{m}_i,\mathsf{n}_i,\mathsf{q}_i\rangle\Big)^{N_i}\right]. \quad (3.6)$$

where the prime symbol denotes that the sum is subject to the constraint (3.5). In the large N limit, the sum is peaked over some average numbers $\{\bar N_0,\bar N_i\}$ of strands, which are related to the complex coefficients A,B_i.

In Section 2.5.1 we reported the results of [103] and [60] concerning non-supercharged superstrata (i.e. concerning the state (3.6) with $q_i=0$). We now generalize this discussion to the states (3.6) with generic q_i: this will enable us to determine the norm of (3.4), the average numbers $\{\bar N_0,\bar N_i\}$ and the relation between the CFT coefficients A,B_i and the supergravity one a,b_i. These results will be used in the following sections. The state $\psi_{\{N_0,N_i\}}$ is univoquely determinated by the distribution of strands $\{N_0,N_i\}$ (which define a conjugacy class of the permutation group S_N), and the quantum numbers $(\mathsf{k}_i,\mathsf{m}_i,\mathsf{n}_i,\mathsf{q}_i)$ carried by each strand. Following [103] (see in particular Section 3), we assign to $\psi_{\{N_0,N_i\}}$ a norm given by the product of the number of ways one can generate the desired distribution of strands starting from the identity element of S_N times the norm of each strand $|\mathsf{k}_i,\mathsf{m}_i,\mathsf{n}_i,\mathsf{q}_i\rangle$. The former is given by

$$\frac{N!}{N_0!\prod_i N_i!\mathsf{k}_i^{N_i}} \quad (3.7)$$

In order to determine the norm of a single strand $|\mathsf{k},\mathsf{m},\mathsf{n},\mathsf{q}\rangle$, we will make use of Eq. (3.2), the fact that an anti-chiral primary is killed by $G^{-A}_{-1/2}$ and J_0^- (beside all pos-

itive modes of the anomaly-free subalgebra) and the following relations on hermitian conjugation:

$$(G_n^{\alpha A})^\dagger = -\epsilon_{\alpha\beta}\epsilon_{AB}G_{-n}^{\beta B} \qquad (J_n^a)^\dagger = J_{-n}^{-a} \quad (L_n)^\dagger = L_{-n} \tag{3.8}$$

We start by considering $\mathsf{m} = \mathsf{n} = \mathsf{q} = 1$, which gives:

$$\langle \mathsf{k}, 1, 1, 1 | \mathsf{k}, 1, 1, 1 \rangle \;=\; \mathsf{k}^2 - 1\,. \tag{3.9}$$

In order to compute the contribution to the norm coming from the contractions of the J_0^+ insertions, it is useful to consider the following state, using the shorthand $\hat{\mathsf{m}} = \mathsf{m} - \mathsf{q}$:

$$\begin{aligned} &J_0^-\big(J_0^+\big)^{\hat{\mathsf{m}}}\Big(G^{+1}_{-\frac{1}{2}}G^{+2}_{-\frac{1}{2}} + \frac{1}{\mathsf{k}}J_0^+L_{-1}\Big)^{\mathsf{q}}\,\big|O^{--}_{\mathsf{k}}\big\rangle \\ &\qquad = \Big(-2(\hat{\mathsf{m}}-1) + \mathsf{k} - 2q + J_0^+J_0^-\Big)\big(J_0^+\big)^{\hat{\mathsf{m}}-1}\Big(G^{+1}_{-\frac{1}{2}}G^{+2}_{-\frac{1}{2}} + \frac{1}{\mathsf{k}}J_0^+L_{-1}\Big)^{\mathsf{q}}\,\big|O^{--}_{\mathsf{k}}\big\rangle \\ &\qquad = \hat{\mathsf{m}}\Big(\mathsf{k} - \hat{\mathsf{m}} + 1 - 2\mathsf{q}\Big)\big(J_0^+\big)^{\hat{\mathsf{m}}-1}\Big(G^{+1}_{-\frac{1}{2}}G^{+2}_{-\frac{1}{2}} + \frac{1}{\mathsf{k}}J_0^+L_{-1}\Big)^{\mathsf{q}}\,\big|O^{--}_{\mathsf{k}}\big\rangle\,. \end{aligned} \tag{3.10}$$

Here we have used the relations $J_0^3\,|\mathsf{k},\mathsf{q},\mathsf{q},\mathsf{q}\rangle = (-\frac{\mathsf{k}}{2}+\mathsf{q})\,|\mathsf{k},\mathsf{q},\mathsf{q},\mathsf{q}\rangle$ and $J_0^-\,|\mathsf{k},\mathsf{q},\mathsf{q},\mathsf{q}\rangle = 0$. Iterating this procedure and using (3.9) one obtains

$$\langle \mathsf{k},\mathsf{m},\mathsf{q},\mathsf{q} | \mathsf{k},\mathsf{m},\mathsf{q},\mathsf{q}\rangle \;=\; \binom{\mathsf{k}-2\mathsf{q}}{\mathsf{m}-\mathsf{q}}(\mathsf{k}^2-1)^{\mathsf{q}}\,. \tag{3.11}$$

We proceed similarly for the Virasoro generators, using $\hat{\mathsf{n}} = \mathsf{n} - \mathsf{q}$:

$$\begin{aligned} &L_1\big(L_{-1}\big)^{\hat{\mathsf{n}}}\Big(G^{+1}_{-\frac{1}{2}}G^{+2}_{-\frac{1}{2}} + \frac{1}{\mathsf{k}}J_0^+L_{-1}\Big)^{\mathsf{q}}\,\big|O^{--}_{\mathsf{k}}\big\rangle \\ &\qquad = \hat{\mathsf{n}}\big(\mathsf{k} + \hat{\mathsf{n}} - 1 + 2\mathsf{q}\big)\Big(G^{+1}_{-\frac{1}{2}}G^{+2}_{-\frac{1}{2}} + \frac{1}{\mathsf{k}}J_0^+L_{-1}\Big)^{\mathsf{q}}\,\big|O^{--}_{\mathsf{k}}\big\rangle\,. \end{aligned} \tag{3.12}$$

Here we have used the relations $L_0\,|\mathsf{k},\mathsf{q},\mathsf{q},\mathsf{q}\rangle = (\frac{\mathsf{k}}{2}+\mathsf{q})\,|\mathsf{k},\mathsf{q},\mathsf{q},\mathsf{q}\rangle$ and $L_1\,|\mathsf{k},\mathsf{q},\mathsf{q},\mathsf{q}\rangle = 0$. Iterating this procedure and using (3.9) one obtains

$$\langle \mathsf{k},\mathsf{q},\mathsf{n},\mathsf{q} | \mathsf{k},\mathsf{q},\mathsf{n},\mathsf{q}\rangle \;=\; \binom{\mathsf{k}+\mathsf{n}+\mathsf{q}-1}{\mathsf{n}-\mathsf{q}}(\mathsf{k}^2-1)^{\mathsf{q}}\,. \tag{3.13}$$

Since the Virasoro generators commute with $J_0^\pm$, we can directly combine the results in (3.9), (3.11) and (3.13) to obtain

$$\langle \mathsf{k},\mathsf{m},\mathsf{n},\mathsf{q} | \mathsf{k},\mathsf{m},\mathsf{n},\mathsf{q}\rangle = \binom{\mathsf{k}-2\mathsf{q}}{\mathsf{m}-\mathsf{q}}\binom{\mathsf{k}+\mathsf{n}+\mathsf{q}-1}{\mathsf{n}-\mathsf{q}}(\mathsf{k}^2-1)^{\mathsf{q}}\,. \tag{3.14}$$

This result, along with (3.7), gives the norm of the building-block state (3.4),

$$|\psi_{\{N_0,N_i\}}|^2 = \frac{N!}{N_0!}\prod_i \frac{1}{N_i!}\Big[\frac{(\mathsf{k}_i^2-1)^{\mathsf{q}_i}}{\mathsf{k}_i}\binom{\mathsf{k}_i-2\mathsf{q}_i}{\mathsf{m}_i-\mathsf{q}_i}\binom{\mathsf{k}_i+\mathsf{n}_i+\mathsf{q}_i-1}{\mathsf{n}_i-\mathsf{q}_i}\Big]^{N_i}. \tag{3.15}$$

This implies that the norm of the full coherent state (3.6) is

$$|\psi(\{A,B_i\})|^2 \equiv \sum_{\{N_0,N_i\}}{}' \frac{N!}{N_0!}|A|^{2N_0}\prod_i \frac{1}{N_i!}\Big[|B_i^2|\frac{\left(\mathsf{k}_i^2-1\right)^{\mathsf{q}_i}}{\mathsf{k}_i}\binom{\mathsf{k}_i-2\mathsf{q}_i}{\mathsf{m}_i-\mathsf{q}_i}\binom{\mathsf{k}_i+\mathsf{n}_i+\mathsf{q}_i-1}{\mathsf{n}_i-\mathsf{q}_i}\Big]^{N_i}. \tag{3.16}$$

We now determine the average number of strands in the coherent state by requiring that the variation of the summand of (3.16) with respect to N_0, N_i vanishes [103], obtaining

$$\bar{N}_0 = |A|^2 \qquad \mathsf{k}_i\bar{N}_i = \left(\mathsf{k}_i^2-1\right)_i^{\mathsf{q}}\binom{\mathsf{k}_i-2\mathsf{q}_i}{\mathsf{m}_i-\mathsf{q}_i}\binom{\mathsf{k}_i+\mathsf{n}_i+\mathsf{q}_i-1}{\mathsf{n}_i-\mathsf{q}_i}|B_i|^2\,. \tag{3.17}$$

This equation, combined with the strand budget constraint (3.5), implies

$$|A|^2+\sum_i\left(\mathsf{k}_i^2-1\right)^{\mathsf{q}_i}\binom{\mathsf{k}_i-2\mathsf{q}_i}{\mathsf{m}_i-\mathsf{q}_i}\binom{\mathsf{k}_i+\mathsf{n}_i+\mathsf{q}_i-1}{\mathsf{n}_i-\mathsf{q}_i}|B_i|^2 = N\,. \tag{3.18}$$

3.2 Supergravity and Superstrata

In this section we briefly review the supergravity theory in which we work, the superstratum solutions we study, and the Kaluza-Klein spectrum of the six-dimensional supergravity theory reduced on S^3.

3.2.1 Six-dimensional supergravity fields

The D1-D5 system admits an AdS_3 decoupling limit leading to configurations that have $AdS_3\times S^3\times\mathcal{M}$ asymptotics [97]. In the limit in which the internal manifold $\mathcal{M}$ is microscopic, dimensional reduction of the 10-dimensional theory on $\mathcal{M}$ gives a $D=6$ supergravity theory with n tensor multiplets[1], whose equations of motion were first derived by Romans in [131]. The bosonic field content of the theory is as follows: a graviton g_{MN} ($M,N=0,...,5$ are curved 6D indices), 5 two-forms whose field strengths H^m are selfdual ($m=1,...,5$ is a vector index of $SO(5)$), n two-forms whose field strengths H^r are anti-selfdual ($r=6,...,n+5$ is a vector index of $SO(n)$) and $5n$ scalars ϕ^{mr}. Dimensional reduction on the T^4 also gives rise to 16 vectors: their CFT duals, however, belong to the short multiplets of fermionic CPOs and we shall not consider them further in the present work. The scalars live in the coset space $SO(5,n)/(SO(5)\times SO(n))$, which can be parametrized by vielbeins (V_I^m, V_I^r) where $I=(m,r)$ is an $SO(5,n)$ vector index. We also introduce field strengths G^I which are related to the selfdual and anti-selfdual

[1]Some details of the theory change depending on whether the internal manifold is T^4 or $K3$. In the first case the number of supersymmetries is $\mathcal{N}=(2,2)$, while in the other one has $\mathcal{N}=(2,0)$. Note that this is the 6D supersymmetry counting. Let us take the case of T^4: $\mathcal{N}=(2,2)$ supersymmetries in 6D means that we have 32 supercharges. The addition of D1 and D5 branes leaves unbroken 1/4 of the supercharges; moreover, when performing the near horizon limit the supercharges get enhanced to 16, which is exactly the number of supercharges of the D1-D5 dual CFT. Moreover, $n=5$ when the internal manifold is T^4 while $n=21$ when $\mathcal{M}=K3$.

field strengths through the vielbeins via $H^m = G^I V_I^m$ and $H^r = G^I V_I^r$. In order to support the global $\mathrm{AdS}_3\times \mathrm{S}^3$ vacuum, one must turn on one of the fluxes, which we will take to be $H^{m=5}$. We parametrize fluctuations of the six-dimensional supergravity fields around the $\mathrm{AdS}_3\times \mathrm{S}^3$ background as follows:

$$g_{MN} = g^0_{MN} + h_{MN}\,, \quad G^{(A)} = g^{0(A)} + g^{(A)}\,, \quad V_I^m = \delta_I^m + \phi^{(mr)}\delta_I^r\,, \quad V_I^r = \delta_I^r + \phi^{(mr)}\delta_I^m\,. \tag{3.19}$$

The explicit expression for the background fields g^0_{MN} and $g^{0(A)}$ is given in Eq. (3.29) below.

3.2.2 Superstrata

In this subsection we briefly review certain aspects of superstrata that will be relevant to the remainder of the chapter.

Superstrata are supersymmetric supergravity solutions in which the isometries preserved by the corresponding black hole solution are broken by momentum-carrying waves, see e.g. [56–64, 132, 133]. These include the first families of smooth horizonless solutions with large BTZ-like AdS_2 throats, general angular momentum, and identified holographic duals in the AdS_3 limit [58, 60]. In the D1-D5-P frame, these are typically constructed in the context of the general 1/8-BPS ansatz of Type IIB supergravity that carries D1, D5, P charges and is invariant on $\mathcal{M}$. This was derived in [134] and is reproduced in Appendix C for completeness.

Upon reduction to $6D$, this ansatz gives rise to minimal 6D supergravity coupled to $n = 2$ tensor multiplets, which we will take to be labelled by $r = 6, 7$. The main interest of this work will be the holographic dictionary involving the field strength G^6 and G^7. Let us therefore discuss the relation between these fields and those given in Appendix C. The 6D metric takes the form

$$ds_6^2 = -\frac{2}{\sqrt{\mathcal{P}}}(dv + \boldsymbol{\beta})(du + \omega + \frac{\mathcal{F}}{2}(dv + \boldsymbol{\beta})) + \sqrt{\mathcal{P}} ds_4^2\,. \tag{3.20}$$

We first define the following three-form field strengths (here and until the end of the subsection we use $a, b = 1, 2, 4$)

$$G^a = d\Big[-\frac{1}{2}\frac{\eta^{ab}Z_b}{P}(du + \omega)\wedge(dv + \boldsymbol{\beta})\Big] + \frac{1}{2}\eta^{ab} \star_4 DZ_b + \frac{1}{2}(dv + \boldsymbol{\beta})\wedge\Theta^a \tag{3.21}$$

where

$$\eta_{12} = \eta_{21} = -\eta_{44} = 1\,, \qquad P = Z_1 Z_2 - Z_4^2\,. \tag{3.22}$$

The field strengths G^a respect the self-duality condition:

$$\star_6 G^a = M^a{}_b G^b, \qquad M_{ab} = \frac{Z_a Z_b}{P} - \eta_{ab}. \tag{3.23}$$

The G^a arise from the dimensional reduction of the type IIB field strengths of C_2, C_6 and B, see App. C. The relation between these three-forms and the field strengths G^5, G^6, G^7 introduced above was derived in [55] and in our conventions is given by

$$G^5 = \frac{Q_1 G^1 + Q_5 G^2}{2Q_1 Q_5}\,, \qquad G^6 = -\frac{Q_1 G^1 - Q_5 G^2}{2Q_1 Q_5}\,, \qquad G^7 = \frac{1}{\sqrt{Q_1 Q_5}} G^4\,. \tag{3.24}$$

The scalar fields $\phi^{(56)}$ and $\phi^{(57)}$ arise from the dilaton, C_0, and the component of C_4 with all legs on $\mathcal{M}$. These can be obtained from the vielbein matrix in [55, Eqs. (3.33), (B.20)], along with Eq. (3.19). In our conventions they take the form

$$\phi^{(56)} = \frac{1}{2\sqrt{Q_1 Q_5}} \left(\frac{Q_1 Z_1 - Q_5 Z_2}{\sqrt{Z_1 Z_2}} \right)\,, \qquad \phi^{(57)} = \frac{Z_4}{\sqrt{Z_1 Z_2}}\,. \tag{3.25}$$

The general structure of superstratum solutions is as follows. The construction begins with a seed solution which is usually taken to be a circular supertube [44, 45] with characteristic length-scale a. Momentum-carrying waves are added by a linear superposition of terms within the linear system of BPS equations, specifically at the level of the "first layer" recorded in Eq. (C.8). These momentum-carrying waves come with a set of dimensionful Fourier coefficients b_i. This construction is designed to correspond to the structure of the CFT states in Eq. (3.6). For further details, see e.g. [60, 63].

Smoothness of the supergravity solutions imposes the relation [63, Eq. (4.13)–(4.14)]

$$\frac{Q_1 Q_5}{R^2} = a^2 + \sum_i \frac{b_i^2}{2} \hat{x}_i\,, \qquad \hat{x}_i = \left(\binom{k_i - 2q_i}{m_i - q_i} \binom{k_i + n_i + q_i - 1}{n_i - q_i} (k_i^2 - 1) \right)^{-1} \tag{3.26}$$

which has the same form of the CFT strand budget constraints (3.5), (3.18), and indeed this is no accident. By comparing the two, the proposed superstratum holographic dictionary involves the following map between the CFT coefficients A, B_i and the supergravity coefficients a b_i:

$$\begin{aligned} \frac{A}{\sqrt{N}} &= R\sqrt{\frac{1}{Q_1 Q_5}} a \;\equiv\; \mathsf{a}\,, \\ \frac{B_i}{\sqrt{N}} &= R\sqrt{\frac{1}{2Q_1 Q_5}} \left(\binom{k_i - 2q_i}{m_i - q_i} \binom{k_i + n_i + q_i - 1}{n_i - q_i} (k^2 - 1)^q \right)^{-1} b_i \\ &= \sqrt{\frac{1}{2}} \left(\binom{k_i - 2q_i}{m_i - q_i} \binom{k_i + n_i + q_i - 1}{n_i - q_i} (k^2 - 1)^q \right)^{-1} \mathsf{b}_i\,, \end{aligned} \tag{3.27}$$

where we have also defined the quantities a, b which will be used later in the chapter.

3.3 Kaluza-Klein spectrum

In order to discuss the Kaluza-Klein spectrum of the 6D theory compactified on the S^3 [128, 130] (see also e.g. [54, 62]), we must expand the six-dimensional fluctuations in harmonics of S^3. Before doing this, however, it is convenient to perform the following rescalings:

$$r \to a_0\,\tilde{r}\,, \quad t \to R_y\,\tilde{t}\,, \quad y \to R_y\,\tilde{y}\,, \quad \beta \to R_y\,\tilde{\beta}\,, \quad \omega \to R_y\,\tilde{\omega}\,, \quad Z_i \to \frac{\tilde{Z}_i}{a_0^2}\,, \tag{3.28}$$

with $a_0^2 \equiv \frac{Q_1 Q_5}{R_y^2}$. We then reabsorb the overall scale factor $\sqrt{Q_1 Q_5}$ in the metric[2] to obtain

$$\begin{aligned} g^{(0)}_{MN} &= \frac{d\tilde{r}^2}{\tilde{r}^2+1} - (\tilde{r}^2+1)d\tilde{t}^2 + \tilde{r}^2 d\tilde{y}^2 + d\theta^2 + \sin^2\theta d\phi^2 + \cos^2\theta d\psi^2\,, \\ g^{0(A=5)} &= \cos\theta\sin\theta d\phi\wedge d\psi\wedge d\theta - \tilde{r}d\tilde{r}\wedge d\tilde{t}\wedge d\tilde{y}\,, \qquad g^{0(A\neq 5)} = 0\,. \end{aligned} \tag{3.29}$$

We now introduce a multi-index I for the S^3 harmonic degree k and $(j_3, \bar{j}_3)$ quantum numbers, $I = (k, m, \bar{m})$. In some places we will write k explicitly, and continue to use I for the remaining quantum numbers $(m, \bar{m})$. Harmonics on S^3 and AdS_3 are reviewed in Appendix A. We split the 6D curved indices into AdS_3 indices $\mu, \nu = 0, 1, 2$ and S^3 indices $a, b = 1, 2, 3$. The subscript (ab) denotes the symmetric traceless component of the field. Then expanding the six-dimensional fluctuations in harmonics of S^3, one obtains [54, 128]

$$\begin{aligned} h_{\mu\nu} &= \sum h^I_{\mu\nu} Y^I \\ h_{\mu a} &= \sum h^I_{(v)\mu} Y^I_a + h^I_{(s)\mu} D_a Y^I \\ h_{(ab)} &= \sum \rho^I Y^I_{(ab)} + \rho^I_{(v)} D_a Y^I_b + \rho^I_{(s)} D_{(a} D_{b)} Y^I \\ h^a_a &= \sum \pi^I Y^I \\ g^A_{\mu\nu\rho} &= \sum 3 D_{[\mu} b^{(A)I}_{\nu\rho]} Y^I \\ g^A_{\mu\nu a} &= \sum b^{(A)I}_{\mu\nu} D_a Y^I + 2 D_{[\mu} Z^{(A)I}_{\nu]} Y^I_a \\ g^A_{\mu ab} &= \sum D_\mu U^{(A)I} \epsilon_{abc} D^c Y^I + 2 Z^{(A)I}_\mu D_{[b} Y^I_{a]} \\ g^A_{abc} &= -\sum \epsilon_{abc} \Lambda^I U^{(A)I} Y^I \\ \phi^{mr} &= \sum \phi^{(mr)I} Y^I\,. \end{aligned} \tag{3.30}$$

In what follows, the main focus will be on the AdS_3 vector fields $Z^{(A=6)I}_\mu \equiv Z^{(6)I}_\mu$ and $Z^{(A=7)I}_\mu \equiv Z^{(7)I}_\mu$, obtained by expanding in S^3 harmonics the field strengths G^6 and G^7 introduced in (3.24).

[2] This step allows us to use Eq. (3.44) in the form given.

3.4 Constructing the supercharged holographic dictionary

In this section we review the single-particle basis and use it derive the correspondence between the operators of interest and their dual bulk fields. In Section 3.4.1 we discuss how the single-particle basis can be used to determine most, but not all, of the mixing between single and multi-trace operators from CFT arguments alone. In Section 3.4.2 we compute the gauge-invariant fluctuations of supergravity fields that are dual to the CFT operators of interest. In Section 3.5 we derive the holographic map in the sector we study, in the single-particle basis. This involves resolving the operator mixing by combining and refining the results of [1] and [107]. In Section 3.5.1 we then generate the superdescendants within this supermultiplet that we use in the remainder of the work. In Section 3.5.2 we record the explicit holographic dictionary in the single-particle basis for convenient reference.

3.4.1 Single-particle operator basis

AdS/CFT duality relates AdS fields and boundary CFT operators through a matching of the observables of the theories; we shall focus on protected correlation functions, which can be compared between supergravity and the orbifold CFT.

On the bulk side, correlation functions can be computed by dimensionally reducing the 6D Lagrangian on S^3: the AdS_3 action takes the schematic form

$$S_{AdS_3} \sim \int_{AdS_3} \Big(\mathcal{L}_2 + \mathcal{L}_3 + \cdots \Big) \tag{3.31}$$

where $\mathcal{L}_n$ contains the interactions between n KK modes and is relevant for computing n-point functions and higher.

The first ingredient in the holographic dictionary is the identification of the quantum numbers of the fields and the dual operators. With linear field redefinitions one can diagonalize the quadratic term $\mathcal{L}_2$, and thus identify the quantum numbers that the CFT operators dual to each supergravity field must carry.

On the CFT side, however, there are degeneracies: in general there are single and multi-trace operators with the same quantum numbers. A further complication in the AdS_3 case (which is absent, for example, in the long-studied case of AdS_5) comes from the fact that there are degeneracies also between the single-traces: as discussed in Section 2.4, the chiral primaries Σ_3 and Ω cannot be distinguished by their quantum numbers.

In order to identify the mixing matrix, one must analyze the three-point functions on both sides of the duality [120, 135–137]. On the gravity side, these are generated by considering the cubic Lagrangian $\mathcal{L}_3$. The cubic Lagrangian was derived in [137] and a priori involves derivative couplings. It was shown, however, that the derivative couplings can

be reabsorbed via a non-linear redefinition of the fields. While this transformation does not change non-extremal three-point functions, it has been emphasized in [108, 109, 116] that extremal three-point functions require special attention. An important fact is that non-derivative extremal cubic couplings vanish. This is no coincidence: in the extremal case, the spacetime integral that occurs in the Witten diagram diverges, so the extremal coupling must vanish in order to avoid a divergence in the value of the correlator. The extremal correlator can still gain contributions from the derivative couplings in the Lagrangian, since they give rise to boundary terms upon partial integration [108]. The field redefinition, however, removes the derivative terms and thus all extremal three-point functions vanish.

The bulk field redefinition is interpreted on the CFT side as a change of basis [109], since it amounts to forming an admixture between the operator dual to the original field and certain multi-trace operators. By AdS/CFT, in this basis all CFT extremal three-point functions vanish. Let us denote by Φ^i the AdS field with respect to which the Lagrangian contains derivative terms, and let us denote its CFT dual by $\mathcal{O}^{\Delta_i}$. Then the operator $\tilde{\mathcal{O}}^{\Delta_i}$ dual to the redefined field $\tilde{\Phi}^i$ will take the form:

$$\tilde{\mathcal{O}}^{\Delta_i} = \mathcal{O}^{\Delta_i} + \frac{1}{\sqrt{N}} \sum_k c_{ik} \mathcal{O}^{\Delta_i - \Delta_k} \mathcal{O}^{\Delta_k} + \dots \,, \tag{3.32}$$

where the ellipses denote other double-traces or higher multi-trace operators, the only constraint being that they must have the same quantum numbers as the operator $\mathcal{O}^{\Delta_i}$. Note that the operators $\mathcal{O}_i^{\Delta}$ and $\tilde{\mathcal{O}}_i^{\Delta}$ coincide if $\Delta_i = 1$, as at dimension one the spectrum of the theory consists only of single-trace operators.

In generic correlators, the contribution of the double-trace operators to the correlator is subleading in the $1/N$ expansion (see e.g. the discussions in [107, 108]). This is the CFT version of the bulk statement that the field redefinition $\Phi^i \to \tilde{\Phi}^i$ leaves non-extremal correlators unchanged. However for certain correlators, the double-traces contribute at leading order in large N. This happens in extremal correlators and also in certain (non-extremal) mixed heavy-light correlators. In this work we are interested in precisely such mixed heavy-light correlators.

In recent work it was proposed that single-particle supergravity excitations around global $AdS_5 \times S^5$ are dual to CFT operators (in short multiplets) that are orthogonal to all multi-trace operators [126]. This was then extensively used in [127] to discuss the properties of the single-particle operator basis in free $\mathcal{N} = 4$ SYM.[3]

We now argue that the redefinition that removes cubic couplings gives rise to precisely the same set of single-particle CFT operators defined as those that are orthogonal to all multi-trace operators. We follow in part the discussions in [108, 139]. First of all, we recall that conformal symmetry implies that a two-point function can be non-zero only

[3] See also [138] for further discussion.

if the two operators have the same dimension. To show that an operator with dimension k_1 is a single-particle operator, we must therefore show that it has vanishing two point function with all multi-traces $\big(\mathcal{O}_{k_2}\mathcal{O}_{k_3}\big)(z)$ such that $k_1 = k_2 + k_3$. The first non-singular term in the OPE $\mathcal{O}_{k_2}(z_2)\mathcal{O}_{k_3}(z_3)$, with coefficient one, is the multi-trace $\big(\mathcal{O}_{k_2}\mathcal{O}_{k_3}\big)(z_2)$. Now consider the extremal ($k_1 = k_2 + k_3$) three-point function (the coefficient c is zero in this basis however we keep it for convenience)

$$\langle \mathcal{O}_{k_1}(z_1)\mathcal{O}_{k_2}(z_2)\mathcal{O}_{k_3}(z_3)\rangle \;=\; \frac{c}{(z_1-z_2)^{2k_2}(z_1-z_3)^{2k_3}}\,. \tag{3.33}$$

By taking the $z_2 \to z_3$ limit (which is smooth at extremality) one obtains

$$\langle \mathcal{O}_{k_1}(z_1)\big(\mathcal{O}_{k_2}\mathcal{O}_{k_3}\big)(z_2)\rangle \;=\; \frac{c}{(z_1-z_2)^{2k_1}}\,. \tag{3.34}$$

This shows the equivalence of the single-particle CFT basis of [126, 127] and the CFT basis dual to supergravity fields with derivative cubic couplings removed. The vanishing of the three-point coefficient c in (3.33) implies the orthogonality between the operator $\mathcal{O}_{k_1}$ and all multi-particle operators in Eq. (3.34), and vice versa[4].

Before proceeding to our analysis let us make a few comments on the derivation of the holographic dictionary for scalar operators of dimension two in Chapter 2. In that chapter we did not use the single-particle basis, however we shall use the single-particle basis in the present work, so let us describe the difference in the two approaches.

The method used in Chapter 2 was as follows. First, the most general linear combination of single and double-trace operators allowed by the quantum numbers was worked out (higher multi-trace operators are trivially absent at dimension two). Then a set of different backgrounds were considered, for which there was already a well-established holographic description (the two-charge Lunin-Mathur solutions [47]). CFT expectation values of these light fields in a selection of these heavy states were then matched to the expansion of the dual bulk fields identified in [54] and [55]. By considering an exhaustive set of examples, the combinations of single and multi-trace operators in the CFT dual to certain supergravity fluctuations were fixed, as were the overall normalization coefficients of the holographic dictionary in this sector.

In the present project we work in the single-particle basis. In this basis, the identification of the single-particle operators partially reduces to the identification of the operators

[4]Following this discussion, in order to make contact with the AdS_5 literature, we find it useful to modify the definition of the multi-trace operators given in Eq. (2.39). In this section we will define scalar multi-trace operators of dimension two as follows:

$$\begin{aligned}
(\Sigma_2\cdot\Sigma_2)^{++} \;&\equiv\; \frac{2}{N^2}\sum_{(r<s),(p<q)}\sigma^{++}_{(rs)}\sigma^{++}_{(pq)}\,, \qquad & (J\cdot\tilde{J})^{++} \;&\equiv\; \frac{1}{N}\sum_{r,s}J^{+}_{(r)}\tilde{J}^{+}_{(s)}\,,\\
(\Sigma_2\cdot O)^{++} \;&\equiv\; \frac{\sqrt{2}}{N^{3/2}}\sum_{\substack{r<s\\ t}}\sigma^{++}_{(rs)}O^{++}_{(t)}\,, \qquad & (O\cdot O)^{++} \;&\equiv\; \frac{1}{N}\sum_{r,s}O^{++}_{(r)}O^{++}_{(s)}
\end{aligned} \tag{3.35}$$

that have the property that all their extremal three point functions vanish. This is purely a CFT computation, which works as an input in constructing the holographic dictionary. Importantly, this does not resolve all the mixing, as we shall discuss shortly.

3.4.2 Gauge-invariant combinations of supergravity fields

We now determine the gauge-invariant combinations of supergravity fluctuations that are dual to the operators we consider.

Not all the fluctuations in the KK harmonic expansion (3.30) are independent: some of them are connected to the background fields or to other fluctuations through small coordinate transformations. For instance, consider the vacuum state, which corresponds to empty global $AdS_3\times S^3$. If one performs a change of coordinates that dies off at infinity, one can turn on some of the AdS_3 fields in the KK harmonic expansion (3.30). Of course these are not physical excitations and there are no boundary operators that source them.

In the study of the KK spectrum in [128], the authors dealt with this redundancy by fixing the (de Donder) gauge. Here we follow instead the gauge-invariant KK reduction method developed in [115]. The strategy is to organize the AdS_3 fields in combinations that have the correct transformation properties under a gauge transformation.

The coordinate transformation

$$x^M \to x'^M = x^M - \xi^M \tag{3.36}$$

generates a perturbation of the metric and three-form which, up to linear order in the gauge parameter, reads

$$\begin{aligned} \delta h_{MN} &= D_M\xi_N + D_N\xi_M + D_M\xi^R h_{RN} + D_N\xi^R h_{RM} + \xi^R D_R h_{MN}\,, \\ \delta g^A_{MNP} &= 3D_{[M}\xi^R g^{oA}_{NP]R} + 3D_{[M}\xi^R g^A_{NP]R} + \xi^R D_R g^A_{MNP}\,. \end{aligned} \tag{3.37}$$

In order to deal with the non-linear terms, one must project onto the basis of S^3 harmonics.

As we will discuss in Section 3.5.2, to study supercharged superstrata we will need to construct the holographic dictionary for the AdS_3 vector fields $Z^6_{k=1}$ and $Z^7_{k=1}$. The operators dual to $Z^{(6)k=1}$ and $Z^{(7)k=1}$ have dimension 3: in principle, we would need the transformation up to second order in the gauge parameter [140, 141], namely the terms quadratic in ξ and linear in $g^{0(A)}$. However, since $g^{0(A)} = 0$ for $A \neq 5$, these terms do not contribute in the analysis of the vector fields in the tensor multiplets and so the gauge-invariant combinations up to the order we are interested in can be obtained using Eq. (3.37). Using the KK spectrum (3.30) together with the decomposition of ξ^M in

harmonics,

$$\xi_\mu = \sum_I \xi^I_\mu Y^I\,, \qquad \xi_a = \sum_{I,J} \xi^I_v Y^I_a + \xi^J_s D_a Y^J\,, \tag{3.38}$$

one obtains that under a small diffeomorphism, the second order transformation of $Z^{(6)k=1}$ and $Z^{(7)k=1}$ reads (here $A \neq 5$, so for us $A = 6, 7$):

$$\begin{aligned}\delta Z^{(A)K}_\mu &= D_\mu U^{(A)J}\big[\xi^I_s(n^v_{IJK} + c^v_{IJK}) + \xi^I_v(p^v_{IJK} + g^v_{IJK})\big] \\ &\quad - \frac{E_{JIK}}{\lambda_k}\big[D_\mu \xi^{I\nu} D_\nu U^{(A)J} + \xi^{I\nu} D_\nu D_\mu U^{(A)J}\big] - \frac{\Lambda_k E_{KIJ}}{\lambda_k^2}\epsilon_{\mu\nu\rho}\xi^{I\nu} D_\rho U^{(A)J} \\ &\quad - \frac{\Lambda_j U^{(A)J}}{\lambda_k}\big[D_\mu \xi^I_v f_{IJK} + D_\mu \xi^I_s E_{IJK}\big]\,,\end{aligned} \tag{3.39}$$

where the degree k associated with the multi-index K must be equal to 1 in order for the equality to hold. The triple overlap coefficients $n^v_{IJK}, c^v_{IJK}, p^v_{IJK}, g^v_{IJK}, E_{IJK}$ are defined in Appendix A.1.3.

The gauge-invariant combination associated with the ($A \neq 5$) field $Z^{(A),k=1}_\mu$ will take the form $\mathbf{Z}^{(A),k=1}_\mu = Z^{(A),k=1}_\mu + \ldots$, where the ellipses represent fields and product of fields such that their transformation properties compensate those on the right-hand side of (3.39), such that the redefined field has the correct transformation properties. With this aim, we consider linear-order variations of

$$\begin{aligned} h_{(ab)} &= \sum_{I,J,K} \rho^I_t Y^I_{ab} + \rho^J_v D_{(a} Y^J_{b)} + \rho^K_s D_{(a} D_{b)} Y^K\,, \\ h_{\mu a} &= \sum_{I,J} h^{v,I}_\mu Y^I_a + h^{s,J}_\mu D_a Y^J\,, \end{aligned} \tag{3.40}$$

where (ab) denotes symmetric traceless. The transformations read:

$$\begin{aligned} \delta h_{(ab)} &= D_a\xi_b + D_b\xi_a = 2\xi^I_v D_{(a} Y^I_{b)} + 2\xi^J_s D_{(a} D_{b)} Y^J\,, \\ \delta h_{\mu a} &= D_\mu \xi_a + D_a \xi_\mu = D_\mu \xi^I_v Y^I_a + (D_\mu \xi^J_s + \xi^J_\mu) D_a Y^J\,. \end{aligned} \tag{3.41}$$

We thus obtain

$$\delta\rho^I_v = 2\xi^I_v\,, \qquad \delta\rho^I_s = 2\xi^I_s\,, \qquad \delta\hat{h}^{s,I}_\mu = \xi^I_\mu\,, \qquad \delta h^{v,I}_\mu = D_\mu \xi^I_v\,, \tag{3.42}$$

where we have defined $\hat{h}^{s,I}_\mu = h^{s,I}_\mu - \frac{1}{2} D_\mu \rho^I_s$. One can further check that the fields $U^{(A\neq 5)k=1}$ are gauge invariant, so one has (again for $A \neq 5$)

$$\begin{aligned}\mathbf{Z}^{(A)K}_\mu &= Z^{(A)K}_\mu + \frac{E^{JIK}}{\lambda_k}(\hat{h}^{s,I,\nu} D_\nu D_\mu U^{(A)J} + D_\mu \hat{h}^{s,I,\nu} D_\nu U^{(A)J}) \\ &\quad + \frac{E^{KIJ}}{\lambda_k^2}\epsilon_{\mu\nu\rho}\hat{h}^{s,I,\nu} D_\rho U^{(A)J} + \frac{\Lambda_j U^{(A)J}}{\lambda_k}(\frac{1}{2} D_\mu \rho^I_v f^{IJK} + \frac{1}{2} D_\mu \rho^I_s E^{IJK}) \\ &\quad - D_\mu U^{(A)J}(\frac{1}{2}\rho^I_s n^v_{IJK} + \frac{1}{2}\rho^I_v p^v_{IJK} + \frac{1}{2}\rho^I_s c^v_{IJK} + \frac{1}{2}\rho^I_v g^v_{IJK})\,.\end{aligned} \tag{3.43}$$

In the following sections, we will also review the holographic dictionary for CPOs of dimension one and scalar chiral primaries of dimension two. Discussing this dictionary in an explicit gauge-invariant fashion requires studying the gauge-invariant combinations associated to other fields. In practise however, it is often convenient to partially fix the gauge and use the holographic dictionary in a preferred system of coordinates, and we will do this explicitly in Appendix E.

3.5 Refining the existing holographic dictionary

The action for the AdS_3 fields is obtained by substituting the KK harmonic expansion (3.30) into the six-dimensional Lagrangian. This procedure leads to a three-dimensional Lagrangian which has a non-diagonal mass matrix. The duality between 3D fields and operators prescribes that the dimension of the operator corresponds to the energy of the bulk excitation. Thus in order to identify the AdS fields dual to the operator of the D1-D5 CFT, one must perform the linear field redefinition that diagonalizes the mass matrix.

Moreover, as discussed in Section 3.4.1, by performing quadratic field redefinitions it is possible to recast the cubic Lagrangian into a form with no derivative couplings: this corresponds to the basis of single-particle excitations. For a general discussion we refer to [128, 137]; here we just discuss the AdS fields that will enter the holographic dictionary we are going to construct. Recall that in [128, 137] the KK spectrum has been studied in de Donder gauge, while we are interested in a gauge independent discussion. It follows from [115] that this can be obtained by simply replacing the fields with the corresponding gauge-invariant combination: in the following, unless explicitly stated, this replacement will be understood.

The field redefinitions that diagonalize the linearized field equations are ($r = 6, 7$)

$$\begin{aligned} s_I^{(r)k} &= \frac{\sqrt{k}}{\sqrt{k+1}}\big(\phi_I^{(5r)k} + 2(k+2)U_I^{(r)k}\big)\,, \\ \sigma_I^k &= \frac{\sqrt{k(k-1)}}{3\sqrt{k+1}}\big(6(k+2)U_I^{(5)k} - \pi_I^k\big)\,, \\ A_{I\mu}^{(\pm)k} &= \pm 2Z_{I\mu}^{(5)(\pm)k} - h_{I\mu}^{(\pm)k}, \qquad Z_{I\mu}^{(r)k} \to 4\sqrt{k+1}Z_{I\mu}^{(r)k}\,, \end{aligned} \tag{3.44}$$

where the superscripts $(\pm)$ are used to distinguish the fields that couple to left $(+)$ and right $(-)$ $SU(2)$ vector harmonics. The overall k-dependent factors are needed to canonically normalize the quadratic Lagrangian [137]. These fields have masses:

$$m^2_{s^{(r)k}} = m^2_{\sigma^k} = k(k-2)\,, \qquad m_{A^{(\pm)k}} = k-1\,, \qquad m_{Z^{(r)k}} = k+1\,. \tag{3.45}$$

Restriction to fields with low k

We focus on the low-order fields, in particular we shall restrict to $s^{(r)k}$ with $k = 1, 2$; σ^k with $k = 2$; $A^{(\pm)k}$ with $k = 1$; and $Z^{(r)k}$ with $k = 1$. Among these fields, only $\sigma^{k=2}$ has a cubic coupling involving derivatives: the equation of motion reads[5]

$$\Box\sigma_I^{(k=2)} = \frac{11}{12\sqrt{2}} \sum_{r=6,7} \big(s_i^{r(k=1)} s_j^{r(k=1)} - D_\mu s_i^{r(k=1)} D^\mu s_j^{r(k=1)}\big) a_{Iij}\,, \tag{3.46}$$

where a_{Iij} is defined as the following triple overlap in Eq. (A.9).

Following the discussion in Section 3.4.1, we wish to remove the derivative couplings, which can be done with the following field redefinition:

$$\sigma_I^{(k=2)} \;\to\; \tilde{\sigma}_I^{(k=2)} = \sigma_I^{(k=2)} + \frac{11}{24\sqrt{2}} \sum_{r=6,7} s_i^{r(k=1)} s_j^{r(k=1)} a_{Iij}\,. \tag{3.47}$$

We now identify the single-particle operators of the D1-D5 CFT that are dual to the fields in Eqs. (3.44) and (3.47). At dimension one there are no multi-trace operators, nor there are degeneracies among the single traces, so the basis of single-trace and single-particle operators coincide. The explicit dictionary for these fields was derived in [103] and is recorded in Table 3.2 below.

For dimension two operators the situation is more complicated, as follows. The spectrum of single-trace CPOs discussed in Section 2.3 splits into two subsectors, according to the quantum numbers. The supergravity theory has an $SO(n)$ symmetry that acts on the tensor multiplets. However, in the full string theory theory, only an $SO(n-1)$ subgroup is preserved [107]. From a CFT point of view, the symmetry breaking to $SO(n-1)$ is related with a marginal deformation (see e.g. [142] for a discussion on the marginal deformation of the D1-D5 CFT) that connects the orbifold point with the supergravity point in the moduli space. This means that the dimension two operator O_2 can only mix with the double trace $(\Sigma_2 \cdot O)$. By contrast, since Σ_3 and Ω are scalars under this $SO(n-1)$, they mix with each other and with the multi-traces $(\Sigma_2 \cdot \Sigma_2)$, $(J \cdot \bar{J})$ and $(O \cdot O)$. This has been explicitly verified in [1] (see Chapter 2).

We have already observed around Eq. (2.59) that all extremal three-point functions involving the operator $\tilde{O}_2$ introduced in Section 2.3.1 vanish. This implies that the single-particle CPO in the first of these subsectors is [1]

$$\tilde{O}_2^{++} = \Big(\frac{\sqrt{2}\, O_2^{++}}{N} - \frac{1}{\sqrt{N}} (\Sigma_2 \cdot O)^{++}\Big). \tag{3.48}$$

The coefficient in front of O_2^{++} is chosen such that this first term on the right-hand side is a unit-normalized operator in the large N limit. Since $(\Sigma_2 \cdot O)$ is unit-normalized at

[5] This is [54, Eq. (5.8)] with implemented $SO(h^{1,1}(\mathcal{M}) + 1)$ invariance.

large N, the full operator $\tilde{O}_2^{++}$ also has unit norm at large N. We observe that the mixing coefficient between the unit-normalized operators scales as $1/\sqrt{N}$. We will see that this is a general feature of all the examples we study.[6] As noted above, in generic correlators the multi-trace contribution is subleading at large N, however in extremal or certain heavy-light correlators it can contribute at leading order in large N. We note that for this operator, all coefficients are fixed from CFT considerations: this is a consequence of the fact that there is no degeneracy among single trace operators in this sector.

In the second subsector, Σ_3 and Ω mix among themselves, and also with the multi-traces $(\Sigma_2 \cdot \Sigma_2)$, $(J \cdot \bar{J})$ and $(O \cdot O)$. CFT considerations alone are not sufficient to identify the two individual single-particle CPOs: if one imposes orthonormality and orthogonality with all multi-traces, one is left with a one-parameter family of possible pairs of candidate single-particle operators. We discuss this and the following steps in more detail in Appendix D. To proceed, we fix the mixing among the single-traces Σ_3 and Ω using additional information from comparison with supergravity, using the mixing matrix derived in [107]. Once we incorporate this single-trace mixing, imposing orthonormality and orthogonality with all multi-traces determines all the remaining admixture coefficients, resulting in the single-particle operators:

$$\begin{aligned}
\tilde{\Sigma}_3^{++} &\equiv \frac{3}{2}\left[\left(\frac{\Sigma_3^{++}}{N^{\frac{3}{2}}} - \frac{\Omega^{++}}{3N^{\frac{1}{2}}}\right) + \frac{1}{N^{\frac{1}{2}}}\left(-\frac{2}{3}(\Sigma_2\cdot\Sigma_2)^{++} + \frac{1}{6}(O\cdot O)^{++} + \frac{1}{3}(J\cdot\bar{J})^{++}\right)\right], \\
\tilde{\Omega}^{++} &\equiv \frac{\sqrt{3}}{2}\left[\left(\frac{\Sigma_3^{++}}{N^{\frac{3}{2}}} + \frac{\Omega^{++}}{N^{\frac{1}{2}}}\right) + \frac{1}{N^{\frac{1}{2}}}\left(-(\Sigma_2\cdot\Sigma_2)^{++} - \frac{1}{2}(O\cdot O)^{++} - (J\cdot\bar{J})^{++}\right)\right].
\end{aligned} \tag{3.49}$$

Let us make a similar comment on the factors of N and numerical coefficients in Eq. (3.49). The linear combinations of the single-particle operators inside Σ_3^{++} and Ω^{++} ensure that these single-trace combinations (and thus the full single-particle operators) are orthonormal in the large N limit, as we discuss in more detail in Appendix D. Again the admixture coefficients between the unit-normalized single-traces and multi-traces are of order $1/\sqrt{N}$; in generic correlators the contributions from the multi-traces are subleading; but in extremal or certain heavy-light correlators, the multi-traces contribute at leading order in large N.

We now make two observations. We note that in this work, the coefficients of the multi-traces have been derived from a purely CFT calculation of orthogonality with all multi-traces. The only direct supergravity input here is the mixing between Ω and Σ_3 derived in [107]. This contrasts with the method of [1] which fixed the multi-trace coefficients holographically. The fact that these two methods agree is non-trivial, and is

[6] The scaling of $1/\sqrt{N}$ per additional trace for the mixing coefficients of multi-trace operators has appeared before in discussions of extremal correlators [107]. Note that in the case of a bound state of N_3 D3 branes giving rise to $SU(N_3)$ $\mathcal{N} = 4$ SYM, the analogous scaling of such admixture coefficients is $1/N_3$ per additional trace (see e.g. [127] and references within).

AdS_3 field	Dual operator	$(j_{\rm sl}, \bar{j}_{\rm sl})$	$(j_{\rm su}, \bar{j}_{\rm su})$
$s^{(6)k=1}$	Σ_2	$(\frac{1}{2}, \frac{1}{2})$	$(\frac{1}{2}, \frac{1}{2})$
$s^{(6)k=2}$	$\tilde{\Sigma}_3$	$(1,1)$	$(1,1)$
$s^{(7)k=1}$	O	$(\frac{1}{2}, \frac{1}{2})$	$(\frac{1}{2}, \frac{1}{2})$
$s^{(7)k=2}$	$\tilde{O}_2$	$(1,1)$	$(1,1)$
$\tilde{\sigma}^{k=2}$	$\tilde{\Omega}$	$(1,1)$	$(1,1)$
$A_\mu^{(+)k=1}$	J	$(1,0)$	$(1,0)$
$A_\mu^{(-)k=1}$	$\bar{J}$	$(0,1)$	$(0,1)$
$Z_\mu^{6(-)k=1}$	$GG\tilde{\Sigma}_3$	$(2,1)$	$(0,1)$
$Z_\mu^{7(-)k=1}$	$GG\tilde{O}_2$	$(2,1)$	$(0,1)$

Table 3.2: This table shows the duality between AdS_3 fields and the CFT operator. We denote with $(j_{\rm sl}, \bar{j}_{\rm sl})$ the quantum numbers associated with the Casimirs of the two copies of $SL(2,\mathbb{R})$ and with $(j_{\rm su}, \bar{j}_{\rm su})$ those associated to the Casimir of the two copies of $SU(2)$

explored further in Appendix E.

Secondly, let us emphasize that the non-trivial mixing between Ω and Σ_3 demonstrates that there is no one-to-one correspondence between k-cycles in the CFT and single-particle supergravity excitations, even at the level of single traces: single-particle states in the bulk are dual to a linear combination of single cycles of the symmetric group (c.f. the discussions in [62, 107]).

3.5.1 Supercharged CFT operators

In the following, we will construct the holographic dictionary for the bosonic 1/8-BPS supercharged descendants of the single-particle operators $\tilde{O}_2$ and $\tilde{\Sigma}_3$. We denote these by $GG\tilde{O}_2$ and $GG\tilde{\Sigma}_3$ respectively, and we obtain:

$$\begin{aligned}
\big(GG\tilde{O}_2\big)^{(0,a)} &\equiv \frac{1}{\sqrt{3}}\big(G^{+1}_{-\frac{1}{2}}G^{+2}_{-\frac{1}{2}} + \frac{1}{2}J_0^+L_{-1}\big)\tilde{O}_2^{-,a} \\
&= \frac{1}{\sqrt{3}}\big(G^{+1}_{-\frac{1}{2}}G^{+2}_{-\frac{1}{2}} + \frac{1}{2}J_0^+L_{-1}\big)\left[\frac{\sqrt{2}\,O_2}{N} - \frac{1}{N^{1/2}}(\Sigma_2\cdot O)\right]^{-,a}, \qquad (3.50)\\
\big(GG\tilde{\Sigma}_3\big)^{(0,a)} &\equiv \frac{1}{\sqrt{3}}\big(G^{+1}_{-\frac{1}{2}}G^{+2}_{-\frac{1}{2}} + \frac{1}{2}J_0^+L_{-1}\big)\tilde{\Sigma}_3^{-,a} \\
&= \frac{\sqrt{3}}{2}\big(G^{+1}_{-\frac{1}{2}}G^{+2}_{-\frac{1}{2}} + \frac{1}{2}J_0^+L_{-1}\big)\left[\left(\frac{\Sigma_3}{N^{\frac{3}{2}}} - \frac{\Omega}{3N^{\frac{1}{2}}}\right) - \frac{1}{N^{\frac{1}{2}}}\left(\frac{2}{3}(\Sigma_2\cdot\Sigma_2) - \frac{1}{6}(O\cdot O) - \frac{1}{3}(J\cdot\bar{J})\right)\right]^{-,a}.
\end{aligned}$$

The overall numerical coefficients follow from Eqs. (3.9), (3.48) and (3.49) and are required to normalize the operators to one at large N. Being descendants of single-particle operators, they are orthogonal to all multi-trace operators. They carry quantum numbers $(j_{\rm sl}, \bar{j}_{\rm sl}) = (2,1)$ associated with the Casimirs of the two copies of $SL(2,\mathbb{R})$ and

quantum numbers $(j_{\rm su}, \bar{j}_{\rm su}) = (0, 1)$ associated to the Casimirs of $SU(2)_L \times SU(2)_R$ (we refer the reader to Appendix A for explicit definitons).

Using the relation between the mass m of a field in AdS_{d+1} and the dimension of the dual operator (see for example [100]) one can identify the map between single-particle operators and AdS_3 fields. The residual degeneracy between $s^{(6)k=2}$ and $\tilde{\sigma}^{k=2}$ can be fixed by comparing non-extremal three-point functions [107]: $s^{(6)k=2}$ is dual to $\tilde{\Sigma}_3$ and $\tilde{\sigma}^{k=2}$ is dual to $\tilde{\Omega}$. These results are recorded in Table 3.2.

3.5.2 Refined holographic dictionary at dimension one and two

For convenient reference we now record the holographic dictionary for CPOs of dimension one and scalar CPOs of dimension two derived in [1, 54, 55, 103], after having recasted it in the single-particle basis. The dictionary relates the asymptotic expansion of the AdS_3 fields in a non-trivial background with the expectation value of the dual operators $\mathcal{O}$ in the dual heavy CFT state $|H\rangle$,

$$\langle \mathcal{O} \rangle \;\equiv\; \langle H | \, \mathcal{O}(\tilde{t}, \tilde{y}) \, | H \rangle \;, \tag{3.51}$$

where $(\tilde{t}, \tilde{y})$ is a generic insertion point on the CFT cylinder. We remind the reader that the coordinates $\tilde{r}, \tilde{t}$ and $\tilde{y}$ are defined in Eq. (3.28).

For scalars, the holographic prescription relates the expectation value of a scalar operator of dimension Δ with the coefficient of $\tilde{r}^{-\Delta}$ of the large $\tilde{r}$ expansion of the dual scalar field. The mass of the scalar fields $s^{(r)k}$ and σ^k in Eq. (3.45) implies that their dual operators have dimension $\Delta = k$. This motivates introducing the following asymptotic expansion of scalar fields: we denote with $\left[\Phi_k\right]$ the first non-vanishing term[7] of the expansion of the scalar field Φ_k,

$$\Phi_k \;=\; \frac{\left[\Phi_k\right]}{\tilde{r}^k} + O(\tilde{r}^{-(k+1)}) \,. \tag{3.52}$$

Similarly, for the one-forms $A^{a(\pm)}_{k=1}$ we expand as [54, 143]

$$A^{a(\pm)}_{k=1} \;=\; \left[A^{a(\pm)}_{k=1}\right](d\tilde{t} \pm d\tilde{y}) + O(\tilde{r}^{-1}) \,. \tag{3.53}$$

[7]Here we are restricting our attentions to solutions describing heavy states within the same holographic CFT, rather than deformations of the holographic CFT, i.e. when there are no non-normalizable modes.

We then have the dictionary

$$\begin{aligned}
&\frac{\sqrt{2}}{N}\langle\Sigma_2^{\alpha\dot\alpha}\rangle = (-1)^{\alpha\dot\alpha}\frac{\sqrt{N}}{\sqrt{2}}\Big[s_{k=1}^{(6)(-\alpha,-\dot\alpha)}\Big], && \frac{1}{\sqrt{N}}\langle O^{\alpha\dot\alpha}\rangle = (-1)^{\alpha\dot\alpha}\frac{\sqrt{N}}{\sqrt{2}}\Big[s_{k=1}^{(7)(-\alpha,-\dot\alpha)}\Big],\\
&\frac{1}{\sqrt{N}}\langle J^{\pm}\rangle = -\frac{\sqrt{N}}{\sqrt{2}}\Big[A_{k=1}^{\mp(+)}\Big], && \frac{1}{\sqrt{N}}\langle \bar J^{\pm}\rangle = -\frac{\sqrt{N}}{\sqrt{2}}\Big[A_{k=1}^{\mp(-)}\Big],\\
&\frac{1}{\sqrt{N}}\langle J^{3}\rangle = -\frac{\sqrt{N}}{2}\Big[A_{k=1}^{0(+)}\Big], && \frac{1}{\sqrt{N}}\langle \bar J^{3}\rangle = -\frac{\sqrt{N}}{2}\Big[A_{k=1}^{0(-)}\Big],\\
&\langle\tilde O_2^{a,\dot a}\rangle = (-1)^{a+\dot a}\frac{\sqrt{N}}{\sqrt{2}}\Big[s_{k=2}^{(7)(-a,-\dot a)}\Big], && \langle\tilde\Sigma_3^{a,\dot a}\rangle = (-1)^{a+\dot a}\frac{\sqrt{N}}{\sqrt{2}}\Big[s_{k=2}^{(6)(-a,-\dot a)}\Big],\\
&\langle\tilde\Omega^{a,\dot a}\rangle = -(-1)^{a+\dot a}\frac{\sqrt{N}}{\sqrt{2}}\Big[\tilde\sigma_{k=2}^{(-a,-\dot a)}\Big].
\end{aligned} \tag{3.54}$$

The numerical coefficients and factors of N on the left hand side of each equality are such that the operators are unit-normalized at large N. With this choice, we note that the coefficients in the first and fourth lines of the dictionary respect the $SO(n)$ symmetry between the n tensor multiplets of the supergravity theory.

3.6 Supercharged holographic dictionary

In this section we construct the precision holographic dictionary for the single-particle operators $GG\tilde O_2^{(0,a)}$ and $GG\tilde\Sigma_3^{(0,a)}$ defined in (3.50). We saw in Table 3.2 that the expectation value of these operators corresponds to the bulk asymptotic expansion of the vector fields $Z_\mu^{7(-)k=1}$ and $Z_\mu^{6(-)k=1}$. The linearized equation of motion for these fields is [137]

$$\star\, dZ_k^{(A)(-)} \;=\; -(k+1)Z_k^{(A)(-)}\,, \tag{3.55}$$

for $A = 6, 7$. We note that this is the equation obeyed by the left AdS_3 harmonics $B_{\mathrm{L},l}^{(\pm)l,\bar l}$ in Eq. (A.28), with the identification $l = k+3$. Left vector harmonics on AdS_3 are discussed in Appendix A.2.2: their large $\tilde r$ expansion reads

$$B_{\mathrm{L},l}^{(\pm)l,\bar l} \;\sim\; \frac{d\tilde t + d\tilde y}{\tilde r^{(l-2)}} + O\Big(\frac{1}{r^{l-1}}\Big)\,. \tag{3.56}$$

This motivates, for $k = 1$, the following asymptotic expansion of the bulk fields, where we use the same square bracket notation introduced in the previous subsection for the leading term:

$$Z_{k=1}^{7(a,-)} = \Big[Z_{k=1}^{7(a,-)}\Big]\frac{d\tilde t + d\tilde y}{\tilde r^2} + O\Big(\frac{1}{\tilde r^3}\Big)\,, \qquad Z_{k=1}^{6(a,-)} = \Big[Z_{k=1}^{6(a,-)}\Big]\frac{d\tilde t + d\tilde y}{\tilde r^2} + O\Big(\frac{1}{\tilde r^3}\Big)\,. \tag{3.57}$$

We consider the following ansatz for the dictionary involving supercharged operators

dual to vector fields in the tensor multiplet:

$$\begin{aligned}\left\langle GG\tilde{O}_2^{(0,a)}\right\rangle &= \alpha\Big[Z_{k=1}^{7(a,-)}\Big]\,,\\ \left\langle GG\tilde{\Sigma}_3^{(0,a)}\right\rangle &= \beta\Big[Z_{k=1}^{6(a,-)}\Big]\,.\end{aligned} \tag{3.58}$$

where α and β are unknown coefficients that we will determine by evaluating the ansatz (3.58) on some reference heavy states. Consistency of the dictionary requires that α and β are universal, i.e. they depend neither on the $SU(2)_R$ quantum number a nor on the heavy state considered.

Moreover, based on the $SO(n)$ symmetry between the tensor multiplets of the supergravity theory, one expects to find $\alpha = \beta$, and we shall verify explicitly that this is the case.

3.6.1 Normalizing the supercharged holographic dictionary

In this section we fix the coefficient α in the supercharged holographic dictionary in Eq. (3.58) by looking at one of the simplest examples of supercharged superstrata: the one sourced by the mode $(\mathsf{k},\mathsf{m},\mathsf{n},\mathsf{q}) = (2,1,\mathsf{n},1)$. This supergravity solution was constructed in [62]. Since we work in the conventions of [63], a slightly more convenient reference for the explicit form of the supergravity quantities we need in the following[8] is [63, Eqs. (2.4), (4.1), (4.4), (4.13), (4.14)].

The CFT state that is proposed to be dual to this bulk solution is

$$\sum_p \Big(A\,|0\rangle_1\Big)^{N-2p}\Big(B\frac{L_{-1}^{\mathsf{n}-1}}{(\mathsf{n}-1)!}\big(G^{+1}_{-\frac{1}{2}}G^{+2}_{-\frac{1}{2}}+\frac{1}{2}J_0^+L_{-1}\big)\,\big|O_2^{--}\big\rangle\Big)^p\,. \tag{3.59}$$

The single-particle operator $GG\tilde{O}_2$ has a non-vanishing expectation value on this state, sourced by its single-trace constituent. In order to compute the correlator, we first consider the basic process described by the correlator

$$\begin{aligned}&\big\langle O_2^{++}\big|\Big(-G^{-1}_{\frac{1}{2}}G^{-2}_{\frac{1}{2}}+\frac{J_0^-L_{+1}}{2}\Big)\frac{L_1^{\mathsf{n}-1}}{(\mathsf{n}-1)!}\Big(G^{+1}_{-\frac{1}{2}}G^{+2}_{-\frac{1}{2}}+\frac{J_0^+L_{-1}}{2}\Big)O_2^{--}(\tilde{t},\tilde{y})\,|0\rangle_1^{\otimes 2}\\ &=z^2\bar{z}\,\big\langle O_2^{++}\big|\Big(-G^{-1}_{\frac{1}{2}}G^{-2}_{\frac{1}{2}}+\frac{J_0^-L_{+1}}{2}\Big)\frac{L_1^{\mathsf{n}-1}}{(\mathsf{n}-1)!}\Big(G^{+1}_{-\frac{1}{2}}G^{+2}_{-\frac{1}{2}}+\frac{J_0^+L_{-1}}{2}\Big)O_2^{--}(z,\bar{z})\,|0\rangle_1^{\otimes 2}\,,\end{aligned} \tag{3.60}$$

where we have mapped the one-point function from the cylinder to the plane and inserted the appropriate conformal factor.
Upon expanding, we obtain four terms. The one with four supercharge modes evaluates

[8] In what follows we will label with b the supergravity coefficient that is denoted by c_4 in [63].

to

$$
\begin{aligned}
&-\big\langle O_2^{++}\big|\big(G^{-1}_{\frac12}G^{-2}_{\frac12}\big)\frac{L_1^{\mathsf{n}-1}}{(\mathsf{n}-1)!}\big(G^{+1}_{-\frac12}G^{+2}_{-\frac12}\big)O_2^{--}(z,\bar z)\,|0\rangle_1^{\otimes 2}\\
&\qquad=-\frac{1}{(\mathsf{n}-1)!}\big\langle O_2^{++}\big|\,\big(G^{-1}_{\frac12}G^{-2}_{\frac12}\big)\Big[(\mathsf{n}^2-3\mathsf{n})G^{+2}_{\frac12}G^{+1}_{\frac12}L_1^{\mathsf{n}-3}+(\mathsf{n}-1)G^{+2}_{\frac12}G^{+1}_{-\frac12}L_1^{\mathsf{n}-2}\\
&\qquad\qquad+(\mathsf{n}-1)G^{+2}_{-\frac12}G^{+1}_{\frac12}L_1^{\mathsf{n}-2}+G^{+1}_{-\frac12}G^{+2}_{-\frac12}L_1^{\mathsf{n}-1}\Big]O_2^{--}(z,\bar z)\,|0\rangle_1^{\otimes 2}\\
&\qquad=\frac{(\mathsf{n}^2+2\mathsf{n}+1)}{(\mathsf{n}-1)!}\big\langle O_2^{++}\big|\,L_1^{\mathsf{n}-1}O_2^{--}(z,\bar z)\,|0\rangle_1^{\otimes 2}\ ,
\end{aligned}
\tag{3.61}
$$

where we have used the anomaly-free algebra (3.2). By similar standard manipulations the other three terms evaluate to

$$
-\frac{1}{2(\mathsf{n}-1)!}\big\langle O_2^{++}\big|\,L_1^{\mathsf{n}}L_{-1}O_2^{--}(z,\bar z)\,|0\rangle\ =\ \frac{\mathsf{n}(\mathsf{n}+1)}{(\mathsf{n}-1)!}\big\langle O_2^{++}\big|\,L_1^{\mathsf{n}-1}O_2^{--}(z,\bar z)\,|0\rangle_1^{\otimes 2}\ .
\tag{3.62}
$$

We note that the commutation relation between L_1^{n} and a primary with left dimension h is

$$
[L_1^{\mathsf{n}},O_h]\ =\ \sum_{m=0}^{\mathsf{n}}\frac{\mathsf{n}!}{(\mathsf{n}-m)!m!}w^{\mathsf{n}+m}\frac{(2h+\mathsf{n}-1)!}{(2h+m-1)!}\partial^m O_h\,.
\tag{3.63}
$$

Collecting all terms and using (3.60) and (3.63) we obtain

$$
\begin{aligned}
&\big\langle O_2^{++}\big|\big(-G^{-1}_{\frac12}G^{-2}_{\frac12}+\frac12 J_0^-L_{+1}\big)\frac{L_1^{\mathsf{n}-1}}{\mathsf{n}-1!}\big(G^{+1}_{-\frac12}G^{+2}_{-\frac12}+\frac12 J_0^+L_{-1}\big)O_2^{--}(\tilde t,\tilde y)\,|0\rangle_1^{\otimes 2}\\
&\qquad=\frac{\mathsf{n}(\mathsf{n}+1)(\mathsf{n}+2)}{2}e^{i((\mathsf{n}+2)\tilde t+\mathsf{n}\tilde y)}\,.
\end{aligned}
\tag{3.64}
$$

This basic process describes the contribution to the expectation value of the single-particle operator when it acts on two copies of the CFT vacuum. We now use this to compute the effect of the single-particle operator acting on the full state (3.59). To do so, we must compute a combinatorial factor, as we shall describe momentarily. Combining the amplitude in (3.64) with this combinatorial factor, the relevant contribution is represented by

$$
\begin{aligned}
&GG\tilde O_2^{(0,-)}(\tilde t,\tilde y)\Big[\Big(\,|0\rangle_1^{N-2p}\Big)\Big(\frac{L_{-1}^{\mathsf{n}-1}}{(\mathsf{n}-1)!}\big(G^{+1}_{-\frac12}G^{+2}_{-\frac12}+\frac12 J_0^+L_{-1}\big)\,\big|O_2^{--}\big\rangle\Big)^p\Big]\\
&=\frac{\sqrt{2}(p+1)}{\sqrt{3}N}e^{i((\mathsf{n}+2)\tilde t+\mathsf{n}\tilde y)}\Big[\Big(\,|0\rangle_1^{N-2p-2}\Big)\Big(\frac{L_{-1}^{\mathsf{n}-1}}{(\mathsf{n}-1)!}\big(G^{+1}_{-\frac12}G^{+2}_{-\frac12}+\frac12 J_0^+L_{-1}\big)\,\big|O_2^{--}\big\rangle\Big)^{p+1}\Big]\,.
\end{aligned}
\tag{3.65}
$$

The factors in (3.65) arise as follows (c.f. [103]). The norm of the states on each side of the equality must match. The factor of $\sqrt{2}/(\sqrt{3}N)$ comes from the normalization of $\tilde O_2$, (3.50). The factor of $(p+1)$ is a combination of a combinatorial factor and the n-dependent factor in (3.64). The norm of the state on the left-hand side (LHS) of the equation is given by the norm of the state in square brackets (on the LHS) multiplied by the number of ways in which the single-particle operator can act on any two of the

$N-2p$ vacua, namely $\binom{N-2p}{2}$. The norm of the states in square brackets on both the LHS and RHS are given in Eq. (3.15). These factors all combine with the n-dependent prefactor in (3.64) to give (3.65).

When we compute the amplitude with the full coherent state (3.59), we obtain an additional factor of A^2/B due to the fact that the process annihilates two A-type strands and creates one B-type strand (c.f. [103, Eq. (4.19)]). Furthermore, we work at large N and with coherent states in which the average $\bar{p}$ is of order N, so we approximate $(\bar{p}+1) \simeq \bar{p}$. We then obtain the amplitude

$$\big\langle GG\tilde{O}_2^{(0,-)}\big\rangle \;=\; \frac{\sqrt{2}\bar{p}}{\sqrt{3}N}\,\frac{A^2}{B}\,e^{i((\mathsf{n}+2)\tilde{t}+\mathsf{n}\tilde{y})}\,. \tag{3.66}$$

From Eq. (3.17), $\bar{p}$ is of order B^2. Using Eqs. (3.17) and (3.27), we obtain the final result for the correlator,

$$\big\langle GG\tilde{O}_2^{(0,-)}\big\rangle \;=\; \sqrt{N}\frac{\mathsf{a}^2\mathsf{b}}{2\sqrt{3}}e^{i((\mathsf{n}+2)\tilde{t}+\mathsf{n}\tilde{y})}\,. \tag{3.67}$$

Since $GG\tilde{O}_2^{(0,+)} = \big(GG\tilde{O}_2^{(0,-)}\big)^\dagger$, the expectation value of the operator $GG\tilde{O}_2^{(0,+)}$ must also be non-vanishing. We thus obtain

$$\big\langle GG\tilde{O}_2^{(0,+)}\big\rangle = \big\langle GG\tilde{O}_2^{(0,-)}\big\rangle^* = \sqrt{N}\frac{\mathsf{a}^2\mathsf{b}}{2\sqrt{3}}e^{-i((\mathsf{n}+2)\tilde{t}+\mathsf{n}\tilde{y})}\,. \tag{3.68}$$

In order to evaluate the coefficient α in Eq. (3.58), we must perform an asymptotic expansion of the gauge-invariant combination $\mathbf{Z}^7_{k=1}$, given in Eq. (3.43). The supergravity solution with modes $(\mathsf{k},\mathsf{m},\mathsf{n},\mathsf{q}) = (2,1,\mathsf{n},1)$ is characterized by $U^7_{k=1}=0$, which implies that the field $Z^7_{k=1}$ that appears in the Kaluza-Klein reduction (3.30) coincides with the gauge-invariant combination $\mathbf{Z}^7_{k=1}$. We thus obtain (recall $\mathsf{n}\geq 1$)

$$\begin{aligned}
\mathbf{Z}^{7(--)}_{k=1} \;&=\; Z^{7(--)}_{k=1} \;=\; -\mathsf{a}^2\mathsf{b}\,e^{-i((\mathsf{n}+2)\tilde{t}+\mathsf{n}\tilde{y})}\,\frac{\tilde{r}^{\mathsf{n}-1}}{(\tilde{r}^2+1)^{\mathsf{n}/2+2}}\Big(+id\tilde{r}+\tilde{r}(\tilde{r}^2+1)(d\tilde{t}+d\tilde{y})\Big)\,,\\
\mathbf{Z}^{7(+-)}_{k=1} \;&=\; Z^{7(+-)}_{k=1} \;=\; -\mathsf{a}^2\mathsf{b}\;e^{i((\mathsf{n}+2)\tilde{t}+\mathsf{n}\tilde{y})}\,\frac{\tilde{r}^{\mathsf{n}-1}}{(\tilde{r}^2+1)^{\mathsf{n}/2+2}}\Big(-id\tilde{r}+\tilde{r}(\tilde{r}^2+1)(d\tilde{t}+d\tilde{y})\Big)\,,
\end{aligned} \tag{3.69}$$

where we recall that the rescaling in Eq. (3.44) has been performed, and where the superscript $(\pm-)$ indicates that the field couples to the $Y^{(\pm-)}$ harmonic respectively. The large $\tilde{r}$ expansion of (3.69) gives

$$\Big[Z^{7(--)}_{k=1}\Big] \;=\; -\mathsf{a}^2\mathsf{b}\,e^{-i((\mathsf{n}+2)\tilde{t}+\mathsf{n}\tilde{y})}\,,\qquad \Big[Z^{7(+-)}_{k=1}\Big] \;=\; -\mathsf{a}^2\mathsf{b}\,e^{i((\mathsf{n}+2)\tilde{t}+\mathsf{n}\tilde{y})}\,. \tag{3.70}$$

Using the ansatz for the holographic dictionary in Eq. (3.58), along with Eqs. (3.67),

(3.68) and (3.70), we obtain

$$\alpha = -\frac{N^{1/2}}{2\sqrt{3}} \,. \tag{3.71}$$

We observe that the value of α is independent of the quantum numbers that specify the state, as required.

3.6.2 Holographic test of general non-supercharged superstrata

We now compute the coefficient β defined in Eq. (3.58) and find that $\alpha = \beta$, verifying the expectation discussed below Eq. (3.58). In doing so, we will also test the coiffuring proposal for general multi-mode superstrata developed in [63, 64]. In the present subsection we test the non-supercharged part of this proposal, and in the following subsection we shall test the hybrid supercharged plus non-supercharged part.

Recall that "coiffuring" refers to imposing a set of algebraic relations on the parameters in the supergravity solution, required for smoothness [124, 125, 144]. A significant achievement of [63] was a proposal for particular families of multi-mode superstrata that had proven impossible to construct with previous methods, as we describe in more detail below. This came as part of a more general proposal for the coiffuring of multi-mode superstrata, where the modes could be either of supercharged or non-supercharged type. This was expressed in a more general holomorphic formalism in [64].

From the supergravity point of view, coiffuring relations are often not easy to give an interpretation to, beyond being a consequence of requiring solutions to be smooth. By contrast, holographic calculations can give a microscopic interpretation to coiffuring relations, as has been done in [1, 103]. We will now test the new type of coiffuring relation proposed in [63, 64], and we will find perfect agreement.

We focus on the family of $(1, \mathsf{m}, \mathsf{n})$ muiltimode non-supercharged superstrata constructed in [132, App, D]. This family of solutions is given in terms of two holomorphic functions F_0, F_1 of a complex variable ξ which is related to the standard six-dimensional coordinates in Eq. (3.3) via

$$\xi \;=\; \frac{\tilde{r}}{\sqrt{\tilde{r}+1}} e^{i(\tilde{t}+\tilde{y})} \,. \tag{3.72}$$

We consider the two-mode solution in which both F_0 and F_1 consist of a single mode,

$$F_0(\xi) \;=\; b\xi^{\mathsf{n}_b} \,, \qquad F_1(\xi) \;=\; d\xi^{\mathsf{n}_d} \,. \tag{3.73}$$

The explicit supergravity solution is given in full detail in [132, Eqs. (D.15)–(D.29)] and we shall not reproduce it here.

The proposed family of dual CFT states is

$$\sum_{p,q}\Big(A\,|0\rangle_1\Big)^{N-p-q}\Big(B\frac{1}{\mathsf{n}_b!}L_{-1}^{\mathsf{n}_b}\,|O^{--}\rangle\Big)^{p}\Big(D\frac{1}{\mathsf{n}_d!}J_0^+L_{-1}^{\mathsf{n}_d}\,|O^{--}\rangle\Big)^{q}. \tag{3.74}$$

The supergravity mode parameters (b,d), the CFT parameters (B,D), and the convenient parameters (b,d) are related as before by Eq. (3.27), which in this specific case takes the form

$$\frac{B}{\sqrt{N}} \;=\; \frac{R}{\sqrt{2\,Q_1Q_5}}b \;=\; \frac{\mathsf{b}}{\sqrt{2}}\,, \qquad \frac{D}{\sqrt{N}} \;=\; \frac{R}{\sqrt{2\,Q_1Q_5}}d \;=\; \frac{\mathsf{d}}{\sqrt{2}}\,. \tag{3.75}$$

When $\mathsf{n}_b\neq\mathsf{n}_d$, this is a class of multimode superstrata where $(\mathsf{k}_b\mathsf{m}_d-\mathsf{k}_d\mathsf{m}_b)(\mathsf{k}_b\mathsf{n}_d-\mathsf{k}_d\mathsf{n}_b)\neq 0$. This is the class of superstrata that had evaded construction since [60] until the proposal of [63]. We have taken $k_b=k_d=1$, since higher values of k_b and/or k_d would require extending the holographic dictionary even further beyond the sector of conformal dimensions that we consider in this work. With $k_b=k_d=1$, this family of states essentially contains the full class of states in which $(\mathsf{k}_b\mathsf{m}_d-\mathsf{k}_d\mathsf{m}_b)(\mathsf{k}_b\mathsf{n}_d-\mathsf{k}_d\mathsf{n}_b)\neq 0$: since $\mathsf{m}\leq\mathsf{k}$, we must have one excited strand with $\mathsf{m}=0$ and one with $\mathsf{m}=1$. Furthermore, once one has control over the general two-mode family (3.73)–(3.74), adding further modes of the same type is a straightforward generalization in both supergravity and CFT.

We start from the CFT side. We shall see that when $\mathsf{n}_b\neq\mathsf{n}_d$, the operator $GG\tilde{\Sigma}_3^{(0,a)}$ has a non-vanishing expectation value in this state. Expanding the definition of $GG\tilde{\Sigma}_3^{(0,a)}$, we have

$$\begin{aligned}\big\langle GG\tilde{\Sigma}_3^{(0,a)}\big\rangle &\equiv \Big\langle\frac{1}{\sqrt{3}}\big(G^{+1}_{-\frac12}G^{+2}_{-\frac12}+\frac12J_0^+L_{-1}\big)\tilde{\Sigma}_3^{-,a}\Big\rangle = \\ &\Big\langle\frac{\sqrt{3}}{2}\big(G^{+1}_{-\frac12}G^{+2}_{-\frac12}+\frac12J_0^+L_{-1}\big)\left[\left(\frac{\Sigma_3}{N^{\frac32}}-\frac{\Omega}{3N^{\frac12}}\right)+\frac{1}{N^{\frac12}}\left(-\frac23(\Sigma_2\cdot\Sigma_2)+\frac16(O\cdot O)+\frac13(J\cdot\bar{J})\right)\right]^{-,a}\Big\rangle.\end{aligned} \tag{3.76}$$

This expectation value is sourced only by the double-trace term (we suppress overall factors and restore them at the end)

$$GG(O\cdot O) \;=\; \frac{1}{N}\Big(G^{+1}_{-\frac12}G^{+2}_{-\frac12}+\frac12J_0^+L_{-1}\Big)\sum_{r,s}O_r^{--}O_s^{--}\,. \tag{3.77}$$

Expanding this product, the GG combination of modes can act either on strand r or strand s, giving rise to eight terms. Two of these terms give rise to fermionic strands, and so do not contribute to the correlator. The remaining terms can be written as

$$\frac{1}{N}\sum_{r,s}\left[-\frac12O_r^{--}\big(J_0^+L_{-1}O_s^{--}\big)+\frac12\big(L_{-1}O_r^{--}\big)\big(J_0^+O_s^{--}\big)\right], \tag{3.78}$$

where we have used the relation $\big(G^{+1}_{-\frac12}G^{+2}_{-\frac12}+J_0^+L_{-1}\big)O^{--}=0$, which holds because O^{--} is a scalar operator of dimension one.

The operator in Eq. (3.78) transforms two copies of the vacuum into one strand of type $|1,0,\mathsf{n}_b,0\rangle$ and another of type $|1,1,\mathsf{n}_d,0\rangle$. We now compute the contribution of this fundamental process. After doing so, we will again dress it with the appropriate combinatorial factor. The initial state is given by two copies of the vacuum $|0\rangle_{r=1}|0\rangle_{r=2}$, which can be transformed into the state $|1,0,\mathsf{n}_b,0\rangle_{r=1}|1,1,\mathsf{n}_d,0\rangle_{r=2}$ or $|1,0,\mathsf{n}_d,0\rangle_{r=1}|1,1,\mathsf{n}_b,0\rangle_{r=2}$: the two processes contribute with equal amplitudes, so we compute only one of them, and multiply the result by two. For ease of notation (and to avoid confusion with the twist-two operator O_2), we shall abbreviate the subscripts $r=1,2$ to $(1),(2)$.

We proceed to compute

$$\begin{aligned}
&{}_{(1)}\langle O^{++}|\frac{L_1^{\mathsf{n}_b}}{\mathsf{n}_b!}\,{}_{(2)}\langle O^{++}|\frac{L_1^{\mathsf{n}_d}}{\mathsf{n}_d!}J_0^-\Big[\big(G^{+1}_{-\frac{1}{2}}G^{+2}_{-\frac{1}{2}}+\frac{1}{2}J_0^+L_{-1}\big)O^{--}_{(1)}O^{--}_{(2)}\Big](\tilde{t},\tilde{y})\;|0\rangle_{(1)}|0\rangle_{(2)}\\
&=z^2\bar{z}\Big[-\frac{1}{2}\,{}_{(1)}\langle O^{++}|\frac{L_1^{\mathsf{n}_b}}{\mathsf{n}_b!}O^{--}_{(1)}(z,\bar{z})\,|0\rangle_{(1)}\;\;{}_{(2)}\langle O^{++}|\frac{L_1^{\mathsf{n}_d}}{\mathsf{n}_d!}J_0^-\big(J_0^+L_{-1}O^{--}_{(2)}\big)(z,\bar{z})\,|0\rangle_{(2)}\\
&\quad+\frac{1}{2}\,{}_{(1)}\langle O^{++}|\frac{L_1^{\mathsf{n}_b}}{\mathsf{n}_b!}\big(L_{-1}O^{--}_{(1)}\big)(z,\bar{z})\,|0\rangle_{(1)}\;\;{}_{(2)}\langle O^{++}|\frac{L_1^{\mathsf{n}_d}}{\mathsf{n}_d!}J_0^-\big(J_0^+O^{--}_{(2)}\big)(z,\bar{z})\,|0\rangle_{(2)}\Big].
\end{aligned}\tag{3.79}$$

Using standard manipulations, together with the commutation relation in Eq. (3.63) and the anomaly-free algebra (3.2), one can rewrite this amplitude as

$$\begin{aligned}
&{}_{(1)}\langle O^{++}|\frac{L_1^{\mathsf{n}_b}}{\mathsf{n}_b!}\,{}_{(2)}\langle O^{++}|\frac{L_1^{\mathsf{n}_d}}{\mathsf{n}_d!}J_0^-\Big[\big(G^{+1}_{-\frac{1}{2}}G^{+2}_{-\frac{1}{2}}+\frac{1}{2}J_0^+L_{-1}\big)O^{--}_{(1)}O^{--}_{(2)}\Big](\tilde{t},\tilde{y})\;|0\rangle_{(1)}|0\rangle_{(2)}\\
&\qquad=\frac{1}{2}\Big[-(\mathsf{n}_d+1)+(\mathsf{n}_b+1)\Big]e^{i(\mathsf{n}_b+\mathsf{n}_d+2)\tilde{t}+i(\mathsf{n}_b+\mathsf{n}_d)\tilde{y}}\\
&\qquad=\frac{1}{2}(\mathsf{n}_b-\mathsf{n}_d)e^{i(\mathsf{n}_b+\mathsf{n}_d+2)\tilde{t}+i(\mathsf{n}_b+\mathsf{n}_d)\tilde{y}}\,.
\end{aligned}\tag{3.80}$$

Already we see that the expectation value is non-zero only when $\mathsf{n}_b\neq\mathsf{n}_d$.

We now dress this with the combinatorial factor as before. The relevant contribution can be represented as

$$\begin{aligned}
&\big(GG(O\cdot O)\big)^{0-}(\tilde{t},\tilde{y})\Big[\Big(|0\rangle_1^{N-p-q}\Big)\Big(\frac{1}{\mathsf{n}_b!}L_{-1}^{\mathsf{n}_b}|O^{--}\rangle\Big)^p\Big(\frac{1}{\mathsf{n}_d!}J_0^+L_{-1}^{\mathsf{n}_d}|O^{--}\rangle\Big)^q\Big]\\
&\qquad=\Big((\mathsf{n}_b-\mathsf{n}_d)e^{i(\mathsf{n}_b+\mathsf{n}_d+2)\tilde{t}+i(\mathsf{n}_b+\mathsf{n}_d)\tilde{y}}\Big)\frac{(p+1)(q+1)}{N}\\
&\qquad\quad\times\Big[\Big(|0\rangle_1^{N-p-q-2}\Big)\Big(\frac{1}{\mathsf{n}_b!}L_{-1}^{\mathsf{n}_b}|O^{--}\rangle\Big)^{p+1}\Big(\frac{1}{\mathsf{n}_d!}J_0^+L_{-1}^{\mathsf{n}_d}|O^{--}\rangle\Big)^{q+1}\Big].
\end{aligned}\tag{3.81}$$

The first term on the RHS is the contribution of the fundamental process, given by twice the result in Eq. (3.80). The second term comes requiring that the normalization of the two sides of the equality are the same. The expectation value of the single-particle operator is then obtained by combining Eq. (3.81) with the normalization factors we suppressed from Eq. (3.76), along with the relation between the CFT and the supergravity

coefficients in Eq. (3.75). This gives

$$\begin{aligned}
\langle GG\tilde{\Sigma}_3^{0-}\rangle &= \frac{1}{8\sqrt{3}N^{1/2}}\langle \big(GG(O\cdot O)\big)^{0-}\rangle \\
&= \frac{1}{4\sqrt{3}}\frac{\bar{p}\,\bar{q}}{N^{3/2}}\frac{A^2}{BD}(\mathsf{n}_b-\mathsf{n}_d)\,e^{i(\mathsf{n}_b+\mathsf{n}_d+2)\tilde{t}+i(\mathsf{n}_b+\mathsf{n}_d)\tilde{y}} \\
&= \frac{\sqrt{N}}{8\sqrt{3}}\mathsf{a}^2\,\mathsf{b}\,\mathsf{d}\,(\mathsf{n}_b-\mathsf{n}_d)\,e^{i(\mathsf{n}_b+\mathsf{n}_d+2)\tilde{t}+i(\mathsf{n}_b+\mathsf{n}_d)\tilde{y}}\,, \qquad (3.82)\\
\langle GG\tilde{\Sigma}_3^{0+}\rangle &= \big(\langle GG\tilde{\Sigma}_3^{0-}\rangle\big)^* \\
&= \frac{\sqrt{N}}{8\sqrt{3}}\mathsf{a}^2\,\mathsf{b}\,\mathsf{d}\,(\mathsf{n}_b-\mathsf{n}_d)\,e^{-i(\mathsf{n}_b+\mathsf{n}_d+2)\tilde{t}-i(\mathsf{n}_b+\mathsf{n}_d)\tilde{y}}\,.
\end{aligned}$$

These CFT expectation values are holographically encoded in the expansion of the gauge-invariant vector field $\mathbf{Z}^6_{k=1}$. The supergravity solution is obtained combining [132, Eqs. (D.15)-(D.29)] with the holomorphic functions F_0 and F_1 in Eq. (3.73). One can check that, as in the example studied in Section 3.6.1, the AdS_3 scalar field $U^6_{k=1}$ vanishes on this background. Eq. (3.43) then implies that $\mathbf{Z}^6_{k=1}=Z^6_{k=1}$. The vector fields are given by

$$\begin{aligned}
Z^{6(+-)}_{k=1} &= \frac{\mathsf{a}^2\,\mathsf{b}\,\mathsf{d}}{4}(\mathsf{n}_d-\mathsf{n}_b)\frac{\tilde{r}^{\mathsf{n}_b+\mathsf{n}_d-1}\,e^{i((\mathsf{n}_b+\mathsf{n}_d+2)\tilde{t}+(\mathsf{n}_b+\mathsf{n}_d)\tilde{y})}}{(1+\tilde{r}^2)^{\frac{(\mathsf{n}_b+\mathsf{n}_d+4)}{2}}}\Big(-id\tilde{r}+\tilde{r}(\tilde{r}^2+1)(d\tilde{t}+d\tilde{y})\Big)\,,\\
Z^{6(--)}_{k=1} &= \frac{\mathsf{a}^2\,\mathsf{b}\,\mathsf{d}}{4}(\mathsf{n}_d-\mathsf{n}_b)\frac{\tilde{r}^{\mathsf{n}_b+\mathsf{n}_d-1}\,e^{-i((\mathsf{n}_b+\mathsf{n}_d+2)\tilde{t}+(\mathsf{n}_b+\mathsf{n}_d)\tilde{y})}}{(1+\tilde{r}^2)^{\frac{(\mathsf{n}_b+\mathsf{n}_d+4)}{2}}}\Big(id\tilde{r}+\tilde{r}(\tilde{r}^2+1)(d\tilde{t}+d\tilde{y})\Big)\,,
\end{aligned} \qquad (3.83)$$

where we have used the normalization in Eq. (3.44) and the relation between the CFT and the supergravity modes in Eq. (3.75).

The coefficient β in Eq. (3.58) is obtained performing the asymptotic expansion (3.57) of the three-dimensional vectors (3.83) and comparing it with the CFT result in Eq. (3.82). We find that

$$\beta=-\frac{N^{1/2}}{2\sqrt{3}}\,, \qquad (3.84)$$

thus explicitly verifying that $\alpha=\beta$.

We emphasize again that this amplitude is non-vanishing only when $n_b\neq n_d$. This can be interpreted as the CFT telling us that for the set of states (3.74), when $n_b\neq n_d$ the bulk solution must involve an extra field that is not turned on when $n_b=n_d$. This is precisely the field that was introduced in the more general coiffuring proposal of [63]. So we have seen that a very non-trivial holographic test of this more general coiffuring is passed.

3.6.3 Holographic test of hybrid supercharged superstrata

At this point we have fixed all coefficients of the holographic dictionary in the sector in which we work. We now use the dictionary to make a precision holographic test of a "hybrid" superstratum solution that combines non-supercharged and supercharged elements. Our computation tests both the proposed holographic dictionary for hybrid superstrata and the supergravity coiffuring procedure for combining non-supercharged and supercharged modes of [63, 64]. This test also serves as an additional non-trivial cross-check of the operator mixing in the dictionary. Note that this operator mixing has already passed thorough holographic tests [1]. The tests in [1] were performed in a different basis to the single-particle basis, however our results are equivalent, as demonstrated in Appendix E. The test that follows involves a non-trivial and delicate cancellation between a set of terms.

We consider the multi-mode hybrid superstratum composed of modes $(\mathsf{k}_1, \mathsf{m}_1, \mathsf{n}_1, \mathsf{q}_1) = (2, 1, 0, 0)$, and $(\mathsf{k}_2, \mathsf{m}_2, \mathsf{n}_2, \mathsf{q}_2) = (2, 1, 1, 1)$, constructed in [64, App. (B.1)]. There, the solution was given in terms of two holomorphic functions F and S of the complex variable ξ defined in Eq. (3.72). In our conventions, we have

$$F(\xi) \;=\; b\,, \qquad S(\xi) \;=\; d\,\frac{\xi}{6}\,. \tag{3.85}$$

The supergravity solution is given explicitly in [64, Eqs. (6.8), (6.9), (B.1)–(B.12)] and so we shall not reproduce it here. Performing the Kaluza-Klein reduction of this background, one obtains that the gauge-invariant field $\mathbf{Z}^6_{k=1}$ in Eq. (3.43) vanishes. The holographic dictionary in Eq. (3.58) then predicts that the expectation values of the single-particle operator $(GG\tilde{\Sigma}_3)^{0a}$ on the dual CFT state must vanish. We will now explicitly check that this is indeed the case.

The proposed dual CFT state is

$$\sum_{p,q} \Big(A\,|0\rangle_1\Big)^{N-2p-2q} \Big(B J_0^+\,|O_2^{--}\rangle\Big)^p \Big(D\big(G^{+1}_{-\frac{1}{2}} G^{+2}_{-\frac{1}{2}} + \frac{1}{2} J_0^+ L_{-1}\big)\,|O_2^{--}\rangle\Big)^q . \tag{3.86}$$

The CFT coefficients (B, D) and the supergravity Fourier coefficients (b, d) in (3.85) are again related via Eq. (3.27), which in the present example becomes

$$\frac{B}{\sqrt{N}} \;=\; \frac{R}{2\sqrt{2\,Q_1 Q_5}}\,b\,, \qquad \frac{D}{\sqrt{N}} \;=\; \frac{R}{3\sqrt{2\,Q_1 Q_5}}\,d\,. \tag{3.87}$$

The only $SU(2)_L \times SU(2)_R$ component of the single-particle operator $(GG\tilde{\Sigma}_3)^{0a}$ that can have a non-vanishing expectation value is $(GG\tilde{\Sigma}_3)^{00}$. Indeed, this single-particle operator contains three operators that have non-zero expectation values in the state (3.86): the single-trace operators $(GG\Sigma_3)^{00}$, $(GG\Omega)^{00}$ and the double-trace operator $(GGJ\bar{J})^{00}$.

First, we compute the expectation value of $(GG\Sigma_3)^{00}$, which arises from the basic process

in which one B-type strand plus one A-type vacuum strand are converted into one D-type strand plus one A-type vacuum strand:

$$\begin{aligned}
&\Big({}_1\langle 0|\,\langle O_2^{++}|\big(-G^{-1}_{\frac{1}{2}}G^{-2}_{\frac{1}{2}}+\frac{1}{2}J_0^-L_{+1}\big)\Big)\Big(\big(G^{+1}_{-\frac{1}{2}}G^{+2}_{-\frac{1}{2}}+\frac{1}{2}J_0^+L_{-1}\big)\Sigma_3^{-0}\Big)\Big(J_0^+\,|O_2^{--}\rangle\,|0\rangle_1\Big)\\
&\qquad=\;3\,{}_1\langle 0|\,\langle O_2^{++}|\,\Sigma_3^{-0}J_0^+\,|O_2^{--}\rangle\,|0\rangle_1\\
&\qquad=\;-3\Big(\sqrt{2}\,{}_1\langle 0|\,\langle O_2^{++}|\,\Sigma_3^{00}\,|O_2^{--}\rangle\,|0\rangle-{}_1\langle 0|\,\langle O_2^{++}|\,J_0^+\Sigma_3^{-,0}\,|O_2^{--}\rangle\,|0\rangle_1\Big)\\
&\qquad=\;-3\sqrt{2}\,{}_1\langle 0|\,\langle O_2^{++}|\,\Sigma_3^{00}\,|O_2^{--}\rangle\,|0\rangle_1\\
&\qquad=-\frac{1}{\sqrt{2}}\,.
\end{aligned}\tag{3.88}$$

In the equation above, following the prescription after Eq. (2.39), the descendant is normalized so that it has the same norm as the highest weight state, that is $\Sigma_3^{00}=\frac{1}{\sqrt{2}}[J_0^+,\Sigma_3^{-0}]$. This three-point function is independent of the insertion point of the light operator on the cylinder. The last equality follows from

$${}_1\langle 0|\,\langle O_2^{++}|\,\Sigma_3^{00}\,|O_2^{--}\rangle\,|0\rangle_1\;=\;\frac{1}{6}\,,\tag{3.89}$$

which can be derived using the covering-space method of Lunin-Mathur [120, 145] analogously to the computation in B.2.

We now use the basic amplitude in Eq. (3.88) to compute the expectation value of the single-trace operator $(GG\Sigma_3)^{00}$ on the full coherent state (3.86). The relevant contribution can be represented by

$$\begin{aligned}
&\big(GG\Sigma_3\big)^{00}\Big[\big(\,|0\rangle_1^{N-2p-2q}\big)\Big(J_0^+\,|O_2^{--}\rangle\Big)^p\Big(\big(G^{+1}_{-\frac{1}{2}}G^{+2}_{-\frac{1}{2}}+\frac{1}{2}J_0^+L_{-1}\big)\,|O_2^{--}\rangle\Big)^q\Big]\\
&\qquad=-\frac{2\sqrt{2}}{3}\big(N-2(p+q)\big)(q+1)\\
&\qquad\quad\times\Big[\Big(\,|0\rangle_1^{N-2(p+q)}\Big)\Big(J_0^+\,|O_2^{--}\rangle\Big)^{p-1}\Big(\big(G^{+1}_{-\frac{1}{2}}G^{+2}_{-\frac{1}{2}}+\frac{1}{2}J_0^+L_{-1}\big)\,|O_2^{--}\rangle\Big)^{q+1}\Big]\,.
\end{aligned}\tag{3.90}$$

The overall factor on the RHS is obtained as before by requiring that the norms on the two sides of the equality sign are the same. In doing so, we combined Eq. (3.88) with a combinatorial factor that represents the number of ways in which the operator $(GG\Sigma_3)^{00}$ can act on the state on the LHS. In particular, it can act on any of the $(N-2p-2q)p$ pairs of strands $|0\rangle_1\,\big(J_0^+\,|O^{--}\rangle_2\big)$ and can cut-and-join these in two inequivalent ways.

We now use Eq. (3.17) to express the average number of strands in a coherent state with the CFT coefficients A,B,D. We obtain that, in the large N-limit,

$$\big\langle\big(GG\Sigma_3\big)^{00}\big\rangle\;=\;-\frac{2\sqrt{2}}{3}(N-2\bar{p}-2\bar{q})\,\bar{q}\,\frac{B}{D}\;=\;-\sqrt{2}A^2BD\,.\tag{3.91}$$

Second, we compute the expectation value of the single-trace operator $GG\Omega$, which arises

from the basic process in which a B-type strand is converted into a D-type strand:

$$\begin{aligned}\Big(\langle O_2^{++}|\big(-G^{-1}_{\frac{1}{2}}G^{-2}_{\frac{1}{2}}+\frac{1}{2}J_0^-L_{+1}\big)\Big)\Big(\big(G^{+1}_{-\frac{1}{2}}G^{+2}_{-\frac{1}{2}}+\frac{1}{2}J_0^+L_{-1}\big)\Omega^{-0}\Big)\Big(J_0^+\,|O_2^{--}\rangle\Big)\\ =\ 3\,\langle O_2^{++}|\,\Omega_3^{-0}J_0^+\,|O_2^{--}\rangle\\ =\ -3\sqrt{2}\,\langle O_2^{++}|\,\Omega^{00}\,|O_2^{--}\rangle\\ =-3\sqrt{2}\,.\end{aligned} \tag{3.92}$$

The last equality follows from [1, Eq. (5.40)]. To compute the expectation value of the operator on the full coherent state we again combine the above result with a combinatorial factor. Doing so, we obtain

$$\begin{aligned}\big(GG\Omega\big)^{00}\Big[\Big(|0\rangle_1^{N-2p-2q}\Big)\Big(J_0^+\,|O_2^{--}\rangle\Big)^p\Big(\big(G^{+1}_{-\frac{1}{2}}G^{+2}_{-\frac{1}{2}}+\frac{1}{2}J_0^+L_{-1}\big)\,|O_2^{--}\rangle\Big)^q\Big]\\ =-2\sqrt{2}\big(q+1\big)\\ \times\Big[\Big(|0\rangle_1^{N-2p-2q}\Big)\Big(J_0^+\,|O_2^{--}\rangle\Big)^{p-1}\Big(\big(G^{+1}_{-\frac{1}{2}}G^{+2}_{-\frac{1}{2}}+\frac{1}{2}J_0^+L_{-1}\big)\,|O_2^{--}\rangle\Big)^{q+1}\Big]\,.\end{aligned} \tag{3.93}$$

Here we have used the fact that the operator $(GG\Omega)$ can act on any of the p strands of type $J_0^+\,|O^{--}\rangle_2$, and we have matched the norms on the two sides of the equation. The expectation value on the full coherent state then follows from Eq. (3.17). We obtain

$$\big\langle\big(GG\Omega\big)^{00}\big\rangle\ =\ -\frac{2\sqrt{2}\,\bar{q}\,B}{D}\ =\ -\frac{3\sqrt{2}}{N}BD\big(A^2+3D^2+2B^2\big)\,. \tag{3.94}$$

For later convenience, in the last equality we have used the strand budget constraint (3.18).

The final operator that contributes to the expectation value of $(GG\tilde{\Sigma}_3)^{00}$ is

$$(GGJ\bar{J})^{00}\ =\ \sqrt{2}\Big(\big(G^{+1}_{-\frac{1}{2}}G^{+2}_{-\frac{1}{2}}+\frac{1}{2}J_0^+L_{-1}\big)J^-\Big)\bar{J}^3\,, \tag{3.95}$$

where the factor of $\sqrt{2}$ follows from the normalization of the $SU(2)_R$ descendant. This operator contributes through the basic process in which a B-type strand is converted into a D-type strand. This process is mediated only by the holomorphic part of the operator $(GGJ\bar{J})^{00}$. Both B-type and D-type strands are eigenstates of $\bar{J}_0^3$, so we treat this contribution separately below. Focusing for now on the holomorphic part, we have the amplitude

$$\begin{aligned}\Big(\langle O_2^{++}|\,\big(-G^{-1}_{\frac{1}{2}}G^{-2}_{\frac{1}{2}}+\frac{1}{2}J_0^-L_{+1}\big)\Big)\Big(\big(G^{+1}_{-\frac{1}{2}}G^{+2}_{-\frac{1}{2}}+\frac{1}{2}J_0^+L_{-1}\big)J^-\Big)\Big(J_0^+\,|O_2^{--}\rangle\Big)\\ =-6\,\langle O_2^{++}|\,J^3\,|O_2^{--}\rangle\\ =6\,.\end{aligned} \tag{3.96}$$

We now compute the expectation value of the multi-trace operator in the full coherent state (3.86). We include the antiholomorphic part at this point. The relevant contribu-

tion can be represented by

$$\begin{aligned}
&\big(GGJ\bar{J}\big)^{00}\Big[\Big(\,|0\rangle_1^{N-2p-2q}\Big)\Big(J_0^+\,\big|O_2^{--}\big\rangle\Big)^p\Big(\big(G^{+1}_{-\frac{1}{2}}G^{+2}_{-\frac{1}{2}}+\frac{1}{2}J_0^+L_{-1}\big)\,\big|O_2^{--}\big\rangle\Big)^q\Big]\\
&=-4\sqrt{2}\,(p+q)(q+1)\\
&\times\Big[\Big(\,|0\rangle_1^{N-2p-2q}\Big)\Big(J_0^+\,\big|O_2^{--}\big\rangle\Big)^{p-1}\Big(\big(G^{+1}_{-\frac{1}{2}}G^{+2}_{-\frac{1}{2}}+\frac{1}{2}J_0^+L_{-1}\big)\,\big|O_2^{--}\big\rangle\Big)^{q+1}\Big]\,.
\end{aligned}\tag{3.97}$$

The prefactor on the RHS is a combination of the basic amplitude (3.96), the action of $\bar{J}$, and a combinatorical factor. The combinatorics has two parts: first, the operator $\bar{J}$ can act either on one of the p strands of type $J_0^+\,\big|O_2^{--}\big\rangle$ or on one of the q strands of type $GG\,\big|O_2^{--}\big\rangle$. Second, the operator GGJ can only act upon strands of type $GG\,\big|O_2^{--}\big\rangle$. Using Eqs. (3.17) and (3.18) we obtain

$$\big\langle\big(GGJ\bar{J}\big)^{00}\big\rangle\;=\;-\frac{4\sqrt{2}\bar{q}(\bar{p}+\bar{q})B}{D}\;=\;-6\sqrt{2}BD\Big(\frac{3}{2}D^2+B^2\Big)\,.\tag{3.98}$$

Finally, we combine the three contributions in Eqs. (3.91), (3.94) and (3.98) using the definition of the single-particle operator $GG\tilde{\Sigma}$ in Eq. (3.50) to obtain the anticipated cancellation:

$$\big\langle GG\tilde{\Sigma}_3^{00}\big\rangle=0\,.\tag{3.99}$$

This result agrees with the vanishing of the dual AdS_3 field $\mathbf{Z}^6_{k=1}$ in the proposed dual supergravity solution. Thus we see that the proposed holographic dictionary for hybrid superstrata has passed a non-trivial test. This computation also represents a non-trivial cross-check of the operator mixing involved in the single-particle operator dual to the AdS_3 vector field $\mathbf{Z}^6_{k=1}$.

3.7 Summary of precision holographic dictionary

For convenient reference we record here a summary of the precision holographic dictionary for single-particle scalar operators of dimension one and two given in Eq. (3.54),

together with our new results for the superdescendant operators $GG\tilde{\Sigma}_3$, $GG\tilde{O}_2$.

$$\begin{aligned}
&\frac{\sqrt{2}}{N}\langle\Sigma_2^{\alpha\dot\alpha}\rangle = (-1)^{\alpha\dot\alpha}\frac{\sqrt{N}}{\sqrt{2}}\left[s_{k=1}^{(6)(-\alpha,-\dot\alpha)}\right], && \frac{1}{\sqrt{N}}\langle O^{\alpha\dot\alpha}\rangle = (-1)^{\alpha\dot\alpha}\frac{\sqrt{N}}{\sqrt{2}}\left[s_{k=1}^{(7)(-\alpha,-\dot\alpha)}\right],\\
&\frac{1}{\sqrt{N}}\langle J^{\pm}\rangle = -\frac{\sqrt{N}}{\sqrt{2}}\left[A_{k=1}^{\mp(+)}\right], && \frac{1}{\sqrt{N}}\langle \bar{J}^{\pm}\rangle = -\frac{\sqrt{N}}{\sqrt{2}}\left[A_{k=1}^{\mp(-)}\right],\\
&\frac{1}{\sqrt{N}}\langle J^{3}\rangle = -\frac{\sqrt{N}}{2}\left[A_{k=1}^{0(+)}\right], && \frac{1}{\sqrt{N}}\langle \bar{J}^{3}\rangle = -\frac{\sqrt{N}}{2}\left[A_{k=1}^{0(-)}\right],\\
&\langle\tilde{\Omega}^{a,\dot a}\rangle = -(-1)^{a+\dot a}\frac{\sqrt{N}}{\sqrt{2}}\left[\tilde{\sigma}_{k=2}^{(-a,-\dot a)}\right],\\
&\langle\tilde{\Sigma}_3^{a,\dot a}\rangle = (-1)^{a+\dot a}\frac{\sqrt{N}}{\sqrt{2}}\left[s_{k=2}^{(6)(-a,-\dot a)}\right], && \langle\tilde{O}_2^{a,\dot a}\rangle = (-1)^{a+\dot a}\frac{\sqrt{N}}{\sqrt{2}}\left[s_{k=2}^{(7)(-a,-\dot a)}\right],\\
&\left\langle GG\tilde{\Sigma}_3^{(0,a)}\right\rangle = -\frac{\sqrt{N}}{2\sqrt{3}}\left[Z_{k=1}^{6(-a,-)}\right], && \langle GG\tilde{O}_2^{(0,a)}\rangle = -\frac{\sqrt{N}}{2\sqrt{3}}\left[Z_{k=1}^{7(-a,-)}\right].
\end{aligned} \tag{3.100}$$

3.8 Discussion

In this Chapter we have derived the precision holographic dictionary in a new sector of the theory, which involves superdescendants of scalar chiral primary operators of dimension two. In doing so we also expressed the existing dictionary in the single-particle basis. Our results are summarized in Eq. (3.100).

We translated into AdS_3 holography the proposal that single-particle supergravity fluctuations are holographically dual to half-BPS operators that are orthogonal to all multi-trace operators [126, 127]. We observed that this property is not sufficient to determine the single-particle basis in the D1-D5 CFT. We thus combined this proposal with the mixing between single-trace operators worked out in [107] to obtain the refined dictionary for scalar operators of dimension two summarized in the first five lines of Eq. (3.100). We then derived the new part of the dictionary in the last line of Eq. (3.100).

Let us note that the structure of the dictionary in Eq. (3.100) is quite robust: it is constrained by the $SO(n)$ symmetry of the supergravity theory, the feature that the single-particle states are orthogonal to all multi-particle states and the mixing between single-trace operators mentioned above. Furthermore, the overall normalization of each subsector of the dictionary has been calibrated successively on the well-established holographic description of two-charge microstates with $\mathbb{R}^4$ base polarizations, and non-supercharged superstrata, in [1]. Our computation of the coefficient β in Section 3.6.2 can also be regarded as a calibration on a non-supercharged superstratum, and is consistent with the value of α that we obtained by comparison with a supercharged superstratum. We used the new dictionary for superdescendant operators to perform tests of a special set of non-supercharged superstrata, and a set of 'hybrid' superstrata involving both su-

percharged and non-supercharged elements. We find precise agreement between gravity and CFT.

It is worth remarking that the agreement we find in this work does not prove that the proposal for the dual CFT states of supercharged superstrata is precisely correct. The reason is simply the standard limitation of precision holographic studies: for a given superstratum solution in supergravity, and a given precision involving a finite set of expectation values of light operators, there can be other CFT states that have the same values of those correlators. Having made this standard caveat, our results support the proposed holographic description of both non-supercharged and supercharged superstrata and demonstrate that this existing proposal for the dual CFT states passes all available state-of-the-art tests.

Let us now discuss the possibility of extending the present precision holographic dictionary to higher dimensional operators. While we do not expect that such extension requires novel conceptual ingredients, we note that the various sources of non-linearities in the dictionary imply considerably more involved computations as one analyzes operators of higher dimension. First, the operators mixing will involve multi-trace operators with a higher number of traces. Analogously, the identification of the single-particle basis on the supergravity side (i.e. the identification of the quadratic field redefinitions that remove derivative couplings in the cubic lagrangian) will be more involved. Last, a gauge invariant formulation of the dictionary would require retaining higher order terms in the perturbation of the metric and three-forms in Eq. (3.37). Despite these complications, the recipe that we have followed in this work is general, and can be applied to operators of increasing dimension.

Part II

Shockwaves on microstate geometries

Chapter 4

Shockwaves in black hole microstate geometries

4.1 Introduction

This chapter reports the work presented in [3], where the first family of three-charge black hole microstates containing a shockwave in their core region was constructed. Shockwaves are gravitational solutions describing the backreaction of high-energy massless point particles [146]. These solutions have attracted recent interest in the context of black hole physics: for example, shockwave collisions near black hole horizons have been used to probe its absorptive nature and give insights on black hole chaotic behaviour [147–149].

Shockwaves have been also considered in the context of black hole microstates. In particular, a two-charge solution describing the backreaction of a shockwave located in the core of a supertube was constructed in [101, 150]. This is a deformation of the circular supertube that represents the backreaction of a uniform distribution of high-energy massless point particles that does not break supersymmetry and whose details are not resolved in supergravity. It can be derived as a coarse-grained limit of the general family of two-charge microstate solutions [47, 53, 55, 110], as we will describe in due course.

This solution containing a shockwave has proven useful in the analysis of black hole microstates instability. In recent years, several studies of perturbations of black hole microstates have been conducted. In the context of two-charge microstate solutions and three-charge spectral flowed supertubes (also known as GLMT solutions) [78, 85, 151–159], a classical perturbation analysis was performed in [160]. These microstates do not have an ergoregion and are linearly stable: indeed, being extremal solution, they belong to the ensamble of a black hole at zero temperature, which does not evaporate. However,

they present an evanescent ergosurface [161]: this is a surface of infinite redshift with respect to infinity where a killing vector ceases to be time-like and becomes null. On this surface, the geodesics are trapped, meaning that they remain confined in a finite region of space.

It was suggested in [160] that the presence of the evanescent ergosurface leads to a non-linear instability. The heuristic argument is as follows. Consider a massive particle near the evanescent ergosurface of the GLMT background. If the backreaction of the particle is taken into account (i.e. if one couples it to the supergravity fields), the particle will radiate energy. Due to this process, it will follow a trajectory that minimizes its energy, approaching the evanescent ergosurface. Even though the energy measured at infinity will be very small, the energy measured by a local observer will be large, which implies that the backreaction on the microstate will be large. This suggests an instability at the non-linear level, in the sense that the instability requires taking into account the interaction between the massive particle and the supergravity fields.

The implication of this process for the fuzzball program depends on the endpoint of the instability. It was argued in [162] that the deformed supertube of [101, 150] can be used to describes the backreaction of massive probe particles approaching the evanescent ergosurgace in the adiabatic limit. It was suggested that the endpoint of this instability is not a near-extremal black hole or black ring as proposed in [160], but that the instability drives the evolution from less typical to more typical microstates.

In this chapter we construct the first family of three-charge microstate solutions containing a shockwave. By starting with the AdS limit of the deformed supertube containing a shockwave, we apply a spectral flow transformation to construct the near horizon limit of a GLMT solution containing a shockwave in the core regions. Next, we exploit the multi-center formalism developed in [67, 68, 163–165] to extend these solutions to new asymptotically flat BPS solutions. Beside the physical singularity due to the shockwave, our solution is everywhere smooth (up to possible orbifold singularities), horizonless and free of closed time-like curves. By refining the proposal of [101] for the CFT states dual to the two-charge configuration containing a shockwave, we identify the CFT states dual to the solutions constructed in this work and show that the proposal passes a precision holographic test. In these new configurations the shockwave is not located on the evanescent ergosurface, thus we cannot make direct contact with the discussion in [162]. Nevertheless these new solutions might provide a useful guide for the construction of more general smooth microstate geometries describing pure states.

As already mentioned, the shockwave describes the backreaction of massless particles whose details are not fully resolved in supergravity. As a result, the solutions derived in this chapter do not describe a single gravitational pure state, but rather provide an approximate description of a family of microstates. On the CFT side, the dual statement is that any CFT pure state within a family of CFT pure states that we identify is

approximately described by our bulk solution at the resolution of supergravity.

This chapter is organized as follows. In Section 4.2 we review the two-charge BPS supertube solutions with shockwaves. In Section 4.3 we construct new three-charge microstate solutions containing shockwaves. In Section 4.4 we refine the proposal for the CFT states dual to circular supertube solutions with shockwaves, propose a family of CFT states dual to our new solutions, and perform tests of this proposal. We discuss our results in Section 4.5.

4.2 Shockwaves in supertube backgrounds

In this section we review the supergravity solution that describes a shockwave in a circular supertube background [101, 150], and make a straightforward generalization to introduce an orbifold parameter k.

As in the previous chapters, we consider Type IIB string theory compactified on $\mathcal{M}\times S^1$, where $\mathcal{M}$ is T^4 or K3. We take T^4 for concreteness. We consider the T^4 to be microscopic and the S^1 to be macroscopic. We consider bound states of D1 branes wrapped on S^1 and D5 branes wrapped on $S^1\times T^4$. We work in the supergravity limit, with D1 and D5 supergravity charges Q_1 and Q_5 respectively. We consider configurations that are invariant on the T^4, and mostly work in six dimensions. Furthermore, we work in the truncation that corresponds to minimal 6D supergravity coupled to one tensor multiplet; the corresponding Type IIB ansatz and BPS equations are recorded in Appendix C.

We begin in the $\mathrm{AdS}_3\times\mathrm{S}^3$ decoupling limit, in which the original asymptotic S^1, coordinatized by y, has become the angular direction of AdS_3. We consider the background obtained by taking a $\mathbb{Z}_k$ orbifold of the global $\mathrm{AdS}_3\times S^3$ vacuum, supported by the self-dual two-form potential C_2:

$$\begin{aligned} ds_6^2 &= \sqrt{Q_1Q_5}\left(-\frac{1+k^2r^2}{k^2}dt^2+\frac{k^2}{1+k^2r^2}dr^2+r^2dy^2+d\theta^2+\sin^2\theta d\phi^2+\cos^2\theta d\psi^2\right),\\ C_2 &= \sqrt{Q_1Q_5}\Big(\cos^2\theta d\phi\wedge d\psi+r^2dt\wedge dy\Big). \end{aligned} \tag{4.1}$$

In this limit the dilaton is a fixed scalar, $e^{2\Phi}=Q_1/Q_5$. One can deform this background to add a shockwave while preserving supersymmetry [101, 150]. Let us consider a distribution of massless quanta at the center of AdS ($r=0$) and at $\theta=\frac{\pi}{2}$ on the S^3, moving in the ϕ direction. We take the energy of each quantum to be large such that we can treat the quanta as massless point particles, and we consider a uniform distribution of such quanta along the ϕ coordinate.

The backreaction of this distribution of quanta can be described by a stationary solution involving an Aichelburg-Sexl type shockwave on the above background. For $k=1$ this

solution was constructed in [150] and further studied in [101]. The generalization to $k > 1$ is straightforward and is given in terms of a parameter q with $0 \leq q < 1$ that parametrises the strength of the shockwave:

$$\begin{aligned} ds^2 \;=\; & \sqrt{Q_1 Q_5}\left[-\frac{1+k^2r^2}{k^2}dt^2 + \frac{k^2}{1+k^2r^2}dr^2 + r^2dy^2 + d\theta^2 + \sin^2\theta d\phi^2 + \cos^2\theta d\psi^2 \right. \\ & \left. + q\frac{\big((kr^2+1/k)dt + \sin^2\theta d\phi\big)^2 - \big(kr^2dy - \cos^2\theta d\psi\big)^2}{k^2r^2+\cos^2\theta}\right], \\ C_2 \;=\; & \sqrt{Q_1 Q_5}\Big[\cos^2\theta\, d\phi\wedge d\psi + r^2 dt\wedge dy \\ & - \frac{q}{k(k^2r^2+\cos^2\theta)}\Big(k\sin^2\theta\big(-\cos^2\theta d\phi\wedge d\psi + kr^2 d\phi\wedge dy\big) \\ & + (1+k^2r^2)\big(\cos^2\theta d\psi\wedge dt + kr^2 dt\wedge dy\big)\Big)\Big]. \end{aligned} \tag{4.2}$$

Near the locus $(r = 0, \theta = \pi/2)$, the metric is approximately

$$ds^2 \simeq \sqrt{Q_1 Q_5}\Big[-\frac{dt^2}{k^2} + k^2dr^2 + r^2dy^2 + d\theta^2 + \cos^2\theta d\psi^2 + d\phi^2 + \frac{q}{k^2r^2+\cos^2\theta}\Big(\frac{dt}{k} + d\phi\Big)^2\Big] \tag{4.3}$$

which has a shockwave singularity at $(r = 0, \theta = \pi/2)$. For $k = 1$ this is an Aichelburg-Sexl-type shockwave generalized to 5+1 dimensions and smeared along the shockwave locus [150]. For $k > 1$ the shockwave singularity is located at the $\mathbb{Z}_k$ orbifold singularity of the solution in Eq. (4.1).

Upon spectral flow to the Ramond-Ramond (RR) sector, this solution gives an approximate description of a family of RR ground states of the dual CFT, as we shall review in Section 4.4.2. The relevant spacetime (fractional) spectral flow coordinate transformation is as follows:

$$\phi \to \phi + \frac{t}{k}\,, \qquad \psi \to \psi + \frac{y}{k}\,. \tag{4.4}$$

The result of this coordinate transformation is a 1/4-BPS two-charge microstate solution describing the backreaction of a shockwave on a circular supertube geometry, still so far in the AdS_3 decoupling limit.

We now extend the AdS solution to an asymptotically flat ($\mathbb{R}^{1,4}\times S^1$) solution. For $k = 1$ this was done in [101] and we make the straightforward generalization to $k > 1$. To do so we introduce the scale R_y that will become the asymptotic radius of the y circle, and a scale a defined in the following equation. We define dimensionful coordinates via the rescaling

$$r \to \frac{r}{a}\,, \qquad t \to tR_y\,, \qquad y \to yR_y\,, \qquad a^2 \;=\; \frac{Q_1Q_5}{k^2R_y^2}. \tag{4.5}$$

The extension of this solution to an asymptotically flat one was obtained, for $k = 1$, in [101], generalizing the two-charge circular supertube solutions (without shockwaves)

of [44, 45]. The straightforward generalization to arbitrary k gives the following solution:

$$\begin{aligned}
ds^2 &= -\frac{1}{\bar{h}_{(0)}}(dt^2-dy^2)+\bar{h}_{(0)}\bar{f}_{(0)}\left(d\theta^2+\frac{k^2d\bar{r}^2}{k^2\bar{r}^2+\bar{a}^2}\right)\\
&\quad-\xi\frac{2a\sqrt{Q_1Q_5}}{k\bar{h}_{(0)}\bar{f}_{(0)}}(\cos^2\theta\,dy\,d\psi+\sin^2\theta\,dt\,d\phi)+\bar{h}_{(0)}\Big[\Big(\bar{r}^2+\xi\frac{\bar{a}^2Q_1Q_5\cos^2\theta}{k^2\bar{h}^2_{(0)}\bar{f}^2_{(0)}}\Big)\cos^2\theta\,d\psi^2\\
&\quad+\Big(\bar{r}^2+\frac{\bar{a}^2}{k^2}-\xi\frac{\bar{a}^2Q_1Q_5\sin^2\theta}{k^2\bar{h}^2_{(0)}\bar{f}^2_{(0)}}\Big)\sin^2\theta\,d\phi^2\Big]\,,\\
C_2 &= -\frac{Q_1dt\wedge dy}{\bar{f}_{(0)}\bar{h}_{1(0)}}-\frac{a\,\xi\sqrt{Q_1Q_5}}{k\bar{f}_{(0)}\bar{h}_{1(0)}}\Big(\cos^2\theta dt\wedge d\phi+\sin^2\theta dy\wedge d\phi\Big)\\
&\quad+\Big(\frac{\bar{a}^2q\,Q_1Q_5\sin^2\theta}{k^2\bar{f}^2_{(0)}\bar{h}_{1(0)}}+\frac{Q_5(k^2Q_1+k^2\bar{f}_{(0)}+\bar{a}^2\sin^2\theta)}{k^2\bar{f}_{(0)}\bar{h}_{1(0)}}\Big)\cos^2\theta d\phi\wedge d\psi\,,\\
e^{2\Phi} &= \frac{\bar{h}_{1(0)}}{\bar{h}_{5(0)}}\,,
\end{aligned}\tag{4.6}$$

where $\xi=1-q$ parametrises the strength of the shockwave, and where

$$\begin{aligned}
\bar{r} &= \sqrt{\xi}r\,, & \bar{a} &= \sqrt{\xi}a\,, & \bar{f}_{(0)} &= \xi(r^2+\frac{a^2}{k^2}\cos^2\theta)\,,\\
\bar{h}_{1(0)} &= 1+\frac{Q_1}{\bar{f}_{(0)}}\,, & \bar{h}_{5(0)} &= 1+\frac{Q_5}{\bar{f}_{(0)}}\,, & \bar{h}_{(0)} &= \sqrt{\bar{h}_{1(0)}\bar{h}_{5(0)}}\,.
\end{aligned}\tag{4.7}$$

The subscript (0) denotes supertube quantities and we use it to distinguish the above functions from those that characterize the new solutions that we will report in the next section.

4.3 Shockwaves in fractionally spectral flowed supertubes

In this section we first review the three-charge, 1/8-BPS, fractionally spectral flowed supertube solutions constructed and studied in [78, 151–154], as well as their decomposition into two-center solutions of the multi-center formalism of [67, 68, 163–165]. We then proceed to construct a novel family of BPS solutions involving shockwave deformations of these solutions.

4.3.1 Fractionally spectral flowed circular supertubes

Fractionally spectral flowed circular supertubes are a family of 1/8-BPS microstates of the D1-D5-P system. In addition to their D1 and D5 charges, they carry momentum

charge along y that we denote by Q_p. The solutions take the form [152–154]

$$\begin{aligned}
ds^2 \;=\; & -\frac{1}{h}(dt^2-dy^2)+\frac{Q_p}{hf}(dt-dy)^2+hf\left(\frac{dr^2}{r^2+a^2(\gamma_1+\gamma_2)^2\eta}+d\theta^2\right)\\
& +h\Big(r^2+a^2\gamma_1(\gamma_1+\gamma_2)\eta-\frac{Q_1Q_5a^2(\gamma_1^2-\gamma_2^2)\eta\cos^2\theta}{h^2f^2}\Big)\cos^2\theta d\psi^2\\
& +h\Big(r^2+a^2\gamma_1(\gamma_1+\gamma_2)\eta+\frac{Q_1Q_5a^2(\gamma_1^2-\gamma_2^2)\eta\sin^2\theta}{h^2f^2}\Big)\sin^2\theta d\phi^2\\
& +\frac{Q_p\,a^2(\gamma_1+\gamma_2)^2\eta^2}{hf}(\cos^2\theta d\psi+\sin^2\theta d\phi)^2\\
& -\frac{2\sqrt{Q_1Q_5}\,a}{hf}(\gamma_1\cos^2\theta d\psi+\gamma_2\sin^2\theta d\phi)(dt-dy)\\
& -\frac{2\sqrt{Q_1Q_5}\,a(\gamma_1+\gamma_2)\eta}{hf}(\cos^2\theta d\psi+\sin^2\theta d\phi)dy\,,\\
C_2 \;=\; & -\frac{\sqrt{Q_1Q_5}\,a\cos^2\theta}{H_1f}(\gamma_2dt+\gamma_1dy)\wedge d\psi-\frac{\sqrt{Q_1Q_5}\,a\sin^2\theta}{H_1f}(\gamma_1dt+\gamma_2dy)\wedge d\phi\\
& +\frac{(\gamma_1+\gamma_2)\,a\,\eta\,Q_p}{\sqrt{Q_1Q_5}H_1f}(Q_1dt+Q_5dy)\wedge(\cos^2\theta d\psi+\sin^2\theta d\phi)\\
& -\frac{Q_1}{H_1f}dt\wedge dy-\frac{Q_5\cos^2\theta}{H_1f}(r^2+\gamma_2(\gamma_1+\gamma_2)\eta+Q_1)d\psi\wedge d\phi\,,
\end{aligned} \tag{4.8}$$

$$e^{2\Phi}\;=\frac{H_1}{H_5}\,, \tag{4.9}$$

where the parameters γ_1,γ_2 are determined by integer parameters s and k through

$$\gamma_1\;=\;-\frac{s}{k}\,,\qquad \gamma_2\;=\;\frac{s+1}{k}\,, \tag{4.10}$$

and where

$$\begin{aligned}
a\;&=\;\frac{\sqrt{Q_1Q_5}}{R}\,,\qquad Q_p\;=\;a^2\gamma_1\gamma_2\,,\qquad \eta\;=\;\frac{Q_1Q_5}{Q_1Q_5+Q_1Q_p+Q_5Q_p}\,,\\
f\;&=\;r^2+a^2(\gamma_1+\gamma_2)\eta(\gamma_1\sin^2\theta+\gamma_2\cos^2\theta)\,,\\
H_1\;&=\;1+\frac{Q_1}{f}\,,\qquad H_5\;=\;1+\frac{Q_5}{f}\,,\qquad h\;=\;\sqrt{H_1H_5}\,.
\end{aligned} \tag{4.11}$$

In the limit $s\to 0$ these solutions reduce to the two-charge circular supertube solution of [44, 45].

One can decompose these solutions into the form of the general BPS ansatz for such solutions [134, 166]; this was done in [163, 165] (see also [164]). We will use this formalism to construct our solutions, so we now briefly review it and introduce appropriate notation.

The relevant supergravity ansatz is recorded in Appendix C. Supersymmetry and the $U(1)\times U(1)$ isometries along ϕ and ψ imply that the base metric $ds_4^2(\mathcal{B})$ introduced in

the second line of (C.1) is of Gibbons-Hawking form,

$$ds_4^2(\mathcal{B}) \,=\, V^{-1}(d\varphi_1 + A)^2 + V ds_3^2\,, \tag{4.12}$$

where ds_3^2 is the flat metric on $\mathbb{R}^3$, V is a harmonic function on $\mathbb{R}^3$, A is a one-form related to V via $\star_3\, dA = dV$, and where $\varphi_1 = \phi - \psi$. On such a base metric, solutions can be constructed in terms of a set of multi-center harmonic functions on $\mathbb{R}^3$ [67, 68], which have poles (centers) at the same points x^i on $\mathbb{R}^3$ (here $I = 1, 2, 3$):

$$\begin{aligned} V \,&=\, \sum_i \frac{q^{(i)}}{|x - x^i|}\,, \qquad K_I \,=\, \sum_i \frac{d_I^{(i)}}{|x - x^i|}\,, \\ L_I \,&=\, \ell_I + \sum_i \frac{Q_I^{(i)}}{|x - x^i|}\,, \qquad M \,=\, \sum_i \frac{m^{(i)}}{|x - x^i|}\,. \end{aligned} \tag{4.13}$$

The relations between these harmonic functions and the quantities Z_I, Θ^I, β, ω and $\mathcal{F}$ that appear in the BPS ansatz in Appendix C are given by (see e.g. [51, 59, 154])

$$\begin{aligned} &Z_I \,=\, L_I + \frac{1}{2} C_{IJK} \frac{K_J K_K}{V}\,, \qquad \Theta_I \,=\, dB_I\,, \qquad B_I \,=\, \frac{K_I}{V}(d\varphi_1 + A) + \xi_I\,, \\ &\mathcal{F} \,=\, -Z_3\,, \qquad \beta \,=\, \frac{K_3}{V}(d\varphi_1 + A) + \xi_3\,, \qquad \omega \,=\, \mu(d\varphi_1 + A) + \bar{\omega}\,, \end{aligned} \tag{4.14}$$

where

$$\begin{aligned} \star_3 dK_I \,&=\, -d\xi_I\,, \qquad \mu \,=\, \frac{M}{2} + \frac{K_I L_I}{2V} + \frac{1}{6} C_{IJK} \frac{K_I K_J K_K}{V^2}\,, \\ \star_3 d\bar{\omega} \,&=\, \frac{1}{2}\Big(V dM - M dV + K_I dL_I - L_I dK_I\Big)\,. \end{aligned} \tag{4.15}$$

Asymptotically flat solutions are obtained by setting $\ell_I = 1 \;\; \forall\; I$, while in the AdS_3 decoupling limit we have instead $\ell_1 = \ell_2 = 0, \;\; \ell_3 = 1$. Furthermore, in smooth horizonless solutions, the set of coefficients $q^{(i)}, d_I^{(i)}, Q_I^{(i)}, m^{(i)}$ in (4.13) must obey certain constraints [164, 165]. Firstly, flat $\mathbb{R}^{1,4}\times S^1$ asymptotics and at most local orbifold singularities require that $q^{(i)} \in \mathbb{Z}$ and $\sum_i q^{(i)} = 1$. Next, the coefficients $d_I^{(i)}$ are quantized in terms of integers $k_I^{(i)}$ as (see e.g. [154])

$$d_1^{(i)} \,=\, \frac{g_s \alpha'}{2R_y} k_1^{(i)}\,, \qquad d_2^{(i)} \,=\, \frac{g_s \alpha'^3}{2V_4 R_y} k_2^{(i)}\,, \qquad d_3^{(i)} \,=\, \frac{R_y}{2} k_3^{(i)}\,, \tag{4.16}$$

where the volume of T^4 is $(2\pi)^4 V_4$. Regularity of the solution (up to possible orbifold singularities) requires a cancellation of the poles in the harmonic functions (4.13): this is ensured if

$$Q_I^{(i)} \,=\, -\frac{|\epsilon_{IJK}|}{2} \frac{d_J^{(i)} d_K^{(i)}}{q^{(i)}}\,, \qquad m^{(i)} \,=\, \frac{d_1^{(i)} d_2^{(i)} d_3^{(i)}}{(q^{(i)})^2}\,. \tag{4.17}$$

Moreover, a necessary condition for absence of CTCs partially constrains the positions

of the poles x^i, via by the so called "bubble equations", which are given by:

$$\sum_{j\neq i}\Pi_1^{(ij)}\Pi_2^{(ij)}\Pi_3^{(ij)}\frac{q^{(i)}q^{(j)}}{|x^i-x^j|} = -\sum_I d_I^{(i)}, \qquad \text{with} \qquad \Pi_I^{(ij)} = \frac{d_I^{(i)}}{q^{(j)}} - \frac{d_I^{(j)}}{q^{(i)}}\,. \tag{4.18}$$

Fractionally spectral flowed supertubes are two-center solutions [154, 163]. Indeed they are the most general asymptotically flat such solutions that are regular up to orbifold singularities (which in turn are known to be resolved in the string theory description of these backgrounds [155–158]). We introduce spherical polar coordinates centered on the locations of the two centers, (r_+,θ_+,φ_2) and (r_-,θ_-,φ_2), where $\varphi_2=-(\psi+\phi)$. The poles in the harmonic functions (4.13) are then located at $r_+=0$ and $r_-=0$. The flat ds_3^2 base takes the form

$$ds_3^2 = dr_+^2 + r_+^2(d\theta_+^2+\sin^2\theta_+ d\varphi_2^2) = dr_-^2 + r_-^2(d\theta_-^2+\sin^2\theta_- d\varphi_2^2)\,, \tag{4.19}$$

where

$$\begin{aligned} r_+ &= \frac{r^2+a^2(\gamma_1+\gamma_2)^2\eta\sin^2\theta}{4}\,, \qquad \cos\theta_+ = \frac{r^2\cos 2\theta - a^2(\gamma_1+\gamma_2)^2\eta\sin^2\theta}{r^2+a^2(\gamma_1+\gamma_2)^2\eta\sin^2\theta}\,,\\ r_- &= \frac{r^2+a^2(\gamma_1+\gamma_2)^2\eta\cos^2\theta}{4}\,, \qquad \cos\theta_- = \frac{r^2\cos 2\theta + a^2(\gamma_1+\gamma_2)^2\eta\cos^2\theta}{r^2+a^2(\gamma_1+\gamma_2)^2\eta\cos^2\theta}\,. \end{aligned} \tag{4.20}$$

In our conventions the functions L_I for $I=1,2,3$ correspond to the (electric) D1, D5 and P charges respectively. Writing $Q_2^\pm = Q_5^\pm, Q_3^\pm = Q_p^\pm$, the coefficients of the poles in the decomposition of the fractionally spectral flowed solutions (4.8) are

$$\begin{aligned} &q^- = -s\,, \qquad q^+ = s+1\,, \qquad d_1^- = -d_1^+ = Q_5\frac{s(s+1)}{2R_y k}\,, \qquad d_2^- = -d_2^+ = Q_1\frac{s(s+1)}{2R_y k}\,,\\ &d_3^- = -d_3^+ = \frac{R_y k}{2}\,, \qquad Q_1^- = \frac{Q_1(s+1)}{4}\,, \qquad Q_1^+ = -\frac{sQ_1}{4}\,, \qquad Q_5^- = \frac{Q_5(s+1)}{4}\,,\\ &Q_5^+ = -\frac{sQ_5}{4}\,, \qquad Q_p^- = \frac{Q_1Q_5 s(s+1)^2}{4R_y^2k^2}\,, \qquad Q_p^+ = -\frac{Q_1Q_5 s^2(1+s)}{4k^2R_y^2}\,,\\ &m^- = \frac{Q_1Q_5(s+1)^2}{8kR_y}\,, \qquad m^+ = -\frac{Q_1Q_5 s^2}{8kR_y}\,, \qquad \ell_I = 1 \quad \forall\, I\,. \end{aligned} \tag{4.21}$$

We note that the relations (4.17), (4.18) are satisfied.

In the AdS_3 decoupling limit, the solution (4.8) is related via a fractional spectral flow large coordinate transformation to the vacuum solution (4.1). In order to exhibit this, we first take the limit in which the R_y is much larger than the scale set by the Q_1 and Q_5 charges:

$$\epsilon = \frac{(Q_1Q_5)^{1/4}}{R_y} \ll 1 \qquad \Rightarrow \qquad Q_p \ll \sqrt{Q_1Q_5}\,, \qquad \eta\simeq 1\,. \tag{4.22}$$

Physically, this regime implies that the geometry (4.8) has an AdS throat whose proper length is large in AdS units (see e.g. [167]). The AdS throat is the region of spacetime where $r \ll \sqrt{Q_1 Q_5}$. To take the decoupling limit, we rescale coordinates as

$$r \to a\, r\,, \qquad t \to \frac{t}{R_y}\,, \qquad y \to \frac{y}{R_y}\,, \tag{4.23}$$

and send $R_y \to \infty$ holding fixed the rescaled dimensionless coordinates (r, t, y) and the charges Q_1, Q_5. From (4.11) this sends $a \to 0$, and likewise $\epsilon \to 0$. We then obtain the decoupled metric

$$\begin{aligned} ds^2 \;=\; \sqrt{Q_1 Q_5}\Big[& -\frac{1+k^2 r^2}{k^2} dt^2 + \frac{k^2}{1+k^2 r^2} dr^2 + r^2 dy^2 + d\theta^2 \\ & + \sin^2\theta (d\phi - \gamma_2 dt - \gamma_1 dy)^2 + \cos^2\theta (d\psi - \gamma_2 dy - \gamma_1 dt)^2 \Big]\,. \end{aligned} \tag{4.24}$$

The fractional spectral flow coordinate transformation

$$\phi \to \phi + \gamma_2 t + \gamma_1 y\,, \qquad \psi \to \psi + \gamma_1 t + \gamma_2 y\,, \tag{4.25}$$

maps the geometry in Eq. (4.24) into the k-orbifolded global $\mathrm{AdS}_3 \times \mathrm{S}^3$ solution given in Eq. (4.1).

4.3.2 Shockwaves in fractionally spectral flowed supertubes

We now construct three-charge solutions involving shockwaves using a straightforward two-step procedure. In the first step we take the solution involving a shockwave on global AdS (4.2) and apply the inverse of the fractional spectral flow coordinate transformation (4.25) to obtain a shockwave deformation of the AdS_3 limit of the fractionally spectral flowed circular supertubes. For later use we record the resulting metric:

$$\begin{aligned} ds^2 \;=\; \sqrt{Q_1 Q_5}\Big[& -\frac{(1+k^2 r^2)}{k^2} dt^2 + r^2 dy^2 + \frac{k^2 dr^2}{1+k^2 r^2} + d\theta^2 \\ & + \cos^2\theta (-\gamma_1 dt - \gamma_2 dy + d\psi)^2 + (-\gamma_2 dt - \gamma_1 dy + d\phi)^2 \sin^2\theta \\ & + \frac{q}{k^2 r^2 + \cos^2\theta} \Big(-\big(k r^2 dy - (-\gamma_1 dt - \gamma_2 dy + d\psi)\cos^2\theta\big)^2 \\ & \qquad + \Big(\frac{1+k^2 r^2}{k} dt + (-\gamma_2 dt - \gamma_1 dy + d\phi)\sin^2\theta\Big)^2 \Big) \Big]. \end{aligned} \tag{4.26}$$

In the second step we extend this solution to an asymptotically flat solution. The method is again straightforward, however the calculation is more involved than the trivial first step. The method is to decompose the solution obtained in the first step into the harmonic functions of the multi-center formalism, and then "add back the 1" in the relevant harmonic functions.

To write the decomposition of the solution obtained in the first step, we rescale the

location of the two poles of the harmonic functions of the undeformed solution as

$$r^{\pm} \;\to\; \xi\, r^{\pm}\,. \tag{4.27}$$

The coefficients of the two poles are then

$$\begin{aligned}
&q^- = -s\,, \qquad q^+ = s+1\,, \qquad d_1^- = -d_1^+ = Q_5\frac{s(s+1)}{2R_y k}\,, \qquad d_2^- = -d_2^+ = Q_1\frac{s(s+1)}{2R_y k}\,,\\
&d_3^- = -d_3^+ = \frac{R_y k}{2}\,, \qquad Q_1^- = \frac{Q_1(s+1)}{4}\,, \qquad Q_1^+ = -\frac{sQ_1}{4}\,, \qquad Q_5^- = \frac{Q_5(s+1)}{4},\\
&Q_5^+ = -\frac{sQ_5}{4}\,, \qquad Q_p^- = \frac{Q_1Q_5 s(s^2+2s+\xi)}{4R_y^2k^2}\,, \qquad Q_p^+ = -\frac{Q_1Q_5 s^2(1+s)}{4k^2R_y^2}\,,\\
&m^- = \frac{Q_1Q_5(s^2+2s+\xi)}{8kR_y}\,, \qquad m^+ = -\frac{Q_1Q_5 s^2}{8kR_y}, \qquad \ell_1=\ell_2=0\,, \quad \ell_3=1\,.
\end{aligned} \tag{4.28}$$

Having expressed the AdS_3 solution in this form, we trivially extend the solution to asymptotically flat space by replacing $\ell_I = 1 \;\; \forall\, I$.

To generate the closed-form solution describing a shockwave on the fractional spectral flowed supertube background, we use Eqs. (4.14) and (4.15) to obtain

$$\begin{aligned}
ds^2 =\; & \frac{\sqrt{\bar h_1\bar h_5}\,\bar f\, dr^2}{b^2+r^2} + \bar f\sqrt{\bar h_1\bar h_5}\,d\theta^2 + \frac{(-dt^2+dy^2)}{\bar h_1\bar h_5}\\
&+\frac{\cos^2\theta}{\bar f^2\sqrt{\bar h_1\bar h_5}}\Big[\xi\bar h_1\bar h_5\,\bar f^2(r^2-s\,b^2) + b^2\,Q_1Q_5\,(2s+1)\,\xi^2\cos^2\theta\\
&\qquad -q\Big(b^2\,s\,(-Q_1Q_5+r^2\,(s+1)(Q_1+Q_5))\,\xi + Q_1Q_5\,r^2\Big(\eta\,\xi - \frac{\bar f}{r^2+b^2\cos^2\theta}\Big)\Big)\Big]d\psi^2\\
&+q\frac{2a\,\sqrt{Q_1Q_5}\,\sin^2\theta(r^2-b^2\,s)(dt-dy)d\phi}{k\bar f\sqrt{\bar h_1\bar h_5}(r^2+b^2\cos^2\theta)} + \frac{a^2\,s(dt-dy)^2(\bar f + s\,(r^2+b^2\sin^2\theta))}{k^2\bar f\sqrt{\bar h_1\bar h_5}(r^2+b^2\cos^2\theta)}\\
&+\frac{\sin^2\theta}{\bar f^2\sqrt{\bar h_1\bar h_5}}\Big(\bar h_1\bar h_5\bar f^2(r^2+b^2\,(s+1))\xi - b^2\,Q_1Q_5(2s+1)\,\xi\,\sin^2\theta + \frac{q\,b^2\bar f\,Q_1Q_5\sin^2\theta}{r^2+b^2\cos^2\theta}\Big)d\phi^2\\
&-\frac{2a\,\sqrt{Q_1Q_5}\,\eta\,\xi\,dy\,(\cos^2\theta d\psi + \sin^2\theta d\phi)}{k\bar f\sqrt{\bar h_1\bar h_5}} + \frac{a^4\,s\,(1+s)\,\eta^2\,\xi^2(\cos^2\theta d\psi^2 + \sin^2\theta d\phi^2)}{k^4\,\bar f\sqrt{\bar h_1\bar h_5}}\\
&-\frac{2a\sqrt{Q_1Q_5}(r^2+b^2\xi\cos^2\theta)\,(dt-dy)\,(\gamma_1\cos^2\theta d\psi + \gamma_2\sin^2\theta d\phi)}{\bar f\sqrt{\bar h_1\bar h_5}(r^2+b^2\cos^2\theta)}\,,
\end{aligned} \tag{4.29}$$

$$\begin{aligned}
C_2 =\; & -\,Q_1\frac{dt\wedge dy}{h_1\bar f} + \frac{Q_5\cos^2\theta}{\bar h_1\bar f}\Big(Q_1 + r^2\xi + b^2(s+1)\xi + \frac{b^2Q_1q\sin^2\theta}{r^2+b^2\cos^2\theta}\Big)d\phi\wedge d\psi\\
&+\frac{q\,a\,\sqrt{Q_1Q_5}(r^2+b^2)\cos^2\theta}{k\bar h_1\bar f\,(r^2+b^2\cos^2\theta)}dt\wedge dy + \frac{q\,a\,\sqrt{Q_1Q_5}\,r^2\sin^2\theta}{k\bar h_1\bar f(r^2+b^2\cos^2\theta)}dy\wedge d\phi\\
&-\sin^2\theta\Big(a\,\sqrt{Q_1Q_5} - \frac{q\,a\,b^2\sqrt{Q_1Q_5}\cos^2\theta}{r^2+b^2\cos^2\theta}\Big)\frac{(\gamma_1\,dt+\gamma_2\,dy)\wedge d\phi}{\bar h_1\bar f}\\
&-\cos^2\theta\Big(a\sqrt{Q_1Q_5} + \frac{q\,a\,b^2\,\sqrt{Q_1Q_5}\sin^2\theta}{r^2+b^2\cos^2\theta}\Big)\frac{(\gamma_2\,dt+\gamma_1\,dy)\wedge d\psi}{\bar h_1\bar f}\\
&+\frac{a\,b^2\,s\,(1+s)\,\xi}{k\sqrt{Q_1Q_5}\,\bar h_1\bar f}\Big(Q_1dt\wedge\big(\sin^2\theta d\phi + \cos^2\theta d\psi\big) + Q_5dy\wedge\big(\sin^2\theta d\phi + \cos^2\theta d\psi\big)\Big)\,,
\end{aligned}$$

$$e^{2\Phi} = \frac{\bar{h}_1}{\bar{h}_5}\,,$$

where

$$\bar{f} = \xi f\,, \qquad b^2 = \frac{a^2\,\eta}{k^2}\,. \tag{4.30}$$

We note that in the limit $s = 0$, this solution reduces to that in Eq. (4.6); in this limit $\bar{f}, \bar{h}_1$ and $\bar{h}_5$ reduce to $\bar{f}_{(0)}, \bar{h}_{1(0)}$ and $\bar{h}_{5(0)}$.

In our new solutions the regularity constraints (4.17) are satisfied only by the coefficients of the pole at $r_+ = 0$ and not by the coefficients of the pole at $r_- = 0$ in (4.28). This is as it should be, since the solution has a shockwave singularity at $\bar{f}_{(0)} = 0$, i.e. at $(r = 0, \theta = \pi/2)$.

We now analyse the absence of CTCs for the solutions we have constructed. First, we note that Eq. (4.18) is not satisfied. This condition, however, is a necessary condition for absence of CTCs when the solutions are smooth [51]. For the case at hand the solutions are not smooth because of the shockwave singularity located at $\bar{f}_{(0)} = 0$; therefore, we investigate the conditions for absence of CTCs directly. We do so by completing the squares in the periodic coordinates (y, ϕ, ψ) and by checking that the overall coefficient is globally non-negative. We first analyze the solution (4.29) in the decoupling limit, where the form of the metric is simple enough to perform an analytic analysis. Since the $g_{\phi\phi}$ and $g_{\psi\psi}$ are not affected by the spectral flow transformation (4.25), we complete the squares in the following order: first ϕ, then ψ, and finally y. In doing so, the conditions for absence of CTCs are independent of the spectral flow parameters γ_1, γ_2. We obtain the conditions

$$\begin{aligned}
&\phi \text{ coordinate:} && \sin^2\theta + \frac{q\sin^4\theta}{k^2r^2 + \cos^2\theta} \;\geq\; 0\,,\\
&\psi \text{ coordinate:} && k^2r^2\cos^2\theta + (1-q)\cos^4\theta \;\geq\; 0\,,\\
&y \text{ coordinate:} && \frac{(1-q)(k^2r^2 + \cos^2\theta)}{k^2r^2 + (1-q)\cos^2\theta} \;\geq\; 0\,,
\end{aligned} \tag{4.31}$$

which are always satisfied for $0 \leq q < 1$.

For the full asymptotically flat solution (4.29), as is often done we have performed a numerical analysis, based on which we can rule out CTCs with a high level of confidence.

Note that in our spectral flowed supertube solutions with shockwaves, Eq. (4.29), the evanescent ergosurface is located at $f = 0$, where f is given in Eq. (4.11). By contrast, the shockwave is located at $(r = 0, \theta = \pi/2)$ which is not on the evanescent ergosurface for $s \neq 0$. Correspondingly, for $s \neq 0$ the addition of the shockwave does not come at zero cost in energy, and indeed we will now see that the momentum charge Q_p is modified.

We now record the conserved quantities of our solutions (4.29). As usual we wish to compare with five-dimensional D1-D5-P BPS black holes [40, 168], so we are interested

in the five-dimensional conserved mass and angular momenta obtained after dimensional reduction along the y direction. These quantities are computed in Appendix F and are given by Eqs. (F.2) and (F.5), which we record here as

$$\begin{aligned} M_{ADM} &= \frac{\pi}{4G_5}\left(Q_1+Q_5+\frac{Q_1Q_5}{R_y^2}\frac{s(s+\xi)}{k^2}\right), \\ J^3 &= \frac{1}{2}(J^\phi - J^\psi) = \frac{1}{2}\frac{\xi N}{k}+\frac{sN}{k}, \\ \bar{J}^3 &= \frac{1}{2}(J^\phi + J^\psi) = \frac{1}{2}\frac{\xi N}{k}. \end{aligned} \tag{4.32}$$

The condition $0 \leq q < 1$ has a natural interpretation in the holographically dual CFT, as we shall see in the next section. Although the value $q = 1$ is excluded, and the natural regime is small (but not infinitesimal) q, let us comment here on the form of the solutions as they approach the singular limit $q \to 1$ ($\xi \to 0$) with $\bar{r} = \sqrt{\xi}r$ fixed. As $q \to 1$, our solutions approach small rotating D1-D5-P (BMPV [168]) black holes, where here 'small' means zero horizon size in supergravity. In the AdS_3 limit, the fractional spectral flow transformation (4.25) relates these solutions to the AdS_3 limit of the two-charge D1-D5 BPS (non-rotating) small black hole solution. Similarly, this two-charge black hole solution is approached in the $q \to 1$ limit of the two-charge solutions with shockwaves (4.6). It is known that the two-charge black hole solution does not correspond to a microscopic profile function (or superposition of such functions), as discussed in [47, 49, 50]. These small black hole solutions are approached here because the $q \to 1$ limit is a singular limit which effectively coarse grains over all the microscopic details of the bound state; we shall elaborate on this in the next section once we have proposed the holographic description of these solutions.

4.4 Holographic description of shockwave solutions

In this section we identify a family of states of the D1-D5 orbifold CFT and propose that these are holographically dual to the $AdS_3\times S^3$ limits of the supergravity solutions (4.6) and (4.29). We perform tests of this proposal, including a precision holographic test, finding agreement.

4.4.1 D1-D5 CFT

Let us briefly recall some facts about the D1-D5 CFT that we have already introduced in Chapters 2 and 3, highlighting the aspects that will be useful for the discussion in the remainder of this chapter. Moreover, for ease of presentation, we also report some general aspects of the covering space formalism and of the spectral flow transformation (we refer the reader to Appendix B for a complementary discussion).

Being a symmetric product orbifold CFT, the D1-D5 CFT contains twisted sectors. The twist operators are in one-to-one correspondence with the conjugacy classes of the permutation group S_N. These operators change the boundary conditions of the fields: for example, the boundary conditions corresponding to the permutation $(12...k)$ are given (on the cylinder) by

$$\begin{aligned} X_{(1)} \to X_{(2)} \to ... \to X_{(k)} \to X_{(1)} \,, \\ \psi_{(1)} \to \psi_{(2)} \to ... \to \psi_{(k)} \to \pm\psi_{(1)} \,, \end{aligned} \tag{4.33}$$

and analogously for the right-moving fermions. The $\pm$ boundary conditions in (4.33) on the cylinder correspond respectively to the R and NS sectors of the theory on a local covering space [120, 169]; the lowest-dimension ('bare') twist operator corresponds to the NS-NS vacuum in the covering space. For a more detailed discussion of this point, see [85]. In the full symmetric product orbifold theory, twist operators are obtained by symmetrizing over all permutations in a given conjugacy class.

Given a state involving a collection of twist operators of cycle lengths k_i, it is common to describe the state as a collection of effective 'strands' of lengths k_i. Strands of length k_i can occur with multiplicity N_i, subject to the 'strand budget' constraint $\sum_i N_i k_i = N$.

As a first example, consider the state consisting of N/k identical strands of length k, each in the lowest dimension state in the k-twisted sector. We denote this state by

$$|0\rangle_k^{N/k} = |0\rangle_k^{(1)} \otimes |0\rangle_k^{(2)} \otimes \cdots \otimes |0\rangle_k^{(N/k)} \,, \tag{4.34}$$

and we refer to it as the k-twisted NS vacuum. This state is an eigenstate of the left and right Virasoro modes $L_0, \bar{L}_0$ with eigenvalues $h = \bar{h} = \frac{c}{24}(1 - \frac{1}{k^2})$, it is a singlet under the $SU(2)_L \times SU(2)_R$ R-symmetry group and it is holographically dual to the k-orbifolded global $\mathrm{AdS}_3 \times \mathrm{S}^3$ solution given in Eq. (4.1).

Upon mapping twisted states into the local k-fold covering space [120, 169], there are no longer any twist operator insertions and the original k copies of the fields in (4.33) are mapped into single-valued fields. In the k-fold covering space, the dimension h_c and central charge c_c are related to those in the physical CFT via $h = h_c/k$ and $c = k\, c_c$. Moreover, the k-twisted sector of the physical CFT contains fractional modes n/k (and $(n + 1/2)/k$), which correspond to integer modes n (half-integer modes $n + 1/2$) in the covering space.

Our main interest is in black hole microstates in the RR sector of the theory, which arises directly from the AdS_3 decoupling limit of asymptotically flat configurations (see e.g. [100]). One can map the NS sector of the CFT into the R sector using spectral flow [170]. Starting with a state of left scaling dimension h and $SU(2)_L$ J^3 charge m and acting with a left spectral flow transformation with parameter ν, we obtain a state

in the same twist sector with left dimension and charge (h', m') given by

$$h' = h + 2\nu m + \frac{c\nu^2}{6}\,, \qquad m' = m + \frac{c\nu}{6}\,. \tag{4.35}$$

When ν is half integer, a spectral flow transformation maps a state in the NS sector to a state in the R sector. When considering spectral flow of the full CFT, we have $c = 6N$. If we consider an individual strand of length k, we have $c = 6k$. A similar transformation holds for the right sector of the theory, with parameter $\bar{\nu}$.

When $(\nu, \bar{\nu}) = (\frac{1}{2}, \frac{1}{2})$, the untwisted NS vacuum $|0\rangle_1^N$ is mapped into a RR state with $h = \bar{h} = N/4$, which is therefore a RR ground state. It carries R-symmetry charge $m = \bar{m} = N/2$ and we shall denote it with $|{+}{+}\rangle_1^N$. The other RR ground states can be obtained from spectral flow of other anti-chiral primaries (i.e. operators satisfying the bound $h = j = -m,\ \bar{h} = \bar{j} = -\bar{m}$) by applying the same spectral flow transformation. For a given twist k there are (anti-)chiral primaries of dimension $h = k/2,\ h = (k-1)/2$ and $h = (k+1)/2$.

Let us now consider the sector of the full CFT composed of N/k strands of length k. In this sector, there is an enhancement of spectral flow known as *fractional* spectral flow [85, 154, 171, 172]. This operation is naturally thought of as ordinary spectral flow in the k-fold covering space and means that the values $\nu \in \mathbb{Z}/k$ give rise to physical states in the same (R or NS) sector of the theory, while the values $\nu \in (\mathbb{Z} + \frac{1}{2})/k$ map from R to NS in the k-fold cover.

The backgrounds to which we add shockwaves in this work are the heavy BPS RR states obtained by chiral fractional spectral flow of the state $|{+}{+}\rangle_k^{N/k}$, studied in [154]. Specifically, we consider $|{+}{+}\rangle_k^{N/k}$ as our reference state and perform left fractional spectral flow with parameter $\nu = s/k$. These states were proposed to be holographically dual to the bulk configurations in Eqs. (4.8)–(4.11) in [154] and this proposal has passed non-trivial holographic tests [93, 154]. We shall exhibit these CFT states in more detail in Section 4.4.4.

4.4.2 Holographic description of shockwaves in supertube backgrounds

The first shockwave solution we reviewed, in Eq. (4.2), for $k = 1$ describes a shockwave on the global $AdS_3 \times S^3$ vacuum. As we have discussed, the shockwave describes the backreaction of a distribution of high-energy massless particles. Supergravity excitations on the vacuum are holographically dual to CFT states in short multiplets whose top (bottom) component is a chiral (anti-chiral) primary, see e.g. [2, 100]. In our conventions, the shockwave of (4.2) is holographically dual to a set of several anti-chiral primaries of the dual CFT with large conformal dimension and R-charge, and therefore high twist [101].

Upon spectral flow to the RR sector, (anti-)chiral primaries transform into RR ground states. Recall from Chapter 2 that suitably coherent RR ground states of the D1-D5 system can be described in terms of eight profile functions $g_i(v')$ in $\mathbb{R}^8$, where v' is a null coordinate, with periodicity $L = 2\pi Q_5/R_y$ [47, 55, 110].

Let us consider the twisted circular supertube geometry that is generated by a circular profile of radius a/k in the x_1-x_2 plane,

$$g_1(v') + ig_2(v') = \frac{a}{k}\, e^{\frac{2\pi i k}{L} v'}\,, \qquad g_{i\neq 1,2} = 0\,. \tag{4.36}$$

The CFT state dual to the microstate generated by the profile (4.36) is

$$|{+}{+}\rangle_k^{N/k}\,. \tag{4.37}$$

Let us now consider the $AdS_3{\times}S^3$ limit of the solution with shockwave in Eq. (4.6). If we switch off the shockwave excitations by setting $q = 0$, this solution is the one corresponding to the profile (4.36) and CFT state (4.37). For non-zero q, this solution can be generated by an approximate profile function by performing two steps (see [101, Fig. 2] for a pictorial representation). The first step is to consider a profile which initially traverses, k times, a circle of radius $\bar{a}/k = \xi a/k$ in the x_1-x_2 plane on the interval $v' \in [0, \xi L]$, and which then remains in the same x-location for the remainder of its length (recall $\xi = 1 - q$):

$$\begin{aligned} g_1(v') + ig_2(v') &= \frac{\bar{a}}{k} e^{\frac{2\pi i k}{\xi L} v'}\,, \qquad 0 \le v' \le \xi L \\ g_1(v') + ig_2(v') &= \frac{\bar{a}}{k}\,, \qquad\qquad \xi L \le v' \le L \\ g_{i\neq 1,2} &= 0\,. \end{aligned} \tag{4.38}$$

The constant segment represents the high-twist chiral primaries, corresponding to profile Fourier modes with high mode numbers and small amplitudes that are not resolved by supergravity.

The second step is to break this constant segment into several smaller segments and smear over their locations within the overall profile to obtain a uniform distribution (subject to additional conditions described in detail in [101]). The resulting approximate profile reproduces the supergravity solution with shockwave given in Eq. (4.6) [101]. This procedure is most natural when q is small compared to 1 (but not infinitesimally small).

We now discuss the holographic description of these solutions, refining the discussion in [101] given for $k = 1$. The circular segment of the profile function (4.38) corresponds to a set of strands of type $|{+}{+}\rangle_k$. The constant segment that is smeared corresponds to some collection of RR ground state strands whose strand lengths are large in a sense that we will make precise shortly. The polarizations of the RR strands are not resolved in supergravity; for concreteness we will take them to be the five bosonic RR ground

states that are invariant on the T^4, commonly labelled by their R-charges as $|\varepsilon\bar{\varepsilon}\rangle = |\pm\pm\rangle, |\pm\mp\rangle, |00\rangle$. As a first pass, we write this family of CFT states as follows (and arbitrary superpositions thereof):

$$|{+}{+}\rangle_k^{N_0} \, |\varepsilon_1\bar{\varepsilon}_1\rangle_{k_1}^{d_1} \cdots |\varepsilon_{n_s}\bar{\varepsilon}_{n_s}\rangle_{k_{n_s}}^{d_{n_s}} \, , \qquad \frac{k_i}{k} \in \mathbb{Z}, \qquad \frac{k_i}{k} \gg 1 \, , \qquad N_0 k + \sum_{i=1}^{n_s} d_i k_i = N \, . \tag{4.39}$$

Here N_0 is the number of strands representing the supertube background, d_i is the degeneracy of the various strands making up the shockwave and n_s is the number of types of strands that do not represent the supertube background. We work at leading order in large N. We take the parameter k not to scale with N, so that $N_0 \sim N$. We also take q and ξ to be independent of N. For ease of terminology we shall refer to the strands of length k_i as the long strands, and to those of length k as the short strands.

In the long strand sector, neither the parameters k_i, d_i, n_s, nor the distribution of polarizations are fixed. This is the CFT analog of the fact that in the bulk the total energy of the shockwave is known, however it is not known how this energy is distributed among the high-energy supergravity quanta making up the shockwave.

Each segment of the supergravity profile (4.38) corresponds to a component of the dual CFT state that contributes a finite fraction of the total strand budget at large N. Considering the overall strand budget of the set of all long strands, we must also have $\sum_i d_i k_i \sim N$.

We will shortly refine the above to derive that at leading order in large N we must have $kN_0 = \xi N$ and thus $\sum_i d_i k_i = qN$. Thus ξ will be the fraction of the total strand budget taken up by the short strands, and q will be the fraction of the total strand budget taken up by the long strands.

The supergravity profile does not explicitly include any Fourier modes higher than k with finite amplitude. From the two-charge dictionary as made precise in [103] (see Eq. (2.7)), this means that the CFT state cannot contain any long strands with both $k_i \sim N^0$ and $d_i \sim N$. Therefore no d_i can scale as N. We shall derive a stronger condition shortly.

We now refine the condition $k_i \gg k$ stated in [101] (for $k = 1$). Our main analysis will involve a precision holography calculation. However it is instructive to make a brief crude first pass by temporarily making the simplifying assumption that the length of all the long strands scales in the same way, which we write as $k_i \sim N^b$, where a priori $0 \leq b \leq 1$. Similarly we temporarily assume that all the degeneracies of the long strands scale as $d_i \sim N^d$ with $0 \leq d < 1$, recalling that we have excluded $d = 1$ in the previous paragraph. Then the condition $\sum_i d_i k_i \sim N$ requires that $n_s \sim N^A$ with $b + d + A = 1$ and a priori $0 \leq A \leq 1$.

Now, in order for there to be enough different integers k_i to have order N^A types of long

strands, we must have $b \geq A$. Combining this with the constraint $b+d+A=1$, we find

$$A \;\leq\; \frac{1-d}{2}\,, \qquad b \;\geq\; \frac{1-d}{2} \qquad \Rightarrow \qquad b>0\,. \tag{4.40}$$

So in this simplified analysis, we see that the length of the long strands must scale with a positive power of N. Furthermore,

$$\sum_{i=1}^{n_s} d_i \;\sim\; N^{1-b} \qquad \text{with} \quad b>0\,. \tag{4.41}$$

This relation will be important for matching the conserved charges. Using precision holography we will shortly establish it in general, with no assumption on the scaling of the different k_i.

As a side comment, let us note that when we allow the different k_i to scale as different powers of N, it is possible for some strand lengths to scale as $k_i \sim N^0$ with degeneracies that scale as $d_i \sim N^d$ with $d<1$, provided that $k_i \gg k$. Since such strands individually account for a vanishingly small strand budget at large N (of order N^d), one would discard them unless the same is true for all the other long strands present, for instance if all $d_i k_i \sim N^d$ and $n_s \sim N^{1-d}$. However in such a CFT state, the vast majority of types of strands will have lengths that scale as some positive power of N (at least N^{1-d}).

4.4.3 Precision holography analysis

In this section we shall use the holographic dictionary derived in Chapters 2 and 3 to perform our precision holography analysis, in which we will prove for general k_i that the condition (4.41) holds in general. This condition will also be sufficient to ensure agreement between gravity and CFT to the precision we probe. On the bulk side, we work in the AdS_3 decoupling limit. We expand fluctuations in S^3 harmonics and consider a single-particle excitation that is a scalar in AdS_3. Since we are considering a two-charge configuration, the four-dimensional base space of the supergravity ansatz (C.1) is flat $\mathbb{R}^4$. We work in spherical polar coordinates in which it takes the form

$$ds_4^2 = d\bar{r}^2 + \bar{r}^2(d\theta^2 + \sin^2\theta d\phi^2 + \cos^2\theta d\psi^2)\,, \tag{4.42}$$

where we have labeled the radial coordinate by $\bar{r}$, for consistency with the notation used in the two-charge solution with shockwave in Eq. (4.6).

In these coordinates it is useful to expand the harmonic functions Z_1, Z_2 that appear in

the BPS ansatz in Appendix C in scalar S^3 harmonics $Y_{\mathsf{k}}^{m_{\mathsf{k}},\bar{m}_{\mathsf{k}}}$ and for large $\bar{r}$ as follows:

$$\begin{aligned} Z_1 &= \frac{Q_1}{\bar{r}^2}\Big(1+\sum_{\mathsf{k}=1}^{2}\sum_{m_{\mathsf{k}},\bar{m}_{\mathsf{k}}=-\mathsf{k}/2}^{\mathsf{k}/2} a_0^{\mathsf{k}}\, f_{1\mathsf{k}}^{(m_{\mathsf{k}},\bar{m}_{\mathsf{k}})}\,\frac{Y_{\mathsf{k}}^{m_{\mathsf{k}},\bar{m}_{\mathsf{k}}}}{\bar{r}^{\mathsf{k}}}+O(r^{-3})\Big)\,,\\ Z_2 &= \frac{Q_5}{\bar{r}^2}\Big(1+\sum_{\mathsf{k}=1}^{2}\sum_{m_{\mathsf{k}},\bar{m}_{\mathsf{k}}=-\mathsf{k}/2}^{\mathsf{k}/2} a_0^{\mathsf{k}}\, f_{5\mathsf{k}}^{(m_{\mathsf{k}},\bar{m}_{\mathsf{k}})}\,\frac{Y_{\mathsf{k}}^{m_{\mathsf{k}},\bar{m}_{\mathsf{k}}}}{\bar{r}^{\mathsf{k}}}+O(r^{-3})\Big)\,, \end{aligned} \tag{4.43}$$

where $a_0=\frac{\sqrt{Q_1Q_5}}{R_y}$.

The particular AdS_3 scalar we consider is the field $s_{\mathsf{k}=2}^{(6)(a,\dot{a})}$ defined in (3.44)[1]. We use the notation introduced in Section 3.5.2 and denote the coefficient of $\bar{r}^{-2}$ in its large $\bar{r}$ expansion by $\Big[s_{\mathsf{k}=2}^{(6)(a,\dot{a})}\Big]$. Choosing the gauge $f_{11}^{(m_1,\bar{m}_1)}+f_{51}^{(m_1,\bar{m}_1)}=0$, one then has (see Appendix E)

$$\Big[s_{\mathsf{k}=2}^{(6)(a,\dot{a})}\Big] \;=\; \sqrt{\frac{3}{2}}\Big(f_{12}^{(a,\dot{a})}-f_{52}^{(a,\dot{a})}\Big)\,. \tag{4.44}$$

The explicit values of the harmonic functions characterizing the backreaction of shockwave on a supertube background were obtained in [101, Eq. (3.18)]. Changing coordinates to recast the base metric into the form (4.42), performing the asymptotic expansion in (4.43) and using the linear combination in (4.44), one obtains that the AdS_3 limit of the solution describing a two-charge supertube with shockwave in Eq. (4.6) has the property that

$$\Big[s_{\mathsf{k}=2}^{(6)(a,\dot{a})}\Big] \;=\; 0\,. \tag{4.45}$$

By examining Table 3.2, we see that the CFT operator dual to $s_{\mathsf{k}=2}^{(6)(a,\dot{a})}$ is the single-particle operator $\Sigma_3^{a\dot{a}}$ introduced in Eq. (3.49). For convenience, we record below its explicit form

$$\tilde{\Sigma}_3^{a\dot{a}} \;\equiv\; \frac{3}{2}\left[\left(\frac{\Sigma_3^{a\dot{a}}}{N^{\frac{3}{2}}}-\frac{\Omega^{a\dot{a}}}{3N^{\frac{1}{2}}}\right)+\frac{1}{N^{\frac{1}{2}}}\left(-\frac{2}{3}(\Sigma_2\cdot\Sigma_2)^{a\dot{a}}+\frac{1}{3}(J\cdot\bar{J})^{a\dot{a}}+\frac{1}{6}(O\cdot O)^{a\dot{a}}\right)\right]. \tag{4.46}$$

In this sector, the dictionary reads (3.100)

$$\big\langle\tilde{\Sigma}_3^{a\dot{a}}\big\rangle \;=\; (-1)^{a+\dot{a}}\frac{\sqrt{N}}{\sqrt{2}}\Big[s_{\mathsf{k}=2}^{(6)(-a,-\dot{a})}\Big]\,. \tag{4.47}$$

Combined with the result in Eq. (4.45), this implies that the dual CFT state (4.39) must have a vanishing expectation value of the operator $\tilde{\Sigma}_3^{a\dot{a}}$. This requirement will yield the claimed constraint (4.41).

For ease of presentation, we shall make two simplifications: first, we take the twist parameter in (4.39) to be $k=1$ for the remainder of this subsection, and second, we

[1]For consistency with the notation in Chapter 3, we indicate with $a,\dot{a}$ the $SU(2)_L\times SU(2)_R$ charges that are denoted with $m_k,\bar{m}_k$, with $k=2$, in Eq. (4.43).

focus on CFT states involving only strands of polarization type $|{+}{+}\rangle$. The computation and result for generic k and generic long strand polarizations are entirely analogous. A more general case involving both $|{+}{+}\rangle$ and $|{-}{-}\rangle$ polarizations for the long strands is described in Appendix G.1.

We shall focus on a particular $SU(2)_L \times SU(2)_R$ component of the single-particle operator, specifically $\tilde{\Sigma}_3^{00}$. Among the operators that mix in Eq. (4.46), there are three operators that have a non vanishing expectation value on the class of states (4.39): the single-trace operators Σ_3^{00}, Ω^{00} and the double-trace $\left(J\cdot\bar{J}\right)^{00}$. The contribution of the other double-trace operator is subleading in N, so we shall ignore it.

First, we analyze the contribution from the twist-three operator Σ_3^{00}. This operator acquires a non-vanishing expectation value by mapping two strands of different length into themselves, permuting the copies [1] (see the discussion above Eq. (2.110)). The fusion coefficient of the process can be computed holographically; we describe the computation in Appendix G.2. The result is:

$$\sigma_3^{00}\,|{+}{+}\rangle_{k_1}\,|{+}{+}\rangle_{k_2} \;=\; \frac{(k_1+k_2)^2}{6k_1^2k_2^2}\big(1-\delta_{k_1,k_2}\big)\,|{+}{+}\rangle_{k_1}\,|{+}{+}\rangle_{k_2}\;. \tag{4.48}$$

The expectation value of Σ_3^{00} on the full state (4.39) arises from the process

$$\Sigma_3^{00}\Big(\,|{+}{+}\rangle_1^{N_0}\prod_i|{+}{+}\rangle_{k_i}^{d_i}\Big)=\Big(\sum_{i\neq j}\frac{(k_i+k_j)^2}{6k_ik_j}d_id_j+\sum_i\frac{(k_i+1)^2}{6k_i}N_0d_i\Big)\Big(\,|{+}{+}\rangle_1^{N_0}\prod_i|{+}{+}\rangle_{k_i}^{d_i}\Big)\,. \tag{4.49}$$

The two terms in the first parenthesis after the equality sign correspond respectively to the processes in which the twist-three operator acts on two long strands, and on a long and a short strand. Let us consider the first contribution: it is given by combining (4.48) with the fact that Σ_3 can act on any of the d_id_j pairs of strand of different length and can cut each of them in k_i and k_j different positions. The second contribution works analogously.

Second, we analyze the operator Ω^{00}. The states $|{+}{+}\rangle_k$ are eigenstates of this operator with eigenvalue described in Eq. (2.100)

$$\Omega^{00}\,|{+}{+}\rangle_k \;=\; \frac{1}{2k}\,|{+}{+}\rangle_k\;. \tag{4.50}$$

Therefore the operator Ω^{00} acquires a non-vanishing expectation value via the process

$$\Omega^{00}\Big(\,|{+}{+}\rangle_1^{N_0}\prod_i|{+}{+}\rangle_{k_i}^{d_i}\Big)\;=\;\Big(\frac{N_0}{2}+\sum_i\frac{d_i}{2k_i}\Big)\Big(\,|{+}{+}\rangle_1^{N_0}\prod_i|{+}{+}\rangle_{k_i}^{d_i}\Big)\,. \tag{4.51}$$

Third, we consider the double-trace operator $\left(J\cdot\bar{J}\right)^{00}$. Its expectation value arises from

the process

$$\big(J\cdot\bar{J}\big)^{00}\Big(\,|{+}{+}\rangle_1^{N_0}\prod_i|{+}{+}\rangle_{k_i}^{d_i}\Big)\;=\;\frac{2}{N}\Big(\frac{N_0^2}{4}+2\frac{N_0}{2}\sum_i\frac{d_i}{2}+\sum_{i,j}\frac{d_id_j}{4}\Big)\Big(\,|{+}{+}\rangle_1^{N_0}\prod_i|{+}{+}\rangle_{k_i}^{d_i}\Big)\,. \tag{4.52}$$

The three terms after the equality sign correspond respectively to: (i) the action of both the left and the right current on a short strand; (ii) one current acting on a short and one on a long strand; and (iii) both currents acting on a long strand. By combining Eqs. (4.49)–(4.52) we obtain the expectation value of the single-particle operator:

$$\begin{aligned}\langle\tilde{\Sigma}_3^{00}\rangle\;&=\;\frac{3}{2N^{3/2}}\Big[\frac{2}{3}N_0\sum_i d_i+\sum_{i\neq j}d_id_j\frac{(k_i+k_j)^2}{6k_ik_j}-\frac{1}{6}\sum_{i,j}d_id_j\Big(\frac{k_i}{k_j}-1\Big)\Big]\\&=\;\frac{1}{N^{3/2}}\Big[N_0\sum_i d_i+\sum_{i\neq j}d_id_j\frac{k_j^2+3k_ik_j}{4k_ik_j}\Big]\,,\end{aligned} \tag{4.53}$$

where the last equality follows by noticing that the $i=j$ parts of the last term of the first line vanish.

With our normalization of the holographic dictionary, the contribution of an operator is visible in the supergravity approximation if its expectation value is of order $N^{1/2}$ in the large N limit. Therefore the expectation value of $\tilde{\Sigma}_3^{00}$ will agree with Eq (4.45) if and only if its large N scaling is subleading with respect to $N^{1/2}$.

We note that Eq. (4.53) is the sum of two positive terms, so no cancellation can occur. Let us thus consider the first term. We have $N_0\sim N$ and therefore we require that

$$\sum_{i=1}^{n_s}d_i\;\sim\;N^{1-\alpha}\qquad\text{for some}\quad\alpha>0\,. \tag{4.54}$$

We emphasize that we have now established that this condition is necessary in general, for any set of long strand lengths k_i.

Next we consider the second term. Again as a crude first pass, suppose that all the various k_i scale as the same power of N. Then an upper bound on the scaling of this term is $N^{2(1-\alpha)}$ with $\alpha>0$, from squaring (4.54). Then this term, and thus the total expectation value, are subleading compared to $N^{1/2}$ as required.

More generally, suppose instead that there are different values of k_i scaling as different powers of N. The term corresponding to $3k_ik_j$ in the numerator of the second line of (4.53) is subleading compared to $N^{1/2}$ by the same argument as in the last paragraph. An upper bound on the remaining term is given by adding in the $i=j$ terms into the sum, obtaining

$$\frac{1}{N^{3/2}}\Big(\sum_j d_jk_j\Big)\Big(\sum_i\frac{d_i}{k_i}\Big)\,. \tag{4.55}$$

The first sum is of order N, while the second is bounded above by $\sum_i d_i\sim N^{1-\alpha}$.

So (4.55) is also subleading compared to $N^{1/2}$. Therefore the condition (4.54) is also sufficient to ensure that the precision holographic test is passed.

We now use the condition (4.54) to determine N_0, the degeneracy of the twist-k strands, in the large N limit. The analysis of the conserved charges of the metric (4.6) in [162] established that the angular momentum carried by the solution describing a shockwave on a supertube background is suppressed by a factor of ξ with respect to that of the supertube solution:

$$\big\langle J^3 \big\rangle_{\text{Supertube+SW}} \,=\, \xi \big\langle J^3 \big\rangle_{\text{Supertube}} \,=\, \xi \frac{N}{2k}\,. \tag{4.56}$$

The same value is obtained upon setting $s = 0$ in the conserved charges in Eq. (4.32). The CFT state (4.39) is an eigenstate of the current operator J^3, with eigenvalue:

$$\big\langle J^3 \big\rangle \,=\, \frac{N_0}{2} + \sum_{i=1}^{n_s} \varepsilon_i \frac{d_i}{2}\,. \tag{4.57}$$

Recall that we have taken $k \sim N^0$ and $N_0 \sim N$. We have just shown that $\sum d_i \sim N^{1-\alpha}$ with $\alpha > 0$. So at large N the contribution of the long strands to the expectation value of J^3 is subleading. As anticipated above, we thus conclude that at leading order in large N,

$$N_0 \,=\, \xi \frac{N}{k}\,. \tag{4.58}$$

Therefore, as claimed, q is the fraction of the total strand budget taken up by the long strands, and $\xi = 1 - q$ is the fraction of the strand budget taken up by the short strands.

For convenient reference we now record the more refined version of the family of CFT states in Eq. (4.39) as

$$\begin{gathered} |{+}{+}\rangle_k^{N_0} \, |\varepsilon_1 \bar{\varepsilon}_1\rangle_{k_1}^{d_1} \cdots |\varepsilon_{n_s} \bar{\varepsilon}_{n_s}\rangle_{k_{n_s}}^{d_{n_s}}\,, \qquad \frac{k_i}{k} \in \mathbb{Z}, \qquad \frac{k_i}{k} \gg 1\,, \\ k N_0 \,=\, \xi N\,, \qquad \sum_{i=1}^{n_s} d_i k_i \,=\, qN\,, \qquad \sum_{i=1}^{n_s} d_i \,\sim\, N^{1-\alpha}\,, \qquad \alpha > 0\,. \end{gathered} \tag{4.59}$$

We remind the reader that while the presence of the shockwave decreases the angular momentum, the total energy of the system is left unchanged and is given by $h = \bar{h} = \frac{N}{4}$.

Let us return to the condition $0 \leq q < 1$ derived in Section 4.3. We make two brief observations here that shed further light on the condition $q < 1$. First, the string profile (4.38) would become a straight line in the limit $q \to 1$, which is microscopically inconsistent with the fact that the configuration carries two charges (see e.g. [50]). Second, the family of CFT states (4.39) involves long strands of winding $k_i \gg k$ whose details are not resolved by supergravity relative to the short strands of length k. In the limit $q \to 1$, the short strands are no longer present, so the approximation of a smeared

profile is no longer valid. For such CFT states a more refined bulk description is required, and is given by the extrapolation of the general two-charge microstate solutions into the stringy regime [47, 53, 55, 101].

As a final comment on these microstates, we note that the proposed holographic description of the $k = 1$ supertube background with shockwave is similar to the proposed holographic description of small two-charge BPS black rings of the D1-D5 system [173–175], where again here 'small' means zero horizon area in supergravity. It would be interesting to further investigate this similarity.

4.4.4 Holography of fractionally spectral flowed supertubes

In this section we review in more detail the holographic description of the fractionally spectral flowed supertube solutions [154] and discuss some of their physical properties.

As mentioned at the end of Section 4.4.1, the dual CFT states to the fractionally spectral flowed supertube solutions given in Eq. (4.8) are 1/8-BPS microstates obtained by left fractional spectral flow of the 1/4-BPS state $|{+}{+}\rangle_k^{N/k}$ by an amount $\nu = s/k$ with $s \in \mathbb{Z}$. The spectral flow adds left-moving fermionic excitations, while leaving the right movers in the ground state; this results in a non-zero momentum charge $n_p = h - \bar{h}$. The state of each strand takes the explicit form

$$|{+}{+}\rangle_{k,s} \equiv \begin{cases} \left[\psi^{+1}_{-\frac{s}{k}}\psi^{+2}_{-\frac{s}{k}} \cdots \psi^{+1}_{-\frac{1}{k}}\psi^{+2}_{-\frac{1}{k}}\right]|{+}{+}\rangle_k \,, & s \geq 1 \\ \left[\psi^{-1}_{\frac{s+1}{k}}\psi^{-2}_{\frac{s+1}{k}} \cdots \psi^{-1}_{0}\psi^{-2}_{0}\right]|{+}{+}\rangle_k = \left[\psi^{-1}_{\frac{s+1}{k}}\psi^{-2}_{\frac{s+1}{k}} \cdots \psi^{-1}_{-\frac{1}{k}}\psi^{-2}_{-\frac{1}{k}}\right]|{-}{+}\rangle_k \,, & s \leq -1 \,. \end{cases} \tag{4.60}$$

Recall that in the k-twisted sector the level spacing of the excitations is in units of $1/k$. This means that spectral flow is the energetically most convenient way to add charge, corresponding to filling a Fermi sea of excitations up to the fractional level s/k for $s \geq 1$, or the level $-(s+1)/k$ for $s \leq 1$. Fractional spectral flow has an entirely analogous effect on the other RR ground states with polarizations $|{-}{-}\rangle\,, |{\pm}{\mp}\rangle\,, |00\rangle$; for further details see e.g. [57].

Let us record the charges of the state (4.60). The spectral flow transformation involves only the left sector of the theory, so the right charges are the same as those of the two-charge circular supertube. The left charges follow from Eq. (4.35) and are

$$\begin{aligned} h &= \frac{N}{4} + \frac{Ns(s+1)}{k^2} \,, & \bar{h} &= \frac{N}{4} \,, \\ m &= \frac{N}{k}\Big(s + \frac{1}{2}\Big) \,, & \bar{m} &= \frac{N}{2k} \,. \end{aligned} \tag{4.61}$$

Importantly, not all values of s, k are allowed. The momentum per strand p is required

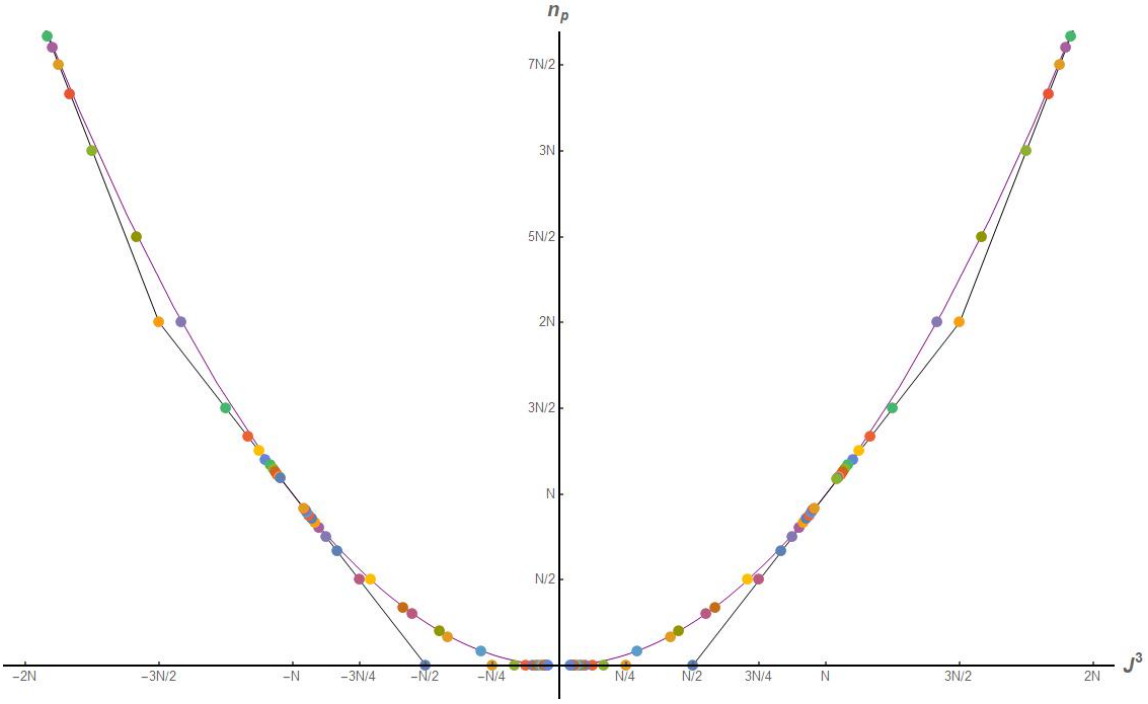

Figure 4.1: Quantum numbers (J^3, n_p) for fractional spectral flowed supertube states with $k \leq 12$ and $|s| \leq 12$ satisfying the condition (4.62) and for which $|J^3| \leq 2N$. All points lie outside the parabola, even though some appear very close to it.

to be an integer:

$$p = \frac{s(s+1)}{k} \in \mathbb{Z}. \tag{4.62}$$

In Figure 4.1 we display the (J^3, n_p) phase diagram for the D1-D5-P system in the RR sector. The black polygon represents the unitarity bound: allowed CFT states exist only on and above this threshold. The parabola $n_p = (J^3)^2/N$ delimits the region of existence of finite-size BMPV black holes, which exist only inside the parabola. Note that inside but very close to the parabola, the small BMPV black holes are sub-dominant to either a BMPV plus supertube or black ring [176]. The fractionally spectral flowed supertube solutions live in the region bounded by the black polygon and the purple parabola. We represent with dots the solutions with $k \leq 12$ and $|s| \leq 12$.

Note that the dots in the corners of the unitarity bound polygon are the states with $k = 1$. In our conventions the interval $0 < J^3 < N/2$ with $n_p = 0$ contains the RR ground states with $k > 1$ and $s = 0$, i.e. the states $|{+}{+}\rangle_k^{N/k}$. Dots in the interval $-N/2 < J^3 < 0$ with $n_p = 0$ correspond to $k > 1$ and $s = -1$, which are the two-charge states $|{+}{+}\rangle_{k,s=-1}^{N/k} = |{-}{+}\rangle_k^{N/k}$. Dots on the remaining lines of the polygon correspond to spectral flowed states that have $s/k \in \mathbb{Z}$ or $(s+1)/k \in \mathbb{Z}$.

The remainder of the states are the most interesting physically. These lie closer to the BMPV parabola, and have $k > 1$ and neither $s/k \in \mathbb{Z}$ nor $(s+1)/k \in \mathbb{Z}$. These were the states of primary interest in [154].

4.4.5 Holography of shockwaves in fractionally spectral flowed supertubes

We now propose the holographic description of the $AdS_3\times S^3$ limit of the solutions describing fractional spectral flowed supertubes with shockwaves in Eq. (4.29). The $AdS_3\times S^3$ limit of the metrics are given in Eq. (4.26).

Recall that the spectral flow large coordinate transformation (4.25) maps the AdS_3 decoupled metric in Eq. (4.26) into that of the supertube with shockwave in (4.2); the same holds for the two-form potential.

Therefore the natural candidate family of dual CFT states is the family obtained by fractional spectral flow with parameter $\nu = s/k$ of the family of two-charge states in Eq. (4.59), subject to the condition of integer momentum per strand. We shall show that this condition is non-trivial, but that it is satisfied by an arbitrarily large number of states in the large N limit. Recall that the lengths of the long strands k_i are required to be multiples of k, in order that we can make this fractional spectral flow transformation.

To describe this family of states in more detail, let us introduce integer parameters s_i which label the amount of spectral flow performed over the strands of length k_i. One has

$$\nu \,=\, \frac{s}{k} \,=\, \frac{s_i}{k_i} \qquad \forall i\,. \tag{4.63}$$

Our proposed dual CFT states of the bulk solutions involving a shockwave on a fractionally spectral flowed supertube background in Eq. (4.29) are the following states (and their superpositions):

$$\begin{gathered}|{+}{+}\rangle_{k,s}^{N_0}\,|\varepsilon_1\bar\varepsilon_1\rangle_{k_1,s_1}^{d_1}\cdots|\varepsilon_{n_s}\bar\varepsilon_{n_s}\rangle_{k_{n_s},s_{n_s}}^{d_{n_s}}\,, \qquad \frac{k_i}{k}\in\mathbb{Z}, \qquad \frac{k_i}{k}\gg 1\,,\\ kN_0 \,=\, \xi N\,, \qquad \sum_{i=1}^{n_s} d_i k_i \,=\, qN\,, \qquad \sum_{i=1}^{n_s} d_i \,\sim\, N^{1-\alpha}\,, \qquad \alpha>0\,,\end{gathered} \tag{4.64}$$

subject to the condition that the momentum on each CFT strand be an integer.

Let us now examine the condition of integer momentum per strand. For the strands corresponding to the background, recall that we have the condition $p = \frac{s(s+1)}{k} \in \mathbb{Z}$, Eq. (4.62). Similarly, for the strands corresponding to the shockwave, we require

$$p_i \,=\, \frac{s_i(s_i+\varepsilon_i)}{k_i} \in \mathbb{Z} \qquad \forall\, i\,. \tag{4.65}$$

This condition is quite non-trivial, because we have noted that the candidate dual CFT states contain strands of parametrically large k_i, and because the numerator is constrained by $s_i = \frac{sk_i}{k}$. Therefore, given an allowed pair (s,k), it is important to ensure

that there is a set of allowed values of k_i that extend to arbitrarily large positive integers. We now prove that this is indeed the case.

Let us assume without loss of generality that $s > 0$, and present the proof first for $\varepsilon_i = 1$. Recall that $k > 0$ by definition. Since s and $(s+1)$ share no common factors and $\frac{s(s+1)}{k} \in \mathbb{Z}$, when we decompose k into its prime factors, a subset of these must divide s, and the rest must divide $(s+1)$. We can then write the prime factorization of k in the form

$$k \,=\, k^{(s)}k^{(s+1)} \,=\, \prod_i n_i^{(s)} \prod_j n_j^{(s+1)}\,, \qquad k^{(s)} \,=\, \prod_i n_i^{(s)}\,, \qquad k^{(s+1)} \,=\, \prod_i n_i^{(s+1)}\,, \tag{4.66}$$

where $n_i^{(s)}$ are primes that divide s, and similarly for $n_i^{(s+1)}$. Repeated primes can of course occur in this decomposition, and $n_i^{(s)} \neq n_j^{(s+1)}$ for all i, j. We can then factorize s and $(s+1)$ as

$$s \,=\, \hat{s}k^{(s)}\,, \qquad s+1 \,=\, \hat{t}k^{(s+1)}\,, \tag{4.67}$$

where $\hat{s}$ and $\hat{t}$ are positive integers but are not necessarily prime. We recall that the k_i are multiples of k, such that we can write $k_i = \hat{k}_i k$ for positive integers $\hat{k}_i$. By using $s_i = s\frac{k_i}{k}$ and the decompositions in Eqs. (4.66), (4.67), we have that the momentum carried by the i-th type of strand is given by

$$p_i \,=\, \frac{s_i(s_i+1)}{k_i} \,=\, \frac{s(s\hat{k}_i+1)}{k} \,=\, \frac{\hat{s}(s\hat{k}_i+1)}{k^{(s+1)}}\,. \tag{4.68}$$

Let us define $\hat{p}_i = p_i/\hat{s}$ and show that there is an infinite sequence of $\hat{k}_i$ such that $\hat{p}_i$ is a positive integer. Rearranging, we have

$$\hat{p}_i k^{(s+1)} - s\hat{k}_i = 1\,. \tag{4.69}$$

Since none of the $n_j^{(s+1)}$ divide s, we have $\gcd(s, k^{(s+1)}) = 1$. Bézout's identity (and the extended Euclidean algorithm) then imply that there is an infinite sequence of positive integer pairs $(\hat{k}_i, \hat{p}_i)$ such that (4.69) is satisfied, and therefore there is an infinite set of k_i such that $p_i \in \mathbb{Z}$.

More generally, the right-hand side of Eq. (4.69) is ε_i. When $\varepsilon_i = -1$, Bézout's identity again ensures the required infinite sequence of positive integer pairs $(\hat{k}_i, \hat{p}_i)$. When $\varepsilon_i = 0$, one can simply take $\hat{k}_i$ to be a multiple of $k^{(s+1)}$ to obtain such an infinite sequence.

The upshot is that there is an infinite family of states of the form (4.64) that obey the non-trivial condition that the momentum on each strand is an integer, including strands with arbitrarily large values of k_i in the large N limit.

Let us compute the charges of the CFT states (4.64) and compare them with the gravity

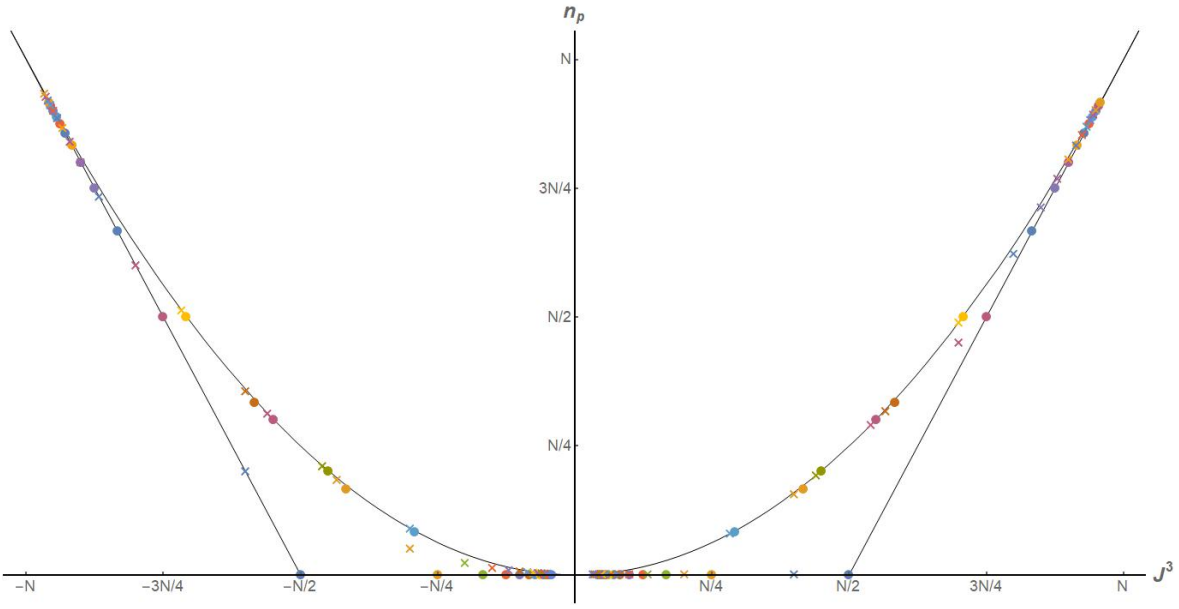

Figure 4.2: Quantum numbers (J^3, n_p) of spectral flowed supertubes without shockwaves (dots) and corresponding solutions with shockwaves, for $q = 0.2$ (crosses). Colour coding and proximity indicate corresponding solutions. Plotted are states with $k \leq 12$, $|s| \leq 12$, satisfying (4.62) and with $|J^3| \leq N$. All plotted points lie outside the parabola, even though some appear very close to it.

result in Eq. (4.32). The scalings in the second line of Eq. (4.64) will again ensure agreement. There is no spectral flow in the right sector, so the right charges $(\bar{h}, \bar{m})$ are the same as those for the two-charge states dual to supertubes with shockwaves (4.59). For the left sector, we compute the charges using Eq. (4.35), and derive their large-N behaviour using the second line of Eq. (4.64). Recalling that $s_i = s\frac{k_i}{k}$ and denoting subleading terms with ellipses, we obtain

$$\begin{aligned} h &= N_0 \frac{k^2 + 4s(s+1)}{4k} + \sum_i d_i \frac{k_i^2 + 4s_i(s_i + \varepsilon_i)}{4k_i} = \frac{N}{4} + \frac{N}{k^2} s(s+\xi) + \frac{s}{k} \sum_i \varepsilon_i d_i \\ \Rightarrow \quad h &= \frac{N}{4} + \frac{N}{k^2} s(s+\xi) + \dots , \\ m &= N_0 \Big(s + \frac{1}{2}\Big) + \sum_i d_i \Big(s_i + \frac{\varepsilon_i}{2}\Big) = \frac{sN}{k} + \xi \frac{N}{2k} + \sum_i \varepsilon_i \frac{d_i}{2} \\ \Rightarrow \quad m &= \xi \frac{N}{2k} + \frac{sN}{k} + \dots . \end{aligned} \tag{4.70}$$

Comparing with the gravity charges given in Eq. (4.32) we see that the angular momentum eigenvalue $J^3 = m$ explicitly agrees. We note in passing that in Eqs. (4.32), (4.70) the s-dependent part of the angular momentum eigenvalue $\langle J^3 \rangle = m$ does not depend on ξ; when $s \neq 0$, the long strands contribute a finite fraction of the angular momentum of the configuration.

To show agreement between the momentum charge Q_p and the value of h, we extract

the quantized CFT y-momentum charge

$$n_p \,=\, h - \bar{h} \,=\, \frac{N}{k^2} s(s+\xi)\,. \tag{4.71}$$

We then translate this CFT charge into supergravity normalization using the general relation between the supergravity charge Q_p and the quantized charge n_p (see e.g. [60, Eq. (6.26)]),

$$Q_p \,=\, \frac{Q_1 Q_5}{R_y^2 N} n_p \,=\, \frac{Q_1 Q_5}{R_y^2} \frac{s(s+\xi)}{k^2}\,. \tag{4.72}$$

This value, derived from the CFT, is in precise agreement with Eq. (4.32). The agreement of conserved charges supports our proposal for the holographic description of our solutions.

In Figure 4.2 we plot both the fractionally spectral flowed supertube solutions without shockwaves (dots) and the microstates obtained adding a shockwave in their core region (crosses). In all examples, the backreaction of the shockwave drives the fractionally spectral flowed supertube solutions toward the BMPV parabola, without ever reaching it except asymptotically in the limit $q \to 1$, which as we have already discussed is a singular limit.

Let us make some observations on the set of solutions with shockwaves and their conserved charges. First, let us consider the right-hand side of the $n_p = 0$ line, i.e. the range $0 < J^3 \leq N/2$. Upon backreaction of the shockwave, the microstate remains on the same line. The shockwave reduces the angular momentum, corresponding to a transition from less typical to more typical two-charge microstates [162].

On the left-hand side of the $n_p = 0$ line, when $-N/2 \leq J^3 < 0$, the behaviour is quite different: upon adding the shockwave, the momentum charge of the microstate increases. The difference between the two sides of the $n_p = 0$ line can be understood by first noticing that in all points plotted, the shockwave adds a negative amount of J^3. When the background has positive J^3, the shockwave decreases $|J^3|$. However when the background has negative J^3, the shockwave increases both $|J^3|$ and the average winding of the strands in the CFT, so it is not possible for the solution with shockwave to remain on the $n_p = 0$ line. A more direct understanding can be obtained by tracing the spectral flow orbits of the points on the right-hand side of the $n_p = 0$ line (by fractional spectral flow with $\nu = -1/k$).

Note that there exists a similar set of configurations with shockwaves in which the shockwave adds a positive amount of J^3. These can be obtained by interchanging $\phi \leftrightarrow \psi$ in the solutions we constructed in Eq. (4.29). Their charges are obtained by reflecting Fig. 4.2 in the n_p axis. So in fact for each background, there exist two solutions with shockwaves of the type we have constructed, only one of which is plotted in Fig. 4.2.

The behaviour on the diagonal lines is similar to the respective halves of the two-charge

line $n_p = 0$. Specifically, the behaviour of the states on the left-most diagonal line is similar to that on the right-hand side of the $n_p = 0$ line, being related by (integer) spectral flow with parameter $\nu = -1$. The configurations with shockwaves remain on the diagonal line. In the same way, the behaviour on the right-most diagonal line is similar to that on the left-hand half of the $n_p = 0$ line. Recall that the dots on these lines include all states that have $k = 1$ and all states that have $s/k \in \mathbb{Z}$ or $(s+1)/k \in \mathbb{Z}$.

The final set of dots are those that already lie close to the parabola, for which $k > 1$ and neither $s/k \in \mathbb{Z}$ nor $(s+1)/k \in \mathbb{Z}$. These are the states that involve 'genuinely' fractional spectral flow, in the sense that they cannot be obtained from any two-charge state by spectral flow with parameter $\nu \in \mathbb{Z}$ [154]. The shockwave drives these states to be closer to the parabola, though in many cases it is not easy to see this from the plot.

We conclude this subsection by returning to the point that for the states with shockwaves that remain on the two-charge line, the process of adding a shockwave is a process that drives the system from less typical to more typical two-charge microstates [162]. For our fractionally spectral flowed supertubes with shockwaves, making a similar interpretation is complicated by the fact that the conserved charge n_p in general changes when the shockwave is added. However in both cases the solutions with shockwaves describe a family of microstates involving strands with unspecified twists k_i, corresponding to the high-frequency quanta making up the shockwave that are not resolved by supergravity.

Typical microstates of the supersymmetric two-charge black hole are those composed of strands with winding $k \sim \sqrt{N}$; for the three-charge supersymmetric black hole, the typical microstates involve strands with length $k \sim N$ [50]. Indeed, our proposed dual CFT states in Eq. (4.64) involve strands with windings that generically are of different lengths, including lengths scaling as positive powers of N. Therefore, relative to other microstates with the same respective values of n_p, the states with shockwaves are naturally thought of as being more typical than the states dual to the fractionally spectral flowed supertube solutions without shockwaves.

4.4.6 Interpolating between different microstates

We now observe that the class of CFT states that we have studied, given in Eq. (4.64), contains some simple examples of states that have attracted recent interest as families that interpolate between different microstate geometries [177, 178]. Those works studied sub-families of states of the general form

$$|{+}{+}\rangle^{N_0}_{k,\nu}\,|{+}{+}\rangle^{d_1}_{k_1,\nu_1}\ , \tag{4.73}$$

where the pair (k, ν) is not equal to the pair (k_1, ν_1), and coherent superpositions of such states. We caution the reader that in this subsection we are parameterizing spectral flow with the rational parameter $\nu = s/k$ rather than the integer s.

This family of states is interesting because in the separate limits in which $d_1 = 0$ or $N_0 = 0$, the state reduces to a spectral flowed supertube state (or a two-charge supertube state). In [177] the sub-family $k = k_1 = 1, \nu = 0, \nu_1 > 0$ was studied (spectral flowed further to the NS-NS sector). In [178] a general discussion was given, as well as an explicit analysis of the sub-family in which $\nu_1 = \nu - \frac{1}{k_1}$. It was found that the bulk description of these states involves codimension-2 sources corresponding to an extra KKM dipole charge in the D1-D5 frame.

The family of states we have analyzed includes another distinct sub-family of states of the form (4.73), namely that in which $k_1 \sim N^b$ with $0 < b \leq 1$, and either $\nu_1 = \nu$ or $\nu_1 = \nu + \frac{1}{k} - \frac{1}{k_1}$, i.e.

$$|{+}{+}\rangle_{k,\nu}^{N_0} \, |{+}{+}\rangle_{k_1,\nu}^{d_1} \ , \qquad\qquad |{+}{+}\rangle_{k,\nu}^{N_0} \, |{+}{+}\rangle_{k_1,\nu+\frac{1}{k}-\frac{1}{k_1}}^{d_1} \ . \tag{4.74}$$

The first of these values of ν_1 is obtained directly by taking the limit of our general family of CFT states (4.64) in which there is only one type of long strand, of polarization $|{+}{+}\rangle$.

The second value of for ν_1 arises because we have the freedom to flip the sign of the left angular momentum J^3 while keeping the right angular momentum $\bar{J}^3$ invariant. This can be implemented by the coordinate transformation $(\psi, \phi) \to (\phi, \psi)$ in our solutions (4.32), as discussed below Eq. (4.72). This gives the bulk solutions dual to a set of CFT states similar to those in Eq. (4.64) but with $|{+}{+}\rangle_k \to |{-}{+}\rangle_k$ and all $\varepsilon_i \to -\varepsilon_i$. This includes states of the form

$$|{-}{+}\rangle_{k,\nu}^{N_0} \, |{-}{+}\rangle_{k_1,\nu}^{d_1} \ . \tag{4.75}$$

By shifting $\nu \to \nu + 1/k$, we can rewrite these states as the second type of state in (4.74).

Note that setting $\nu = 0$ in the second type of state in (4.74), we obtain a set of states of which one is a RR ground state and one is a fractional spectral flowed state,

$$|{+}{+}\rangle_{k}^{N_0} \, |{+}{+}\rangle_{k_1,\frac{1}{k}-\frac{1}{k_1}}^{d_1} \ . \tag{4.76}$$

In our setup, the bulk configurations with $q = 0$ correspond to CFT states with all strands of one type (of the shorter winding k). Dialling q larger, we obtain solutions that describe states of the form (4.73) with $k_1 \sim N^b$ and either $\nu_1 = \nu$ or $\nu_1 = \nu + \frac{1}{k} - \frac{1}{k_1}$. For these states, q controls the fraction of the total strand budget accounted for by the long strands, as discussed around Eq. (4.58).

In the analysis of [178], emphasis was placed on the ability to interpolate from states involving strands of all one type to states involving strands of all the other type. On this point, let us note that there are two limitations to our construction: first, we cannot interpolate all the way to having only long strands, as this would invalidate the shockwave approximation we have made; the approximation relies on both long and short strands contributing an order-one fraction of the overall strand budget. Second,

our bulk solutions do not differentiate between the polarizations of the long strands, so the same bulk solutions describe interpolations between different pairs of fractionally spectral flowed states. In this sense our bulk description is more coarse-grained than that of [178]. Nevertheless, we have found the bulk description of interesting examples of states of the general form (4.73), allowing us to describe a partial interpolation between strands that have different amounts of spectral flow.

4.5 Discussion

In this chapter we have derived the first family of asymptotically flat BPS three-charge black hole microstate geometries containing a shockwave. We have done so by starting with the solution that describes the backreaction of a shockwave on an AdS background. We then exploited the spectral flow transformation together with the multi-center formalism of supersymmetric solutions. The result is reported in Eq. (4.29).

The solution is singular at the location of the shockwave and this is a physical singularity. Besides this, the microstate is smooth everywhere, it is horizonless and free of closed time-like curves. We have analytically checked this last property in the decoupling limit and performed a numerical analysis in the full asymptotically flat solution.

We have proposed a family of CFT states dual to the supergravity solution constructed, refining the proposal in [101]. This identification is supported by computing protected quantities in supergravity and at the free orbifold point in the dual CFT and by matching them. We have found perfect agreement in comparing the conserved charges. Furthermore, we have exploited the holographic dictionary, that relates the expectation value of some CFT operators with the fall off of the dual supergravity fields. Also in this case perfect agreement has been established. We also noted that in a certain limit our new solutions provide a partial interpolation between different three-charge microstate geometries, expanding the class of states discussed in [177, 178].

The new solution describes the backreaction of highly energetic supergravity quanta on a fractionally spectral flowed supertube background. While the total energy of the shockwave is fixed, the solution does not contain information about how the energy is distributed among the supergravity quanta. The dual statement in the CFT is that the number of single copies involved in the long strands in the state (4.64) is fixed, but the length and the number of each long strand is not. In this sense, the shockwave provides a coarse grained description of the high energy quanta. While we know that in the supergravity approximation we do not have access to highly quantum degrees of freedom, the shockwave is able to capture a coarse grained description of the physics.

We also observed that in our asymptotically flat solutions, the location of the shockwave is not on the evanescent ergosurface. As a result, the addition of the shockwave does

not come at zero cost in energy, and instead changes the momentum charge n_p along the y-circle. This is a physical difference from the two-charge solution containing a shockwave [101], discussed in [162] in the context of an evolution from less typical to more typical states, related to the perturbation process described in [160]. Nevertheless, we have argued that the CFT states dual to the solutions constructed in this work are naturally thought of as more typical than the solutions without shockwaves, when each is compared to other microstates with the same respective values of n_p.

Our analysis suggests possible generalizations. One is to generalize this shockwave construction to other supersymmetric two and three-charge microstates. In particular, it may be possible to compute the backreaction of a shockwave that lies on the evanescent ergosurface of a fractionally spectral flowed supertube background: this result would directly connect with the analysis of the non-linear instability of [160]. Second, it would also be interesting to study the backreaction of a shockwave on the ergoregion of a JMaRT background [78]: this would provide the evolution of a non-supersymmetric, linearly unstable microstate solution and might shed light over the unitary evaporation process that should replace Hawking's pair production at the microscopic level.

Part III

Evolutionary algorithms for multi-center solutions

Chapter 5

Evolutionary algorithms for multi-center solutions

5.1 Introduction

This chapter contains the work reported in [4]. We will present an optimization algorithm to construct new approximate multi-center solutions with a high number of centers in generic configurations.

The multi-center formalism has been introduced in Chapter 4 in the context of two centers solutions. We remind the reader that multi-center solutions (also known as bubbling solutions) are described by a set of harmonic functions on a three dimensional euclidean space and the four dimensional base space is of the Gibbons-Hawking form. While this set up might seem simple, deriving physically sensible solutions with several centers is a hard problem. The reason being that asymptotic flatness, charge quantization, regularity and absence of CTCs impose constraints (e.g. the bubble equations introduced in Eq. (4.18)) that make the positions of the centers and the coefficients of the poles of the harmonic functions interdependent. Moreover, only a subset of such solutions share the same asymptotic charges of a macroscopic black hole.

We have a good analytic control of multi-center solutions with a low (≤ 4) number of centers (see e.g. [72–75, 154]), but less examples with higher number of centers are known [69] and they usually take all centers to lie on a line, so that the configuration is axisymmetric. An important step forward to construct multi-center solutions with a high number of centers was provided in [71]: by taking the fluxes, instead of the distances between the centers, as dependent variables, the authors wrote the bubble equations as a linear system of the form $\mathcal{M}_{\alpha\beta}\,\Pi_\beta = B_\alpha$, where $\mathcal{M}$ is a symmetric matrix. They also conjectured that a solution satisfying such equation does not contain CTCs if and only if $\mathcal{M}$ is positive definite. While such perspective simplified the task of finding physically

relevant solutions, it relies on the requirement that the distances between the centers shall be rational. Such a requirements ensures that the resulting fluxes are rational, consistently with flux quantization.

While two-center bubbling solutions have a well-established holographic description [78, 85, 151–154] (which we have reviewed in Section 4.4.4), multi-center solutions with a higher number of centers do not have a proposed holographic dual. It has been suggested in [179] that these configurations are not part of the phase space of a supersymmetric black hole, but they should rather be thought of as microstates of other black objects. Nonetheless, these class of configurations are interesting examples of gravitational solutions that closely resemble black holes. This is especially true in the so called "scaling" regime, in which all the centers are localized deep inside a long-black-hole like throat. For example, multi-center solutions have been used to study potentially observable signatures of fine-grained structure of black holes in gravitational wave observations [180–182].

In recent years, an increasing domain of String Theory and Particle Physics problems have been address with the aid of optimization algorithms and machine learning (see e.g. [183–190]). In this chapter we propose an algorithm, based on Bayesian optimization and evolutionary algorithm, to generate approximate solutions to the bubble equations that are free of CTCs, respect all quantization conditions and describe a high number of centers in a generic configuration.

The starting point is a set of centers in a three dimensional Euclidean space. We use a Bayesian optimization algorithm to assign charges to these centers that give rise to solutions with D1 and D5 charges greater than a desired threshold $\bar{Q}$ ($Q_1, Q_5 > \bar{Q}$). While doing so, we focus on geometries that are in the scaling regime. With this aim, following [73], we solve the $AdS_2 \times S^3$ version of the bubble equations: these equations are scale invariant and are relevant to construct scaling solutions, which have the property that the separation between the centers can be made arbitrarily small while keeping the asymptotic charges practically constant. The fluxes resulting from this procedure are in general irrational. In accordance with the flux quantization condition we round the fluxes and obtain an approximate solution to the bubble equation. Such a solution is approximate for two reasons: first, the fluxes have been rounded; second, we obtained this solution by solving the AdS_2 version of the bubble equations, rather then the fully asymptotically flat ones.

We improve on this approximate solution by implementing an evolutionary algorithm (EA) that changes the positions of the centers to maximize a fitness function (i.e. a function that measures how well the bubble equations are solved). The evolutionary algorithm works by generating a population of individuals starting from the aforementioned approximate solution and making these individuals evolve following the principles of the Darwinian theory: selection, heredity and variation. This algorithm, iterated over several generations, leads to new individuals with higher fitness. Once an individual with

the desired fitness is generated, we check the absence of CTCs by computing the eigenvalues of the matrix $\mathcal{M}$. Our algorithm is designed to generate solutions with an arbitrary number of centers in a generic configuration. We test it explicitly for configurations of three, five and seven centers and will provide explicit examples in due course. Generating solutions with a higher number of centers or higher fitness is feasible, although computationally more expensive.

This chapter is structured as follows. In Section 5.2 we revise the construction of multi-center scaling solutions with the formalism introduced in [71]. In Section 5.3 we describe the Bayesian optimization algorithm and the evolutionary algorithm designed for our task. In Section 5.4 we describe explicit examples of a five-center and a seven-center configuration obtained with our method. In Section 5.4.3 we discuss the performance of the algorithm and compare it with a random search. Section 5.5 contains the conclusions.

5.2 Multi-center scaling supergravity solutions

5.2.1 Multi-center solutions

We begin by resuming and extending the review in Section 4.3.1 on multi-center solutions (also known as bubbling geometries), highlighting the feature that are relevant for the discussion in this chapter.

For concreteness, we shall primarily have in mind 5D $\mathcal{N} = 1$ Super-Einstein-Maxwell-Yang-Mills supergravity, whose bosonic field content is given by the metric, three Abelian vector multiplets, and an SU(2) triplet of non-Abelian vector multiplets.

Multi-center solutions are specified by a set of harmonic functions on a three-dimensional Euclidean "base" space, which have poles at the location of the centers. The index $a = 0, 1, ..., n-1$ labels the centers, and $r_a = |\vec{r} - \vec{r}_a|$ is the distance from the a-th center in the three-dimensional base. In the Abelian sector the harmonic functions are ($i = 0, 1, 2$):

$$H = \sum_{a=0}^{n-1} \frac{q_a}{r_a}\,, \qquad K^i = \sum_{a=0}^{n-1} \frac{k_a^i}{r_a}\,, \qquad L^i = l_0^i + \sum_{a=0}^{n-1} \frac{l_a^i}{r_a}\,, \qquad M = m_0 + \sum_{a=0}^{n-1} \frac{m_a}{r_a}\,, \tag{5.1}$$

where $q_a \in \mathbb{Z}$. In the non-Abelian sector [191], denoting the gauge coupling by g, we have

$$P = 1 + \sum_{a=0}^{n-1} \frac{\lambda_a}{r_a}\,, \qquad Q = \sum_{a=0}^{n-1} \frac{\sigma_a \lambda_a}{r_a}\,. \tag{5.2}$$

The harmonic function H defines a four-dimensional Gibbons-Hawking metric via

$$ds_4^2 = H^{-1}(d\psi + A)^2 + H ds_3^2\,, \tag{5.3}$$

where ds_3^2 is the flat metric on $\mathbb{R}^3$, and A is a one-form related to H via $\star_3\, dA = dH$. For the full five-dimensional fields, we refer the reader to [71].

Only certain subsets of possible coefficients of the poles in Eqs. (5.1) and (5.2) lead to physically sensible solutions: one needs to impose further constraints. First, asymptotic flatness requires $\sum_a q_a = 1$. Second, upon uplifting to Type IIB supergravity compactified on $S^1 \times T^4$, the coefficients k_a^i are quantized in terms of integer flux parameters n_a^i as follows [154],

$$k_a^0 \,=\, \frac{g_s\alpha'}{2R_y} n_a^0\,, \qquad k_a^1 \,=\, \frac{g_s\alpha'^3}{2V_4 R_y} n_a^1\,, \qquad k_a^2 \,=\, \frac{R_y}{2} n_a^2\,, \tag{5.4}$$

where the coordinate volume of T^4 is $(2\pi)^4 V_4$ and that of the S^1 is $2\pi R_y$.

We focus on smooth horizonless supersymmetric solutions.[1] The following relations are imposed by absence of event horizons and singularities (the first three relations) and asymptotic flatness (the last two relations), see e.g. [71, App. A.3],

$$\begin{aligned} l_a^i \,&=\, -\frac{|\epsilon^{ijk}|}{2}\frac{k_a^j k_a^k}{q_a} + \frac{\delta^{0i}}{2g^2}\,, \qquad \sigma_a \,=\, \frac{k_a^0}{q_a}\,, \qquad m_a \,=\, \frac{k_a^0}{2q_a^2}\big(k_a^1 k_a^2 - \frac{1}{2g^2}\big)\,, \\ l_0^0 l_0^1 l_0^2 \,&=\, 1\,, \qquad m_0 \,=\, -\frac{1}{2}\sum_{a,i} l_0^i k_a^i\,. \end{aligned} \tag{5.5}$$

The absence of Dirac-Misner singularities imposes the so-called "bubble equations" [51, 191, 194], which constrain the relation between the positions of the centers and the local charges:

$$\sum_{b\neq a} \frac{q_a q_b}{r_{ab}} \Pi^0_{ab}\Big(\Pi^1_{ab}\Pi^2_{ab} - \frac{1}{2g^2}\mathbb{T}_{ab}\Big) = \sum_{b,i} q_a q_b l_0^i \Pi^i_{ab}\,, \tag{5.6}$$

where

$$\Pi^i_{ab} = \frac{k_b^i}{q_b} - \frac{k_a^i}{q_a}, \qquad \mathbb{T}_{ab} = \frac{1}{q_a^2} + \frac{1}{q_b^2}\,. \tag{5.7}$$

Here r_{ab} is the $\mathbb{R}^3$ Euclidean distance between centers a and b, Π^i_{ab} are the magnetic fluxes, and we will refer to the coefficients k_a^i as flux parameters. The bubble equations are a set of n equations among which only $(n-1)$ are independent: summation over a leads to a trivial identity, due to the antisymmetry of the Π^i_{ab}.

[1] The supersymmetric multi-center formalism can also be used to construct solutions with physical singularities such as shockwaves [3], which give collective descriptions of families of pure states. Similar but different multi-center formalisms exist for non-supersymmetric solutions [86, 87, 192, 193].

The asymptotic charges of the multi-center solutions are [51]:[2]

$$\begin{aligned}
Q_1 &= -\sum_{a,b,c} q_a q_b q_c \Pi^1_{ab}\Pi^2_{ac} + \frac{1}{2g^2}\sum_a \frac{1}{q_a}\,,\\
Q_5 &= -\sum_{a,b,c} q_a q_b q_c \Pi^0_{ab}\Pi^2_{ac}\,,\\
Q_p &= -\sum_{a,b,c} q_a q_b q_c \Pi^0_{ab}\Pi^1_{ac}\,,\\
J_L &= -\frac{1}{2}\sum_{a,b,c,d} q_a q_b q_c q_d \Pi^0_{ab}\Pi^1_{ac}\Pi^2_{ad} + \frac{1}{4g^2}\sum_{a,b}\frac{q_b\Pi^0_{ab}}{q_a}\,,\\
\vec{J}_R &= \frac{1}{4}\sum_{a,b,a\neq b} q_a q_b \Pi^0_{ab}\Big(\Pi^1_{ab}\Pi^2_{ab} - \frac{1}{2g^2}\mathbb{T}_{ab}\Big)\frac{\vec{r}_a-\vec{r}_b}{|\vec{r}_a-\vec{r}_b|}\,.
\end{aligned} \tag{5.8}$$

5.2.2 Scaling solutions and their construction

Of particular interest are solutions to the bubble equations (5.6) in which the distances between the centers can be made uniformly parametrically small by scaling $r_{ab} \to \lambda r_{ab}$ with $\lambda \ll 1$, while keeping the asymptotic charges approximately constant. These solutions are known as "scaling" solutions [51, 69, 70]. Note that the rescaling $r_{ab} \to \lambda r_{ab}$ is equivalent to multiplying the RHS of (5.6) by λ, with $\lambda \ll 1$. It will be useful for us to note that in the limit $\lambda \to 0$, one obtains the homogeneous bubble equations [70] (see also for instance [73]),

$$\sum_{b\neq a}\frac{q_a q_b}{r_{ab}}\Pi^0_{ab}\left(\Pi^1_{ab}\Pi^2_{ab} - \frac{1}{2g^2}\mathbb{T}_{ab}\right) = 0\,. \tag{5.9}$$

Therefore, in the scaling regime of small λ, solutions to the full inhomogeneous bubble equations (5.6) are also approximate solutions to the homogeneous bubble equations (5.9), up to terms of order λ. We will exploit this to construct new scaling solutions.

The full inhomogeneous bubble equations (5.6) have typically been considered as equations in which the variables to be solved for are the distances r_{ab}, see e.g. [51]. This perspective has two disadvantages [71]. First, it is generically difficult to find solutions for r_{ab}. Second, after solving the equations, one often finds that the resulting r_{ab} do not represent possible distances between points in 3D Euclidean space; for example, the triangle inequality might not be respected.

A recently developed alternative approach is to exploit the feature that the bubble equations (5.6) are linear in the flux parameters k^2_a. Thus, instead of solving for the distances, one can first specify the positions of the centers, and then solve for the flux

[2] We use conventions in which J_L and J_R are interchanged with respect to [51].

parameters k_a^2 with $a = 2, 3, ...n$ [71][3]. While this procedure is general and not restricted to scaling solutions, let us now review it in the context of scaling solutions. We introduce a scaling parameter λ that rescales the position of the centers while keeping the shape of the distribution fixed: i.e. we write the distance between the centers as $r_{ab} = \lambda d_{ab}$, where d_{ab} remain constant in the scaling process. We define[4]

$$\begin{aligned} \bar{A}^2_{ab} &= \frac{q_a q_b}{d_{ab}} \Pi^0_{ab} \Pi^1_{ab} \,, \qquad \dot{A}^2_{ab} = -s q_a q_b l_0^2 \,, \\ \bar{B}^2_{ab} &= \sum_{b=0}^{n-1} \frac{q_a q_b}{d_{ab}} \frac{1}{2g^2} \mathbb{T}_{ab} \Pi^0_{ab} \,, \qquad \dot{B}^2_a = s \sum_{b=0}^{n-1} q_a q_b (l_0^0 \Pi^0_{ab} + l_0^1 \Pi^1_{ab}) \,, \end{aligned} \tag{5.10}$$

where we have introduced the constant s which takes values 0 or 1. These values correspond respectively to the homogeneous and inhomogeneous bubble equations, as we shall see momentarily. We then introduce ($\alpha \,, \beta \, = \, 1, ..., n-1$)[5]

$$\begin{aligned} \bar{\mathcal{M}}^2_{\alpha\beta} &= \bar{A}^2_{(\alpha+1)(\beta+1)} - \delta^\beta_\alpha \sum_{c=0}^{n-1} \bar{A}^2_{(\alpha+1)c} \,, \\ \dot{\mathcal{M}}^2_{\alpha\beta} &= \dot{A}^2_{(\alpha+1)(\beta+1)} - \delta^\beta_\alpha \sum_{c=0}^{n-1} \dot{A}^2_{(\alpha+1)c} \,, \end{aligned} \tag{5.11}$$

in terms of which, we write the following linear system of equations in the fluxes Π^2_{ab}:

$$\mathcal{M}^2_{\alpha\beta} \Pi^2_{1(\alpha+1)} \equiv \left(\bar{\mathcal{M}}^2_{\alpha\beta} + \lambda \dot{\mathcal{M}}^2_{\alpha\beta} \right) \Pi^2_{1(\alpha+1)} \, = \, \bar{B}^2_\beta + \lambda \dot{B}^2_\beta \,. \tag{5.12}$$

For $s = 1$ this linear system is equivalent to the inhomogeneous bubble equations (5.6), while for $s = 0$ the system is equivalent to the homogeneous bubble equations (5.9).

Although this perspective has simplified the task of solving the bubble equations, it remains a fact that generic solutions obtained in this way will not respect the quantization conditions in Eq. (5.4). This can be seen as follows. If we choose generic locations of the centers, generic relative distances will be irrational numbers. Then generic solutions will give irrational values of the flux parameters k^2_α, which is in conflict with the quantization conditions in Eq. (5.4).

Using this method one can construct exact solutions with quantized fluxes by arranging a set of non-generic locations of centers, such that all relative distances are rational. For instance one can take all centers to lie on a line, or on a circle, as discussed in [71].[6] While these constructions provide interesting and valuable exact solutions, the requirement to work with non-generic locations of centers is a significant limitation.

[3] The bubble equations are also linear in $k_a^{0,1}$, so a similar analysis can be carried out for them.

[4] A numerical typo in [71, Eq. (3.22)] has been corrected.

[5] To be clear, the '2' are superscript labels for the value of the index i, not exponents. To avoid potential confusion on this point, we have suppressed the superscript '2' on the matrix $\mathcal{M}^2$ in the Introduction and Discussion sections.

[6] For earlier examples of solutions with all centers on a line, see e.g. [69].

To proceed further, an alternative approach is to give up the idea of pursuing exact solutions and construct approximate solutions to the bubble equations. One can do so with an iterative approach, as follows. One first chooses a set of center locations, then solves for k_α^2, generically obtaining irrational values. One then rounds the k_α^2 to nearby rational numbers to a desired precision, obtaining an approximate solution, as discussed in [71] and done in [72, 73].

A further step is to take the rounded flux parameters k_α^2, re-solve the bubble equations (in the traditional way) to obtain a new set of distances r_{ab}, and then arrange center positions to have the resulting relative distances. If this could be done analytically, one can obtain exact solutions, however typically this is hard, for the reasons discussed below Eq. (5.9). More realistically, one can employ this method to improve the precision of the approximate solution, as done in [73]. However, for more than four centers, doubt has been expressed as to the feasibility of this method [71].

In our approach, we first round the flux parameters k_α^2 as above. However, for the next step, we introduce our new method of varying the positions of the centers using an evolutionary algorithm. The resulting method can be used to construct numerical solutions with any number of centers, and with no symmetry imposed on the locations of the centers. The algorithm constructs numerical solutions whose precision improves by several orders of magnitude on that of a given seed solution (obtained by simply rounding irrational quantities). Since we work with the positions of the centers, by construction the distances between them are always well-defined.

Our primary interest is in scaling solutions, and so we tailor the algorithm to construct scaling solutions, which have $J_R \ll 1$, see e.g. [112]. We also ensure that the dimensionful D1 and D5 charges are sufficiently large that the supergravity approximation is valid. We do this by introducing a hyperparameter $\bar{Q}$ and requiring the algorithm to select only solutions satisfying $Q_1, Q_5 > \bar{Q}$, using a Bayesian optimization algorithm.

Following the discussion below (5.9), given a generic set of locations of the centers, we can obtain a configuration in the scaling regime by first solving the homogeneous bubble equations (5.9) for the flux parameters k_α^2, and then rescaling $r_{ab} \to \lambda r_{ab}$ with $\lambda \ll 1$, as done in [73]. Let us consider the homogeneous bubble equations (5.9) for $a = n-1$:

$$\sum_{b\neq n-1} \frac{q_{n-1}q_b}{r_{(n-1)b}} \Pi^0_{(n-1)b} \left(\Pi^1_{(n-1)b}\Pi^2_{(n-1)b} - \frac{1}{2g^2}\mathbb{T}_{(n-1)b} \right) = 0\,. \tag{5.13}$$

Let us further examine the generic case in which all the terms in this sum are non-zero. Then a necessary condition to have a solution is that not all of the terms in the sum have the same sign.
Since the distances are positive, the expressions $q_{n-1}q_b\Pi^0_{(n-1)b}(\Pi^1_{(n-1)b}\Pi^2_{(n-1)b} - \frac{1}{2g^2}\mathbb{T}_{(n-1)b})$ should not all have the same sign.

The next step in the procedure is to round the flux parameters, $k_\alpha^2 \to \tilde{k}_\alpha^2$, to a certain precision, which is a hyperparameter of the algorithm, and which we call `k_rounding`. From here onwards, tildes denote rounded quantities. After rounding, Eq. (5.9) will no longer be exactly satisfied for the same configuration of centers. Our strategy will be to keep the rounded fluxes $\tilde{\Pi}^2$, and change the location of the centers, to construct a high-precision numerical scaling solution. Based on the above discussion, we shall impose that not all of the following expressions have the same sign (note the presence of the rounded fluxes $\tilde{\Pi}^2$):

$$q_{n-1}q_b\Pi^0_{(n-1)b}\left(\Pi^1_{(n-1)b}\tilde{\Pi}^2_{(n-1)b}-\frac{1}{2g^2}\mathbb{T}_{(n-1)b}\right). \tag{5.14}$$

The condition Eq. (5.9) for scaling solutions, and the scaling limit $r_{ab} \to \lambda r_{ab}$, correspond to "zooming in" to the core of the solutions, such that the asymptotics become AdS_2 fibered over S^3; for a general discussion, see [112]. In order to "undo" this limit and construct solutions with $\mathbb{R}^{4,1}$ asymptotics, which requires restoring the inhomogeneous part of the bubble equations (5.6), we will implement an evolutionary algorithm that moves the positions of the centers in space.

The solutions must also satisfy the absence of CTCs. Let us first review the case in which only Abelian fields are turned on. To rule out CTCs, two algebraic combinations of the harmonic functions (5.1) must be globally positive. Generically, the stronger of these conditions is that the quartic $E_{7(7)}$ invariant, as a function of the harmonic functions (5.1), is globally positive [164]. Investigating this condition is non-trivial, and typically done numerically. The generalization to configurations with both Abelian and non-Abelian fields was discussed in [71, 191]. The authors of [71] conjectured that the condition for absence of CTCs is equivalent to requiring that the matrix $\mathcal{M}^2$ defined in (5.12) is positive-definite. We will thus investigate absence of CTCs in the solutions found by the algorithm by examining this condition on $\mathcal{M}^2$.

5.3 The algorithm

In this section we will describe the algorithm developed in this work, which is composed of two main parts. In the first part, we use a Bayesian optimization (BO) algorithm to find points in parameter space that lead to solutions with $Q_1, Q_5 > \bar{Q}$. Upon rounding the flux parameters k_α^2, this procedure leads to a approximate solution of the homogeneous bubble equations (5.9). The second part of the algorithm makes use of an evolutionary algorithm to find numerical solutions to the full inhomogeneous bubble equations (5.6), by varying the positions of the centers.

5.3.1 The Bayesian optimization algorithm

In the first part of the process, we generate solutions of the homogeneous bubble equations (5.9), in the form (5.12). We do so by taking the position of the centers $\vec{r}_a$ and the coefficients q_a, l_0^i, $k_a^{0,1}$ and k_0^2 to be independent variables, and solving for k_α^2 (recall $\alpha = 1, ..., n-1$). However, generically the resulting global charges will not satisfy $Q_1, Q_5 > \bar{Q}$. To construct solutions such that $Q_1, Q_5 > \bar{Q}$, in principle one could maximise the first two expressions in (5.8) as functions of both k_0^2 and the full set of $k_a^{0,1}$. However in practice, it is neither computationally efficient, nor necessary, to maximize Q_1, Q_5 with respect to a substantial fraction of the flux parameters $k_a^{0,1}$ — it suffices to focus on the flux parameters of a small number of the centers. We thus introduce a hyperparameter $n_{\rm B}$ and maximize Q_1, Q_5 only with respect to the flux parameters of $n_{\rm B}$ of the centers. In our examples, it will suffice to take $n_{\rm B}$ to be equal to 1 or 2.

The centers whose flux parameters are dependent variables of the optimization process will be labelled with the index $\bar{a} = 0, \cdots, n_{\rm B} - 1$, and the remainder will be labelled with the index $\dot{a} = n_{\rm B}, \cdots, n-1$. In other words, we will fix the value of the flux parameters $k_{\dot{a}}^{0,1}$ when initializing the algorithm and we then maximize the value of the global charges with respect to k_0^2 and $k_{\bar{a}}^{0,1}$.

In order to maximize the value of the global charges we use a Bayesian optimization algorithm. The reason for this choice is that the global charges Q_1, Q_5 in (5.8) are computationally expensive to evaluate: for any given trial configuration, one must first solve the homogeneous bubble equations for k_α^2, and then use the result to compute Q_1, Q_5.

Let us now provide an intuitive description on how the Bayesian optimization algorithm works. The Bayesian optimization algorithm is an approach to find the global maximum (or minimum) of a black-box function, called the objective function. By black-box function we mean either a function over which we have no analytic control (for example a stochastic function) or a function that is computationally expensive to evaluate, as in the case at hand. As a result, we do not have a global knowledge of the function, i.e. we do not know its value on every point of the domain, but we have the freedom to evaluate it on a finite set points. With this perspective, the Bayesian optimization algorithm is a strategy to obtain the maximum of such functions that works better than a random search. It works as follows, for a review see e.g. [195]. First, a Gaussian process prior is placed on the objective function. Then, the objective function is evaluated on a set of points $[x_1, \cdots, x_{\mathbf{n_0}}]$ of the domain. At this stage, the data $\{[x_1, \cdots, x_{\mathbf{n_0}}], [f(x_1), \cdots, f(x_{\mathbf{n_0}})]\}$ represent all our knowledge on the objective function. Of course, there are infinite functions whose value is $[f(x_1), \cdots, f(x_{\mathbf{n_0}})]\}$ when evaluated on $[x_1, \cdots, x_{\mathbf{n_0}}]$, but, by assuming that the objective function follows a Gaussian process model, these are not all equally probable. Thus, the next step is to obtain the surrogate function, which, among the infinite functions that have the same value of

the objective on the points $[x_1, \cdots, x_{\mathbf{n_0}}]$, has the highest probability of representing the objective[7]: as such, it is our best estimate of the objective based on the knowledge we have so far, and has the advantage of being much quicker to evaluate. The last ingredient of the algorithm is the acquisition function, also known as acquisition strategy. By evaluating the surrogate function on a finite set of points of the domain, it chooses the next sampling point of the objective (i.e. the point of the domain that is more likely to pay off when the objective is evaluated on it), according to some specified strategy (there are many different possible acquisition strategies, we refer to [195] for further reading on this topic). By evaluating the objective on this new point we increase the knowledge we have on the objective, thus after each additional sampling point the surrogate is updated and the acquisition function is iteratively used to choose the next sampling point, until an acceptably good approximate maximum (in our case, $Q_1, Q_5 > \bar{Q}$) of the objective is found, or a previously set computational limit is reached (in our case, a maximum number of iterations N).

We now explain this first part of our algorithm in more detail. We initialize the independent variables as follows. The q_a must all sum to 1. If n is odd, we use alternating values ± 1, starting and ending with 1. If n is even, the first $n-1$ use alternating values ± 1, starting and ending with -1, while $q_n = 2$:

$$q_a = \begin{cases} (1, -1, 1, \ldots, -1, 1) & n \text{ odd} \\ (-1, 1, -1, \ldots, -1, 2) & n \text{ even} \end{cases} \quad ; \qquad l_0^i = 1 \quad \forall\, i\,. \tag{5.15}$$

Furthermore, we choose the position of the n centers so that they lie inside a cube with edge length equal to two. We set up the coordinate system in such a way that the first center is at the origin, the second is at $y = 0$, $z = 0$ and the third center is at $z = 0$, so that we have a total of $3n - 6$ free coordinates. We sample the remaining non-zero r_a^i from the following uniform distribution:

$$r_a^i \;\sim\; U\big(-1, 1\big)\,. \tag{5.16}$$

In practice, this sampling is obtained from a discrete distribution whose step-size is controlled by the hyperparameter `prec_pos`. Similarly, the coefficients $k_{\bar{a}}^{0,1}$ are sampled with the discrete uniform distribution $U\big(-10^{\texttt{prec\_k}}, 10^{\texttt{prec\_k}}\big)$, with step-size equal to 1. In the following we will set the parameter `prec_k` $= 2$.

Having initialized all the parameters we are not optimizing over, we now maximize the objective function

$$f_{\text{OBJ}} \;=\; \min\big(Q_1, Q_5\big)\,, \tag{5.17}$$

as a function of the variables $\{k_{\bar{a}}^{0,1}, k_0^2\}$, which (having set `prec_k` $= 2$) we also allow to

[7] This is why this optimization algorithm is called Bayesian: given the knowledge on the objective, the prior is used to obtain a posterior, which in this case is the surrogate function.

take integer values in $[-100, 100]^{\otimes(2n_{\text{B}}+1)}$. The evaluation of f_{OBJ} works as follows. We first solve the homogeneous bubble equations (5.9). Next, we round the flux parameters $k_\alpha^2 \to \tilde{k}_\alpha^2$. Last, we use (5.8) to compute Q_1, Q_5 and select the minimum of the two.

We evaluate the objective function on $\mathbf{n_0}$ points in the $(2n_{\text{B}}+1)$-dimensional space of $\{k_{\bar{a}}^{0,1}, k_0^2\}$ sampled from the discrete uniform distribution $U\big(-10^2, 10^2\big)^{\otimes(2n_{\text{B}}+1)}$. Assuming a Gaussian process prior with a Radial Basis Function as kernel, we use knowledge of f_{OBJ} evaluated at this set of points to generate the surrogate function. We use $\mathbf{n_0} = 200$.

We then evaluate the surrogate function on a much higher number (of order 10^4) of randomly sampled points, with discrete uniform distribution $U\big(-10^2, 10^2\big)^{\otimes(2n_{\text{B}}+1)}$ and step-size 1. We use an acquisition function based on the Probability of Improvement method (see e.g. [196]) to choose the next point of the domain that is most worth evaluating with the objective function. The knowledge of f_{OBJ} at this new point is then used to update the surrogate function. This process is iterated until a point $\{k_{\bar{a}}^{0,1}, k_0^2\}$ such that $f_{\text{OBJ}}\big(\{k_{\bar{a}}^{0,1}, k_0^2\}\big) > \bar{Q}$ is found, or a previously set computational limit (the maximum number of iterations N) is reached. This procedure is summarized in Algorithm 1.

Algorithm 1 BO algorithm

function $f_{\text{OBJ}}(\{k_{\bar{a}}^{0,1}, k_0^2\})$
  $k_\alpha^2 \leftarrow$ Solve the homogeneous bubble equations (5.9)
  $\tilde{k}_\alpha^2 \leftarrow$ Round k_α^2
  Compute Q_1, Q_5 via (5.8)
  return $\min\big(Q_1, Q_5\big)$

Assume Gaussian process prior
Evaluate f_{OBJ} on $\mathbf{n_0}$ points $\{k_{\bar{a}}^{0,1}, k_0^2\}$ sampled with $U\big(-10^2, 10^2\big)^{\otimes(2n_{\text{B}}+1)}$
$Q_{\max} \leftarrow$ The maximum output of f_{OBJ} found so far
Generate the surrogate function using the available data
while $n < N$ or $Q_{\max} < \bar{Q}$ **do**
  Let $\{k_{\bar{a}}^{0,1}, k_0^2\}_n$ be the point returned by the acquisition function
  Evaluate $f_{\text{OBJ}}\big(\{k_{\bar{a}}^{0,1}, k_0^2\}_n\big)$
  $Q_{\max} \leftarrow$ if $f_{\text{OBJ}}\big(\{k_{\bar{a}}^{0,1}, k_0^2\}_n\big) > Q_{\max}$, update $Q_{\max}$
  Update the surrogate function with the new data
  $n{+}{+}$

While this algorithm is not guaranteed to find a solution, we found that in practice this approach is much more successful than a random search.

After a successful run of the BO algorithm, we have an approximate solution to the homogeneous bubble equations, with charges Q_1, Q_5 in the desired range. We next generate another approximate solution by rescaling the positions of the centers obtained in Eq. (5.16):

$$r_a^i \to \bar{r}_a^i \equiv \lambda\, r_a^i\,, \qquad \lambda \ll 1\,, \tag{5.18}$$

where for concreteness we take $\lambda = 10^{-5}$. We wish to use the resulting configurations as inputs to the evolutionary algorithm that will find numerical solutions to the inho-

mogeneous bubble equations. However, before proceeding, we examine two conditions to check whether the configurations are indeed good seed solutions.

The first condition is the condition that the expressions in Eq. (5.14) do not all have the same sign, so that it is possible that there is a nearby scaling solution to be found. Next, we check that the matrix $\mathcal{M}^2$ is positive-definite. Even if $\mathcal{M}^2$ depends on the positions of the centers (and thus will be modified by the EA), we have observed that small modifications of the distances do not tend to change the eigenvalues much. Of course, after the evolutionary algorithm, one must recheck the condition on $\mathcal{M}^2$. However, checking the condition at this stage provides a good indication of whether the condition will be respected in the final solution. If both conditions are satisfied, we use this configuration as a seed for the evolutionary algorithm.

5.3.2 The evolutionary algorithm

A successful run of the Bayesian optimization algorithm outputs an approximate solution to the homogeneous bubble equations (5.9) with the desired characteristics. The approximate nature of this solution is due to the rounding of the flux parameters k_α^2. Our task is now to obtain a numerical solution of the inhomogeneous bubble equations (5.6) by moving the positions of the centers in the $\mathbb{R}^3$ base space.

We shall do so by using an evolutionary algorithm (EA), which is an optimization algorithm inspired by Darwin's theory of evolution. The starting point is a population, i.e. a set of individuals that are approximate solutions to the problem we wish to solve. The properties of each individual are called genes. We measure how good an approximate solution is via the fitness function, which is the function we want to maximize. The fittest individuals are selected to reproduce, by passing some of their genes to their offspring and in the reproduction process some mutations are implemented, i.e. random modifications of the genes of the offspring. Then the offspring take the place of the less fit individuals, which die, such that the population size is constant. This process is iterated until a sufficiently good solution is found, or a previously set computational limit is reached.

For the case at hand, each individual is an approximate solution to the bubble equations (5.6) and is characterized by the positions of the centers and a set of strategy parameters, whose role will be described shortly. After implementing the translational and rotational symmetry, the number of free coordinates is $3n-6$, while the number of independent bubble equations is $n-1$. Implementing a genetic algorithm on all the $3n-6$ coordinates would be computationally expensive. Thus, we select a subset of the coordinates to be fixed to the values of the BO algorithm output, $\bar{r}_a^i$ of Eq. (5.18). We observed that fixing approximately one coordinate on each of the last $n-3$ centers provides a good balance between effectiveness and computational cost, and we shall give

explicit examples of this in Section 5.4. We shall denote by d the number of degrees of freedom, i.e. the number of unfixed coordinates over which we run the EA.

To describe the algorithm further, we introduce the multi-index $A = (a, i)$ combining the center label a and the three Euclidean coordinates i. For the p^{th} individual in the population, we denote the set of coordinates to be varied by $r_A^{(p)}$. As noted above, we work directly with the positions of the centers as genes, so the distances between the centers are always well-defined. In the reproduction process random mutations can occur and the magnitude of the mutations is controlled by a strategy parameter $\sigma_A^{(p)}$. Each direction has an independent strategy parameter, which is a gene of the individual that undergoes variation and selection itself. As we will describe in the following, we will initialize the positions of the individuals in the population by sampling from a Gaussian distribution with fixed standard deviation, which will be taken as the initial value of the strategy parameter for every individual and every direction.

The genes of the p-th individual in the population are then

$$\{r_A^{(p)}, \sigma_A^{(p)}\}\,, \qquad A = (a, i)\,. \tag{5.19}$$

All genes $r_A^{(p)}, \sigma_A^{(p)}$ undergo variation and selection. An individual whose genes are likely to survive in the evolutionary process will have a good set of positions $r_A^{(p)}$, that will be quantified by having high fitness, and a set of strategy parameters $\sigma_A^{(p)}$ that are likely to give rise to fit offspring, as will become clearer when we discuss reproduction and mutation. The evolutionary mechanism is iterated over a certain number of generations controlled by the hyperparameter `generations`; in each new generation a number of offspring is generated, specified by the hyperparameter `offspring_per_generation`. The optimal values of these hyperparameters depend on the number of degrees of freedom of the problem, i.e. the number of centers of the configuration, as we shall see in examples.

Fitness function

We now define the fitness function, i.e. the function the EA algorithm seeks to maximize. We seek solutions to the inhomogeneous bubble equations (5.6), so we use these to construct the fitness function. By rearranging the bubble equations, we write:

$$\sum_{a\neq b} \frac{q_a q_b}{r_{ab}} \Pi^0_{ab} \Big(\Pi^1_{ab} \Pi^2_{ab} - \frac{1}{2g^2} \mathbb{T}_{ab} \Big) - \sum_{b,i} q_a q_b l_0^i \Pi^i_{ab} \;=\; \epsilon_a\,, \tag{5.20}$$

where if $\epsilon_a \;=\; 0 \;\; \forall a$ then the solution is exact. We seek configurations $\{r_A\}$ that minimize $\sum_a |\epsilon_a|$. We thus define our fitness function to be

$$f(r_A) \;=\; \frac{1}{\sum_a |\epsilon_a|}\,. \tag{5.21}$$

It will also be useful to define the following inverse fitness function:

$$f_{\text{inv}}(r_A) = \sum_a |\epsilon_a| \,. \tag{5.22}$$

Population initialization

We initialize a population of `pop_size` individuals by starting with the configuration of centers obtained in (5.18), and adding to it a random variable $\delta r_A^{(p)}$ sampled from the Gaussian distribution $\mathcal{N}(0, \texttt{var\_pos})$ with mean 0 and standard deviation `var_pos`, where `var_pos` is a hyperparameter of the algorithm:

$$r_A^{(p)} = \bar{r}_A + \delta r_A^{(p)} \qquad \text{for } p = 1, \cdots, \texttt{pop\_size} \,. \tag{5.23}$$

The optimal value of `var_pos` depends on the number of centers. If `var_pos` is too small, we generate a population that is too similar to the seed solution; if `var_pos` is too large, we obtain a large number of unfit individuals in the initial population. It is not practical to compute optimal value of `var_pos` directly from the bubble equations Eq. (5.6), so we optimize it via a simple grid search. Concretely, we examine the populations generated by a set of candidate values of `var_pos`, and use the population fitness to select the optimal `var_pos`.

Once an individual is generated, we implement the opposition-based technique [197, 198], i.e. we compare this individual with the one obtained through reflection symmetry with respect to the initial configuration (5.18), and keep the one which has the highest fitness. In other words, given the individual with position $r_A^{(p)}$, we consider the individual with position $r_A'^{(p)}$ given by:

$$r'^{(p)}_A = 2\bar{r}_A - r_A^{(p)} \,, \tag{5.24}$$

and add to the population (only) the fitter of the two individuals. We initialize the strategy parameter as $\sigma_A^{(p)} = \texttt{var\_pos}$ for all p, A.

Selection

The selection mechanism of the evolutionary algorithm dictates which individuals pass their genes to the offspring, and which individuals are replaced in the new generation. Recall that the number of new offspring per generation is a hyperparameter of the algorithm. To produce an offspring, the algorithm selects two parents that reproduce and one individual that will be replaced. This selection process occurs probabilistically, favouring potential parents with highest fitness, and where those with highest inverse fitness are most likely to die off.

Our algorithm implements two different selection mechanisms, amongst which the user can choose. The two methods are (see e.g. [199] for more details):

- Fitness proportional selection. The probability of an individual to be chosen as a parent is:

$$P^{(p)} = \frac{f(r_A^{(p)})}{\sum_p f(r_A^{(p)})}\,, \tag{5.25}$$

  where f is the fitness function (5.21). The probability of an individual to die off is governed by the same equation, with the fitness function replaced by the inverse fitness function, defined in Eq. (5.22).

- Sigma scaling. The probability of an individual to be chosen as parent is given by a modified version of Eq. (5.25), with the fitness function being replaced by the following auxiliary fitness function f', which involves a shift controlled by the mean $\bar{f}$ and standard deviation σ_f of the fitnesses of the population:

$$f'(r_A^{(p)}) = \max\Big(f(r_A^{(p)}) - \big(\bar{f} - c\sigma_f\big), 0\Big)\,, \tag{5.26}$$

  where c is a constant which is usually set to 2. Similarly, we also apply this method to the selection of the individual that dies by replacing the fitness function with the inverse fitness function.

The first method is less computationally expensive, however it can be less effective due to the following disadvantages. It is sensitive to adding a constant shift to all f, and depending on this shift there can be too much or too little selection pressure. For instance, if there is too much selection pressure, the best individuals tend to dominate the population very quickly, which can lead to premature convergence.

By contrast, the second method is more computationally expensive, but tends to produce an appropriate amount of selection pressure.

Reproduction and mutation

Once two parents $\{r_A^{(1)}, \sigma_A^{(1)}\}$ and $\{r_A^{(2)}, \sigma_A^{(2)}\}$ are selected, their offspring $\{r_A, \sigma_A\}$ is generated as follows. First, separately for each gene, i.e. for each element of the multi-index A, we assign equal probability to one of the following three reproduction methods to occur. Before possible mutation, this gene will be set equal to the gene of a parent, or the average of the two parental genes:

$$\begin{aligned}
&1) \qquad \{r_A, \sigma_A\} = \{r_A^{(1)}, \sigma_A^{(1)}\}\,;\\
&2) \qquad \{r_A, \sigma_A\} = \{r_A^{(2)}, \sigma_A^{(2)}\}\,;\\
&3) \qquad \{r_A, \sigma_A\} = \Big\{\frac{r_A^{(1)} + r_A^{(2)}}{2}, \frac{\sigma_A^{(1)} + \sigma_A^{(2)}}{2}\Big\}\,.
\end{aligned} \tag{5.27}$$

Next, we implement a mutation mechanism to enable the population to escape from local minima of the fitness function. Recall that each offspring has a total of d genes

$(A = 1, \ldots, d)$. For each gene of an offspring, we assign a probability of order $2/d$ for the gene to mutate away from the value assigned in (5.27). So on average, approximately two genes of each offspring will mutate.

We implement uncorrelated mutation with different step sizes for different genes (see e.g. [199]). If a gene is selected for mutation, first σ_A mutates, then the mutated σ'_A sets the scale for the mutation of the position r_A. The mutation of σ_A is controlled by two Gaussian random variables: $\delta\sigma$ is sampled only once for each offspring, while $\delta\sigma_A$ is sampled separately for each gene. Both are sampled from the Gaussian distribution $\mathcal{N}(0, 1)$. The mutation strength of σ_A is controlled by the parameters τ' and τ as follows:

$$\sigma_A \;\to\; \sigma'_A \;=\; \sigma_A \exp\Big\{\Big(\tau'\,\delta\sigma + \tau\,\delta\sigma_A\Big)\Big\}\,. \tag{5.28}$$

The motivation behind this choice is to treat different dimensions differently: while the mutation $\exp(\tau'\,\delta\sigma)$ is common to all direction and allows for an overall change of the mutation step-size that preserves all degrees of freedom; the term $\exp(\tau\,\delta\sigma_A)$ provides the flexibility to use different mutation strategies in different directions. Following [199], we set $\tau' = 1/\sqrt{d}$ and $\tau = 1/\sqrt{2\sqrt{d}}$. Then the position r_A mutates with a Gaussian random variable δr_A drawn from $\mathcal{N}(0, 1)$, with mutation strength set by the new σ'_A:

$$r_A \;\to\; r'_A \;=\; r_A + \sigma'_A\,\delta r_A\,. \tag{5.29}$$

As the fitness of the population improves, and the algorithm explores narrower regions of the phase space, we improve upon the mutation mechanism (5.28) to achieve a set of goals. The mutation should enable an appropriately fine exploration of the narrower region, while not becoming too small in magnitude. Separately, the mutation should be able to jump outside local minima. To enable this, we introduce a hyperparameter `generation_update`. After `generation_update` generations, we update the strategy parameter of the individuals according to the following prescription. After this update, the algorithm returns to the mutation (5.28) for the next `generation_update` generations. The algorithm contains two different methods to update the strategy parameter, among which the user can choose. These are:

- Random update. We introduce the hyperparameters `percentage_random_update` and `factor_random_update`, randomly select (`percentage_random_update`)% of the individuals and rescale $\sigma_A \to \sigma_A/$`factor_random_update`, while rescaling the strategy parameter of the remaining individuals as $\sigma_A \to$ (`factor_random_update`) σ_A .

- Variance update. We update the strategy parameter according to the variance of

the positions, as follows. For each A, we define the average position

$$\hat{r}_A \;=\; \frac{1}{\texttt{pop\_size}} \sum_q r_A^{(q)} \,, \tag{5.30}$$

and reset the strategy parameters in direction A of all individuals to have the same value,

$$\sigma_A^{(p)} \;\to\; \sigma_A'^{(p)} \;=\; \sqrt{\frac{1}{\texttt{pop\_size}} \sum_q \left(r_A^{(q)} - \hat{r}_A \right)^2} \qquad \forall p \,. \tag{5.31}$$

The variance update method works as follows. If, for instance, the whole population is concentrated in a particular region of parameter space, it tends to enable finer exploration of the local region. By contrast, if for instance the population is concentrated in two or more separate regions, the variance update tends to enable the population to explore a larger region of the parameter space.

We performed several runs with both Random and Variance updates. The Variance update has the advantage that it does not depend on the number of centers, while in the Random update we are introducing two new hyperparameters that could in principle be optimized over, depending for instance on the number of centers. Of the two methods, typically the Variance update is more computationally expensive, and typically the performance of the algorithm is better than or comparable to the Random update, depending on the other parameters of the configuration.

For the sake of clarity, suppose we have chosen the variance update method and let us make an example. Suppose we set the evolutionary algorithm to run for 1000 generations and `generation_update` = 100. The evolution of the strategy parameter will work as follows. For the first 100 generations, the σ_A of each individual will evolve via Eq. (5.28), then at the 100^{th} generation we will transform the strategy parameters of each individual in the population by using Eq. (5.31). Next, from the 101^{th} generation we get back to Eq. (5.28), and we do so until the 200^{th} generation, when we impose Eq. (5.31), etc. We do so until the 1000^{th} generation, when the algorithm ends.

5.4 Results

In this section we present two explicit examples of numerical scaling solutions obtained with the algorithm described above, which have five and seven centers respectively. In both of these examples we use the fitness proportional selection method and the variance update mechanism described in Section 5.3.2. We discuss the performance of the algorithm, showing that its performance is several orders of magnitude better than a random search algorithm. In the examples that we present, the non-Abelian coupling constant g will be set equal to 1.

5.4.1 A five-center scaling configuration

As a first application of our algorithm, we provide an example of a five-center configuration. We first optimize the hyperparameters of the EA for a five-center configuration. We do so with a grid search and obtain the values reported in Table 5.1.

`pop_size`	`off_per_gen`	`generations`	`var_pos`	`generation_update`
2000	50	10000	3.34×10^{-5}	666

Table 5.1: Hyperparameters of the algorithm optimized for five-center configurations. In this table the hyperparameter `off_per_gen` is a shorthand for `offspring_per_generation`.

We then follow the procedure described in Section 5.3.1. We use the BO algorithm to obtain initial positions and flux parameters, recorded in Table 5.2, that give a solution with global charges $Q_1 \approx 2938$ and $Q_5 \approx 2015$.

	1^{st}	2^{nd}	3^{rd}	4^{th}	5^{th}
x	0	$\underline{0.3314}$	$\underline{0.7491}$	-0.6923	$\underline{0.4644}$
y	0	0	$\underline{0.5648}$	-0.684	$\underline{0.4799}$
z	0	0	0	$\underline{-0.0792}$	0.549
q	1	1	-1	-1	1
k^0	17	-18	63	47	29
k^1	-61	66	25	72	80
k^2	60	-	-	-	-

Table 5.2: Input parameters of the solution. For ease of notation, the rescaling in Eq. (5.18) with $\lambda = 10^{-5}$ is understood: in the first three rows of this table the coordinates of the centers are in units of 10^{-5}, i.e. $r_2^1 = 0.3314 \times 10^{-5}$. The underlined coordinates are those that are genes of the EA, i.e. the coordinates over which the evolution process occurs.

By solving the homogeneous bubble equations (5.9), we obtain the $(n-1)$ remaining k_α^2 parameters. After rounding to a precision of `k_rounding` $= 10^{-4}$, we report their values in Table 5.3.

	1^{st}	2^{nd}	3^{rd}	4^{th}	5^{th}
k^2	-	56.0815	-48.5265	-51.1402	47.9087

Table 5.3: Solution of the homogeneous bubble equations, with the input parameters given in Table 5.2, after rounding.

The parameters in Tables 5.2 and 5.3 define a numerical solution to the inhomogeneous bubble equations (5.6) with fitness $f(\bar{r}_a^i) \approx 4.26$. The configuration respects the condition discussed around (5.14), and the matrix $\mathcal{M}^2$ is positive-definite. Therefore we

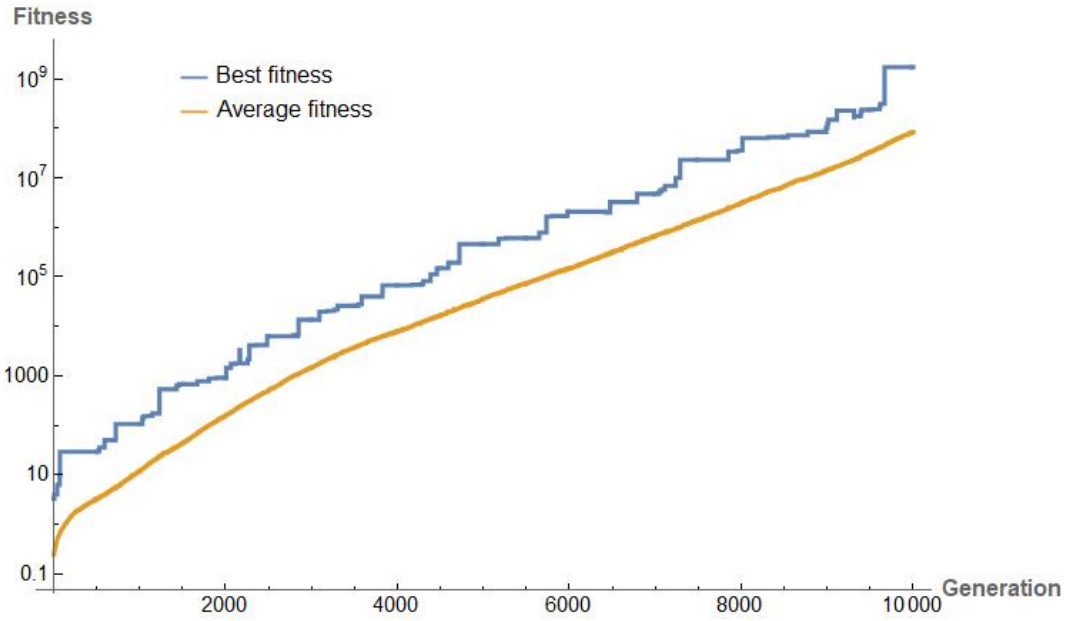

Figure 5.1: Fitness of the fittest five-center configuration, and average fitness of the population over the generations.

proceed to use the configuration as a seed configuration in the EA. We use as genes the coordinates underlined in Table 5.2.

We plot in Figure 5.1 how the fitness of the fittest individual and the average fitness of the population change over the generations. By starting with a seed solution with fitness ~ 1 we obtain, after 10000 generations, a numerical solution with fitness $\sim 10^9$. This means that the EA generated a numerical solution that solves each bubble equation with a precision of at least 10^{-9}.

The associated matrix $\mathcal{M}^2$ is positive-definite, thus we can have confidence that the geometry does not contain any CTCs. We report in Table 5.4 the coordinates of the centers of this numerical solution.

	1^{st}	2^{nd}	3^{rd}	4^{th}	5^{th}
x	0	0.3314021729760	0.7491065875679	-0.6923	0.4644006034503
y	0	0	0.5648006365055	-0.6839943823786	0.4799
z	0	0	0	-0.0792018993574	0.549

Table 5.4: Output of the EA with highest fitness. Similarly to those in Table 5.2, these coordinates are in units of 10^{-5}.

We compute the global charges of this solution using Eq. (5.8), obtaining:

$$\begin{aligned} &Q_1 \simeq 2938\,, \qquad Q_5 \simeq 2015\,, \qquad Q_P \simeq 3\times 10^4\,, \\ &J_L \simeq 4\times 10^5\,, \qquad J_R \simeq 0.0015\,. \end{aligned} \tag{5.32}$$

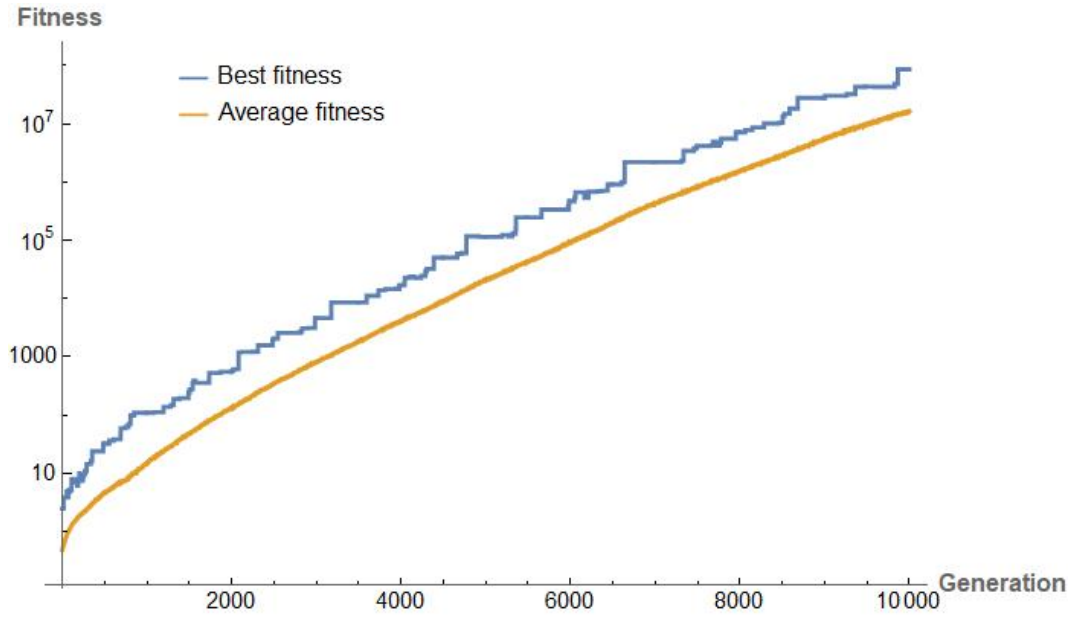

Figure 5.2: Fitness of the fittest seven-center configuration, and average fitness of the population over the generations.

We note that $J_R \ll 1$ as desired. We emphasize that the highest fitness value of order 10^9 is an improvement of eight orders of magnitude from the fitness of the seed configuration.

5.4.2 A seven-center scaling configuration

We now present a seven-center example configuration. We report in Table 5.5 the hyperparameters of the EA optimized for seven-center configurations.

`pop_size`	`off_per_gen`	`generations`	`var_pos`	`generation_update`
2200	90	10000	10^{-4}	666

Table 5.5: Hyperparameters of the algorithm optimized for seven-center configurations. In this table the hyperparameter `off_per_gen` is a shorthand for `offspring_per_generation`.

After running the BO algorithm, we obtain an initial configuration with global charges $Q_1 \approx 736$ and $Q_5 \approx 410$, which is described in Table 5.6.

The homogeneous bubble equations (5.9) give the $n-1$ remaining flux parameters k_α^2; we round them to a precision of 10^{-5}, and report the result in Table 5.7.

The coefficients in Tables 5.6 and 5.7 provide an approximate solution to the inhomogeneous bubble equations (5.6) with fitness $f\left(\vec{r}_a^{\,i}\right) \approx 3.21$. As in the five-center example, only the underlined coordinates in Table 5.6 are taken to be genes of the EA. As shown in Figure 5.2, we obtain, after 10000 generations, a numerical solution with fitness of order 10^7.

	1st	2nd	3rd	4th	5th	6th	7th
x	0	0.8409	0.3858	-0.0195	0.2188	-0.6853	-0.6294
y	0	0	-0.4476	-0.8449	-0.2569	-0.82	0.8284
z	0	0	0	-0.2854	-0.9864	-0.3303	-0.9516
q	1	-1	1	-1	1	-1	1
k^0	66	-38	56	38	86	85	15
k^1	99	57	39	30	48	37	72
k^2	39	-	-	-	-	-	-

Table 5.6: Input parameters of the solution. Similarly to those in Table 5.2, the coordinates in the first three rows are in units of 10^{-5}, and underlined coordinates are genes of the EA.

	1st	2nd	3rd	4th	5th	6th	7th
k^2	-	-37.2187	38.5597	-38.568	38.4874	-38.6549	38.8499

Table 5.7: Solution of the homogeneous bubble equations, with input parameters given in Table 5.6, after rounding.

The coordinates of the centers of the fittest configuration discovered by the EA are reported in Table 5.8.

	1st	2nd	3rd	4th	5th	6th	7th
x	0	0.84089461	0.38578914	0.0195	0.21881058	-0.68529754	-0.62943306
y	0	0	-0.44760652	-0.84485779	-0.2569	-0.82006997	0.82837416
z	0	0	0	-0.28533642	-0.98638654	-0.33036306	-0.9516

Table 5.8: Output of the EA with highest fitness. Again, coordinates are in units of 10^{-5}.

The matrix $\mathcal{M}^2$ is positive-definite, and thus we can have confidence that the configuration is free of CTCs. Finally, we record the global charges of the solution:

$$\begin{aligned} &Q_1 \approx 736\,, \qquad Q_5 \approx 410\,, \qquad Q_P \approx 8.9\times 10^4\,, \\ &J_L \approx 1.6\times 10^5\,, \qquad J_R \approx 0.007\,. \end{aligned} \tag{5.33}$$

We observe that $J_R \ll 1$ as desired.

5.4.3 Performance of the algorithm

We now make some general comments regarding the algorithm's performance. We have run the algorithm in detail for configurations of three, five, and seven centers. As the number of centers increases, naturally the runtime increases. This is primarily due to two factors. First, the number of bubble equations that need to be evaluated increases

linearly with n. Second, a higher number of centers means a higher number of degrees of freedom of the evolutionary algorithm, thus the population size and the number of offspring per generation should be increased accordingly, to optimize the algorithm's performance.

When run on a three-center configuration, the algorithm typically found of order 10 numerical solutions with fitness $\gtrsim 10^6$ in around 10 hours (all run-times refer to a high-specification mainstream desktop machine). For a five-center configuration, typically around 13 hours runtime produced two solutions with fitness $\gtrsim 10^6$. For a seven-center configuration, in 40 hours runtime the algorithm produced two solutions with fitness $\gtrsim 10^5$, including the one reported above.

In light of the No Free Lunch Theorem, we have compared our algorithm with a random search on several examples, and observed it is always preferable, as follows. The random search is obtained by generating `offspring_per_generation` new individuals via Eq. (5.23) for `generations` generations, and evaluating their fitness. We did so for different values of the standard deviation `var_pos`. For large values of `var_pos`, the relevant sampling space is too big, and the probability of finding good solutions is low. As we decrease `var_pos`, the performance of the random search increases until an optimized value. Decreasing `var_pos` further results in a loss of performance, as the individuals are too close to the seed solution $\bar{r}_A$, and thus their fitness is of the same order of $f(\bar{r}_A)$.

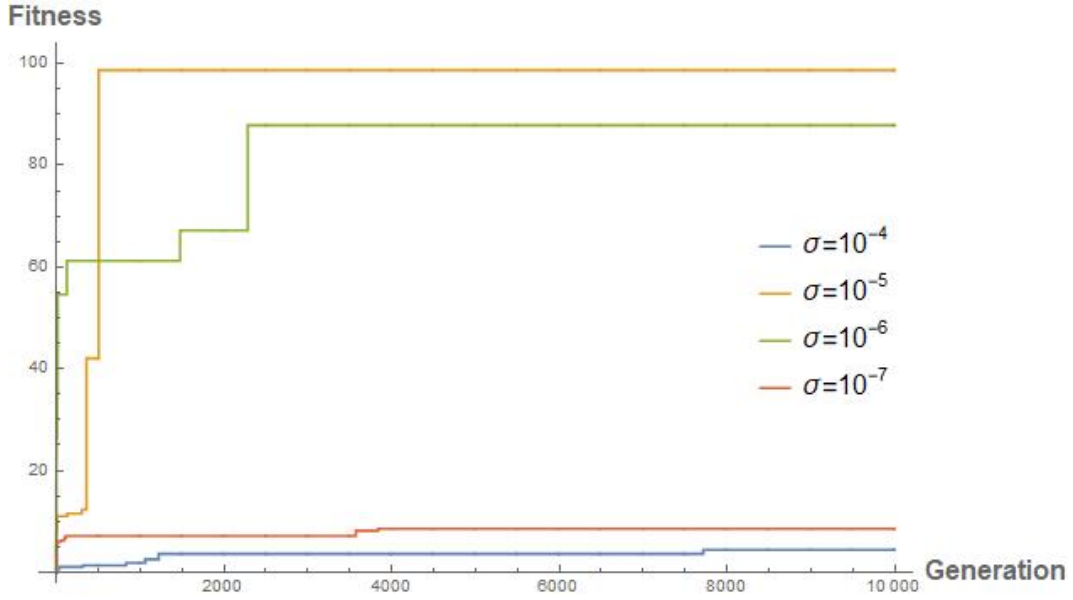

Figure 5.3: Random search over the initial configuration described in Tables 5.2 and 5.3. We repeat the analysis for four different values of `var_pos`, which are denoted with σ in the plot's legend.

In all the examples we analysed, the random search provided an approximate solution with fitness no higher than around 10^2. For completeness, in Figure 5.3 we present an example of such a random search for the five-center configuration discussed in 5.4.1, with the values of `generations` and `offspring_per_generation` given in Table 5.1.

This contrasts with the far superior performance of the evolutionary algorithm.

5.5 Discussion

In the present work we developed an optimization algorithm, based on Bayesian optimization and an evolutionary algorithm, to find multi-center solutions with a high number of centers in generic configurations, satisfying all flux quantization constraints.

The Bayesian optimization algorithm enables to focus on a region of the parameter space with high D1 and D5 charges and provides an approximate solution to the bubble equations (5.6). Such solution contains two approximations: first, we derived it from the homogeneous version of the bubble equations; second, we have rounded the flux parameters to satisfy all flux quantization conditions. The evolutionary algorithm uses this solution as a seed to generate individuals with improving fitness. In Section 5.4 we reported two examples of solutions found. In the five center case, by starting with a seed solution of fitness of order ~ 1, we obtained an approximate solution with fitness $\sim 10^9$. In the seven-center case, the algorithm improved the fitness of the seed solution by a factor of $\sim 10^7$. This is much better than any example we analyzed with a random search, and we gave example of this in Section 5.4.3.

Given a seed solution the evolutionary algorithm may fail to give a good enough approximate solution. On the one hand, this is a limitation of evolutionary algorithms: they not always find optimal solutions and might get stuck in local minima. On the other hand, given a seed solution a corresponding exact solution not always exist: for instance, by rounding the flux parameters, one could access a region of parameter space that does not admit solutions. It is thus possible that the EA fails in giving a sufficiently good solution simply because such a solution does not exist. Indeed, we found three-center examples in which the evolutionary algorithm could not improve the fitness above a certain value: a detailed analysis of one such example then revealed that a nearby exact solution did not exist. Despite these inherent limitations, most of the time the algorithm is very successful at finding high-precision solutions.

As the number of centers grows, naturally, more computational resources are required. Let us note that the task of finding a good seed configuration to pass on to the evolutionary algorithm becomes more computationally expensive as the number of centers increases. The reason being that, as the number of centers grows, the Bayesian algorithm has to be run an increasingly number of times before it finds a solution with appropriately large Q_1, Q_5 charges and such that the matrix $\mathcal{M}$ is positive-definite (for absence of CTCs). In particular, apart from choosing the flux parameters that we initialize to have the same sign, as suggested in [71, Footnote 17], finding a good $\mathcal{M}$ is otherwise left to a random search. Note that the probability of randomly selecting initial parameters that lead to an $\mathcal{M}$ with all positive eigenvalues decreases as the number of centers, and

thus the dimension of $\mathcal{M}$, increases. It would be interesting to explore more efficient ways to select parameters that lead to absence of CTCs; we leave this task to future work.

While we have tested the algorithm for configurations with three, five and seven centers, it is designed to generate more generic configurations, upon tuning the hyper-parameters accordingly (this is of course subject to the available computational resources and the desired fitness of the final solution). The code is publicly available at: `https://github.com/SamiRawash/Multicenter-Scaling-Solutions`.

To conclude, we have implemented a novel application of evolutionary algorithms and Bayesian optimization to the study of multi-centered solutions to supergravity, and have presented in detail two state-of-the-art high-precision numerical solutions. The prospects for harnessing the power of computer science algorithms to solve physically interesting problems in String Theory and related fields appear bright, with an exciting future ahead.

Chapter 6

Conclusions and Outlook

In this thesis, we have developed various tools to corroborate the Fuzzball proposal, which conjectures that strong quantum gravity effects occur already at the horizon scale due to the size of the underlying quantum bound state. As a consequence, a classical black hole solution represents a coarse-grained representation of the system which is not detailed enough to correctly describe fine-grained processes, such as the Hawking evaporation process.

The main playground for analysing this proposal is the D1-D5 system. We have a complete understanding of the microstates responsible of the entropy of the two-charge, supersymmetric D1-D5 black hole: these microstates are well understood in term of smooth supergravity solutions and limits thereof, and their CFT dual states are known. Of more interest are the microstates of the three-charge supersymmetric D1-D5-P black hole: this black hole is macroscopic (unlike the two-charged one, it does not have zero horizon area in supergravity) and it is important to understand how much of the physics learn in the two-charge context is carried over by the microstates of this black hole. The two main classes of such microstates constructed so far are represented by superstrata [56–66, 89], smooth geometries obtained by backreacting a coherent combination of (conventionally) left-moving excitations in the CFT, and multi-center geometries [51, 67–75], solutions specified by a set of harmonic functions on a three-dimensional Euclidean space that involve a non-trivial topologies supported by fluxes in their core region. Despite this advances, it has been shown that these solutions can account only for a small fraction of the entropy of the supersymmetric D1-D5-P black hole [66, 76, 77].

Last, we should extend our understanding of microstates on non-supersymmetric black-hole, for which much less is known. Beside the JMaRT solution [78] and the set of works in [86, 87] which describes a non-extremal generalization of multi-center solutions, recent advances in this direction are provided by the construction of "microstrata" [88, 200], a non-extremal generalization of superstrata where the backreaction of both left and right-excitations are taken into account.

Let us now summarize the results discussed in this thesis and outline some future research directions, in the light of the above discussion.

In Chapters 2 we have refined the precision holographic dictionary pioneered in [54, 55] that relates the fall off of supergravity fields in the bulk with the expectation value of chiral primary operators of dimension $(1,1)$ in the dual CFT state. The relevant operators in the CFT involve a mixing between single and double-trace operators and this mixing has been interpreted as the holographic origin of the coiffuring relations, i.e. relations that arise in the bulk after demanding smoothness of the geometry.

In Chapter 3 we have recasted the holographic dictionary in the single-particle basis: this choice has the advantage that the CFT operators mixing relevant for the dictionary can be predicted by (almost) only CFT computations. By exploiting this basis, we have extended the holographic dictionary to a new sector of the theory: superdescendats of chiral primary operators of dimension $(1,1)$.

After performing consistency checks of the dictionary, we have used it to test proposed CFT dual states to families of recently constructed superstrata solutions. As already discussed in Chapter 2, this tests cannot prove that the holographic description of these geometries is correct in all its details: given the holographic dictionary for a finite set of light operators, there can be many CFT states with the same expectation value of such operators. Despite this limitation, the checks we have conducted provide a strong indication of validity of the holographic description. Let us briefly discuss the current status of precision holographic tests:

- General classes of superstrata with a single-mode, such as the family $(2,m,n,0)$ and $(k,1,0,0)$, passed the precision holographic tests reported in Section 2.5.
- The family of single-mode supercharged superstrata $(2,0,n-1,1)$ has been analyzed in Section 3.6.1
- Among the families of multimode $(k_1,m_1,n_1,0)$-$(k_2,m_2,n_2,0)$, non-supercharged superstrata, the class of solution for which $(k_1m_2-k_2m_1)(k_1n_2-k_2n_1)\neq 0$ is of particular interest: this family evaded construction since [60] until the proposal of [63]. The work of [63] showed that to construct such solutions a novel type of coiffuring relation is required, which turns on an extra supergravity field that is not present when $(k_1m_2-k_2m_1)(k_1n_2-k_2n_1)=0$. We give a CFT interpretation of this phenomenon in Section 3.6.2.
- A family of hybrid supercharged superstrata has been analysed in Section 3.6.3.
- The precision holographic dictionary has been used in [200] to identify the CFT state dual to a non-BPS solution and perform some checks on the proposed holographic description.

A detailed analysis of more recently constructed, supersymmetric, three-charge microstates, such as those reported in [65, 89], is still lacking. As for multi-center solutions, their CFT interpretation is not well understood: it has been suggested in [179] that, when the number of centers is > 3, the resulting configurations should not be thought of as part of the phase space of a supersymmetric black hole, but they should rather be interpreted as microstates of other black objects.

The recipe outlined in Chapter 3 can be used to extend the present holographic dictionary to higher dimensional operators. This will be technically more involved due to the non linearities coming from: i) the mixing between the single and the multi-trace operators, ii) the identification of the single-particle basis in supergravity and iii) the identification of the gauge invariant combination of the supergravity fields. Nonetheless, we do not expect such extension to involve conceptual novelties.

It is perhaps more interesting, however, to generalizie the present dictionary to novel sectors of the theory. The linearized supergravity spectrum studied in [128] suggests that there are other excitations that should lead to new smooth superstrata solutions. Of particular interest are the excitations that lead to a deformed base space (roughly speaking, the operators dual to these excitations are $GG\bar{J}$ and $\bar{G}\bar{G}J$): these solutions are computationally harder to construct and it is possible that building an holographic dictionary for these sectors could inform and guide the construction of the corresponding bulk solutions.

In Chapter 4 we constructed the first family of three-charge supersymmetric solutions containing a shockwave in their core region and we made a proposal for their holographic duals, which passed a set of non-trivial precision holography tests. These solutions represent a collective description of a family of microstates whose details are not resolved in supergravity. While not representing a single pure state in gravity, this coarse grained description has the advantage of being relatively simple: the equations of motion have a simpler form than those for generic single pure states and this could open up the analysis of several generalizations of our construction. First, it would be interesting to place the shockwave on the evanescent ergosurface of the of the GLMT solution: this would enable a discussion of the non-linear instability for this class of solutions on the line of the one made in [160] for the supertube. Second, it could be possible to use this set up to study the properties of non-extremal solutions, for example computing the backreaction of a shockwave on a JMaRT background or considering shockwave configurations that break all the supersymmetries of the theory.

Last, in Chapter 5 we developed an optimization algorithm, base on Bayesian optimization and the evolutionary algorithm, to construct new approximate multi-center solutions with a high number of centers in generic configurations. We provided two examples of such numeric solutions with five and seven centers, that solve each bubble equation up to orders of 10^{-9} and 10^{-7} respectively. This work pioneers the use

of computer science tools to find new approximate black hole microstates and opens different research directions. First, one could optimize the code using techniques of parallel computing: this would enable the use of greater computer resources by exploiting the power of modern High Performance Computers. As a consequence, it would be feasible to obtain solutions with a higher number of centers and fitness then those of the examples presented in 5. Second, it would be interesting to adapt the code to let the algorithm solve the non-extremal generalization of the multi-center configurations developed in [86, 87].

To summarize, the work presented in this thesis supports the ideas of the fuzzball paradigm, develops techniques which can prove useful to examine and test the conjecture in future scenarios and opens different research directions. Despite the progress made in the last 20 years, the fuzzball conjecture is still a proposal at the present state of things. It is reasonable to expect that a deeper understanding of the theoretical framework beyond supergravity will be necessarily to fully understand and resolve the entropy puzzle and the information paradox.

Appendix A

Harmonics on S^3 and AdS_3

A.1 Harmonics on S_3

A.1.1 Spherical harmonics

The spherical harmonics on S^3 are a representation of the isometry group of the three-sphere $SO(4) \simeq SU(2)_L \times SU(2)_R$. We will use spherical coordinates in the $\mathbb{R}^4$ base space that are related to the Cartesian coordinates via

$$\begin{aligned} x^1 &= r\sin\theta\cos\phi\,, \qquad x^2 = r\sin\theta\sin\phi\,, \\ x^3 &= r\cos\theta\cos\psi\,, \qquad x^4 = r\cos\theta\sin\psi\,, \end{aligned} \tag{A.1}$$

where $\theta \in [0, \frac{\pi}{2}]$ and $\psi, \phi \in [0, 2\pi)$. With this coordinate choice, the S^3 line element ds_3^2 is given by $ds_3^2 = d\theta^2 + \sin^2\theta d\phi^2 + \cos^2\theta d\psi^2$. We use conventions in which $\epsilon_{\theta\phi\psi}$=1. The generators of the isometry group of S^3, written in terms of the standard $SU(2)$ generators, are

$$\begin{aligned} J^{\pm} &= \frac{1}{2}e^{\pm i(\phi+\psi)}\big(\pm\partial_\theta + i\cot\theta\partial_\phi - i\tan\theta\partial_\psi\big)\,, \quad J^3 = -\frac{i}{2}\big(\partial_\phi + \partial_\psi\big)\,, \\ \bar{J}^{\pm} &= \frac{1}{2}e^{\pm i(\phi-\psi)}\big(\mp\partial_\theta - i\cot\theta\partial_\phi - i\tan\theta\partial_\psi\big)\,, \quad \bar{J}^3 = -\frac{i}{2}\big(\partial_\phi - \partial_\psi\big)\,, \end{aligned} \tag{A.2}$$

which satisfy the $SU(2)_L \times SU(2)_R$ algebra:

$$\begin{aligned} \big[J^+, J^-\big] &= 2J^3\,, \qquad \big[J^3, J^+\big] = J^+\,, \qquad \big[J^3, J^-\big] = -J^-\,, \\ \big[\bar{J}^+, \bar{J}^-\big] &= 2\bar{J}^3\,, \qquad \big[\bar{J}^3, \bar{J}^+\big] = \bar{J}^+\,, \qquad \big[\bar{J}^3, \bar{J}^-\big] = -\bar{J}^-\,. \end{aligned} \tag{A.3}$$

The left quadratic Casimir operator is $J^2 = \frac{1}{2}\big(J^+J^- + J^-J^+\big) + \big(J^3\big)^2$, and likewise for $\bar{J}^2$. A state in a representation with principal quantum number $j_{\rm su}$ has J^2 eigenvalue $j_{\rm su}(j_{\rm su}+1)$.

Degree k scalar harmonics live in the $(j_{\rm su}, \bar{j}_{\rm su}) = (k/2, k/2)$ representation of $SU(2)_L \times SU(2)_R$. We denote these by $Y_k^{m,\bar{m}}$, and $(m, \bar{m})$ are the spin charges under $(J^3, \bar{J}^3)$. They satisfy the following Laplace equation:

$$\Box_{S_3} Y_k^{m_1,\bar{m}_2} = -k(k+2) Y_k^{m_1,\bar{m}_2} \,. \tag{A.4}$$

Denoting the volume of S^3 by $\Omega_3 = 2\pi^2$, we use normalized spherical harmonics

$$\int Y_{k_1}^{*m_1,\bar{m}_1} Y_{k_2}^{m_2,\bar{m}_2} \;=\; \Omega_3 \, \delta_{k_1,k_2} \delta^{m_1,m_1} \delta^{\bar{m}_1,\bar{m}_2} \,. \tag{A.5}$$

One can generate the degree k scalar spherical harmonic wavefunctions acting with the lowering operators in (A.2) on the highest-weight wavefunctions, which are

$$Y_k^{\pm\frac{k}{2},\pm\frac{k}{2}} = \sqrt{k+1}\sin^k\theta e^{\pm ik\phi} \,. \tag{A.6}$$

We make use of the degree $k = 1, 2$ normalized scalar spherical harmonics, given by:

$$\begin{aligned} Y_1^{+\frac{1}{2},+\frac{1}{2}} &= \sqrt{2}\sin\theta\, e^{i\phi} \quad , \quad Y_1^{+\frac{1}{2},-\frac{1}{2}} = \sqrt{2}\cos\theta\, e^{i\psi} \,, \\ Y_1^{-\frac{1}{2},+\frac{1}{2}} &= -\sqrt{2}\cos\theta\, e^{-i\psi} \quad , \quad Y_1^{-\frac{1}{2},-\frac{1}{2}} = \sqrt{2}\sin\theta\, e^{-i\phi} \,; \end{aligned} \tag{A.7}$$

$$\begin{aligned} &Y_2^{+1,+1} = \sqrt{3}\sin^2\theta\, e^{2i\phi} \quad , \quad Y_2^{+1,0} = \sqrt{6}\sin\theta\cos\theta\, e^{i(\phi+\psi)} \quad , \quad Y_2^{+1,-1} = \sqrt{3}\cos^2\theta e^{2i\psi} \,, \\ &Y_2^{0,+1} = -\sqrt{6}\sin\theta\cos\theta\, e^{i(\phi-\psi)} \quad , \quad Y_2^{0,0} = -\sqrt{3}\cos 2\theta \quad , \quad Y_2^{0,-1} = \sqrt{6}\sin\theta\cos\theta\, e^{-i(\phi-\psi)} \\ &Y_2^{-1,+1} = \sqrt{3}\cos^2\theta\, e^{-2i\psi} \quad , \quad Y_2^{-1,0} = -\sqrt{6}\sin\theta\cos\theta\, e^{-i(\phi+\psi)} \quad , \quad Y_2^{-1,-1} = \sqrt{3}\sin^2\theta\, e^{-2i\phi} \,. \end{aligned} \tag{A.8}$$

We also define the triple overlap:

$$\int Y_k^{M_k,\bar{M}_k} Y_{k_1}^{m_1,\bar{m}_1} \left(Y_{k_2}^{m_2,\bar{m}_2}\right)^* = \Omega_3 \; a^{M_k,\bar{M}_k}_{(m_1,\bar{m}_1)(m_2,\bar{m}_2)} \tag{A.9}$$

A.1.2 Vector harmonics

Degree k left vector harmonics live in the $(j_{\rm su}, \bar{j}_{\rm su}) = (\frac{k+1}{2}, \frac{k-1}{2})$ representation of $SU(2)_L \times SU(2)_R$. We denote these by $Y_{{\rm L},k}^{m,\bar{m}}$ where L stands for left; we shall suppress the label L when we write explicit S^3 vector indices (which will be denoted by a, b). Similarly, degree k right vector harmonics have $(j_{\rm su}, \bar{j}_{\rm su}) = (\frac{k-1}{2}, \frac{k+1}{2})$ and we denote them by $Y_{{\rm R},k}^{m,\bar{m}}$. We shall use $Y_{v,k}^{m,\bar{m}}$ to denote a vector harmonic which can be either right or left. Vector harmonics satisfy

$$\nabla^2_{S^3} Y_{v,k}^{m,\bar{m}} = -(k^2+2k-1) Y_{v,k}^{m,\bar{m}} \,, \qquad D^a (Y_{v,k}^{m,\bar{m}})_a = 0 \,, \tag{A.10}$$

where $\nabla^2_{S^3} = g^{ab} D_a D_b$ and D_a is the covariant derivative with Levi-Civita connection.

One could generate the $(1,0)$ and $(0,1)$ vector harmonics by dualizing (A.2), i.e. through $V_a = g_{ab} V^b$. We choose a different normalizion for these harmonics by imposing

$$\int (Y_1^{\hat{a}A})^*_a (Y_1^{\hat{b}B})^a \;=\; \Omega_3\, \delta^{\hat{a},\hat{b}} \delta^{A,B}\,, \tag{A.11}$$

where $\hat{a}, \hat{b} = \pm, 0$ denote the range of m and $A, B = \pm$ denotes left/right vector harmonics. With this choice, the degree one vector spherical harmonics expressed as one-forms are

$$\begin{aligned}
Y_1^{++} &= \frac{1}{\sqrt{2}} e^{i(\phi+\psi)} \left[-i\, d\theta + \sin\theta\cos\theta\, d(\phi-\psi)\right]\,,\\
Y_1^{-+} &= \frac{1}{\sqrt{2}} e^{-i(\phi+\psi)} \left[i\, d\theta + \sin\theta\cos\theta\, d(\phi-\psi)\right]\,,\\
Y_1^{0+} &= -\cos^2\theta\, d\psi - \sin^2\theta\, d\phi\,,\\
Y_1^{+-} &= \frac{1}{\sqrt{2}} e^{i(\phi-\psi)} \left[i\, d\theta - \sin\theta\cos\theta\, d(\phi+\psi)\right]\,,\\
Y_1^{--} &= -\frac{1}{\sqrt{2}} e^{-i(\phi-\psi)} \left[i\, d\theta + \sin\theta\cos\theta\, d(\phi+\psi)\right]\,,\\
Y_1^{0-} &= \cos^2\theta\, d\psi - \sin^2\theta\, d\phi\,.
\end{aligned} \tag{A.12}$$

One can generate a degree k vector harmonic using the $SU(2)$ tensor product decomposition

$$(\frac{k}{2}, \frac{k}{2}) \otimes (1,0) = (\frac{k}{2}+1, \frac{k}{2}) \oplus (\frac{k}{2}, \frac{k}{2}) \oplus (\frac{k}{2}-1, \frac{k}{2})\,. \tag{A.13}$$

The highest weight state of $(\frac{k}{2}+1, \frac{k}{2})$ is obtained just by multiplying the highest weight states of $(\frac{k}{2}, \frac{k}{2})$ and that of $(1,0)$ (the Clebsch-Gordan coefficient in this case is always one). One can then generate all the descendants by acting with the lowering operator J^-. In order to satisfy the generalized normalization condition

$$\int (Y^{m_1,\bar{m}_1}_{v,k_1})^*_a (Y^{m_2,\bar{m}_2}_{v,k_2})^a \;=\; \Omega_3\, \delta^{k_1,k_2} \delta^{m_1,m_2}\, \delta^{\bar{m}_1,\bar{m}_2}\,, \tag{A.14}$$

one can use the $SU(2)$ algebra to write

$$Y^{\frac{k+1}{2}-m, \frac{k-1}{2}-\bar{m}}_{\mathrm{L},k} = \sqrt{\frac{(k+1-m)!}{(k+1)!m!}} \sqrt{\frac{(k-1-\bar{m})!}{(k-1)!\bar{m}!}} \Big[(J^-)^m (\bar{J}^-)^{\bar{m}}, Y^{\frac{k+1}{2}, \frac{k-1}{2}}_{\mathrm{L},k}\Big] \tag{A.15}$$

All the previous discussion proceeds analogously for right vector harmonics. We define the following triple integral:

$$\int Y_k^{(m_k,\bar{m_k})} \big(Y_1^{a-}\big)_\mu \big(Y_1^{b+}\big)^\mu \;=\; \Omega_3 f^{(k)}_{(m_k,\bar{m_k})ab}\,. \tag{A.16}$$

The explicit value of the components of $f^{(k)}_{(m_k,\bar{m_k})ab}$, defined in (A.16), that have been

used in this work are

$$f^{(2)}_{(0,0)00} = \frac{1}{\sqrt{3}}\,, \qquad f^{(2)}_{(1,1)--} = \frac{1}{\sqrt{3}}\,, \qquad f^{(2)}_{(\pm1,\pm1)00} = 0\,. \tag{A.17}$$

One also has $\epsilon_{abc}D^b(Y^{m,\bar{m}}_{\mathrm{L},k})^c = (k-1)(Y^{m,\bar{m}}_{\mathrm{L},k})_a$ and $\epsilon_{abc}D^b(Y^{m,\bar{m}}_{\mathrm{R},k})^c = -(k-1)(Y^{m,\bar{m}}_{\mathrm{R},k})_a$.

A.1.3 Useful definitions

Due to the non linearity of the gauge-invariant combinations at higher order, one has to project products of harmonics into harmonics of higher order. The following definitions are useful:

- $(Y^I)^\mu Y^J = \frac{E^{IJK}}{\Lambda_K} D^\mu Y^K + f^{IJK}(Y^K)^\mu$
- $\epsilon_{\mu\nu\rho}D^\sigma Y^I D_\sigma D_\rho Y^J = c^s_{IJK}\epsilon_{\mu\nu\rho}D^\rho Y^K + c^v_{IJK}D_{[\nu}Y^K_{\mu]}$
- $Y^{\sigma,I}\epsilon_{\mu\nu\rho}D_\sigma D^\rho Y^J = g^s_{IJK}\epsilon_{\mu\nu\rho}D^\rho Y^K + g^v_{IJK}D_{[\nu}Y^K_{\mu]}$
- $2D_{[\mu}D^\rho Y^I\epsilon_{\nu]\rho\sigma}D^\sigma Y^J = n^s_{IJK}\epsilon_{\mu\nu\rho}D^\rho Y^K + n^v_{IJK}D_{[\nu}Y^K_{\mu]}$
- $2D_{[\mu}(Y^I)^\rho\epsilon_{\nu]\rho\sigma}D^\sigma Y^J = p^s_{IJK}\epsilon_{\mu\nu\rho}D^\rho Y^K + p^v_{IJK}D_{[\nu}Y^K_{\mu]}$

where I, J, K are the multi-indices defined above, and where on the right-hand side the index K is summed over.

A.2 Harmonics on AdS_3

A.2.1 Scalar harmonics

The scalar harmonics are a representation of the AdS_3 isometry group $SO(2,2) \simeq SL(2,\mathbb{R}) \times SL(2,\mathbb{R})$. We use coordinates where the line element reads:

$$ds^2_{AdS_3} = -(\tilde{r}^2+1)d\tilde{t}^2 + \frac{d\tilde{r}^2}{\tilde{r}^2+1} + \tilde{r}^2 d\tilde{y}^2\,. \tag{A.18}$$

In our conventions $\epsilon_{\tilde{t}\tilde{r}\tilde{y}}$=1. The generators of the isometry group are given by:

$$\begin{aligned} L_{\pm1} &= ie^{\pm i(\tilde{t}+\tilde{y})}\Big(-\frac{1}{2}\frac{\tilde{r}}{\sqrt{\tilde{r}^2+1}}\partial_{\tilde{t}} - \frac{1}{2}\frac{\sqrt{\tilde{r}^2+1}}{r}\partial_{\tilde{y}} \pm \frac{i}{2}\sqrt{r^2+1}\,\partial_{\tilde{r}}\Big)\,, \qquad L_0 = \frac{i}{2}\big(\partial_{\tilde{t}}+\partial_{\tilde{y}}\big) \\ \bar{L}_{\pm1} &= ie^{\pm i(\tilde{t}-\tilde{y})}(-\frac{1}{2}\frac{\tilde{r}}{\sqrt{\tilde{r}^2+1}}\partial_{\tilde{t}} + \frac{1}{2}\frac{\sqrt{\tilde{r}^2+1}}{\tilde{r}}\partial_{\tilde{y}} \pm \frac{i}{2}\sqrt{\tilde{r}^2+1}\,\partial_{\tilde{r}})\,, \qquad \bar{L}_0 = \frac{i}{2}(\partial_{\tilde{t}}-\partial_{\tilde{y}}) \end{aligned} \tag{A.19}$$

They respect the algebra

$$\big[L_0, L_\pm\big] = \mp L_\pm \qquad \big[L_1, L_{-1}\big] = 2L_0 \qquad \big[\bar{L}_0, \bar{L}_\pm\big] = \mp \bar{L}_\pm \qquad \big[\bar{L}_1, \bar{L}_{-1}\big] = 2\bar{L}_0 \tag{A.20}$$

The quadratic Casimirs are $L^2 = \frac{1}{2}\big(L_1 L_{-1} + L_{-1}L_1\big) - \big(L_0\big)^2$ and the corresponding antiholomorphic operator $\bar{L}^2$. For a state of L^2 quantum number $j_{\rm sl}$, we have $L^2\,|j_{\rm sl}\rangle = -j_{\rm sl}(j_{\rm sl}-1)\,|j_{\rm sl}\rangle$.

Scalar harmonics have $j_{\rm sl} = \bar{j}_{\rm sl}$. We introduce for convenience $l = 2j_{\rm sl}$. We introduce scalar harmonics $B_l^{(\pm)}$, where the superscript $\pm$ denotes the positive and negative frequency modes. $B_l^{(+)00}$ is the lowest-weight state in the discrete series representation D_+, and $B_l^{(-)00}$ is the highest-weight state in the discrete series representation D_-. For ease of language we refer to these both as highest-weight states. These harmonics solve the following Laplace equation:

$$\Box_{AdS_3} B_l^{(\pm)} = l(l-2) B_l^{(\pm)} \tag{A.21}$$

We then have

$$B_l^{(\pm)} = \frac{e^{\mp i l \tilde{t}}}{\sqrt{\tilde{r}^2+1}^{\,l}} \qquad L_0 B_l^{(\pm)} = \bar{L}_0 B_l^{(\pm)} = \pm\frac{l}{2} B_l^{(\pm)} \tag{A.22}$$

The fact that this is the highest-weight state can be seen as follows:

$$\big[L_1, B_l^{(+)}\big] = \big[\bar{L}_1, B_l^{(+)}\big] = 0 \qquad \big[L_{-1}, B_l^{(-)}\big] = \big[\bar{L}_{-1}, B_l^{(-)}\big] = 0 \tag{A.23}$$

A.2.2 Vector Harmonics

We now introduce vector harmonics on AdS_3: these live in the representation labeled by L^2 quantum numbers $(j_{\rm sl}, \bar{j}_{\rm sl}) = (\frac{l-2}{2}, \frac{l}{2})$ and will be denoted with $B^{(\pm)}_{\mathrm{R},l}$, where R stands for right. Analogously, there is also the left representation with quantum numbers $(j_{\rm sl}, \bar{j}_{\rm sl}) = (\frac{l}{2}, \frac{l-2}{2})$, and we will denote it by $B^{(\pm)}_{\mathrm{L},l}$. The vector harmonics satisfy the following Laplace equation

$$(d\delta + \delta d) B_{v,l}^{(\pm)} = (l-2)^2 B_{v,l}^{(\pm)} \tag{A.24}$$

Here the subscript v stands for vector, meaning that the formula applies to both left and right vector harmonics. The $l = 0$ vector harmonics are the killing one forms, which

can be obtained can be obtained dualizing Eq. (A.19)

$$\begin{aligned}
L_0 &= -\frac{i}{2}\big((\tilde{r}^2+1)d\tilde{t} - \tilde{r}^2 d\tilde{y}\big) \\
L_\pm &= e^{\pm i(\tilde{t}+\tilde{y})}\frac{\tilde{r}}{2\sqrt{\tilde{r}^2+1}}\big(\mp\frac{d\tilde{r}}{\tilde{r}} + i(\tilde{r}^2+1)(d\tilde{t}-d\tilde{y})\big) \\
\bar{L}_0 &= -\frac{i}{2}\big((\tilde{r}^2+1)d\tilde{t} + \tilde{r}^2 d\tilde{y}\big) \\
\bar{L}_\pm &= e^{\pm i(\tilde{t}-\tilde{y})}\frac{\tilde{r}}{2\sqrt{\tilde{r}^2+1}}\big(\mp\frac{d\tilde{r}}{\tilde{r}} + i(\tilde{r}^2+1)(d\tilde{t}+d\tilde{y})\big)
\end{aligned} \tag{A.25}$$

One can generate degree l vector harmonics, as in the S^3 case, by multiplying scalar harmonics with the one forms in Eq. (A.25) exploiting the $SL(2,\mathbb{R})$ tensor product decomposition. For concreteness, let us consider right vector harmonics, which live in the representation in the first term of the direct sum

$$\Big(\frac{l}{2},\frac{l}{2}\Big)\otimes\big(-1,0\big) = \Big(\frac{l-2}{2},\frac{l}{2}\Big)\oplus\Big(\frac{l}{2},\frac{l}{2}\Big)\oplus\Big(\frac{l+2}{2},\frac{l}{2}\Big) \tag{A.26}$$

Let's focus on the positive modes: it is important to note that $B^{(+)}_l$ is a lowest weight state; in order to obtain the lowest weight of the vectorial representation we need to take the product with L_1, and one has:

$$\begin{aligned}
&B^{(+)}_{\mathrm{R},l} = B^{(+)}_{\frac{l}{2},\frac{l}{2}}\otimes L_1, \qquad \big[L_0, B^{(+)}_{\mathrm{R},l}\big] = \frac{l-2}{2}B^{(+)}_{\mathrm{R},l} \\
&\big[\bar{L}_0, B^{(+)}_{\mathrm{R},l}\big] = \frac{l}{2}B^{(+)}_{\mathrm{R},l}, \qquad \big[L_1, B^{(+)}_{\mathrm{R},l}\big] = \big[\bar{L}_1, B^{(+)}_{\mathrm{R},l}\big] = 0
\end{aligned} \tag{A.27}$$

Analogous relations hold for the left vector harmonics. Vector harmonics on AdS_3 are also eigenstates of the following operator:

$$\star\, dB^{(\pm)}_{\mathrm{R},l} = (l-2)B^{(\pm)}_{\mathrm{R},l} \qquad \star\, dB^{(\pm)}_{\mathrm{L},l} = -(l-2)B^{(\pm)}_{\mathrm{L},l} \tag{A.28}$$

Appendix B

Computations of CFT correlators

In this appendix we compute the CFT correlators (B.17) and (B.27), which are used in Eqs. (2.151) and (2.53) respectively, using the method developed in [120, 145]. In order to do so, and for reference in the main part of the thesis, we also record some conventions and notation.

B.1 Conventions and notation

We introduce on the CFT cylinder Euclidean coordinates $\tau = it/R_y$, $\sigma = y/R_y$. With coordinate $w = \tau + i\sigma$, the bare twist operator σ_k corresponding to the permutation $(12\cdots k)$ is defined to introduce the following boundary conditions on the fields $X^i_{(r)}$, $\psi^{\alpha A}_{(r)}$, $r = 1, 2, \ldots k$ as they circle the insertion point w_* (see e.g. [201, Eq. (2.12)]):

$$\begin{aligned} &X_{(1)} \to X_{(2)} \to \cdots \to X_{(k)} \to X_{(1)}\,, \\ &\psi_{(1)} \to \psi_{(2)} \to \cdots \to \psi_{(k)} \to \pm\psi_{(1)}\,, \end{aligned} \tag{B.1}$$

where the $\pm$ boundary condition correspond to R and NS sector as in Eq. (4.33), and an analogous relation holds for the right-moving sector. We have of course suppressed some indices to lighten the notation here.

In the full symmetric orbifold CFT, a bare twist operator is obtained symmetrizing over all the copies. We define:

$$\Sigma_k \;=\; \sum_{k\text{-cycles}} \sigma_k\,. \tag{B.2}$$

The conformal dimension of σ_k is $h = \bar{h} = \frac{1}{4}(k - \frac{1}{k})$ and it is neutral under $SU(2)_L \times SU(2)_R$.

The insertion of a twist operator σ_k allows the existence of fractional modes of the operators. Switching to the CFT plane with coordinate $z = e^w$, for a primary operator

O with conformal dimension h, these are defined by [120]:

$$O_{-\frac{m}{k}} \equiv \int \frac{dz}{2\pi i} \sum_{r=1}^{k} O_{(r)}(z) e^{-2\pi i \frac{m}{k}(r-1)} z^{-\frac{m}{k}+h-1} \,. \tag{B.3}$$

To construct a chiral primary operator starting from the bare twist σ_k we must raise its charge until $h = j$ and $\bar{h} = \bar{j}$. This is achieved by using fractional modes of the current operators and, for even k, spin fields $S^{\pm}$, $\bar{S}^{\pm}$ [120]. A set of twist-k chiral primary operators is given by [120] (see also [111, 201])

$$\sigma_k^{\frac{k-1}{2},\frac{k-1}{2}} \equiv \begin{cases} \tilde{J}^+_{-(k-2)/k} \ldots \tilde{J}^+_{-1/k} J^+_{-(k-2)/k} \ldots J^+_{-1/k} \sigma_k(z) & k \text{ odd} \\ \tilde{J}^+_{-(k-2)/k} \ldots \tilde{J}^+_{-2/k} J^+_{-(k-2)/k} \ldots J^+_{-2/k} (S^+ \bar{S}^+) \sigma_k(z) & k \text{ even} \end{cases} \tag{B.4}$$

These operators have dimension and charge $h = \bar{h} = j = \bar{j} = \frac{k-1}{2}$.

The covering-space method of [120, 145] for computing correlators of twist operators involves mapping to a local covering space (with coordinate t), given by a map that is locally of the form

$$z - z_* \simeq b_*(t - t_*)^k \,. \tag{B.5}$$

The k sets of fields $X^i_{(r)}$, $\psi^{\alpha A}_{(r)}$, which had untwisted boundary conditions in the absence of the twist operator, are mapped to one set of single-valued fields in the covering space, and in the t-plane there are no twist operator insertions; the only parts of the z-plane operator (B.4) that survive in the covering t-plane are the currents and spin fields. When the operator is inserted at the origin of the t-plane, the spin fields in (B.4) for even n create the RR vacuum $|{+}{+}\rangle^{(t)}$. For more discussion and recent related work, see e.g. [83, 201–209].

Passing to the t-plane via the map (B.5), one obtains the following relation between the modes in the z-plane (given in Eq. (B.3)) and those in the covering space:

$$O^{(z)}_{-\frac{m}{k}} \;\to\; \int \frac{dt}{2\pi i} \left(\frac{dz}{dt}\right)^{-h+1} O(t) \left(b_t t^k\right)^{-\frac{m}{k}+h-1} \;=\; b_t^{-\frac{m}{k}} k^{1-h} O^{(t)}_{-m} \tag{B.6}$$

where the superscripts (z) and (t) distinguish the operators in the z-plane from those in the t-plane.

We are interested in (normalized) three-point functions in the z-plane of the following form:

$$\frac{\langle O_1^\dagger(\infty) O_2(a) O_3(0) \rangle}{\langle O_1^\dagger(\infty) O_1(0) \rangle} \tag{B.7}$$

where O_i is an operator that is composed of a bare twist contribution σ_{k_i} with conformal dimension $h_i = \frac{1}{4}(k_i - \frac{1}{k_i})$ and a spin contribution which we denote schematically by S_i, i.e. $O_i = S_i \sigma_{k_i}$. As discussed in [120, Eq. (3.18)], the contributions of the twist fields

and the spin fields in the correlator (B.7) factorize as follows:

$$\frac{\langle O_1^\dagger(\infty)O_2(a)O_3(0)\rangle}{\langle O_1^\dagger(\infty)O_1(0)\rangle} \;=\; |C_{1,2,3}|^{12}|a|^{-2(h_1+h_2-h_3)}\,\frac{\langle S_1^\dagger(\infty)S_2(a)S_3(0)\rangle}{\langle S_1^\dagger(\infty)S_1(0)\rangle} \tag{B.8}$$

where the a dependence is given by conformal invariance and $C_{1,2,3}$ is the fusion coefficient of a bosonic theory with $c = 1$. The exponent 12 appears because we have $c = 6$ on a single copy. The coefficient $C_{1,2,3}$ was computed in [145]; we will thus focus on the spin field correlator, which can be computed using bosonization [120].

We introduce holomorphic (antiholomorphic) bosonic fields $\phi_5(z)$ and $\phi_6(z)$ ($\tilde{\phi}_5(\bar{z})$ and $\tilde{\phi}_6(\bar{z})$). We write only the holomorphic expressions for brevity. We bosonize the fermions as

$$\psi^{++} \;=\; e^{i\phi_5}\,, \qquad \psi^{+-} \;=\; e^{-i\phi_6}\,, \qquad \psi^{-+} \;=\; e^{i\phi_6}\,, \qquad \psi^{--} \;=\; -e^{-i\phi_5}\,. \tag{B.9}$$

Normal ordering is implicit as usual, and we shall suppress cocycles as these will not be important for our purposes. We also introduce the notation

$$\phi_- \;\equiv\; \phi_5 - \phi_6 \qquad\qquad \Rightarrow \quad e^{i\alpha\phi_-(z)}e^{i\beta\phi_-(w)} \;\sim\; e^{i\alpha\phi_-(z)+i\beta\phi_-(w)}(z-w)^{2\alpha\beta}\,. \tag{B.10}$$

In terms of ϕ_-, the $SU(2)_L$ currents are

$$J^+(z) \;=\; e^{i\phi_-(z)}\,, \qquad J^-(z) \;=\; e^{-i\phi_-(z)}\,, \qquad J^3(z) \;=\; \frac{i}{2}\partial\phi_-(z)\,. \tag{B.11}$$

We will also need the expression for the operator O^{--}:

$$O^{--}(z,\bar{z}) \;=\; \frac{-i}{\sqrt{2}}\Big(e^{-i\phi_5(z)+i\tilde{\phi}_6(\bar{z})} - e^{i\phi_6(z)-i\tilde{\phi}_5(\bar{z})}\Big)\,. \tag{B.12}$$

Using Eqs. (B.6) and (B.11) we obtain the following expression for the twist-k primaries in Eq. (B.4) lifted to the covering space:

$$\sigma_k^{\frac{k-1}{2},\frac{k-1}{2}}(t,\bar{t}) \;=\; |b|^{-\frac{2p^2}{k}}e^{ip\phi_-(t)}e^{ip\tilde{\phi}_-(\bar{t})}\,, \qquad\qquad p \;=\; \tfrac{k-1}{2}\,. \tag{B.13}$$

We conclude this section by recording our conventions for spectral flow. Spectral flow acts on states and operators as

$$|\phi\rangle \;\to\; \big|\phi'\big\rangle \;=\; U_\nu\,|\phi\rangle\,, \qquad O \;\to O' \;=\; U_\nu O U_\nu^\dagger\,, \tag{B.14}$$

where $U_\nu = e^{i\nu\phi_-}$ in the z-plane, and where on the covering t-plane of a strand of length k, $U_\nu = e^{ik\nu\phi_-}$. Analogous expressions hold in the antiholomorphic sector. The spectral flow transformations for the modes of the $SU(2)_L$ currents are (for the rest of the chiral

algebra, see e.g. [111, App. A]):[1]

$$J^3_m \;\to\; J^3_m - \frac{c\nu}{6}\delta_{m,0}\,, \qquad\qquad J^\pm_m \;\to\; J^\pm_{m\mp 2\nu}\,. \tag{B.15}$$

The weight and $SU(2)$ charge (h, j) of states transform as

$$h \;\to\; h + 2\nu j + \frac{c\nu^2}{6}\,, \qquad\qquad j \;\to\; j + \frac{c\nu}{6}\,; \tag{B.16}$$

for example, spectral flow with parameters $(\nu, \bar\nu) = (\frac{1}{2}, \frac{1}{2})$ maps the NS-NS vacuum to the RR ground state $|{+}{+}\rangle$.

B.2 Expectation value of Σ_3^{00} on a three-charge state

We are now ready to compute the following normalized three-point function, for use in Eqs. (2.151):

$$\frac{{}_1\langle{+}{+}|_k \langle 00|\, J^-_{+1}\sigma_3^{00}(a)\, J^+_{-1}\,|00\rangle_k\,|{+}{+}\rangle_1}{{}_1\langle{+}{+}|_k \langle 00|\, J^-_{+1}J^+_{-1}\,|00\rangle_k\,|{+}{+}\rangle_1} \;\equiv\; C^{00(m=1)}_{k3k}|a|^{-2}\,. \tag{B.17}$$

In order to exploit the machinery worked out so far, we map the correlator Eq. (B.17) to the NS-NS sector using spectral flow with parameters $(-\frac{1}{2}, -\frac{1}{2})$. This is a unitary transformation (B.14) that leaves invariant the value of the correlator.

This spectral flow transformation maps the RR vacuum $|{+}{+}\rangle_1$ to the untwisted NS-NS vacuum. From (B.15), the operator J^+_{-1} becomes J^+_0 in the NS sector.

Next, σ_3^{00} is defined by $\sigma_3^{00} \equiv \frac{1}{2}[J^-_0, [\tilde J^-_0, \sigma_3^{11}]]$. Using Eqs. (B.4) and (B.13), we see that in the covering space $\sigma_3^{00} \to 2|b|^{-2/3}J^3\tilde J^3$, so this operator is invariant under spectral flow.

To derive the spectral flow of the state $|00\rangle_k$, recall that it is defined by:

$$|00\rangle_k \;\equiv\; O_0^{--}\,|{+}{+}\rangle_k \;=\; \frac{-i}{\sqrt{2}}\epsilon_{\dot A\dot B}\psi_0^{-\dot A}\tilde\psi_0^{-\dot B}\,|{+}{+}\rangle_k\,. \tag{B.18}$$

In the z-plane, $\psi_0^{-\dot A}$ is spectral flowed to $\psi^{-\dot A}_{-\frac{1}{2}}$, which is related to the corresponding covering-space mode through Eq. (B.6), giving

$$\psi^{-\dot A}_{-\frac{1}{2}} \;\to\; b_t^{-\frac{1}{2}}\sqrt{k}\,\psi^{-\dot A(t)}_{-\frac{k}{2}}\,. \tag{B.19}$$

Under spectral flow with parameters $(-\frac{1}{2}, -\frac{1}{2})$, the RR ground state $|{+}{+}\rangle_k$ is mapped to an anti-chiral primary state; moving to the covering t-plane gives (normal ordering

[1] The convention map to the spectral flow parameters of [111] is $\alpha_{\rm there} = 2\nu_{\rm here}$.

of exponentials should be understood; we leave this implicit to lighten the notation)

$$|{+}{+}\rangle_k \;\to\; \sigma_k^{-\frac{k-1}{2},-\frac{k-1}{2}}\,|0\rangle^{(t)}_{\rm NS} \;=\; |b|^{-\frac{2p^2}{k}} e^{-ip\phi_-(0)} e^{-ip\tilde\phi_-(0)}\,|0\rangle^{(t)}_{\rm NS} \tag{B.20}$$

where $|0\rangle^{(t)}_{\rm NS}$ is the NS-NS vacuum of the covering t-plane and again $p=\frac{k-1}{2}$. Then from Eqs. (B.12) and (B.18) we obtain

$$\begin{aligned}
|00\rangle_k \;&\to\; \frac{i\sqrt{k}}{\sqrt{2}}|b|^{-\frac{2p^2}{k}-1}\Big(\psi^{--(t)}_{-\frac{k}{2}}\tilde\psi^{-+(t)}_{-\frac{k}{2}} - \psi^{-+(t)}_{-\frac{k}{2}}\tilde\psi^{--(t)}_{-\frac{k}{2}}\Big) e^{-ip\phi_-(0)}e^{-ip\tilde\phi_-(0)}\,|0\rangle^{(t)}_{\rm NS}\\
&= \frac{i\sqrt{k}}{\sqrt{2}}|b|^{-\frac{2p^2}{k}-1}\int\frac{dtd\bar t}{(2\pi i)^2}t^{-\frac{k+1}{2}}\bar t^{-\frac{k+1}{2}}\big(e^{-i\phi_5(t)+i\tilde\phi_6(\bar t)} - e^{i\phi_6(t)-i\tilde\phi_5(\bar t)}\big)e^{-ip\phi_-(0)}e^{-ip\tilde\phi_-(0)}\,|0\rangle^{(t)}_{\rm NS}\\
&= \frac{i\sqrt{k}}{\sqrt{2}}|b|^{-\frac{2p^2}{k}-1}\int\frac{dtd\bar t}{(2\pi i)^2}t^{-1}\bar t^{-1}\Big(e^{-i\phi_5(t)-ip\phi_-(0)+i\tilde\phi_6(\bar t)-ip\tilde\phi_-(0)}\\
&\qquad\qquad -e^{i\phi_6(t)-ip\phi_-(0)-i\tilde\phi_5(\bar t)-ip\tilde\phi_-(0)}\Big)\,|0\rangle^{(t)}_{\rm NS}\\
&= \frac{i\sqrt{k}}{\sqrt{2}}|b|^{-\frac{2p^2}{k}-1}\Big(e^{-i\frac{k+1}{2}\phi_5(0)+i\frac{k-1}{2}\phi_6(0)-i\frac{k-1}{2}\tilde\phi_5(0)+i\frac{k+1}{2}\tilde\phi_6(0)}\\
&\qquad\qquad -e^{-i\frac{k-1}{2}\phi_5(0)+i\frac{k+1}{2}\phi_6(0)-i\frac{k+1}{2}\tilde\phi_5(0)+i\frac{k-1}{2}\tilde\phi_6(0)}\Big)\,|0\rangle^{(t)}_{\rm NS}
\end{aligned} \tag{B.21}$$

so we obtain

$$\begin{aligned}
J^+_{-1}\,|00\rangle_k \;\to\; \frac{i\sqrt{k}}{\sqrt{2}}|b|^{-\frac{2p^2}{k}-1}\Big(&e^{-i\frac{k-1}{2}\phi_5(0)+i\frac{k-3}{2}\phi_6(0)-i\frac{k-1}{2}\tilde\phi_5(0)+i\frac{k+1}{2}\tilde\phi_6(0)}\\
&- e^{-i\frac{k-3}{2}\phi_5(0)+i\frac{k-1}{2}\phi_6(0)-i\frac{k+1}{2}\tilde\phi_5(0)+i\frac{k-1}{2}\tilde\phi_6(0)}\Big)\,|0\rangle^{(t)}_{\rm NS}\,.
\end{aligned} \tag{B.22}$$

Before computing the spin correlator in Eq. (B.8), we recall the value of the twist fusion coefficient we require [145, Eq. (6.25)],

$$|C_{k,3,k}|^{12} \;=\; \frac{(k+1)^{\frac{k^2+1}{k}+\frac{2}{3}}}{2^{\frac{4}{3}}3^{\frac{5}{3}}k^{\frac{4}{3}}(k-1)^{\frac{k^2+1}{k}-\frac{2}{3}}}\,. \tag{B.23}$$

The map from the z-plane to the covering space used to compute this is given in [145, Eq. (4.34)]. Since it will be needed in the following, we report here the behaviour of this map near the insertion points $z=0,a,\infty$, as given in [120, Eq. (6.18)–(6.20)][2]:

$$\begin{aligned}
z \;&\sim\; b_0 t^k \;=\; a\frac{k+1}{k-1}t^k && \text{near } z=0\,,\\
z \;&\sim\; a+b_1(t-1)^3 \;=\; a+a\frac{(k+1)k(k-1)}{12}(t-1)^3 && \text{near } z=a\,,\\
z \;&\sim\; b_\infty t^k \;=\; a\frac{k-1}{k+1}t^k && \text{near } z=\infty\,.
\end{aligned} \tag{B.24}$$

Note that the map has been chosen so that the point $z=a$ is mapped to $t=1$. Because of the normalization in (B.8), the spin field correlator in the case of (B.17) arises from con-

[2] We note a typo in [120, Eq. (6.20)]: $(d-1-d_2)\to(d_1-d_2)$.

tracting the covering-space operator $\sigma_3^{00(t)}(1) = 2|b_1|^{-\frac{2}{3}} J^3 \tilde{J}^3(1) = -\frac{1}{2}|b_1|^{-\frac{2}{3}} \partial\phi_- \bar{\partial}\tilde{\phi}_-(1)$ with the operator in Eq. (B.22). The result reads:

$$\frac{\langle S_1^\dagger(\infty) S_2(a) S_3(0)\rangle}{\langle S_1^\dagger(\infty) S_1(0)\rangle} = \frac{k(k-2)}{2}|b_0|^{-\frac{2p^2}{k}-1}|b_1|^{-\frac{2}{3}}|b_\infty|^{\frac{2p^2}{k}+1}, \qquad p = \tfrac{k-1}{2}. \tag{B.25}$$

Using Eqs. (B.8), (B.23) and (B.24) we find

$$C_{k3k}^{00(m=1)} = \frac{k-2}{6k}. \tag{B.26}$$

B.3 Expectation value of Σ_2^{++} in the state $|00\rangle_1 |{+}{+}\rangle_2$

In Eq. (2.53) we make use of the relation $\sigma_2^{++}|00\rangle_1 |00\rangle_1 = \frac{1}{4}|{+}{+}\rangle_2$, which we now derive. The coefficient corresponds to computing the following correlator:

$$\frac{{}_2\langle {+}{+}| \sigma_2^{++}|00\rangle_1 |00\rangle_1}{{}_2\langle {+}{+}|{+}{+}\rangle_2}. \tag{B.27}$$

We lift this correlator to the covering space with the map (c.f. [201])

$$z = t(t-1). \tag{B.28}$$

The point $z = 0$ corresponds to the points $t = 0, 1$, where we have the insertions

$$(O^{--}S^+\bar{S}^+)(0), \quad (O^{--}S^+\bar{S}^+)(1). \tag{B.29}$$

Writing only the holomorphic expressions, the operators $S^\pm$ take the following form in the covering space:

$$S^\pm(t) = |b_t|^{-\frac{1}{4k}} e^{\pm\frac{i}{2}\phi_-(t)}. \tag{B.30}$$

The operator σ_2^{++} is inserted at the point $t = 1/2$ in the covering space (see e.g. [201, Sec. 4]). The asymptotic behaviour of the map (B.28) at the insertion points $t = 0, 1/2, 1, \infty$ is given in [201, Eq. (C.45)]. Factorizing the correlator as in (B.8), we compute the spin contribution

$$\frac{\langle (S^-\bar{S}^-)(\infty)(S^+\bar{S}^+)(\frac{1}{2})(O^{--}S^+\bar{S}^+)(1)(O^{--}S^+\bar{S}^+)(0)\rangle}{\langle (S^-\bar{S}^-)(\infty)(S^+\bar{S}^+)(0)\rangle} = |b_\infty|^{\frac{1}{4}}|b_{\frac{1}{2}}|^{-\frac{1}{4}}|b_1|^{-\frac{1}{2}}|b_0|^{-\frac{1}{2}}. \tag{B.31}$$

The remaining contributions to the correlator are given in [201, Eqs. (C.5), (C.39)]. Combining these results with (B.31), we obtain the value of the desired coefficient,

$$\sigma_2^{++}|00\rangle_1 |00\rangle_1 = \frac{1}{4}|{+}{+}\rangle_2. \tag{B.32}$$

Appendix C

Type IIB supergravity ansatz and BPS equations

The general solution to Type IIB supergravity compactified on T^4 that is 1/8-BPS, has D1-D5-P charges, and is invariant on the T^4 directions is [134, Appendix E.7]:

$$
\begin{aligned}
ds_{10}^2 &= \sqrt{\alpha}\, ds_6^2 + \sqrt{\frac{Z_1}{Z_2}}\, d\hat{s}_4^2 \,, && \text{(C.1a)}\\
ds_6^2 &= -\frac{2}{\sqrt{\mathcal{P}}}\,(dv+\boldsymbol{\beta})\left[du+\omega+\frac{\mathcal{F}}{2}(dv+\boldsymbol{\beta})\right] + \sqrt{\mathcal{P}}\, ds_4^2 \,, && \text{(C.1b)}\\
e^{2\Phi} &= \frac{Z_1^2}{\mathcal{P}} \,, && \text{(C.1c)}\\
B &= -\frac{Z_4}{\mathcal{P}}\,(du+\omega)\wedge(dv+\boldsymbol{\beta}) + a_4\wedge(dv+\boldsymbol{\beta}) + \gamma_4 \,, && \text{(C.1d)}\\
C_0 &= \frac{Z_4}{Z_1} \,, && \text{(C.1e)}\\
C_2 &= -\frac{Z_2}{\mathcal{P}}\,(du+\omega)\wedge(dv+\boldsymbol{\beta}) + a^1\wedge(dv+\boldsymbol{\beta}) + \gamma_2 \,, && \text{(C.1f)}\\
C_4 &= \frac{Z_4}{Z_2}\,\widehat{\mathrm{vol}}_4 - \frac{Z_4}{\mathcal{P}}\,\gamma_2\wedge(du+\omega)\wedge(dv+\boldsymbol{\beta}) + x_3\wedge(dv+\boldsymbol{\beta}) \,, && \text{(C.1g)}\\
C_6 &= \widehat{\mathrm{vol}}_4\wedge\left[-\frac{Z_1}{\mathcal{P}}\,(du+\omega)\wedge(dv+\boldsymbol{\beta}) + a^2\wedge(dv+\boldsymbol{\beta}) + \gamma_1\right] , && \text{(C.1h)}
\end{aligned}
$$

where

$$
\alpha = \frac{Z_1 Z_2}{Z_1 Z_2 - Z_4^2} \,, \qquad \mathcal{P} = Z_1 Z_2 - Z_4^2 \,. \tag{C.2}
$$

In the above, $d\hat{s}_4^2$ denotes the flat metric on T^4, and $\widehat{\mathrm{vol}}_4$ stands for the corresponding volume form. This ansatz contains all fields known to arise from worldsheet calculations of the backreaction of D1-D5-P bound states invariant on $\mathcal{M}$ [210].

The BPS equations have the following structure. The base metric, ds_4^2, and the one-form $\boldsymbol{\beta}$ satisfy non-linear equations. Having solved these initial equations, the remaining ansatz quantities are organized into two layers of linear equations [134, 211].

We denote the exterior differential on the spatial base $\mathcal{B}$ by $\tilde{d}$, and introduce [166]

$$\mathcal{D} \equiv \tilde{d} - \boldsymbol{\beta} \wedge \frac{\partial}{\partial v} . \tag{C.3}$$

In the present thesis we consider only solutions where the four-dimensional base space is flat $\mathbb{R}^4$, and in which $\boldsymbol{\beta}$ does not depend on v. Then the BPS equation for $\boldsymbol{\beta}$ is

$$d\boldsymbol{\beta} = *_4 d\boldsymbol{\beta} , \tag{C.4}$$

where $*_4$ denotes the flat $\mathbb{R}^4$ Hodge dual.

To write the remaining BPS equations in a covariant form, we rescale $(Z_4, a_4, \gamma_4) \to (Z_4, a_4, \gamma_4)/\sqrt{2}$ for the remainder of this appendix (and only here). We introduce the $SO(1,2)$ Minkowski metric η_{ab} $(a = 1, 2, 4)$ via

$$\eta_{12} = \eta_{21} = 1 , \qquad \eta_{44} = -1 . \tag{C.5}$$

This is used to raise and lower a, b indices. We introduce the two-forms Θ^1, Θ^2, Θ^4 via[1]

$$\Theta^b \equiv \mathcal{D}a^b + \eta^{bc}\dot{\gamma}_c . \tag{C.6}$$

We now have

$$\mathcal{P} \equiv \tfrac{1}{2}\eta^{ab} Z_a Z_b = Z_1 Z_2 - \tfrac{1}{2} Z_4^2 . \tag{C.7}$$

The first layer of the BPS equations then takes the form

$$*_4 D\dot{Z}_a = \eta_{ab} D\Theta^b , \qquad D *_4 DZ_a = -\eta_{ab}\Theta^b \wedge d\boldsymbol{\beta} , \qquad \Theta^a = *_4 \Theta^a . \tag{C.8}$$

The second layer becomes

$$\begin{aligned} D\omega + *_4 D\omega + \mathcal{F}\, d\boldsymbol{\beta} &= Z_a \Theta^a , \\ *_4 D *_4 \Big(\dot{\omega} - \tfrac{1}{2} D\mathcal{F}\Big) &= \ddot{\mathcal{P}} - \tfrac{1}{2}\eta^{ab}\dot{Z}_a\dot{Z}_b - \tfrac{1}{4}\eta_{ab} *_4 \Theta^a \wedge \Theta^b . \end{aligned} \tag{C.9}$$

[1] The relation to the notation of [60] is that $\Theta^1_{\text{here}} = \Theta^{\text{there}}_1$, $\Theta^2_{\text{here}} = \Theta^{\text{there}}_2$, $(1/\sqrt{2})\Theta^{\text{here}}_4 = \Theta^{\text{there}}_4$.

Appendix D

Extremal three-point functions

In this appendix we derive the scalar chiral primary operators of dimension two in the single-particle basis. The vanishing of extremal three-point functions built with the operator $\tilde{O}_2$ in (3.48) was discussed in Section 2.3.1; here we shall focus on the operators $\tilde{\Omega}$ and $\tilde{\Sigma}_3$ defined in Eq. (3.49). These operators involve a mixing between the single-trace operators Σ_3, Ω and the double-trace operators $(\Sigma_2 \cdot \Sigma_2)$, $(J \cdot \bar{J})$ and $(O \cdot O)$. Let us first discuss the mixing matrix between the single-traces: the single-particle operators take the form

$$\tilde{\Omega} \;\sim\; a_1 \frac{\Sigma_3}{N^{\frac{3}{2}}} + a_2 \frac{\Omega}{N^{\frac{1}{2}}}\,, \qquad \tilde{\Sigma}_3 \;\sim\; b_1 \frac{\Sigma_3}{N^{\frac{3}{2}}} + b_2 \frac{\Omega}{N^{\frac{1}{2}}}\,, \tag{D.1}$$

where $\sim$ means that we are retaining only the single-trace contributions and we have arranged the factors of N so that each term contributes at order N^0 to the norm of the single-particle operators. As we shall discuss below, at large N, the multi-trace contribution to norm of the single-particle operator is subleading. Thus, the orthonormality conditions

$$\langle \tilde{\Sigma}_3^{++} \tilde{\Sigma}_3^{--} \rangle \;=\; \langle \tilde{\Omega}^{++} \tilde{\Omega}^{--} \rangle \;=\; 1\,, \qquad \langle \tilde{\Sigma}_3^{++} \tilde{\Omega}^{--} \rangle \;=\; 0\,, \tag{D.2}$$

give three constraints on the four coefficients a_1, a_2, b_1 and b_2. In order to completely fix the mixing matrix in Eq. (D.1) we need a fourth constraint, which was derived in [107] from comparison with non-extremal supergravity correlators. The result is

$$\tilde{\Omega} = \frac{\sqrt{3}}{2} \left(\frac{\Sigma_3}{N^{\frac{3}{2}}} + \frac{\Omega}{N^{\frac{1}{2}}} \right), \qquad \tilde{\Sigma}_3 = \frac{3}{2} \left(\frac{\Sigma_3}{N^{\frac{3}{2}}} - \frac{\Omega}{3N^{\frac{1}{2}}} \right). \tag{D.3}$$

We now focus on the mixing of multi-trace operators in the single-particle basis: as we shall see, it can be completely fixed by CFT computations. Let us consider the most general linear combination allowed by the quantum numbers that can give rise to the single-particle operators:

$$\alpha \frac{\Sigma_3}{N^{3/2}} + \beta \frac{\Omega}{N^{1/2}} + \gamma (\Sigma_2 \cdot \Sigma_2) + \delta (J \cdot \bar{J}) + \epsilon (O \cdot O)^{++}\,. \tag{D.4}$$

The coefficients α and β are given by the single-trace mixing matrix in Eq. (D.3). We now fix the coefficients γ, δ and ϵ by imposing that all extremal three-point functions built with this operator and two operators of dimension one vanish. For ease of notation we will suppress the standard space-time dependence in the following correlators.

- The first constrain comes by imposing that the three-point function obtained inserting the operator in (D.4) with two O^{--} vanishes. Since the latter belongs to the untwisted sector of the theory, the contributions coming from the twist operators in (D.4) are trivially zero; moreover the contribution of the multi-trace $(J\bar{J})$ is subleading at large N. We obtain:

$$\langle\Big(\beta\frac{\Omega^{++}}{N^{1/2}}+\epsilon(O\cdot O)^{++}\Big)O^{--}O^{--}\rangle \;=\; \beta N^{1/2}+2\epsilon N \;=\; 0\,. \tag{D.5}$$

  where we have used the definitions in Eqs. (2.19), (2.38) and (3.35).

- Let us now consider the currents insertions: again, since they carry no twist, the twist operators in Eq. (D.4) do not contribute to the correlator; the contribution of the double-trace $(O\cdot O)^{++}$ is subleading in N and we shall ignore it. The computation leads to

$$\langle\Big(\beta\frac{\Omega^{++}}{N^{1/2}}+\delta(J\cdot\bar{J})^{++}\Big)J^{-}\bar{J}^{-}\rangle \;=\; \beta N^{1/2}+\delta N \;=\; 0\,. \tag{D.6}$$

  where we have used the definitions in Eqs. (2.16), (2.38) and (3.35).

- The last constraint comes from inserting two twist operators Σ_2^{--}. Leading order contributions to the extremal three-point function come from the twist operators and the Ω^{++} in (D.4). The contraction with Σ_3 gives the large-N result

$$\langle\sum_{r<s<t}\big(\sigma^{++}_{(rst)}+\sigma^{++}_{(rts)}\big)\sum_{a<b}\sigma^{--}_{(ab)}\sum_{c<d}\sigma^{--}_{(cd)}\rangle \;=\; \frac{3N^{3/2}}{4},\,. \tag{D.7}$$

  The combinatorics works as follows. The choice of the copies r,s,t gives $\binom{N}{3}$ and, for each choice, there are two inequivalent cycles so that the twist-three operator can glue three strands out of N in $2\binom{N}{3}$ ways. To fix the ideas, let us suppose that the orientation of the 3 copies r,s,t is chosen to be (123): we can still choose the first σ_2 to be the two-cycle (12), (23) or (13) (this fixes the second σ_2 to be (23), (13) and (12) respectively): this gives a factor of three. Eq. (D.7) follows from combining this combinatorial factor with the building block

$$\langle\sigma^{++}_{(123)}\sigma^{--}_{(12)}\sigma^{--}_{(23)}\rangle \;=\; 3/4,\,, \tag{D.8}$$

derived in [120, Eq. (5.25)]. The double-trace $(\sigma_2 \cdot \sigma_2)^{++}$ contributes with

$$\langle \frac{2}{N^2} \sum_{(r<s)\neq(p<q)} \sigma^{++}_{(rs)} \sigma^{++}_{(pq)} \sum_{a<b} \sigma^{--}_{(ab)} \sum_{c<d} \sigma^{--}_{(cd)} \rangle \;=\; N^2, . \tag{D.9}$$

The computation goes as follows: the choice of the copies r, s and p, q gives the combinatorial factors $N(N-1)/2$ and $(N-2)(N-3)/2$ respectively; moreover, one can perform two inequivalent Wick contractions, which give an extra factor of two. Taking into account the normalization of the multi-trace operator, one gets Eq. (D.9). The last contribution comes from the operator Ω^{++}. One could evaluate it using the techniques developed in [120, 145], or exploiting Ward identities that relate different n-point functions in the same R-symmetry multiplet together with some results obtained in [1]: we are going focus on the latter method. We write the operator Σ_2^{--} as $[J_0^- \bar{J}_0^-, \Sigma_2^{++}]$ and make use the permutation property of the correlator (e.g. [119, Eq. (2.2.48)]) . Moving the current modes on the other operators we obtain

$$\begin{aligned} \langle \Omega^{++}\, \Sigma_2^{--}\, \Sigma_2^{--} \rangle &= \langle \Sigma_2^{--}\, \Omega^{++}\, \Sigma_2^{--} \rangle \\ &= \left\langle \Sigma_2^{++} \left(2\Omega^{00}\right) \Sigma_2^{--} \right\rangle = \frac{N^2}{4} \,. \end{aligned} \tag{D.10}$$

The last equality is obtained spectral flowing the correlator to the R sector, noticing that Ω carries no twist so that the twist operators need to act on the same copies carrying a combinatorial factor of $\binom{N}{2}$ and using eq. [1, Eq. (5.40)].

Eq.s (D.5), (D.6), (D.7), (D.9), (D.10) imply that all three-point functions in which the operator (D.4) is the one with highest dimension vanish if

$$\gamma = -\frac{3\alpha}{4N^{1/2}} - \frac{\beta}{4N^{1/2}} \qquad \delta = -\frac{\beta}{N^{1/2}} \qquad \epsilon = -\frac{\beta}{2N^{1/2}} \tag{D.11}$$

Combining this result with the single-trace mixing matric in Eq. (D.3) one obtains

$$\begin{aligned} \tilde{\Sigma}_3^{++} &\equiv \frac{3}{2}\left[\left(\frac{\Sigma_3^{++}}{N^{\frac{3}{2}}} - \frac{\Omega^{++}}{3N^{\frac{1}{2}}}\right) + \frac{1}{N^{\frac{1}{2}}}\left(-\frac{2}{3}(\Sigma_2\cdot\Sigma_2)^{++} + \frac{1}{6}(O\cdot O)^{++} + \frac{1}{3}(J\cdot\bar{J})^{++}\right)\right] \\ \tilde{\Omega}^{++} &\equiv \frac{\sqrt{3}}{2}\left[\left(\frac{\Sigma_3^{++}}{N^{\frac{3}{2}}} + \frac{\Omega^{++}}{N^{\frac{1}{2}}}\right) + \frac{1}{N^{\frac{1}{2}}}\left(-(\Sigma_2\cdot\Sigma_2)^{++} - \frac{1}{2}(O\cdot O)^{++} - (J\cdot\bar{J})^{++}\right)\right]. \end{aligned} \tag{D.12}$$

Note that while the factors of N that go with the single-trace operators are such that they contribute at order N^0 to the norm of the operators, since the double-trace operators are already unit normalized, they are naturally suppressed by a factor of $1/\sqrt{N}$. This implies, in particular, that the double-trace contribution to the norm of the single-particle operators is subleading in the large N limit.

Appendix E

Gauge-fixed holographic dictionary

In Section 3.5.2 we provided the holographic dictionary that relates the expectation value of single-particle operators at dimension one and scalar single-particle operators at dimension two in terms of gauge-invariant combination of KK fields. This formulation has the advantage of being general and manifestly gauge invariant: it can be used to probe any microstate solution in any coordinate system. From a practical point of view, however, it is useful to formulate the dictionary in a preferred gauge, as it makes it more manageable to use.

We choose coordinates such that the four-dimensional metric ds_4^2 in (3.20) takes the form:

$$ds_4^2 = dr^2 + r^2(d\theta^2 + \sin^2\theta d\phi^2 + \cos^2\theta d\psi^2)\,. \tag{E.1}$$

Note that this choice is always possible for the class of solutions discussed in Section 3.2.2, namely for geometries whose base space is flat $\mathbb{R}^4$. One can consider, however, constructing superstrata with a non-flat base: for example, solutions that carry excitations of the field ρ^I in (3.30) do not fall in this category (on the CFT side, they correspond to states for which, roughly speaking, the operators $GG\bar{J}$ and $\bar{G}\bar{G}J$ have a non trivial expectation value [62]). For this class of geometries one should apply the gauge-invariant formulation of the dictionary in Eq. (3.54).

From Eq. (C.8) one can see that for 1/4-BPS solutions, charactered by $\Theta_1 = \Theta_2 = \Theta_4 = 0$, the functions Z_1, Z_2 and Z_4 are harmonic. For 1/8-BPS solutions, they obey a Poisson-type equation, where the Θ_i play the role of sources. For the superstrata solution discussed in Section 3.3, the first term in the large r expansion of the sources is ≥ 7. Again, it is convenient to perform the transformation in Eq. (3.28) and reabsorb the

overall factor $\sqrt{Q_1Q_5}$ in the metric. Thus, we define the following expansion[1] [54, 55]:

$$\begin{aligned}
\tilde{Z}_1 &= \frac{Q_1}{\tilde{r}^2}\left(1+\sum_{k=1}^{2}\sum_{m_k,\bar{m}_k=-k/2}^{k/2} f_{1k}^{(m_k,\bar{m}_k)}\,\frac{Y_k^{m_k,\bar{m}_k}}{\tilde{r}^k}+O(\tilde{r}^{-3})\right),\\
\tilde{Z}_2 &= \frac{Q_5}{\tilde{r}^2}\left(1+\sum_{k=1}^{2}\sum_{m_k,\bar{m}_k=-k/2}^{k/2} f_{5k}^{k\,(m_k,\bar{m}_k)}\,\frac{Y_k^{m_k,\bar{m}_k}}{\tilde{r}^k}+O(\tilde{r}^{-3})\right),\\
\tilde{Z}_4 &= \frac{\sqrt{Q_1Q_5}}{\tilde{r}^2}\left(\sum_{k=1}^{2}\sum_{m_k,\bar{m}_k=-k/2}^{k/2} \mathcal{A}_k^{(m_k,\bar{m}_k)}\,\frac{Y_k^{m_k,\bar{m}_k}}{\tilde{r}^k}+O(\tilde{r}^{-3})\right),\\
\tilde{A} &= \frac{1}{\tilde{r}^2}\sum_{a=1}^{3}(a_{a+}Y_1^{a+}+a_{a-}Y_1^{a-})+O(\tilde{r}^{-3}),\qquad \mathcal{F}=-\frac{2Q_p}{a_0\tilde{r}^2}+O(r^{-3}),
\end{aligned}\tag{E.2}$$

where we have denoted with $Y_k^{m_k,\bar{m}_k}$ the scalar harmonics on S^3 of degree k and with $Y_1^{a\pm}$ the vector harmonics of degree one (see Appendix A). We are still left with the freedom of choosing the origin of the coordinate system on the flat base. We fix this redundancy by requiring

$$f_{11}^{(\alpha,\dot{\alpha})}+f_{51}^{(\alpha,\dot{\alpha})}=0\,,\tag{E.3}$$

which corresponds to placing the origin in the center of mass of the D1-D5 system. The choices in Eqs. (E.2) and (E.3) imply that all the unphysical fields in (3.30) at order $k=1$ vanish [54]. With these choices, the expansion of the bulk quantities in the dictionary (3.54) in terms of (E.2) yields the gauge-fixed single-particle fields in supergravity:

$$\begin{aligned}
\left[s_{k=1}^{(6)(\alpha,\dot{\alpha})}\right] &= -2\sqrt{2}f_{51}^{(\alpha,\dot{\alpha})}\,,\qquad \left[s_{k=2}^{(6)(a,\dot{a})}\right]=\sqrt{\frac{3}{2}}(f_{12}^{(a,\dot{a})}-f_{52}^{(a,\dot{a})})\,,\\
\left[s_{k=1}^{(7)(\alpha,\dot{\alpha})}\right] &= 2\sqrt{2}\mathcal{A}_1^{(\alpha,\dot{\alpha})}\,,\qquad \left[s_{k=2}^{(7)(a,\dot{a})}\right]=\sqrt{6}(\mathcal{A}_2^{(a,\dot{a})})\,,\\
\left[\tilde{\sigma}_{k=2}^{(a,\dot{a})}\right] &= -\frac{1}{\sqrt{2}}\big(f_{12}^{(a,\dot{a})}+f_{52}^{(a,\dot{a})}\big)+2\sqrt{2}\big(f_{51}^{(\alpha,\dot{\alpha})}f_{51}^{(\beta,\dot{\beta})}+\mathcal{A}_1^{(\alpha,\dot{\alpha})}\mathcal{A}_1^{(\beta,\dot{\beta})}\big)a^{(a,\dot{a})}_{(\alpha,\dot{\alpha})(\beta,\dot{\beta})}\\
&\quad +4\sqrt{2}a^{c+}a^{d-}f^1_{(a,\dot{a})cd}\,,\\
\left[A_{k=1}^{a(\pm)}\right] &= -2a^{-a,\pm}\,,
\end{aligned}\tag{E.4}$$

where $a^{(a,\dot{a})}_{(\alpha,\dot{\alpha})(\beta,\dot{\beta})}$ and $f^1_{(a,\dot{a})cd}$ are triple overlap coefficients defined in (A.9) and (A.16).

Let us compare the dictionary for operators of dimension two given in Eq. (3.54) with the one given in Chapter 2 . To do so, we first note that the dictionary for the operator $\tilde{O}_2$ given in Eq.s (2.95) and (2.96) is already formulated in the single-particle basis.

Next, we take Eq.s (2.93) and (2.94) and rotate them to express them in terms of the geometric quantities $g_{a,\dot{a}}$, $\tilde{g}_{a,\dot{a}}$. We note that the operator dual to $g_{a,\dot{a}}$ coincides with $\tilde{\Sigma}_3$, thus this sector of holographic dictionary is already given in terms of single-particles.

[1] Note that this equation is more general than [1, Eq. (3.6)], which applies only to two-charge solutions

The resulting dictionary for $\tilde{g}_{a,\dot{a}}$ reads:

$$\begin{aligned}\tilde{g}_{a,\dot{a}} &= \sqrt{2}\Big(- \big(f_{12}^{(a,\dot{a})} + f_{52}^{(a,\dot{a})}\big) + 8a^{c+}a^{d-}f^{1}_{(a,\dot{a})cd}\Big) \\ &= -(-1)^{a+\dot{a}}\sqrt{6}\Big(\frac{1}{N^{3/2}}\langle\Sigma_3^{a\dot{a}}\rangle + \frac{1}{N^{3/2}}\big(\langle\Omega^{a\dot{a}}\rangle - \frac{1}{3}\langle(\Sigma_2\cdot\Sigma_2)^{a\dot{a}}\rangle \\ &\qquad\qquad - \langle(J\cdot\bar{J})^{a\dot{a}}\rangle + \frac{1}{6}\langle(O\cdot O)^{a\dot{a}}\rangle\big)\Big)\end{aligned} \tag{E.5}$$

We observe that the right-hand side of the first line of (E.5) differs from the second-last line of Eq. (E.4) through the (gauge-invariant) terms of f_{51} and $\mathcal{A}_1$. The holographic dictionary for f_{51} and $\mathcal{A}_1$ is obtained by combining Eqs. (E.4) and (3.54). We can thus improve on the dictionary (E.5) by adding the terms in f_{51} and $\mathcal{A}_1$ to both sides of the equation. Doing so results precisely in the dictionary given in Eq. (E.4). We note that this shift corresponds to Eq. (5.30) of [54]: in that paper the authors used the basis of Chapter 2; in that basis the precise dictionary is given by Eqs. (2.93) and (2.94). In the light of the present work, Eq. (5.30) of [54] should be interpreted as follows. First, the CFT operator on the left hand side is not a single trace, but the linear combination of single and multi-trace operators reported in the right hand side of Eq. (E.5). The momentum $\pi^{\Sigma_I^2}_{(2)}$ is proportional to the right hand side of the third line of Eq. (E.4), while the product $a_{Iij}\pi^{S_i^1}_{(1)}\pi^{S_j^1}_{(1)}$ corresponds to the shift that links Eq.s (E.5) and (E.4). Note that, as discussed in Section 5.4.2 of [54], Eq. (5.30) does not have an analog for the operators $\tilde{\Sigma}_3$ and $\tilde{O}_2$: this is consistent with the fact that for these two sectors, the dictionaries in Chapters 2 and 3 coincide.

This demonstrates the consistency of the results in Chapters 2 and 3 (i.e. in [1] and [2]), and is a non-trivial check of the independent methods used in the two works.

Appendix F

Conserved charges of three-charge solutions with shockwaves

In this appendix we compute the five-dimensional conserved ADM mass and angular momenta carried by our three-charge microstate solutions with shockwaves, given in Eq. (4.29). The asymptotic metric to leading order has sphere radius $\bar{r} = \sqrt{\xi} r$ in the presence of the shockwave. With this in mind, we use [212, Eqs. (2.17), (2.18)] (see also [213, Eqs. (3.3), (3.5)]) to calculate the ADM mass of the solution in (4.29),

$$M_{ADM} = \frac{\Omega_3 L}{16\pi G_6}(3c_t - c_y) \tag{F.1}$$

$$= \frac{\pi}{4G_5}\left(Q_1 + Q_5 + \frac{Q_1 Q_5}{R_y^2}\frac{s(s+\xi)}{k^2}\right), \tag{F.2}$$

where $G_6 = LG_5,\ L = 2\pi R_y,$ and $\Omega_3 = 2\pi^2$ is the area of the unit sphere $S^3,$ and where we have used $a = \frac{\sqrt{Q_1 Q_5}}{R_y}$.

To calculate the conserved five-dimensional ADM angular momenta, we dimensionally reduce on the y-circle. Following the discussion around [214, Eq. (1.58)–(1.65)] and again using the coordinate $\bar{r}$, we compute the angular momentum along ψ, finding

$$J^\psi = -\frac{\pi}{4G_5}\frac{as\sqrt{Q_1 Q_5}}{k} = -\frac{sn_1 n_5}{k}, \tag{F.3}$$

where in the second equality we have used $a = \frac{\sqrt{Q_1 Q_5}}{R_y}$, $G_5 = \frac{G_{10}}{2\pi R_y (2\pi)^4 V_4}$, $G_{10} = 8\pi^6 g_s^2 l_s^8$, $Q_1 = \frac{g_s n_1 \alpha'^3}{V_4}$ and $Q_5 = g_s n_5 \alpha'$. Similarly the angular momentum along ϕ is

$$J^\phi = \frac{\pi a(s+\xi)\sqrt{Q_1 Q_5}}{4G_5 k} = \frac{(s+\xi)n_1 n_5}{k}. \tag{F.4}$$

Therefore the left and right angular momenta for our new solutions are

$$\begin{aligned} J^3 &= \frac{1}{2}(J^\phi - J^\psi) = \frac{1}{2}\frac{\xi n_1 n_5}{k} + \frac{s n_1 n_5}{k}\,, \\ \bar{J}^3 &= \frac{1}{2}(J^\phi + J^\psi) = \frac{1}{2}\frac{\xi n_1 n_5}{k}\,. \end{aligned} \tag{F.5}$$

We note that to compute the ADM mass, we could equally well have used dimensional reduction combined with [214, Eq. (1.65)].

Appendix G

Precision holographic computations

In this appendix we record several details of our precision holographic computation of Section 4.4.2. We refer the reader to Sections 2.2 and 2.3 for the definitions of the single-trace operators and to Eq. (3.35) for the definition of double-trace operators that we will use in this appendix.

G.1 Precision holographic test for more general states

We now describe the computation of the expectation value of the single-particle operator $\tilde{\Sigma}_3^{00}$ on the following class of states, which is more general than that considered in Section 4.4.2.

$$|{+}{+}\rangle_1^{N_0} \left(\prod_{i=1}^{n_s^+} |{+}{+}\rangle_{k_i^+}^{d_i^+} \right) \left(\prod_{j=1}^{n_s^-} |{-}{-}\rangle_{k_j^-}^{d_j^-} \right), \qquad N_0 + \sum_{i=1}^{n_s^+} d_i^+ k_i^+ + \sum_{i=1}^{n_s^-} d_i^- k_i^- = N\,. \tag{G.1}$$

Here the superscript $\pm$ refers to the strand polarizations $|{+}{+}\rangle$ and $|{-}{-}\rangle$; for ease of notation we introduce the index $m = \pm$ which we shall use in some of the following expressions.

Let us first consider the contribution from Σ_3^{00}. Proceeding as explained after Eq. (4.49), and using Eqs. (G.22) and (G.23) in the following subsection, one obtains that the

expectation value of Σ_3^{00} on the full state (4.39) arises from the process

$$\Sigma_3^{00}\Big(\,|{+}{+}\rangle_1^{N_0}\prod_{i=1}^{n_s^+}|{+}{+}\rangle_{k_i^+}^{d_i^+}\prod_{j=1}^{n_s^-}|{-}{-}\rangle_{k_j^-}^{d_j^-}\,\Big)\;=$$
$$\Bigg[\sum_i\frac{(k_i^++1)^2}{6k_i^+}N_0d_i^+ + \sum_i\frac{(k_i^-)^2+6k_i^-+1}{6k_i^-}N_0d_i^- + \sum_{m,i\neq j}\frac{(k_i^m+k_j^m)^2}{6k_i^mk_j^m}d_i^md_j^m$$
$$+\sum_{i,j}\frac{(k_i^+)^2+6k_i^+k_j^-+(k_j^-)^2}{6k_i^+k_j^-}d_i^+d_j^-\big(1-\delta_{k_i^+k_j^-}\big)\Bigg]\Big(\,|{+}{+}\rangle_1^{N_0}\prod_{i=1}^{n_s^+}|{+}{+}\rangle_{k_i^+}^{d_i^+}\prod_{j=1}^{n_s^-}|{-}{-}\rangle_{k_j^-}^{d_j^-}\,\Big)\,, \tag{G.2}$$

where the indices i,j run from 1 to n_s^+ (n_s^-) when $m=+$ ($m=-$).

Second, we consider the operator Ω^{00}. By using Eq. (4.50), it acquires a non-vanishing expectation value via the process

$$\Omega^{00}\Big(\,|{+}{+}\rangle_1^{N_0}\prod_{i=1}^{n_s^+}|{+}{+}\rangle_{k_i^+}^{d_i^+}\prod_{j=1}^{n_s^-}|{-}{-}\rangle_{k_j^-}^{d_j^-}\,\Big)=\Big(\frac{N_0}{2}+\sum_{i,m}\frac{d_i^m}{2k_i^m}\Big)\Big(\,|{+}{+}\rangle_1^{N_0}\prod_{i=1}^{n_s^+}|{+}{+}\rangle_{k_i^+}^{d_i^+}\prod_{j=1}^{n_s^-}|{-}{-}\rangle_{k_j^-}^{d_j^-}\,\Big)\,. \tag{G.3}$$

Third, we consider the double-trace operator $\big(J\cdot\bar{J}\big)^{00}$. Its expectation value arises from the process described after Eq. (4.52),

$$\big(J\cdot\bar{J}\big)^{00}\Big(\,|{+}{+}\rangle_1^{N_0}\prod_{i=1}^{n_s^+}|{+}{+}\rangle_{k_i^+}^{d_i^+}\prod_{j=1}^{n_s^-}|{-}{-}\rangle_{k_j^-}^{d_j^-}\,\Big)\;= \tag{G.4}$$
$$\Big[\frac{N_0^2}{2}+N_0\sum_i d_i^+ - N_0\sum_i d_i^- + \sum_{m,i,j}\frac{d_i^md_j^m}{2} - \sum_{i,j}d_i^+d_j^-\Big]\Big(\,|{+}{+}\rangle_1^{N_0}\prod_{i=1}^{n_s^+}|{+}{+}\rangle_{k_i^+}^{d_i^+}\prod_{j=1}^{n_s^-}|{-}{-}\rangle_{k_j^-}^{d_j^-}\,\Big)\,.$$

By combining the definition of the single-particle operator $\tilde{\Sigma}_3^{00}$ with Eqs. (G.2)–(G.4), we obtain the expectation value of the single-particle operator. We find cancellation of all terms that are clearly of order $N^{1/2}$, leaving the following remainder:

$$\big\langle\tilde{\Sigma}_3^{00}\big\rangle \;=\; \frac{1}{N^{3/2}}\Big[N_0\sum_{m,i}d_i^m + \sum_{m,i\neq j}d_i^md_j^m\frac{(k_j^m)^2+3k_i^mk_j^m}{4k_i^mk_j^m} + \sum_{i,j}d_i^+d_j^-\Big(1-2\delta_{k_i^+,k_j^-}\Big)\Big]\,. \tag{G.5}$$

We must ensure that this remainder is subleading compared to $N^{1/2}$. When the long strands were all of polarization $|{+}{+}\rangle$, this condition led to the constraint $\sum_i d_i\sim N^{1-\alpha}$ with $\alpha>0$. We will obtain the analogous constraint, however to do so we must take care since now (G.5) is not the sum of positive terms, due to the final term.

Let us therefore examine the final term. Without loss of generality, let us assume $n_s^+\geq n_s^-$. To obtain a bound on this term, let us consider the worst-case scenario in which $k_i^+=k_i^-$ for all $i=1,\ldots,n_s^-$. The magnitude of the negative contribution to this

term is then given by

$$\frac{1}{N^{3/2}}\sum_{i=1}^{n_s^-} d_i^+ d_i^- \,. \tag{G.6}$$

Since no d_i^m can scale as N, and since $N_0 \sim N$, the magnitude of this term is subleading with respect to the first term in (G.5). Therefore these terms cannot cancel each other, and so the first term in (G.5) must by itself be subleading with respect to $N^{1/2}$. This implies that:

$$\left(\sum_{i=1}^{n_s^+} d_i^+ + \sum_{i}^{n_s^-} d_i^-\right) \;\sim\; N^{1-\alpha}\,, \qquad \alpha > 0\,. \tag{G.7}$$

Upon imposing this condition, the other terms in (G.5) are also subleading with respect to $N^{1/2}$, using similar reasoning to that used in the main text. We thus find that the condition (G.7) is necessary and sufficient for the precision holographic test to be passed for this more general class of states. The completely general case, i.e. the one in which the long-strands can have any RR polarization, is analogous.

G.2 Fusion coefficients for Σ_3

In this final section we compute the fusion coefficients $c_{k_1k_2}$ for the following processes:

$$\begin{aligned}
\sigma_3^{00}\,|{+}{+}\rangle_{k_1}\,|{+}{+}\rangle_{k_2} &= c_{k_1k_2}^{(++)}\big(1-\delta_{k_1,k_2}\big)\,|{+}{+}\rangle_{k_1}\,|{+}{+}\rangle_{k_2}\,,\\
\sigma_3^{00}\,|{-}{-}\rangle_{k_1}\,|{-}{-}\rangle_{k_2} &= c_{k_1k_2}^{(--)}\big(1-\delta_{k_1,k_2}\big)\,|{-}{-}\rangle_{k_1}\,|{-}{-}\rangle_{k_2}\,,\\
\sigma_3^{00}\,|{+}{+}\rangle_{k_1}\,|{-}{-}\rangle_{k_2} &= c_{k_1k_2}^{(+-)}\big(1-\delta_{k_1,k_2}\big)\,|{+}{+}\rangle_{k_1}\,|{-}{-}\rangle_{k_2}\,.
\end{aligned} \tag{G.8}$$

The factor $(1-\delta_{k_1,k_2})$ can be explained as follows. The operator σ_3^{00} corresponds to a three-cycle that, when acting on two permutations of length k_1 and k_2, produces another pair of permutations of length k_1 and k_2 by shuffling the copies (see the discussion around Eq. (2.110)): this process can occur only if $k_1 \neq k_2$.

We now give an explicit derivation of the coefficient $c_{k_1k_2}^{(++)}$. The derivation of the coefficients $c_{k_1k_2}^{(--)}$ and $c_{k_1k_2}^{(+-)}$ is analogous, and we simply report their values at the end of the appendix.

We compute the coefficient $c_{k_1k_2}^{(++)}$ by requiring that the precision holography dictionary (4.47) for the single-particle operator $\tilde{\Sigma}_3$ holds on the two-charge CFT state:

$$\sum_{N_1}\Big(A\,|{+}{+}\rangle_{k_1}\Big)^{N_1}\Big(B\,|{+}{+}\rangle_{k_2}\Big)^{N-N_1}\,, \tag{G.9}$$

where, for concreteness, we take $k_1 \neq k_2$. Here A, B are coefficients that we take to be

real; they are related to the average number of strands $\bar{N}_1$ and $N - \bar{N}_1$ via [103]

$$k_1 \bar{N}_1 = A^2 \,, \qquad k_2 (N - \bar{N}_1) = B^2 \,. \tag{G.10}$$

Let us first compute the bulk quantity $\left[s_{k=2}^{(6)(-a,-\dot{a})} \right]$ defined in Eq. (4.44). We do so by generating the harmonic functions Z_1 and Z_2 as in Eq. (2.14), making use of the following profile functions:

$$g_1(v') \;=\; \frac{a}{k_1} e^{\frac{2\pi i k_1}{L} v'} + \frac{b}{k_2} e^{\frac{2\pi i k_2}{L} v'} \,, \qquad g_{i \neq 1}(v') \;=\; 0 \,. \tag{G.11}$$

The supergravity Fourier modes a, b are related to the CFT coefficients A, B via

$$A \;=\; R_y \sqrt{\frac{N}{Q_1 Q_5}} a \,, \qquad B \;=\; R_y \sqrt{\frac{N}{Q_1 Q_5}} b \,, \tag{G.12}$$

and satisfy the usual relation

$$a^2 + b^2 \;=\; \frac{Q_1 Q_5}{R_y^2} \,. \tag{G.13}$$

Upon performing the asymptotic expansion in Eq. (E.2), one finds that the spin component $(0, 0)$ is non-vanishing, with value

$$\left[s_{\mathsf{k}=2}^{(6)(0,0)} \right] \;=\; \sqrt{2} \frac{a^2 b^2}{k_1 k_2} \frac{R_y^4}{(Q_1 Q_5)^2} \,. \tag{G.14}$$

The holographic dictionary in Eq. (4.47) then predicts that the single-particle scalar CPO $\tilde{\Sigma}_3^{00}$ has the following expectation value on the CFT state (G.9):

$$\left\langle \tilde{\Sigma}_3^{00} \right\rangle \;=\; \frac{a^2 b^2}{k_1 k_2} \frac{R_y^4}{(Q_1 Q_5)^2} N^{1/2} \,. \tag{G.15}$$

We now fix the fusion coefficient $c_{k_1 k_2}$ by requiring that this is indeed the case. The CFT operators in the linear combination (4.46) that contribute at leading order at large N to the expectation value of the single-particle operator $\tilde{\Sigma}_3^{00}$ are the single-trace operators Σ_3^{00} and Ω^{00} and the double-trace $\left(J \cdot \bar{J} \right)^{00}$.

First, we consider the operator Σ_3^{00}. Its expectation value is obtained by multiplying the fundamental process (G.8) by the number of different ways the twist operator can act on the coherent state, as we shall describe momentarily. When the operator Σ_3^{00} acts on a term in the coherent state sum (G.9), the contribution is

$$\Sigma_3^{00} \Big[\left| {+}{+} \right\rangle_{k_1}^{N_1} \left| {+}{+} \right\rangle_{k_2}^{N - N_1} \Big] \;=\; c_{k_1 k_2}^{(++)} N_1 (N - N_1) k_1 k_2 \Big[\left| {+}{+} \right\rangle_{k_1}^{N_1} \left| {+}{+} \right\rangle_{k_2}^{N - N_1} \Big] \,. \tag{G.16}$$

The numerical factor $N_1(N - N_1)$ follows from the fact that the twist operator can act on any of the $N_1(N - N_1)$ pairs of $\left| {+}{+} \right\rangle_{k_1}$, $\left| {+}{+} \right\rangle_{k_2}$, while the term $k_1 k_2$ occurs because

each strand can be cut in k_1 and k_2 different positions respectively. Using Eqs. (G.10) and (G.12) we find

$$\langle \Sigma_3^{00} \rangle \;=\; c_{k_1 k_2}^{(++)}\, a^2\, b^2 \frac{R_y^4 N^2}{(Q_1 Q_5)^2}\,. \tag{G.17}$$

Second, we consider the operator Ω^{00}. The relevant contribution to the expectation value of Ω^{00} then follows from Eq. (4.50) via the basic process

$$\Omega^{00}\Big[\,|{+}{+}\rangle_{k_1}^{N_1}\,|{+}{+}\rangle_{k_2}^{N-N_1}\,\Big] \;=\; \Big(\frac{N_1}{2k_1}+\frac{N-N_1}{2k_2}\Big)\Big[\,|{+}{+}\rangle_{k_1}^{N_1}\,|{+}{+}\rangle_{k_2}^{N-N_1}\,\Big]\,. \tag{G.18}$$

It follows from Eqs. (G.10)–(G.13) that

$$\langle \Omega^{00} \rangle \;=\; (a^2+b^2)\left(\frac{a^2}{2k_1^2}+\frac{b^2}{2k_2^2}\right)\frac{R_y^4 N}{(Q_1 Q_5)^2}\,. \tag{G.19}$$

Third, we consider the double-trace operator $\big(J\cdot\bar{J}\big)^{00} = \frac{2}{N}\sum_{r,s} J^3_{(r)}\bar{J}^3_{(s)}$. When acting on a member of the coherent state (G.9), this operator produces three terms, which correspond to: (i) both left and right currents acting on a strand of twist k_1, (ii) both currents acting on a strand of length k_2, and (iii) each current acting on a different type of strand. This produces the following contribution:

$$\big(J\cdot\bar{J}\big)^{00}\Big[\,|{+}{+}\rangle_{k_1}^{N_1}\,|{+}{+}\rangle_{k_2}^{N-N_1}\,\Big] \;=\; \frac{2}{N}\Big(\frac{N_1^2}{4}+\frac{N_1(N-N_1)}{2}+\frac{(N-N_1)^2}{4}\Big)\Big[\,|{+}{+}\rangle_{k_1}^{N_1}\,|{+}{+}\rangle_{k_2}^{N-N_1}\,\Big]\,, \tag{G.20}$$

which implies

$$\big\langle \big(J\cdot\bar{J}\big)^{00} \big\rangle \;=\; \Big(\frac{a^4}{2k_1^2}+\frac{a^2b^2}{k_1k_2}+\frac{b^4}{2k_2^2}\Big)\frac{R_y^4 N}{(Q_1 Q_5)^2}\,, \tag{G.21}$$

where we have used Eqs. (G.10) and (G.12). By using the definition of the single-particle operator $\tilde{\Sigma}_3$ in Eq. (4.46), we have that the holographic prediction in Eq. (G.15) holds provided that

$$c_{k_1 k_2}^{(++)} \;=\; \frac{(k_1+k_2)^2}{6k_1^2k_2^2}\,. \tag{G.22}$$

With similar computations, one obtains

$$c_{k_1 k_2}^{(--)} \;=\; \frac{(k_1+k_2)^2}{6k_1^2k_2^2}\,, \qquad c_{k_1 k_2}^{(+-)} \;=\; \frac{k_1^2+6k_1k_2+k_2^2}{6k_1^2k_2^2}\,. \tag{G.23}$$

Bibliography

[1] S. Giusto, S. Rawash, and D. Turton, "Ads$_3$ holography at dimension two," *JHEP* **07** (2019) 171, arXiv:1904.12880 [hep-th].

[2] S. Rawash and D. Turton, "Supercharged AdS$_3$ Holography," *JHEP* **07** (2021) 178, arXiv:2105.13046 [hep-th].

[3] B. Chakrabarty, S. Rawash, and D. Turton, "Shockwaves in black hole microstate geometries," *JHEP* **02** (2022) 202, arXiv:2112.08378 [hep-th].

[4] S. Rawash and D. Turton, "Evolutionary algorithms for multi-center solutions," arXiv:2212.08585 [hep-th].

[5] **LIGO Scientific Collaboration and Virgo Collaboration** , "Observation of gravitational waves from a binary black hole merger," *Phys. Rev. Lett.* **116** (Feb, 2016) 061102. https://link.aps.org/doi/10.1103/PhysRevLett.116.061102.

[6] **Event Horizon Telescope** , K. Akiyama *et al.*, "First M87 Event Horizon Telescope Results. I. The Shadow of the Supermassive Black Hole," *Astrophys. J.* **875** no. 1, (2019) L1, arXiv:1906.11238 [astro-ph.GA].

[7] C. M. Will, "The confrontation between general relativity and experiment," *Living Reviews in Relativity* **9** no. 1, (Mar, 2006) . https://doi.org/10.12942%2Flrr-2006-3.

[8] M. Heusler, "Stationary black holes: Uniqueness and beyond," *Living Rev.Rel.* **1** (1998) 6. , http://www.livingreviews.org/lrr-1998-6.

[9] J. D. Bekenstein, "Black holes and entropy," *Phys. Rev.* **D7** (1973) 2333–2346.

[10] R. M. Wald, *General Relativity*. Chicago Univ. Pr., Chicago, USA, 1984.

[11] A. Zee, *Einstein Gravity in a Nutshell*. Princeton University Press, New Jersey, 5, 2013.

[12] J. D. Bekenstein, "Generalized second law of thermodynamics in black hole physics," *Phys. Rev.* **D9** (1974) 3292–3300.

[13] S. W. Hawking, "Particle Creation by Black Holes," *Commun. Math. Phys.* **43** (1975) 199–220. Erratum: [Commun. Math. Phys. **46**, 206 (1976)].

[14] J. B. Hartle and S. W. Hawking, "Path-integral derivation of black-hole radiance," *Phys. Rev. D* **13** (Apr, 1976) 2188–2203. https://link.aps.org/doi/10.1103/PhysRevD.13.2188.

[15] J. Polchinski, "The Black Hole Information Problem," in *Theoretical Advanced Study Institute in Elementary Particle Physics: New Frontiers in Fields and Strings*, pp. 353–397. 2017. arXiv:1609.04036 [hep-th].

[16] S. W. Hawking, "Breakdown of Predictability in Gravitational Collapse," *Phys. Rev.* **D14** (1976) 2460–2473.

[17] S. B. Giddings and W. M. Nelson, "Quantum emission from two-dimensional black holes," *Physical Review D* **46** no. 6, (Sep, 1992) 2486–2496. https://doi.org/10.1103%2Fphysrevd.46.2486.

[18] D. N. Page, "Black hole information," arXiv:hep-th/9305040.

[19] S. D. Mathur, "What Exactly is the Information Paradox?," *Lect. Notes Phys.* **769** (2009) 3–48, arXiv:0803.2030 [hep-th].

[20] S. D. Mathur and C. J. Plumberg, "Correlations in Hawking radiation and the infall problem," *JHEP* **09** (2011) 093, arXiv:1101.4899 [hep-th].

[21] A. Almheiri, D. Marolf, J. Polchinski, and J. Sully, "Black Holes: Complementarity or Firewalls?," *JHEP* **1302** (2013) 062, arXiv:1207.3123 [hep-th].

[22] D. Harlow, "Jerusalem lectures on black holes and quantum information," *Reviews of Modern Physics* **88** no. 1, (Feb, 2016) . https://doi.org/10.1103%2Frevmodphys.88.015002.

[23] S. Raju, "Lessons from the information paradox," *Phys. Rept.* **943** (2022) 1–80, arXiv:2012.05770 [hep-th].

[24] Y. Aharonov, A. Casher, and S. Nussinov, "The Unitarity Puzzle and Planck Mass Stable Particles," *Phys. Lett. B* **191** (1987) 51.

[25] D. N. Page, "Average entropy of a subsystem," *Phys.Rev.Lett.* **71** (1993) 1291–1294, arXiv:gr-qc/9305007 [gr-qc].

[26] J. D. Bekenstein, "A Universal Upper Bound on the Entropy to Energy Ratio for Bounded Systems," *Phys. Rev.* **D23** (1981) 287.

[27] J. D. Bekenstein, "Entropy bounds and black hole remnants," *Phys. Rev.* **D49** (1994) 1912–1921, arXiv:gr-qc/9307035.

[28] L. Susskind, "Trouble for remnants," arXiv:hep-th/9501106.

[29] S. B. Giddings, "The Black hole information paradox," arXiv:hep-th/9508151.

[30] S. D. Mathur, "The information paradox: A pedagogical introduction," *Class. Quant. Grav.* **26** (2009) 224001, arXiv:0909.1038 [hep-th].

[31] S. G. Avery, "Qubit Models of Black Hole Evaporation," *JHEP* **1301** (2013) 176, arXiv:1109.2911 [hep-th].

[32] R. P. Feynman, *Feynman lectures on gravitation*. 1996.

[33] A. Almheiri, N. Engelhardt, D. Marolf, and H. Maxfield, "The entropy of bulk quantum fields and the entanglement wedge of an evaporating black hole," *Journal of High Energy Physics* **2019** no. 12, (Dec, 2019) . https://doi.org/10.1007%2Fjhep12%282019%29063.

[34] G. Penington, "Entanglement Wedge Reconstruction and the Information Paradox," *JHEP* **09** (2020) 002, arXiv:1905.08255 [hep-th].

[35] G. Penington, S. H. Shenker, D. Stanford, and Z. Yang, "Replica wormholes and the black hole interior," *JHEP* **03** (2022) 205, arXiv:1911.11977 [hep-th].

[36] A. Almheiri, R. Mahajan, J. Maldacena, and Y. Zhao, "The Page curve of Hawking radiation from semiclassical geometry," *JHEP* **03** (2020) 149, arXiv:1908.10996 [hep-th].

[37] A. Almheiri, T. Hartman, J. Maldacena, E. Shaghoulian, and A. Tajdini, "The entropy of Hawking radiation," *Rev. Mod. Phys.* **93** no. 3, (2021) 035002, arXiv:2006.06872 [hep-th].

[38] G. W. Gibbons and S. W. Hawking, "Action Integrals and Partition Functions in Quantum Gravity," *Phys. Rev. D* **15** (1977) 2752–2756.

[39] B. Guo, M. R. R. Hughes, S. D. Mathur, and M. Mehta, "Contrasting the fuzzball and wormhole paradigms for black holes," *Turk. J. Phys.* **45** no. 6, (2021) 281–365, arXiv:2111.05295 [hep-th].

[40] A. Strominger and C. Vafa, "Microscopic Origin of the Bekenstein-Hawking Entropy," *Phys. Lett.* **B379** (1996) 99–104, arXiv:hep-th/9601029.

[41] K. Sfetsos and K. Skenderis, "Microscopic derivation of the bekenstein-hawking entropy formula for non-extremal black holes," *Nuclear Physics B* **517** no. 1-3, (Apr, 1998) 179–204. https://doi.org/10.1016%2Fs0550-3213%2898%2900023-6.

[42] C. G. Callan and J. M. Maldacena, "D-brane approach to black hole quantum mechanics," *Nuclear Physics B* **472** no. 3, (Jul, 1996) 591–608. https://doi.org/10.1016%2F0550-3213%2896%2900225-8.

[43] S. De Haro, J. van Dongen, M. Visser, and J. Butterfield, "Conceptual analysis of black hole entropy in string theory," *Stud. Hist. Phil. Sci. B* **69** (2020) 82–111, arXiv:1904.03232 [physics.hist-ph].

[44] V. Balasubramanian, J. de Boer, E. Keski-Vakkuri, and S. F. Ross, "Supersymmetric conical defects: Towards a string theoretic description of black hole formation," *Phys. Rev.* **D64** (2001) 064011, arXiv:hep-th/0011217.

[45] J. M. Maldacena and L. Maoz, "De-singularization by rotation," *JHEP* **12** (2002) 055, arXiv:hep-th/0012025.

[46] O. Lunin and S. D. Mathur, "Metric of the multiply wound rotating string," *Nucl. Phys.* **B610** (2001) 49–76, arXiv:hep-th/0105136.

[47] O. Lunin and S. D. Mathur, "AdS/CFT duality and the black hole information paradox," *Nucl. Phys.* **B623** (2002) 342–394, arXiv:hep-th/0109154.

[48] L. Susskind, "Some speculations about black hole entropy in string theory," arXiv:hep-th/9309145.

[49] S. D. Mathur and D. Turton, "The fuzzball nature of two-charge black hole microstates," arXiv:1811.09647 [hep-th].

[50] S. D. Mathur, "The fuzzball proposal for black holes: An elementary review," *Fortsch. Phys.* **53** (2005) 793–827, arXiv:hep-th/0502050.

[51] I. Bena and N. P. Warner, "Black holes, black rings and their microstates," *Lect. Notes Phys.* **755** (2008) 1–92, arXiv:hep-th/0701216.

[52] K. Skenderis and M. Taylor, "The fuzzball proposal for black holes," *Phys. Rept.* **467** (2008) 117–171, arXiv:0804.0552 [hep-th].

[53] M. Taylor, "General 2 charge geometries," *JHEP* **03** (2006) 009, arXiv:hep-th/0507223.

[54] I. Kanitscheider, K. Skenderis, and M. Taylor, "Holographic anatomy of fuzzballs," *JHEP* **04** (2007) 023, arXiv:hep-th/0611171.

[55] I. Kanitscheider, K. Skenderis, and M. Taylor, "Fuzzballs with internal excitations," *JHEP* **06** (2007) 056, arXiv:0704.0690 [hep-th].

[56] I. Bena, S. Giusto, R. Russo, M. Shigemori, and N. P. Warner, "Habemus Superstratum! A constructive proof of the existence of superstrata," *JHEP* **05** (2015) 110, arXiv:1503.01463 [hep-th].

[57] I. Bena, E. Martinec, D. Turton, and N. P. Warner, "Momentum Fractionation on Superstrata," *JHEP* **05** (2016) 064, arXiv:1601.05805 [hep-th].

[58] I. Bena, S. Giusto, E. J. Martinec, R. Russo, M. Shigemori, D. Turton, and N. P. Warner, "Smooth horizonless geometries deep inside the black-hole regime," *Phys. Rev. Lett.* **117** no. 20, (2016) 201601, arXiv:1607.03908 [hep-th].

[59] I. Bena, E. Martinec, D. Turton, and N. P. Warner, "M-theory Superstrata and the MSW String," *JHEP* **06** (2017) 137, arXiv:1703.10171 [hep-th].

[60] I. Bena, S. Giusto, E. J. Martinec, R. Russo, M. Shigemori, D. Turton, and N. P. Warner, "Asymptotically-flat supergravity solutions deep inside the black-hole regime," *JHEP* **02** (2018) 014, arXiv:1711.10474 [hep-th].

[61] I. Bena, D. Turton, R. Walker, and N. P. Warner, "Integrability and Black-Hole Microstate Geometries," *JHEP* **11** (2017) 021, arXiv:1709.01107 [hep-th].

[62] N. Ceplak, R. Russo, and M. Shigemori, "Supercharging Superstrata," *JHEP* **03** (2019) 095, arXiv:1812.08761 [hep-th].

[63] P. Heidmann and N. P. Warner, "Superstratum Symbiosis," *JHEP* **09** (2019) 059, arXiv:1903.07631 [hep-th].

[64] P. Heidmann, D. R. Mayerson, R. Walker, and N. P. Warner, "Holomorphic Waves of Black Hole Microstructure," *JHEP* **02** (2020) 192, arXiv:1910.10714 [hep-th].

[65] N. Čeplak, "Vector Superstrata," arXiv:2212.06947 [hep-th].

[66] M. Shigemori, "Superstrata on Orbifolded Backgrounds," arXiv:2212.13388 [hep-th].

[67] I. Bena and N. P. Warner, "One ring to rule them all ... and in the darkness bind them?," *Adv. Theor. Math. Phys.* **9** (2005) 667–701, arXiv:hep-th/0408106.

[68] J. P. Gauntlett and J. B. Gutowski, "General concentric black rings," *Phys.Rev.* **D71** (2005) 045002, arXiv:hep-th/0408122 [hep-th].

[69] I. Bena, C.-W. Wang, and N. P. Warner, "Mergers and Typical Black Hole Microstates," *JHEP* **11** (2006) 042, arXiv:hep-th/0608217.

[70] I. Bena, C.-W. Wang, and N. P. Warner, "Plumbing the Abyss: Black Ring Microstates," *JHEP* **07** (2008) 019, arXiv:0706.3786 [hep-th].

[71] J. Avila, P. F. Ramirez, and A. Ruiperez, "One Thousand and One Bubbles," *JHEP* **01** (2018) 041, arXiv:1709.03985 [hep-th].

[72] P. Heidmann, "Four-center bubbled BPS solutions with a Gibbons-Hawking base," *JHEP* **10** (2017) 009, arXiv:1703.10095 [hep-th].

[73] I. Bena, P. Heidmann, and P. F. Ramirez, "A systematic construction of microstate geometries with low angular momentum," *JHEP* **10** (2017) 217, arXiv:1709.02812 [hep-th].

[74] M. Bianchi, J. F. Morales, L. Pieri, and N. Zinnato, "More on microstate geometries of 4d black holes," *Journal of High Energy Physics* **2017** no. 5, (May, 2017) . https://doi.org/10.1007%2Fjhep05%282017%29147.

[75] D. R. Mayerson, "Modave Lectures on Horizon-Size Microstructure, Fuzzballs and Observations," arXiv:2202.11394 [hep-th].

[76] M. Shigemori, "Counting Superstrata," *JHEP* **10** (2019) 017, arXiv:1907.03878 [hep-th].

[77] D. R. Mayerson and M. Shigemori, "Counting D1-D5-P microstates in supergravity," *SciPost Phys.* **10** no. 1, (2021) 018, arXiv:2010.04172 [hep-th].

[78] V. Jejjala, O. Madden, S. F. Ross, and G. Titchener, "Non-supersymmetric smooth geometries and D1-D5-P bound states," *Phys. Rev.* **D71** (2005) 124030, arXiv:hep-th/0504181.

[79] V. Cardoso, O. J. C. Dias, J. L. Hovdebo, and R. C. Myers, "Instability of non-supersymmetric smooth geometries," *Phys. Rev.* **D73** (2006) 064031, arXiv:hep-th/0512277.

[80] B. D. Chowdhury and S. D. Mathur, "Radiation from the non-extremal fuzzball," *Class. Quant. Grav.* **25** (2008) 135005, arXiv:0711.4817 [hep-th].

[81] B. D. Chowdhury and S. D. Mathur, "Pair creation in non-extremal fuzzball geometries," *Class. Quant. Grav.* **25** (2008) 225021, arXiv:0806.2309 [hep-th].

[82] B. D. Chowdhury and S. D. Mathur, "Non-extremal fuzzballs and ergoregion emission," *Class. Quant. Grav.* **26** (2009) 035006, arXiv:0810.2951 [hep-th].

[83] S. G. Avery, B. D. Chowdhury, and S. D. Mathur, "Deforming the D1D5 CFT away from the orbifold point," *JHEP* **06** (2010) 031, arXiv:1002.3132 [hep-th].

[84] S. G. Avery, B. D. Chowdhury, and S. D. Mathur, "Excitations in the deformed D1D5 CFT," *JHEP* **06** (2010) 032, arXiv:1003.2746 [hep-th].

[85] B. Chakrabarty, D. Turton, and A. Virmani, "Holographic description of non-supersymmetric orbifolded D1-D5-P solutions," *JHEP* **11** (2015) 063, arXiv:1508.01231 [hep-th].

[86] I. Bena, G. Bossard, S. Katmadas, and D. Turton, "Bolting Multicenter Solutions," *JHEP* **01** (2017) 127, arXiv:1611.03500 [hep-th].

[87] G. Bossard, S. Katmadas, and D. Turton, "Two Kissing Bolts," *JHEP* **02** (2018) 008, arXiv:1711.04784 [hep-th].

[88] B. Ganchev, A. Houppe, and N. Warner, "Q-Balls Meet Fuzzballs: Non-BPS Microstate Geometries," arXiv:2107.09677 [hep-th].

[89] B. Ganchev, A. Houppe, and N. P. Warner, "New Superstrata from Three-Dimensional Supergravity," arXiv:2110.02961 [hep-th].

[90] J. M. Maldacena, "Eternal black holes in anti-de Sitter," *JHEP* **04** (2003) 021, arXiv:hep-th/0106112 [hep-th].

[91] E. Keski-Vakkuri, "Bulk and boundary dynamics in BTZ black holes," *Phys. Rev.* **D59** (1999) 104001, arXiv:hep-th/9808037 [hep-th].

[92] A. L. Fitzpatrick, J. Kaplan, D. Li, and J. Wang, "On information loss in AdS_3/CFT_2," *JHEP* **05** (2016) 109, arXiv:1603.08925 [hep-th].

[93] A. Galliani, S. Giusto, E. Moscato, and R. Russo, "Correlators at large c without information loss," *Journal of High Energy Physics* **2016** no. 9, (Sep, 2016) . http://dx.doi.org/10.1007/JHEP09(2016)065.

[94] A. Bombini, A. Galliani, S. Giusto, E. Moscato, and R. Russo, "Unitary 4-point correlators from classical geometries," *Eur. Phys. J.* **C78** no. 1, (2018) 8, arXiv:1710.06820 [hep-th].

[95] A. Galliani, S. Giusto, and R. Russo, "Holographic 4-point correlators with heavy states," *JHEP* **10** (2017) 040, arXiv:1705.09250 [hep-th].

[96] A. W. Peet, "TASI lectures on black holes in string theory," arXiv:hep-th/0008241.

[97] J. M. Maldacena, "The large N limit of superconformal field theories and supergravity," *Adv. Theor. Math. Phys.* **2** (1998) 231–252, arXiv:hep-th/9711200.

[98] E. Witten, "Anti-de Sitter space and holography," *Adv. Theor. Math. Phys.* **2** (1998) 253–291, arXiv:hep-th/9802150.

[99] S. S. Gubser, I. R. Klebanov, and A. M. Polyakov, "Gauge theory correlators from non-critical string theory," *Phys. Lett.* **B428** (1998) 105–114, arXiv:hep-th/9802109.

[100] O. Aharony, S. S. Gubser, J. M. Maldacena, H. Ooguri, and Y. Oz, "Large N field theories, string theory and gravity," *Phys. Rept.* **323** (2000) 183–386, arXiv:hep-th/9905111.

[101] O. Lunin, S. D. Mathur, and A. Saxena, "What is the gravity dual of a chiral primary?," *Nucl. Phys.* **B655** (2003) 185–217, arXiv:hep-th/0211292.

[102] M. Baggio, J. de Boer, and K. Papadodimas, "A non-renormalization theorem for chiral primary 3-point functions," *JHEP* **07** (2012) 137, arXiv:1203.1036 [hep-th].

[103] S. Giusto, E. Moscato, and R. Russo, "AdS_3 holography for 1/4 and 1/8 BPS geometries," *JHEP* **11** (2015) 004, arXiv:1507.00945 [hep-th].

[104] N. Lashkari and J. Simón, "From state distinguishability to effective bulk locality," *JHEP* **06** (2014) 038, arXiv:1402.4829 [hep-th].

[105] S. Raju and P. Shrivastava, "Critique of the fuzzball program," *Phys. Rev. D* **99** no. 6, (2019) 066009, arXiv:1804.10616 [hep-th].

[106] K. Skenderis and M. Taylor, "Fuzzball solutions and D1-D5 microstates," *Phys. Rev. Lett.* **98** (2007) 071601, arXiv:hep-th/0609154.

[107] M. Taylor, "Matching of correlators in AdS(3) / CFT(2)," *JHEP* **06** (2008) 010, arXiv:0709.1838 [hep-th].

[108] E. D'Hoker, D. Z. Freedman, S. D. Mathur, A. Matusis, and L. Rastelli, "Extremal correlators in the AdS / CFT correspondence," arXiv:hep-th/9908160 [hep-th].

[109] G. Arutyunov and S. Frolov, "On the correspondence between gravity fields and CFT operators," *JHEP* **04** (2000) 017, arXiv:hep-th/0003038 [hep-th].

[110] O. Lunin, J. M. Maldacena, and L. Maoz, "Gravity solutions for the D1-D5 system with angular momentum," arXiv:hep-th/0212210.

[111] S. G. Avery, "Using the D1D5 CFT to Understand Black Holes," arXiv:1012.0072 [hep-th].

[112] I. Bena, P. Heidmann, and D. Turton, "AdS_2 holography: mind the cap," *JHEP* **12** (2018) 028, arXiv:1806.02834 [hep-th].

[113] E. Bakhshaei and A. Bombini, "Three-charge superstrata with internal excitations," *Class. Quant. Grav.* **36** no. 5, (2019) 055001, arXiv:1811.00067 [hep-th].

[114] I. Bena, E. J. Martinec, R. Walker, and N. P. Warner, "Early Scrambling and Capped BTZ Geometries," arXiv:1812.05110 [hep-th].

[115] K. Skenderis and M. Taylor, "Kaluza-Klein holography," *JHEP* **05** (2006) 057, arXiv:hep-th/0603016 [hep-th].

[116] L. Rastelli and X. Zhou, "How to Succeed at Holographic Correlators Without Really Trying," *JHEP* **04** (2018) 014, arXiv:1710.05923 [hep-th].

[117] J. Garcia i Tormo and M. Taylor, "Correlation functions in the D1-D5 orbifold CFT," *JHEP* **06** (2018) 012, arXiv:1804.10205 [hep-th].

[118] S. Giusto and R. Russo, "Entanglement Entropy and D1-D5 geometries," *Phys. Rev.* **D90** no. 6, (2014) 066004, arXiv:1405.6185 [hep-th].

[119] S. Ribault, "Conformal field theory on the plane," arXiv:1406.4290 [hep-th].

[120] O. Lunin and S. D. Mathur, "Three-point functions for M(N)/S(N) orbifolds with N = 4 supersymmetry," *Commun. Math. Phys.* **227** (2002) 385–419, arXiv:hep-th/0103169.

[121] A. Tyukov, R. Walker, and N. P. Warner, "Tidal Stresses and Energy Gaps in Microstate Geometries," *JHEP* **02** (2018) 122, arXiv:1710.09006 [hep-th].

[122] M. Bianchi, D. Consoli, A. Grillo, and J. F. Morales, "The dark side of fuzzball geometries," arXiv:1811.02397 [hep-th].

[123] A. Bombini and A. Galliani, "AdS_3 four-point functions from $\frac{1}{8}$-BPS states," arXiv:1904.02656 [hep-th].

[124] S. D. Mathur and D. Turton, "Oscillating supertubes and neutral rotating black hole microstates," *JHEP* **1404** (2014) 072, arXiv:1310.1354 [hep-th].

[125] I. Bena, S. F. Ross, and N. P. Warner, "On the Oscillation of Species," *JHEP* **1409** (2014) 113, arXiv:1312.3635 [hep-th].

[126] F. Aprile, J. Drummond, P. Heslop, and H. Paul, "Double-trace spectrum of $N = 4$ supersymmetric Yang-Mills theory at strong coupling," *Phys. Rev. D* **98** no. 12, (2018) 126008, arXiv:1802.06889 [hep-th].

[127] F. Aprile, J. Drummond, P. Heslop, H. Paul, F. Sanfilippo, M. Santagata, and A. Stewart, "Single Particle Operators and their Correlators in Free $\mathcal{N} = 4$ SYM," arXiv:2007.09395 [hep-th].

[128] S. Deger, A. Kaya, E. Sezgin, and P. Sundell, "Spectrum of D = 6, N = 4b supergravity on AdS(3) x S(3)," *Nucl. Phys.* **B536** (1998) 110–140, arXiv:hep-th/9804166 [hep-th].

[129] F. Larsen, "The Perturbation spectrum of black holes in N=8 supergravity," *Nucl. Phys.* **B536** (1998) 258–278, arXiv:hep-th/9805208 [hep-th].

[130] J. de Boer, "Six-dimensional supergravity on S**3 x AdS(3) and 2-D conformal field theory," *Nucl. Phys.* **B548** (1999) 139–166, arXiv:hep-th/9806104 [hep-th].

[131] L. Romans, "Selfduality for Interacting Fields: Covariant Field Equations for Six-dimensional Chiral Supergravities," *Nucl. Phys. B* **276** (1986) 71.

[132] D. R. Mayerson, R. A. Walker, and N. P. Warner, "Microstate Geometries from Gauged Supergravity in Three Dimensions," arXiv:2004.13031 [hep-th].

[133] M. Shigemori, "Superstrata," *Gen. Rel. Grav.* **52** no. 5, (2020) 51, arXiv:2002.01592 [hep-th].

[134] S. Giusto, L. Martucci, M. Petrini, and R. Russo, "6D microstate geometries from 10D structures," *Nucl.Phys.* **B876** (2013) 509–555, arXiv:1306.1745 [hep-th].

[135] A. Jevicki, M. Mihailescu, and S. Ramgoolam, "Gravity from CFT on S**N(X): Symmetries and interactions," *Nucl.Phys.* **B577** (2000) 47–72, arXiv:hep-th/9907144 [hep-th].

[136] M. Mihailescu, "Correlation functions for chiral primaries in d = 6 supergravity on ads3 × s3," *Journal of High Energy Physics* **2000** no. 02, (Jan, 2000) 007–007. http://dx.doi.org/10.1088/1126-6708/2000/02/007.

[137] G. Arutyunov, A. Pankiewicz, and S. Theisen, "Cubic couplings in D = 6 N=4b supergravity on AdS(3) x S**3," *Phys. Rev. D* **63** (2001) 044024, arXiv:hep-th/0007061.

[138] P. Yang, Y. Jiang, S. Komatsu, and J.-B. Wu, "D-branes and Orbit Average," arXiv:2103.16580 [hep-th].

[139] K. Intriligator and W. Skiba, "Bonus symmetry and the operator product expansion of super-yang-mills," *Nuclear Physics B* **559** no. 1-2, (Oct, 1999) 165–183. https://doi.org/10.1016%2Fs0550-3213%2899%2900430-7.

[140] P. McFadden and K. Skenderis, "Holographic non-gaussianity," *Journal of Cosmology and Astroparticle Physics* **2011** no. 05, (May, 2011) 013–013. http://dx.doi.org/10.1088/1475-7516/2011/05/013.

[141] M. Bruni, S. Matarrese, S. Mollerach, and S. Sonego, "Perturbations of spacetime: gauge transformations and gauge invariance at second order and beyond," *Classical and Quantum Gravity* **14** no. 9, (Sep, 1997) 2585–2606. http://dx.doi.org/10.1088/0264-9381/14/9/014.

[142] J. R. David, G. Mandal, and S. R. Wadia, "Microscopic formulation of black holes in string theory," *Phys. Rept.* **369** (2002) 549–686, arXiv:hep-th/0203048.

[143] J. Hansen and P. Kraus, "Generating charge from diffeomorphisms," *JHEP* **0612** (2006) 009, arXiv:hep-th/0606230 [hep-th].

[144] I. Bena, S. F. Ross, and N. P. Warner, "Coiffured Black Rings," *Class.Quant.Grav.* **31** (2014) 165015, arXiv:1405.5217 [hep-th].

[145] O. Lunin and S. D. Mathur, "Correlation functions for M(N)/S(N) orbifolds," *Commun. Math. Phys.* **219** (2001) 399–442, arXiv:hep-th/0006196.

[146] P. Aichelburg and R. Sexl, "On the Gravitational field of a massless particle," *Gen.Rel.Grav.* **2** (1971) 303–312.

[147] J. Maldacena, S. H. Shenker, and D. Stanford, "A bound on chaos," *JHEP* **08** (2016) 106, arXiv:1503.01409 [hep-th].

[148] S. H. Shenker and D. Stanford, "Black holes and the butterfly effect," *JHEP* **03** (2014) 067, arXiv:1306.0622 [hep-th].

[149] S. H. Shenker and D. Stanford, "Multiple Shocks," *JHEP* **12** (2014) 046, arXiv:1312.3296 [hep-th].

[150] O. Lunin and S. D. Mathur, "Rotating deformations of AdS(3) x S(3), the orbifold CFT and strings in the pp-wave limit," *Nucl. Phys.* **B642** (2002) 91–113, arXiv:hep-th/0206107.

[151] O. Lunin, "Adding momentum to D1-D5 system," *JHEP* **04** (2004) 054, arXiv:hep-th/0404006.

[152] S. Giusto, S. D. Mathur, and A. Saxena, "Dual geometries for a set of 3-charge microstates," *Nucl. Phys.* **B701** (2004) 357–379, arXiv:hep-th/0405017.

[153] S. Giusto, S. D. Mathur, and A. Saxena, "3-charge geometries and their CFT duals," *Nucl. Phys.* **B710** (2005) 425–463, arXiv:hep-th/0406103.

[154] S. Giusto, O. Lunin, S. D. Mathur, and D. Turton, "D1-D5-P microstates at the cap," *JHEP* **1302** (2013) 050, arXiv:1211.0306 [hep-th].

[155] E. J. Martinec and S. Massai, "String Theory of Supertubes," *JHEP* **07** (2018) 163, arXiv:1705.10844 [hep-th].

[156] E. J. Martinec, S. Massai, and D. Turton, "String dynamics in NS5-F1-P geometries," *JHEP* **09** (2018) 031, arXiv:1803.08505 [hep-th].

[157] E. J. Martinec, S. Massai, and D. Turton, "Little Strings, Long Strings, and Fuzzballs," *JHEP* **11** (2019) 019, arXiv:1906.11473 [hep-th].

[158] E. J. Martinec, S. Massai, and D. Turton, "Stringy Structure at the BPS Bound," *JHEP* **12** (2020) 135, arXiv:2005.12344 [hep-th].

[159] D. Bufalini, S. Iguri, N. Kovensky, and D. Turton, "Black hole microstates from the worldsheet," *JHEP* **08** (2021) 011, arXiv:2105.02255 [hep-th].

[160] F. C. Eperon, H. S. Reall, and J. E. Santos, "Instability of supersymmetric microstate geometries," *JHEP* **10** (2016) 031, arXiv:1607.06828 [hep-th].

[161] G. Gibbons and N. Warner, "Global structure of five-dimensional fuzzballs," *Class.Quant.Grav.* **31** (2014) 025016, arXiv:1305.0957 [hep-th].

[162] D. Marolf, B. Michel, and A. Puhm, "A rough end for smooth microstate geometries," *JHEP* **05** (2017) 021, arXiv:1612.05235 [hep-th].

[163] S. Giusto and S. D. Mathur, "Geometry of D1-D5-P bound states," *Nucl. Phys.* **B729** (2005) 203–220, arXiv:hep-th/0409067.

[164] I. Bena and N. P. Warner, "Bubbling supertubes and foaming black holes," *Phys. Rev.* **D74** (2006) 066001, arXiv:hep-th/0505166.

[165] P. Berglund, E. G. Gimon, and T. S. Levi, "Supergravity microstates for BPS black holes and black rings," *JHEP* **0606** (2006) 007, arXiv:hep-th/0505167 [hep-th].

[166] J. B. Gutowski, D. Martelli, and H. S. Reall, "All supersymmetric solutions of minimal supergravity in six dimensions," *Class. Quant. Grav.* **20** (2003) 5049–5078, arXiv:hep-th/0306235.

[167] S. D. Mathur and D. Turton, "Microstates at the boundary of AdS," *JHEP* **05** (2012) 014, arXiv:1112.6413 [hep-th].

[168] J. Breckenridge, R. C. Myers, A. Peet, and C. Vafa, "D-branes and spinning black holes," *Phys.Lett.* **B391** (1997) 93–98, arXiv:hep-th/9602065 [hep-th].

[169] O. Lunin and S. D. Mathur, "Correlation functions for orbifolds of the type M(N)/S(N)," *Nucl. Phys. Proc. Suppl.* **101** (2001) 296–303.

[170] A. Schwimmer and N. Seiberg, "Comments on the N=2, N=3, N=4 Superconformal Algebras in Two-Dimensions," *Phys.Lett.* **B184** (1987) 191.

[171] E. J. Martinec and W. McElgin, "String theory on AdS orbifolds," *JHEP* **04** (2002) 029, arXiv:hep-th/0106171 [hep-th].

[172] E. J. Martinec and W. McElgin, "Exciting AdS orbifolds," *JHEP* **10** (2002) 050, arXiv:hep-th/0206175 [hep-th].

[173] H. Elvang, R. Emparan, D. Mateos, and H. S. Reall, "Supersymmetric black rings and three-charge supertubes," *Phys.Rev.* **D71** (2005) 024033, arXiv:hep-th/0408120 [hep-th].

[174] I. Bena and P. Kraus, "Microscopic description of black rings in AdS/CFT," *JHEP* **12** (2004) 070, arXiv:hep-th/0408186.

[175] V. Balasubramanian, P. Kraus, and M. Shigemori, "Massless black holes and black rings as effective geometries of the d1–d5 system," *Classical and Quantum Gravity* **22** no. 22, (Oct, 2005) 4803–4837. http://dx.doi.org/10.1088/0264-9381/22/22/010.

[176] I. Bena, B. D. Chowdhury, J. de Boer, S. El-Showk, and M. Shigemori, "Moulting Black Holes," *JHEP* **1203** (2012) 094, arXiv:1108.0411 [hep-th].

[177] S. Hampton, S. D. Mathur, and I. G. Zadeh, "Lifting of d1-d5-p states," *Journal of High Energy Physics* **2019** no. 1, (Jan, 2019) . http://dx.doi.org/10.1007/JHEP01(2019)075.

[178] M. Shigemori, "Interpolating between multi-center microstate geometries," arXiv:2105.11639 [hep-th].

[179] G. Bossard and S. Lüst, "Microstate geometries at a generic point in moduli space," *Gen. Rel. Grav.* **51** no. 9, (2019) 112, arXiv:1905.12012 [hep-th].

[180] I. Bena and D. R. Mayerson, "Multipole Ratios: A New Window into Black Holes," *Phys. Rev. Lett.* **125** no. 22, (2020) 221602, arXiv:2006.10750 [hep-th].

[181] M. Bianchi, D. Consoli, A. Grillo, J. F. Morales, P. Pani, and G. Raposo, "Distinguishing fuzzballs from black holes through their multipolar structure," *Phys. Rev. Lett.* **125** no. 22, (2020) 221601, arXiv:2007.01743 [hep-th].

[182] I. Bah, I. Bena, P. Heidmann, Y. Li, and D. R. Mayerson, "Gravitational footprints of black holes and their microstate geometries," *JHEP* **10** (2021) 138, arXiv:2104.10686 [hep-th].

[183] S. Abel, A. Constantin, T. R. Harvey, and A. Lukas, "Cosmic Inflation and Genetic Algorithms," arXiv:2208.13804 [hep-th].

[184] P. Shanahan *et al.*, "Snowmass 2021 Computational Frontier CompF03 Topical Group Report: Machine Learning," arXiv:2209.07559 [physics.comp-ph].

[185] I. Bena, J. Blåbäck, M. Graña, and S. Lüst, "Algorithmically Solving the Tadpole Problem," *Adv. Appl. Clifford Algebras* **32** no. 1, (2022) 7, arXiv:2103.03250 [hep-th].

[186] F. Ruehle, "Data science applications to string theory," *Phys. Rept.* **839** (2020) 1–117.

[187] S. Abel and J. Rizos, "Genetic Algorithms and the Search for Viable String Vacua," *JHEP* **08** (2014) 010, arXiv:1404.7359 [hep-th].

[188] D. Partipilo, "New methods for old problems: vacua of maximal D = 7 supergravities," *JHEP* **09** (2022) 096, arXiv:2205.06245 [hep-th].

[189] H. Erbin and A. H. Fırat, "Characterizing 4-string contact interaction using machine learning," arXiv:2211.09129 [hep-th].

[190] P. Berglund, G. Butbaia, T. Hübsch, V. Jejjala, D. Mayorga Peña, C. Mishra, and J. Tan, "Machine Learned Calabi–Yau Metrics and Curvature," arXiv:2211.09801 [hep-th].

[191] P. F. Ramirez, "Non-Abelian bubbles in microstate geometries," *JHEP* **11** (2016) 152, arXiv:1608.01330 [hep-th].

[192] I. Bah and P. Heidmann, "Smooth bubbling geometries without supersymmetry," *JHEP* **09** (2021) 128, arXiv:2106.05118 [hep-th].

[193] I. Bah, P. Heidmann, and P. Weck, "Schwarzschild-like topological solitons," *JHEP* **08** (2022) 269, arXiv:2203.12625 [hep-th].

[194] F. Denef, "Supergravity flows and D-brane stability," *JHEP* **0008** (2000) 050, arXiv:hep-th/0005049 [hep-th].

[195] P. Frazier, "A tutorial on bayesian optimization," *ArXiv* **abs/1807.02811** (2018) .

[196] A. Agnihotri and N. Batra, "Exploring bayesian optimization," *Distill* **5** (05, 2020) .

[197] H. R. Tizhoosh, "Opposition-based learning: a new scheme for machine intelligence," in *International conference on computational intelligence for modelling, control and automation and international conference on intelligent agents, web technologies and internet commerce (CIMCA-IAWTIC'06)*, vol. 1, pp. 695–701, IEEE. 2005.

[198] S. Rahnamayan, H. R. Tizhoosh, and M. M. Salama, "Opposition-based differential evolution algorithms," in *2006 IEEE International Conference on Evolutionary Computation*, pp. 2010–2017, IEEE. 2006.

[199] A. E. Eiben, J. E. Smith, *et al.*, *Introduction to evolutionary computing*, vol. 53. Springer, 2003.

[200] B. Ganchev, S. Giusto, A. Houppe, and R. Russo, "AdS_3 holography for non-BPS geometries," arXiv:2112.03287 [hep-th].

[201] Z. Carson, S. Hampton, S. D. Mathur, and D. Turton, "Effect of the deformation operator in the D1D5 CFT," *JHEP* **01** (2015) 071, arXiv:1410.4543 [hep-th].

[202] Z. Carson, S. Hampton, S. D. Mathur, and D. Turton, "Effect of the twist operator in the D1D5 CFT," *JHEP* **1408** (2014) 064, arXiv:1405.0259 [hep-th].

[203] Z. Carson, S. D. Mathur, and D. Turton, "Bogoliubov coefficients for the twist operator in the D1D5 CFT," *Nucl.Phys.* **B889** (2014) 443–485, arXiv:1406.6977 [hep-th].

[204] B. A. Burrington, A. W. Peet, and I. G. Zadeh, "Twist-nontwist correlators in M^N/S_N orbifold CFTs," *Phys.Rev.* **D87** (2013) 106008, arXiv:1211.6689 [hep-th].

[205] B. A. Burrington, A. W. Peet, and I. G. Zadeh, "Operator mixing for string states in the D1-D5 CFT near the orbifold point," *Phys.Rev.* **D87** (2013) 106001, arXiv:1211.6699 [hep-th].

[206] B. A. Burrington, A. W. Peet, and I. G. Zadeh, "Bosonization, cocycles, and the D1-D5 CFT on the covering surface," *Phys. Rev.* **D93** no. 2, (2016) 026004, arXiv:1509.00022 [hep-th].

[207] B. A. Burrington, I. T. Jardine, and A. W. Peet, "Operator mixing in deformed D1D5 CFT and the OPE on the cover," *JHEP* **06** (2017) 149, arXiv:1703.04744 [hep-th].

[208] B. A. Burrington, I. T. Jardine, and A. W. Peet, "The OPE of bare twist operators in bosonic S_N orbifold CFTs at large N," *JHEP* **08** (2018) 202, arXiv:1804.01562 [hep-th].

[209] T. de Beer, B. A. Burrington, I. T. Jardine, and A. W. Peet, "The large N limit of OPEs in symmetric orbifold CFTs with $\mathcal{N} = (4, 4)$ supersymmetry," arXiv:1904.07816 [hep-th].

[210] S. Giusto, R. Russo, and D. Turton, "New D1-D5-P geometries from string amplitudes," *JHEP* **11** (2011) 062, arXiv:1108.6331 [hep-th].

[211] I. Bena, S. Giusto, M. Shigemori, and N. P. Warner, "Supersymmetric Solutions in Six Dimensions: A Linear Structure," *JHEP* **1203** (2012) 084, arXiv:1110.2781 [hep-th].

[212] T. Harmark and N. A. Obers, "New phase diagram for black holes and strings on cylinders," *Class. Quant. Grav.* **21** (2004) 1709, arXiv:hep-th/0309116.

[213] T. Harmark and N. A. Obers, "General definition of gravitational tension," *JHEP* **05** (2004) 043, arXiv:hep-th/0403103.

[214] R. C. Myers, *Myers–Perry black holes*. 2012. arXiv:1111.1903 [gr-qc].